

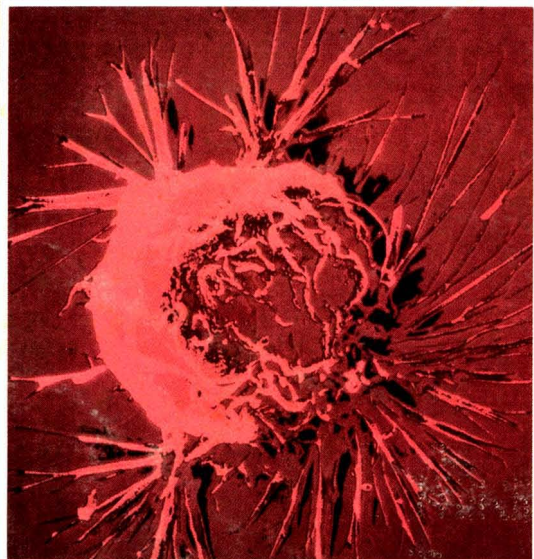
JUNE 1985

ENVIRONMENTAL SCIENCE & TECHNOLOGY

ES&T

**Regulating
cancer risks**

Page 473



PCB SERVICES

Turnkey management is provided for all PCB related clean ups.

- Transformer, Drain-Flush-Disposal • Resulting Liquids
- Capacitors • Articles • Contaminated Soils

Complete packaging, removal, transport and disposal is provided.

- Secure 7,200 sq. ft. PCB Handling Area
- Emergency Spill Response



Stock Brothers Corporation
Great Lakes Environmental Services

22077 Mound Road, P.O. Box 1208
Warren, Michigan 48091-1208
24 Hour Service @ (313) 758-0400
MI 1-800-482-4484 U.S. 1-800-482-4482
Telex 311894DOSS UR

Indoor Air Quality and Human Health

ISAAC TURIEL

Air pollution inside American homes, offices, and public buildings may be far worse than it is outside, according to a recent government report. The first summary of all that is known about the health risks associated with indoor air quality, this book suggests what can be done to lessen the effects of such major contaminants as combustion products (from cooking, heating, and cigarette smoke), chemical evaporants (from building materials and household products), radon, microbes, allergens, etc. It also considers the unhealthy side effects of promoting energy-efficient houses and airtight buildings. \$24.95

Stanford University Press

INTRODUCING

NEW STATE-OF-THE-ART INSTRUMENTATION:

The SEASTAR IN SITU WATER SAMPLER

Uses microprocessor control and extraction columns to make the most significant advance in water sampling technology since the Nansen bottle.

FEATURES:

- Capable of large volume ultra-trace water sampling
- Equally useful for organic and inorganic applications
- Utilizes a variety of types of extraction columns, each with guaranteed blank levels
- Microprocessor-controlled for unprecedented flexibility of sampling, and precise control of flow rate and sample volume
- Can be moored (for days or weeks) or triggered with a messenger from a hydrowire
- Totally self-contained powered by D-cell batteries

BUILT WITH PRIDE BY



SEASTAR INSTRUMENTS LTD

2045 MILLS ROAD, SIDNEY, B.C. CANADA V8L 3S1 (604) 656-0891 TELEEX 049-7529

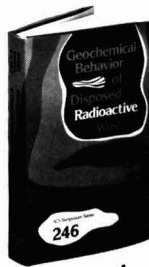
Geochemical Behavior of Disposed Radioactive Waste

G.S. Barney and W.W. Schulz, Editors
Rockwell Hanford Operations
J.D. Navratil, Editor
Rockwell International Rocky Flats Plant

Examines the complex issue of radioactive waste disposal and the health hazards at underground waste sites. Assesses the chemical and physical behavior of wastes from the nuclear fuel cycle, from nuclear weapons testing, and from medical and research activities.

CONTENTS

Sorption and Desorption Reactions with Interbedded Materials • Reactions Between Tc and Fe-Containing Minerals • Radionuclide Sorption Mechanisms and Rates on Granitic Rock • Actinide and Technetium Sorption on Fe-Silicate and Dispersed Clay Colloids • Adsorption of Nuclides on Hydrated Oxides • High-Level Waste Components on Solubility and Sorption of Co, Sr, Np, Pu, Am • Hydrolysis of Am(III) and Pu(IV) • Aging Effect on Solubility and Crystallinity of Np(IV) Hydrated Oxide • Geochemical Controls on Radionuclide Releases from Waste Repository in Basalt • Radionuclide-Humic Acid Interactions • Oxygen Consumption and Redox Conditions in Basalt • Monitoring and Control of pH Conditions in Hydrothermal Experiments • Cs - Feldspars Interaction • Interaction of Groundwater and Basalt Fissure Surfaces and Effect on Actinide Migration • Organics and Radionuclides Subsurfaces Migration • Uranium Mining Releases • Uranium Mobility and Roll-Front Deposits • Crystal Chemistry of ABO₄ Compounds • Transformation Characteristics of LaV, Nb_{1-x}O₄ Compounds • Stability of Tetravalent Actinides in Perovskites • α and β Decay in the Solid State • Effects of Water Flow Rates on Leaching • Borosilicate Glass-Containing Waste • Leach Resistance of Iodine Compounds • Nuclear Waste - View from Washington, D.C.



New!

Order from:
American Chemical Society
Distribution Office Dept. 70
1155 Sixteenth St., N.W.
Washington, DC 20036
or CALL TOLL FREE
800-424-6747 and use your
VISA, MasterCard, or
American Express credit
card.

ACS Symposium Series No. 246
424 pages (1984) Clothbound
Lc 84-3106

ISBN 0-8412-0827-1
Export \$95.95

Environmental Science & Technology
© Copyright 1985 by the American Chemical Society

Editor: Russell F. Christman
Associate Editor: John H. Seinfeld
Associate Editor: Philip C. Singer

ADVISORY BOARD

Julian B. Andelman, Marcia C. Dodge, Steven Eisenreich, William H. Glaze, Michael R. Hoffmann, Lawrence H. Keith, Donald Mackay, Jarvis Moyers, Kathleen C. Taylor, Eugene B. Welch

WASHINGTON EDITORIAL STAFF

Managing Editor: Stanton S. Miller
Associate Editor: Julian Josephson

MANUSCRIPT REVIEWING

Manager: Janice L. Fleming
Associate Editor: Monica Creamer
Assistant Editor: Yvonne D. Curry
Editorial Assistant: Diane Scott

MANUSCRIPT EDITING

Assistant Manager: Mary E. Scanlan
Assistant Editor: Ruth A. Linville

GRAPHICS AND PRODUCTION

Production Manager: Leroy L. Corcoran
Art Director: Alan Kahan
Staff Artist: Julie Katz

Production Editor: Kate Kelly

BOOKS AND JOURNALS DIVISION

Director: D. H. Michael Bowen
Head, Journals Department: Charles R. Bertsch
Head, Production Department: Elmer M. Pusey
Head, Research and Development Department: Lorrin R. Garson

ADVERTISING MANAGEMENT

Centcom, Ltd.

For officers and advertisers, see page 492.

Please send *research* manuscripts to Manuscript Reviewing, *feature* manuscripts to Managing Editor. For editorial policy and author's guide, see the January 1985 issue, page 22, or write Janice L. Fleming, Manuscript Reviewing Office, *ES&T*. A sample copyright transfer form, which may be copied, appears on the inside back cover of the January 1985 issue.

Environmental Science & Technology, *ES&T* (ISSN 0013-936X), is published monthly by the American Chemical Society at 1155 16th Street, N.W., Washington, D.C. 20036; 202-872-4600, TDD 202-872-8733. Second-class postage paid at Washington, D.C., and at additional mailing offices. POSTMASTER: Send address changes to Membership & Subscription Services, P.O. Box 3337, Columbus, Ohio 43210.

SUBSCRIPTION PRICES 1985: Members, \$26 per year; nonmembers (for personal use), \$35 per year; institutions, \$149 per year. Foreign postage, \$8 additional for Canada and Mexico, \$14 additional for Europe including air service, and \$23 additional for all other countries including air service. Single issues, \$13 for current year; \$13.75 for prior years. Back volumes, \$161 each. For foreign rates add \$1.50 for single issues and \$10.00 for back volumes. Rates above do not apply to nonmember subscribers in Japan, who must enter subscription orders with Maruzen Company Ltd., 3-10 Nihon bashi 2-chome, Chuo-ku, Tokyo 103, Japan. Tel: (03) 272-7211.

COPYRIGHT PERMISSION: An individual may make a single reprographic copy of an article in this publication for personal use. Reprographic copying beyond that permitted by Section 107 or 108 of the U.S. Copyright Law is allowed, provided that the appropriate per-copy fee is paid through the Copyright Clearance Center, Inc., 21 Congress St., Salem, Mass. 01970. For reprint permission, write Copyright Administrator, Books & Journals Division, ACS, 1155 16th St., N.W., Washington, D.C. 20036.

REGISTERED NAMES AND TRADEMARKS, etc., used in this publication, even without specific indication thereof, are not to be considered unregistered by law.

SUBSCRIPTION SERVICE: Orders for new subscriptions, single issues, back volumes, and microfiche and microform editions should be sent with payment to Office of the Treasurer, Financial Operations, ACS, 1155 16th St., N.W., Washington, D.C. 20036. Phone orders may be placed, using Visa, Master Card, or American Express, by calling toll free (800) 424-6747 from anywhere in the continental U.S. Changes of address, subscription renewals, claims for missing issues, and inquiries concerning records and accounts should be directed to Manager, Membership and Subscription Services, ACS, P.O. Box 3337, Columbus, Ohio 43210. Changes of address should allow six weeks and be accompanied by old and new addresses and a recent mailing label. Claims for missing issues will not be allowed if loss was due to insufficient notice of change of address, if claim is dated more than 90 days after the issue date for North American subscribers or more than one year for foreign subscribers, or if the reason given is "missing from files."

The American Chemical Society assumes no responsibility for statements and opinions advanced by contributors to the publication. Views expressed in editorials are those of the author and do not necessarily represent an official position of the society.

ES&T CONTENTS

Volume 19, Number 6, June 1985

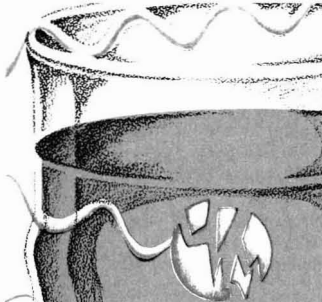
CRITICAL REVIEW



473

Regulating cancer risks. A discussion of cancer risk assessment methods and ways to regulate the risks is presented. Paolo F. Ricci, Electric Power Research Institute, Palo Alto, Calif., and Lawrence S. Molton, Palo Alto, Calif.

FEATURE



480

Contaminant degradation in water. Light and catalysts are used to break up halogenated hydrocarbons. David F. Ollis, North Carolina State University, Raleigh, N.C.

REGULATORY FOCUS

485

Groundwater monitoring. Richard Dowd discusses trends in compliance with groundwater monitoring legislation and regulations.

VIEWS



486

Ocean incineration of hazardous wastes. Desmond Bond discusses the controversy surrounding the ocean incineration issue.

488

Miami meeting report. A review of environmental topics at the April ACS national meeting.

DEPARTMENTS

- 467 Editorial
- 470 Currents
- 493 Consulting services

UPCOMING

Photochemistry of the marine environment

PCBs in the Hudson River

ESTHAG 19(6) 465-560 (1985)
ISSN 0013-936X

Credits: p. 470, courtesy Westinghouse Public Relations; pp. 473, 479, courtesy Walter Reed Army Medical Center
Cover: Raymond B. Weiss, Medical Oncology Service, Walter Reed Army Medical Center; inset photos, National Cancer Institute

RESEARCH

497

New conceptual formulation for predicting filter performance. Vinod Tare* and C. Venkobachar

Surface coverage by media grains, retained particles acting as collectors, and variation of retained particles with depth prove to be important factors when predicting filter performance.

■ 500

Estimation of vapor pressures for polychlorinated biphenyls: A comparison of eleven predictive methods. Lawrence P. Burkhard, Anders W. Andren, and David E. Armstrong*

The predictive ability of these methods for compounds with low vapor pressures and one or fewer experimental determinations is assessed.

■ 507

Phase-transfer-catalyzed methylation of hydroxyaromatic acids, hydroxyaromatic aldehydes, and aromatic polycarboxylic acids. Sowmianarayanan Ramaswamy, Murugan Malaiyandi,* and Gerald W. Buchanan

A phase transfer technique is described with tetra-*n*-butylammonium hydroxide as the catalyst and either idomethane or dimethyl sulfate used for methylation.

512

Identification of intermediates leading to chloroform and C-4 diacids in the chlorination of humic acid. Ed W. B. de Leer,* Jaap S. Sinninghe Damsté, Corrie Erkelens, and Leo de Galan

Intermediates are identified that support Rook's hypothesis that *m*-dihydroxybenzene moieties in humic acid are responsible for chloroform formation.

522

Relationships between octanol-water partition coefficient and aqueous solubility. Michele M. Miller, Stanley P. Wasik, Guo-Lan Huang, Wan-Ying Shiu, and Donald Mackay*

The thermodynamic basis for previous correlations between aqueous solubility and the octanol-water partition coefficient is described, and a new correlating approach is suggested.

529

Composition of fine particle regional sulfate component in Shenandoah Valley. Semra G. Tuncel, Ilhan Olmez, Josef R. Parrington, Glen E. Gordon,* and Robert K. Stevens

To answer some of the questions that prevent the acceptance of regional scale receptor modeling, the fine fractions of the samples of Stevens et al. from 1980 are reanalyzed by INAA.

538

Removal of arsenic from geothermal fluids by adsorptive bubble flotation with colloidal ferric hydroxide. Eric Heinen De Carlo* and Donald M. Thomas

A method is described for the separation of arsenic oxyanions from high ionic strength geothermal fluids employing flotation with ferric hydroxide and alkyl surfactants.

544

Using electrophoresis in modeling sulfate, selenite, and phosphate adsorption onto goethite. Douglas D. Hansmann* and Marc A. Anderson

Electrophoresis is used to determine the electrical component of net adsorption energies and to compare three techniques for assigning maximum available surface site concentrations.

NOTES

552

Acidification of southern Appalachian lakes. Robert W. Talbot and Alan W. Elzerman*

Measurements of the major anions and cations in 10 southeastern U.S. lakes are used to examine effects of atmospheric acid deposition on water chemistry.

557

Improved aqueous scrubber for collection of soluble atmospheric trace gases. Wesley R. Cofer III,* Vernon G. Collins, and Robert W. Talbot

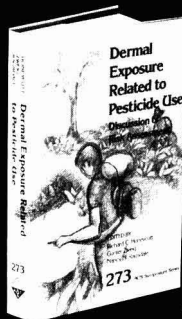
This technique allows for highly efficient extraction of water-soluble gases from large-volume flow rates of air in a minimum of trapping solution.

*To whom correspondence should be addressed.

■ This article contains supplementary material in microform. See ordering instructions at end of paper.

Dermal Exposure Related to Pesticide Use

Discussion of Risk Assessment



Richard C. Honeycutt, *Editor*
CIBA-GEIGY

Gunter Zweig, *Editor*
University of California, Richmond

Nancy Ragsdale, *Editor*
Department of Agriculture

Confronts the issue of a serious chemical risk—pesticide exposure. Reports data vital for assessing and regulating farm worker safety. Looks at dermal absorption, field studies of exposure methodology, exposure assessment and protection, predicting exposure levels, and interpretation of data.

CONTENTS

In Vitro Data and Risk Assessment • Transdermal Absorption Kinetics • In Vitro Methods for Percutaneous Absorption • Radioisotope Approaches to Dermal Studies • Dermal Dose-Cholinesterase Response • Monkey Percutaneous Absorption Studies • Field Studies: Methods Overview • MSMA and Cacodylic Acid Exposure in Forestry • Carbaryl Exposure to Strawberry Harvesters • Applications Exposure to Home Gardener • Monitoring Field Applications Exposure • MeP Residue in Contaminated Fabrics • Pesticide Drift and Quantification from Air/Ground Applications • Mancozeb Exposure • Inhalation Exposure to CCl₄ • Inhalation Exposure to Dowfume 75 • Exposure to DDVP-Treated Residences • Subterranean Termite Control: Chlordane Residues • Measuring Exposure to Paraquat • Exposure to Pesticides Applied to Turfgrass • Orchard and Field Crop Pesticide Exposure • Pesticide Exposure in Greenhouse Operations • Unified Field Model for Reentry Hazards • Data-Base Proposal for Predicting Exposure • EPA's Viewpoint on Dermal Exposure • Exposure Estimates Based on Generic Data • Fluorescent Tracer Methodology • Protective Clothing • Protective Apparel Research • Minimizing Pesticide Exposure Risk • Occupational Pesticide Exposure in Canada • Excess Pesticide Exposure in California • Exposure Studies in Risk Assessment • Farmworker Risk from OPIDN • Pesticide Drift: Toxicological and Social Consequences

Based on a symposium sponsored by the Division of Pesticide Chemistry of the American Chemical Society

ACS Symposium Series No. 273
544 pages (1985) Clothbound
LC 84-28361 ISBN 0-8412-0898-0
US & Canada \$79.95 Export \$95.95

Order from: American Chemical Society
Distribution Office Dept. 26
1155 Sixteenth St., N.W.
Washington, DC 20036
or CALL TOLL FREE 800-424-6747
and use your VISA, MasterCard,
or American Express credit card.

Phosphate here, phosphate there . . .

Most of us have felt a sense of frustration over public environmental debates in which a clearly correct and effective course of action is not obvious. When this is the case, scientists conclude that more research is needed, and more enlightened members of the public conclude, properly, that no one has the answers. These conclusions, however, do not prevent municipalities and state and federal agencies from acting—public and political processes being what they are.

The frustration is particularly intense when relatively old and heavily researched issues fall into this trap, as is the case with eutrophication and public consideration of the favorite political control option of banning phosphates in detergents.

Not many environmental issues have received more scientific thought and research investment than eutrophication. The currently accepted definition is that eutrophication is a process of nutrient enrichment in water bodies that can be accelerated by natural or synthetic means. Even the most respected limnological experts, however, have disagreed over whether the amount of algae present should be included in the definition. While the scientific community has been studying the complex chemical and ecological processes involved, the public has learned that eutrophication can mean unsightly algal blooms, the presence of unpleasant odors, and a tendency to stain and, perhaps, to kill fish.

Eutrophic waters can exist without unsightly or noxious conditions where productivity is limited by nonnutrient factors. More than one factor can control the growth of aquatic plants, although much of the early research base was established on relatively pure north-central lakes sensitive to as little as 10 $\mu\text{g/L}$ of total phosphorus. In southeastern waters, natural phosphorus levels are higher (40–70 $\mu\text{g/L}$) and can exceed 100 $\mu\text{g/L}$ as a result of rainstorm-induced erosion. Much of this phosphorus load is particulate and is removed by natural assimilative processes as streams cut new channels, depositing alluvial soil on flood plains, and as suspended matter settles to the bottom of lakes. High turbidity values associated with this particulate

flux may make algal growth in such waters light limited, but other limiting factors may be equally important. In all such cases control of phosphorus is less directly associated with reductions of nuisance algal growth.

What is known scientifically suggests that natural variations in the complex interrelations among nutrient levels, light availability, and plant growth are so substantial that single control measures (such as phosphate bans) are likely to have extremely variable results if applied over large areas.

Indeed, there are surface waters that benefit from phosphorus reductions, such as Lake Washington in Seattle, but phosphorus bans are not a panacea nationally, regionally, or perhaps even on a statewide level. For one thing, detergents are not the largest source of phosphates in domestic sewage, and in any case it may well be more economical to remove them by sewage treatment than it is to require the use of more expensive soap. At least this is EPA's apparent message in deciding not to pursue national efforts to ban phosphates in detergent. Ban advocates, who often speak as though the entire environmental research community were united behind them, present cost data suggesting the reverse. Which data are more credible? We don't have much national experience with either approach and "actual" cost data are likely site specific.

Another disadvantage of phosphate bans over large areas as a mandatory single solution to eutrophication is the unwitting support it lends to the efforts of community officials to avoid expanded investments in sewage treatment facilities. This is extremely counterproductive in the Southeast, where municipal sewage effluents are a major contaminant of surface water and where phosphate reductions that result from bans may produce no noticeable improvement in water quality.

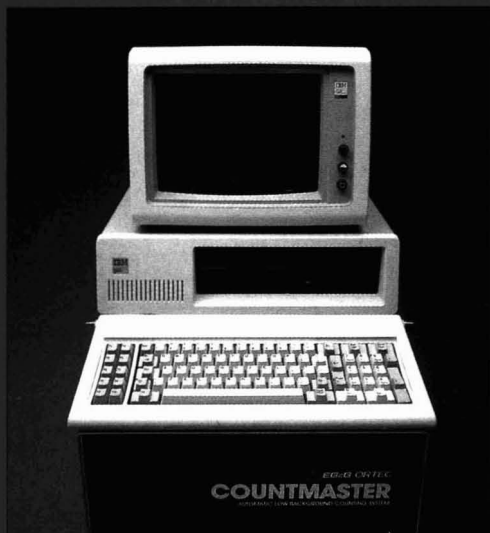


The Countmaster alpha/beta counting

A compact, convenient low-level alpha/beta counting system, the Countmaster™ from EG&G ORTEC has introduced a new era in enhanced counting capabilities. Less than half the size and weight of conventional counters, the Countmaster represents an innovative concept in detector design. Developed by the pioneer in nuclear instrumentation, it provides new dimensions in performance, convenience, flexibility and value.

240 sample capacity

Countmaster from EG&G ORTEC features a standard counting capacity at least twice that of any other low-level alpha/beta counter. For larger sample volume requirements, the Countmaster system can be conveniently and economically expanded to handle 480, 720 or 960 samples. Modular design allows up to four counters to be operated through one master controller (an IBM-PC).



Powerful IBM-PC

Computer control with the IBM-PC combines dramatic power, flexibility and ease of use. Countmaster offers unprecedented analytical power, information handling/storage capacity and flexibility. Software is menu-driven and adapts easily to your specialized requirements. Total alpha/beta counting and analytical functions are standard including multichannel analysis.

The display monitor prompts and guides users through each task. Special function keys enhance convenience. BASIC allows simple programming for special requirements. It all adds up to easy, user-friendly operation.

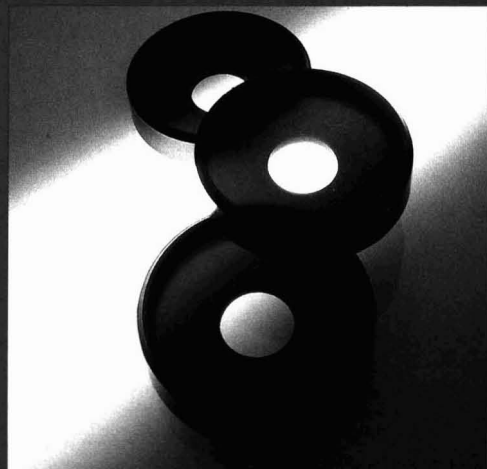
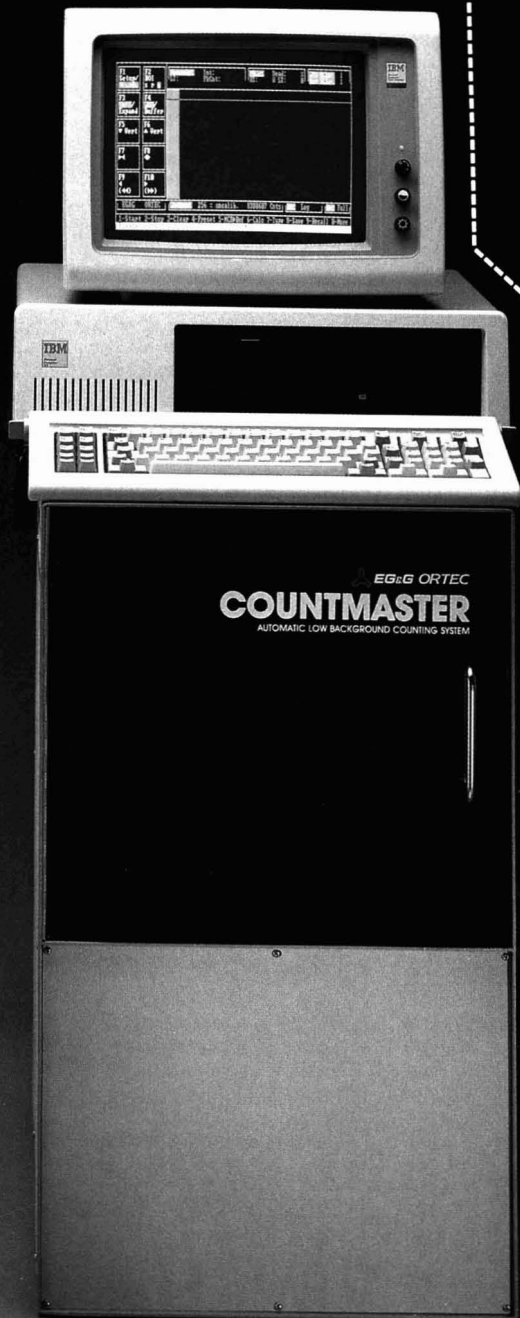
**TWICE THE
CAPACITY
IN HALF
THE SPACE.**

low-level automatic system from EG&G ORTEC

In addition, the Countmaster can be networked with a central mainframe via IEEE-488 or RS-232-C port.

Countmaster is available separately to use with any in-place IBM computer.

Optional HP-85 computer and/or software is available.



Jam-free sample changer

Reliability is inherent by design in the Countmaster. A special automatic sample changer assures reliable performance. The robotic manipulator has no square edges to catch or jam. Round sample holders facilitate smooth changing. Any misaligned sample is readjusted automatically by an exclusive anti-jamming feature to insure trouble-free operation.

Exclusive sample tracking system

Keeping track of all samples—from receipt to storage—is easy with the Countmaster. Each sample holder has an exclusive magnetic recording system. Special read and record heads allow 16 bits of information in any format. A message-repeat feature insures coding is always read accurately.

Find out how the Countmaster can enhance your low-level alpha/beta counting capabilities. Contact your EG&G ORTEC Regional Sales Manager or write/call:

 **EG&G ORTEC**
100 Midland Road, Oak Ridge, TN 37830
Phone: 1-800-251-9750 or 615-483-2157/Telex: 55-7450

ES&T

CURRENTS

INTERNATIONAL



Sabimbona: Environmental plans

The central African Republic of Burundi has begun "environmental protection initiatives," Simon Sabimbona, Burundi's ambassador to the U.S., tells *ES&T*. He says that the first tasks of this program will be floral and faunal preservation and water pollution prevention and control. Ambassador Sabimbona explains his government's view that preserving the diversity of animal and plant species is important because it may serve to draw tourists and provide future sources of chemicals and pharmaceuticals. Another important objective is the protection of Lake Tanganyika. The Earth's second oldest and second deepest lake, it supports the world's most intensive lake fishery industry. He adds that vigorous development of renewable resources of energy is another top-priority objective.

FEDERAL

The Occupational Safety and Health Administration (OSHA) is expected to issue new rules to protect more than 1.4 million workers exposed to formaldehyde. OSHA is under considerable pressure from organized labor and environmental advocacy groups to make the move. The advocates of control cite laboratory evidence that formaldehyde causes cancer in rats. The current exposure limit, set in 1970, is 3 ppm in workplace air; some scientific studies have recommended lowering that limit by as much as 50%. About 777,000 workers in the textile industry are exposed to formaldehyde;

other industries in which workers are exposed include auto manufacturing and metal casting. OSHA estimates that tightening the rules could result in a loss of 135,000 jobs.

Speaker of the House Thomas P. (Tip) O'Neill (D-Mass.) has called for rapid reauthorization of Superfund in the amount of at least \$7.5 billion (the present federal funding is \$1.6 billion). In April, he told a Chemical Manufacturers Association forum in Washington, D.C., that he expects passage of laws that will require industries to inform communities of their right to know what chemical hazards are in their vicinity—perhaps attached to any new Superfund legislation. He also brought up the strong possibility of compensation for victims of exposure to hazardous wastes. O'Neill told *ES&T* that he expects reauthorization of the Clean Water Act and the Clean Air Act during the 1986 session of Congress.

EPA has proposed granting federal and state agencies emergency exemptions from pesticide regulations. This would allow the use of pesticides for applications for which they were not registered, such as combating a target pest not covered in the chemical's registration. Section 18 of the Federal Insecticide, Fungicide and Rodenticide Act allows exemptions of this kind under emergency conditions. The term "emergency condition" means an unusual set of circumstances calling for nonconventional use of a pesticide. One example would be a heavy infestation of insects that would cause a substantial reduction in expected farm yields and profits. Another would entail a loss in the value of fixed assets, such as land, brought about by the pest emergency.

The Nuclear Regulatory Commission (NRC) may have to reduce the number of safety inspections it conducts and curtail its research activities because of constraints in its fiscal year 1986 budget. The 1986 budget request for NRC was for \$429 million, \$20 million below its 1985 level. Chairman Nunzio Palladino notes that research funds will

have been reduced by 40% from the 1981 level. One effort to be curtailed is the development of simplified regulations for new generations of reactors, which cannot be licensed until final regulations are in place. NRC Commissioner James Asseltine added that budget cuts also will translate to fewer inspections for maintenance, equipment testing, and fire protection.

Sen. David Durenberger (R-Minn.) has introduced a bill (S. 124) to reauthorize the Safe Drinking Water Act of 1974 (SDWA). He complains that EPA has been too slow to regulate contaminants in drinking water and says he is considering adding language that would force the agency to set enforceable standards within a given time. This language would be similar to the "hammer provisions" of the Resource Conservation and Recovery Act Amendments of 1984. They force EPA to promulgate regulations by a certain deadline; otherwise, rules that Congress approves automatically become law by the deadline date. In the House, Rep. Edward Madigan (R-Ill.) introduced H.R. 1650 to reauthorize the SDWA with provisions that will force control of contaminants.

As of 1982, there were 42,407 environmental scientists at work in the U.S., according to the National Science Foundation. Most of them, 26,442, worked in business and industry, whereas about 9000 worked for federal, state, or local governments. Almost 11,000 were employed by educational institutions. More than 22,000 were involved with energy and fuel research, and about 6100 worked in pollution abatement, hazardous waste, and related areas. Approximately 3600 were employed in the field of mineral resources other than those used for energy and fuel, and nearly 1600 worked in national defense.

Existing federal air pollution regulations soon may become less defensible, according to members of EPA's science advisory board (SAB). During April, the board cited increasing evidence that indoor air quality and personal lifestyles (use of

tobacco, for example) are very important in determining the effects of human exposure to air pollution. The SAB also notes that although most persons are outdoors only 5-10% of the time, they encounter pollutants from automobiles at concentrations several times higher than those detected by monitoring stations. The board called for a systematic review of the ways that exposure to criteria pollutants, such as particulates and NO_x , occurs. The SAB is especially interested in particulates less than $10 \mu\text{m}$ in diameter and is calling for better linkage between health effects studies and studies of actual exposure to pollutants.

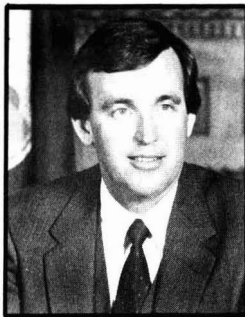
A "perfect" scientific answer to the question of when to impose restrictions on SO_x and NO_x pollutants to control acid rain may never be available, says Christopher Bernabo, executive director of the National Acid Precipitation Assessment Program. In April, he told the House Subcommittee on Natural Resources, Agriculture Research and Environment that information about which pollutants cause forest damage or how quickly lakes become acidified is being gathered but will not be available for months or even years. Bernabo added that although scientists can provide technical data on acid rain, they are not qualified to make decisions about when controls must be imposed. He said that Congress must judge when such controls are necessary.

STATES

Acid rain in the western U.S. is more attributable to NO_x emissions than is acid rain in eastern states, according to a report by scientists from the World Resources Institute (WRI, Washington, D.C.) and the University of California (Berkeley). WRI president Gus Speth said that although there was "no real evidence of acid rain damage" in the West yet, precursors to damage, such as the loss of acid-neutralizing ability in lakes, are showing up. John Harte of the University of California agreed and added a warning about biological damage with long-term effects. He noted that soil in high elevations, such as the Colorado Rockies and Washington State's Cascade Mountains, has little natural capacity for neutralizing airborne acids.

On March 31, New York banned all commercial fishing for striped bass in the New York harbor and on

the north and south shores of western Long Island. The reason is that polychlorinated biphenyls (PCBs) were found to exceed the permissible level of 2 ppm. Commercial fishing for striped bass is still allowed off the shore of eastern Long Island despite the detection of PCBs in fish from those waters. In addition, the state Health Department is advising women and children to eat no striped bass from New York waters because of possible adverse effects. Adult males are urged to eat striped bass no more than once a month.



Carlin: Banning waste burial

No hazardous waste may be buried underground in Kansas after July 1, 1985, under a law signed by Gov. John Carlin. The ban would not apply to companies generating less than 110 lb/month of hazardous wastes after July 1, 1985, or less than 55 lb/month after July 1, 1986. Also, the state secretary of health and environment is to decide whether exceptions will be made for cases in which no economically or technically feasible alternative to burial exists. Most hazardous waste in Kansas is currently stored at company sites or disposed of by deep-well injection. There is one land disposal site near Furlley, in south-central Kansas, but that was closed in 1982 when it was found to be leaking into area groundwater.

New Jersey is the first state to propose tough regulations on groundwater. The state is expected to require utilities and communities to develop alternative sources of supply. For example, sellers of water would have to keep track of water withdrawn but not used. A water loss over a certain percentage would lead to an order for a company to plug leaks in its supply system within one year. Another provision requires water suppliers to set aside a minimum of 10% of their revenues for rehabilitation of storage and distribution systems. The regulations apply

to places where groundwater supplies are threatened. Middlesex, Monmouth, and Ocean Counties fall into this category; Camden and Atlantic Counties may be next in line.

SCIENCE

Parathion, a highly toxic organophosphate pesticide, can now be decomposed by a bacterium.

Pseudomonas diminuta is a soil microorganism that generates an enzyme, parathion hydrolase, which breaks parathion into biodegradable products. Recombinant-DNA techniques developed by Cunev Serdar and Douglas Munneke of the University of Texas at Austin (Munneke is now with Genencor, South San Francisco, Calif.) make the bacterium secrete increased amounts of the enzyme. Serdar estimates that the toxicity of parathion can be reduced about 120-fold after treatment with parathion hydrolase.

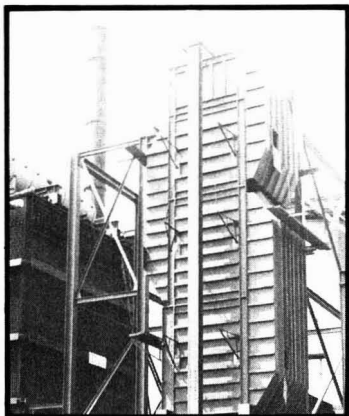
Groundwater is affected for several years by the one-time application of almost any soluble chemical. Scientists from the North Appalachian Experimental Watershed Research Laboratory, (Coshocton, Ohio), a part of the U.S. Agricultural Research Service, set out to verify this hypothesis. They applied potassium bromide (KBr), a tracer, in amounts and rates similar to those used for nitrogen fertilizer on two three-acre watersheds. Groundwater samples showed peak KBr concentrations 21-24 months after application. Even after 45 months, there was no significant decrease.

Retinoids may be instrumental in preventing cancer, says Don Hill of the Southern Research Institute (Birmingham, Ala.). Retinoids are derivatives of vitamin A that have shown the ability to prevent cancer in some animals. Hill explained that if a group of rats is dosed with a carcinogen, 80-90% may contract cancer. "But if you give them retinoids, you may reduce the incidence of cancer to 40-50%," he noted. Hill's research indicates that retinoids can prevent mammary, skin, and possibly bladder cancers in rats.

TECHNOLOGY

The Solar Energy Research Institute (SERI, Golden, Colo.) dedicated its field test laboratory building earlier this year. The 70,000-ft² building will house 60 researchers, many of whom will be involved with biofuel and thermal work. Biofuels research

will include biotechnology, electro-chemistry, fermentation, genetic engineering, microbiology, and thermochemical research. Gasification, pretreatment, and pyrolysis also will be studied. Researchers will evaluate materials, desiccant cooling systems, heliostats, and high-temperature heat transfer and storage systems.



FBC system burns low-grade fuel

Low-grade fuels can be converted to energy through a fluidized-bed combustion (FBC) and boiler system developed by Cockerill Mechanical Industries (Liège, Belgium). According to the company, advantages include smaller energy needs for crushing fuel particles to 1–8 mm and lower combustion temperatures (850–900 °C), which substantially reduce NO_x emissions. Other features Cockerill lists are a close combustion mixture of fuel, air, and limestone, so that sulfur, chlorine, and cyanide emissions are largely suppressed; this obviates the need for flue gas desulfurization. The company, which is to furnish three such systems to companies in Belgium, displayed the technology at the 12th Energy Technology Conference and Exposition in Washington, D.C., in late March.

Oil shales of the eastern U.S. could contain more than 400 billion bbl of recoverable oil, D. V. Punwani of the Institute of Gas Technology (IGT, Chicago, Ill.) told the 12th Energy Technology Conference and Exposition in Washington, D.C. He added that conventional shale retorting results in “a much lower yield” for eastern shales; however, retorting in a hydrogen-rich atmosphere could raise the oil output by 250%. Punwani says that IGT has been doing government- and industry-funded research in extracting oil from eastern shales for the past 10 years.

Wastewater can be cleansed of uranium, vanadium, chromium, and silver with various species of *Pseudomonas* bacteria, says Robert Clyde of Clyde Engineering (New Orleans, La.). *Thiobacillus ferrooxidans* can be used to remove palladium. Clyde reported at the meeting of the American Chemical Society in Miami, Fla., that when the bacteria are attached to high-area fibers, filtering is avoided (free cells of the microbe would plug the filter). He added that the bacteria perform efficiently at concentrations ranging between 0.01% and 1%.

Incineration of hazardous waste on land and at sea is one of the safest disposal methods, according to Milton Russell, EPA's assistant administrator for policy, planning, and evaluation. He says that the use of land and ocean incineration will increase because it consists of proven technologies. Russell foresees heightened demand for incineration of landfill restrictions in the Resource Conservation and Recovery Act amendments of 1984 are put into full effect. He also forecasts that incinerator ship operators will have an increased market because of public resistance to placing waste burners on land and because the three ships awaiting permits would double U.S. hazardous waste incineration capacity. About 2.64×10^8 t of hazardous waste is generated in the U.S. each year. Europe plans to ban at-sea incineration of hazardous wastes beginning in 1990.

BUSINESS

The National Environmental Development Association (NEDA, Washington, D.C.) has called for reauthorization of the Clean Water Act this year. NEDA representatives told the Senate's Pollution Subcommittee that there should be a continued commitment to federally funded sewage treatment plant construction. NEDA also recommends extending industrial pollutant discharge permits from five to ten years and extending treatment technology deadlines by three years. It opposes legislation that would end variances for certain nontoxic pollutants under Section 301(g) of the Clean Water Act.

Southern Company (Atlanta, Ga.) plans to join in the support of the development of a 160-MW fluidized-bed combustion (FBC) boiler at Paducah, Ky. This boiler will be the largest demonstration of FBC technology in the world. The FBC boiler

works by injecting a combination of limestone and fuel—mainly coal—into the combustor; the limestone suppresses the SO_x by removing about 90% of the sulfur from the coal during the combustion process. Principal cosponsors of the project are the Department of Energy, the Tennessee Valley Authority, and Duke Power Company.

Environmental regulations have not significantly raised costs or lowered productivity in U.S. businesses, according to a report published in March by the Congressional Budget Office (CBO). The report does acknowledge, however, that in recent years costs have been somewhat higher and productivity slightly lower in the U.S. than in Canada, Japan, or West Germany, even though those countries' laws now mandate similar levels of environmental protection. Still, compliance costs in some industries have been high. One example is the elaborate air pollution control technology needed by the nonferrous metals industry. The report recommends allowing standards to be met with the least costly control technique, rather than by mandating a control method such as precipitators or fabric filters.



Santoro: Evaluation by computer

Westinghouse (Pittsburgh, Pa.) is offering risk management and reliability engineering services, developed for its nuclear business, to other industries. The services involve computerized techniques that could be used in the hazardous waste disposal, chemicals, and petroleum industries. Joe Santoro, marketing manager of Westinghouse's nuclear technology division, says the services identify potential hazards, analyze their consequences and risks, and make recommendations based on the evaluations. He adds that even mini-computers and personal computers can be programmed to analyze faults, failures, consequences, and safety and financial risks.

Regulating cancer risks

Paolo F. Ricci

*Electric Power Research Institute
Palo Alto, Calif. 94303*

Lawrence S. Molton

*3172 Middlefield Road
Palo Alto, Calif. 94306*

There is much debate on how to regulate chemical carcinogens (1, 2). Regu-

lation must reflect the desire to reduce the incidence of cancer and to ease the large uncertainty about its causation. If the magnitude of the response that results from exposure to carcinogens could be measured accurately using dose-response functions, then for selected levels of risk the associated dose could be determined.

Although this is a simple task, it is confounded by an important uncertainty: the biological mechanism of cancer. This uncertainty, particularly at low environmental doses, in turn creates uncertainty in cancer policies.

Legislation ordinarily must contain broad language, and policy must attempt to provide answers when science



cannot. We approach the regulation of cancer by reviewing the mechanisms of cancer induction, their relationship to dose-response functions, and the epidemiologic and animal studies used to estimate the coefficients of those functions. These factors form the basis of cancer regulatory policy.

Cancer processes

The simplified process of cancer induction can be thought of as initiation, promotion, and progression (3). Initiation consists of an irreversible lesion in the DNA that can lead to a cancer if further attack on the DNA occurs. Promotion is a biochemical process that can accelerate the progression of an initiated cell to cancer. But if a promoter attacks a "normal" (uninitiated) cell, the damage is thought to be reversible. What governs these steps and the eventual progression to a tumor or cancer is not clear.

Recent work on the actual mechanism of cancer has examined certain fragments of DNA—the oncogenes, both cellular and viral (4). It is widely believed that cellular oncogenes are necessary to the initiation of cancer and that they can be activated by lesions to the DNA. In the case of human bladder cancer, the lesion is the smallest that can occur in DNA: It is the substitution of a single base for another. The gene thus affected will code for an inappropriate amino acid, changing the structure of a protein and leading to a cancerous cell. This has been observed for

the *ras* oncogene (5).

There are other mechanisms for cancer induction. For instance, in the case of Burkitt's lymphoma, the oncogene *myc* is activated by a break in a chromosome and by the insertion of the oncogene in a different chromosome. This disturbs the normal temporal expression of genes and thus the mitosis of the cell. In both of these examples, the attack on the DNA can occur through exposure to chemicals or other agents such as viruses. In a study of normal cells from a rat embryo, the two oncogenes were found to affect the cancer process if they acted in concert; however, each alone would not be able to convert a healthy cell into a tumorigenic one (6). Current work is examining the role of genes and oncogenes in different biological units, to explain not only the tumor process but the cancer process as well (7-9). Genetic carcinogens attack the DNA, whereas epigenetic agents such as hormones or asbestos involve other cellular controls and do not attack the DNA itself.

Cancer can be caused by the "hit" of a toxicant on a DNA molecule in the target organ; a hit may be a point mutation. The resulting change may or may not be reversible. Reversibility can mean that the resulting carcinogen-DNA complex (known as an adduct) is removed from the DNA molecule as new, unaffected DNA comes into being through the excision-repair process. If a DNA adduct forms and is retained it is likely to dramatically alter cellular

control, initiating the cancer process. However, adduct formation is an index of exposure but not necessarily of initiation; continued attack on the DNA does not mean that a cancer necessarily must develop.

Some chemicals are transformed into carcinogens through human metabolism. For example, benzo[*a*]pyrene must be metabolized to an epoxide, which then reacts with DNA in the cell to induce cancer. Other chemicals, such as bis(chloromethyl) ether, do not appear to need metabolic conversion to be reactive. Chemical carcinogens also can interact with one another. For example, asbestos and smoking appear to act synergistically; azo-dye and 3-methylcholanthrene act antagonistically (10, 11).

The chemical kinetics of a carcinogen describe the relationship that exists between external dose (exposure) and the metabolized dose (12). Unfortunately, kinetic rates often are unavailable for many of the chemicals that are of interest to risk assessors; exposure data are used instead.

One well-known example of the difficulties in describing the cancer process is summarized by Cairns (9). Individuals with defective DNA repair mechanisms have a sharply higher incidence of a specific skin cancer (xeroderma pigmentosum) than do normal individuals. Although the repair mechanism is affected in all tissues that have been tested, these persons do not experience an increase in cancers at other

TABLE 1
Dose-response formulas in risk assessment of carcinogens

Formula ^a	Discussion of parameters	Remarks ^b
$p(D) = 1 - \exp(-kD)$	$k > 0$. The proportion unaffected is $\exp(-kD)$. The reaction rate is first order in the concentration of the pollutant. The exposure rate is constant, over some period of time t , that is, $p(D) = 1 - \exp(-\alpha t D)$; $\alpha \geq 0$.	Single-hit model; a single hit causes irreversible damage to DNA, leading to tumor development. At low doses the function is linear; once the biological target is hit, the process leading to tumor continues independently of dose.
$p(D) = 1/\Gamma(k) \int_0^D u^{k-1} e^{-u} du$	Γ is the gamma function; for k integer $\Gamma = k!$ Where $k=1$, $P(D) = 1 - \exp(-kD)$. When $k > 1$ (2) is convex; $k < 1$ (2) is concave. At low doses $p(D) \approx (\lambda D)^k / \Gamma(k)$.	Gamma multihit model; k shows the sensitivity of the biological unit to insult, i.e., the number of hits required for irreversible damage.
$p(D, t) = 1 - \exp(-g(D)h(t))$	$g(D) = \sum_{i=1}^k (\alpha_i + \beta_i D)$; t is time. ^c $\alpha_i > 0$ and $\beta_i > 0$; $h(t) = \int_0^t f(t-u)u^{k-1} du$, where $f(t)$ is the density of time for cancer induction.	This is the multistage model. ^d The incidence of a tumor, given dose D , at age t , requires k stages before the tumor is initiated in a single line of cells. $h(t)$, in the nonparametric multistage function, is an arbitrary increasing function.

^a $p(D)$ is the proportion affected; D is the dose per unit time. In dose-response modeling at low doses, there are two hypotheses: That the same mechanism that causes cancer at high doses also operates at low doses (the dependence hypothesis) or that two different mechanisms exist. In the former case, the doses are additive; in the latter, the probabilities are multiplicative.

^bFor dose-response functions applicable to radiation carcinogenesis see Reference 15.

^cThis equation includes time-to-tumor; the others do not.

^dPeto discusses the meaning of stage: "What is a 'stage'? If, after one change, a cell is likely to suffer another change in the near future, they would not both count as stages. Stages have to be slow and improbable. . . . A rough general rule is that if a change is not likely to have happened within 10 years of a cell being ready for it, then it would count as a stage, but if it is likely to take less than a year it would not. (For example, the process of DNA damage and faulty repair would only comprise one stage, not two.)" (16)

sites. A better understanding of DNA repair and other protective mechanisms might resolve the question of whether thresholds exist.

The existence of a threshold for cancer is a point of contention among risk assessors. Whether a threshold exists, or is assumed to exist, can affect cancer risk estimates at low doses. The argument against a threshold assumes that a single insult (hit) to the DNA—a point mutation—can lead to the uncontrolled growth of a somatic cell, eventually producing cancer. A probabilistic argu-

ment can be made that although an individual may have a threshold, different persons have different thresholds, and some persons may have none.

The arguments for a threshold are based on the existence of gene repair mechanisms, immune defenses, and the epigenetic mechanism. As Weisburger and Williams note, the effect of epigenetic carcinogens may be reversible (13). Nevertheless, when the single cell is the unit at risk, if initiation is a threshold phenomenon and there is a random distribution of cell thresholds

(in dose), then “low dose response on the whole tissue over background will be approximately linear” (14). However, linearity at low doses may lead to such concepts as a practical threshold.

Quantitative cancer risk assessment relies on dose-response functions to establish the likelihood that cancer can occur in individuals exposed to low doses of chemicals. The process of cancer provides biologically plausible bases for some of the functions. Several dose-response functions are summarized in Table 1. Quantal functions describe whether the adverse effect is present or not. Time-to-response functions account for the differences in longevity among exposed individuals. Such models as the one-hit, the probit, the logit, the multihit, and the multistage do not explicitly model those dependencies. Figure 1 illustrates the application of several models to one set of data.

The one-hit model assumes that a single hit causes irreversible damage to DNA and leads to cancer. In the multistage model, a cell line must pass through k stages before a tumor is irreversibly initiated. The rate at which cell lines pass through one or more of the stages is a function of the dose rate. In the multihit model, k dose-related hits to the sensitive tissue are required to initiate a cancer. The more reasonable assumption—that these hits must occur in a single cell line and that different cell lines compete independently in producing a tumor—results in the Weibull model.

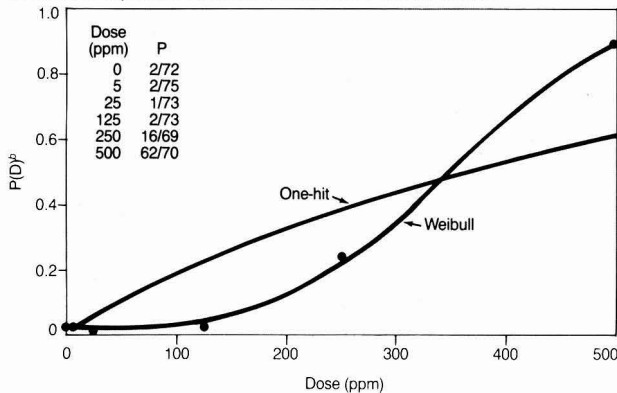
In all of these models it is assumed that the rate at which dose-related hits occur is a linear function of the dose rate. The most important difference between the multistage and the Weibull and multihit models is that in the Weibull and multihit models all hits must result from the dose, whereas in the multistage model passage through some of the stages can occur spontaneously. The practical implication of this is that the Weibull and multihit models are generally much flatter at low doses and consequently predict a lower risk than the multistage model.

The quantal multistage model is the generalization of the multistage model that has been applied frequently by regulatory agencies. The multiplicative hazard model of Hartley and Sielken accounts for the ages of the exposed individuals but is similar in form to the quantal multistage model (17).

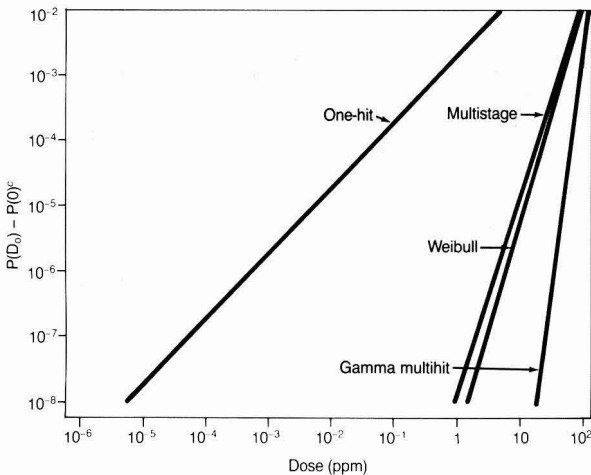
The remaining models—probit and logistic—are not derived from mechanistic assumptions about the cancer process. They may be thought of as representing distributions of tolerances to the carcinogenic insult in a large population. However, there is no evi-

FIGURE 1. Models for assessment of risk from ethylene thiourea^a

(a) The fit to experimental data for the one-hit and Weibull models



(b) Extrapolations to the low-dose region for the one-hit, multistage, Weibull, and multihit functions. The multistage, Weibull, and multihit functions have an acceptable goodness of fit within the data; the one-hit does not



^aEthylene thiourea causes thyroid carcinomas in rats

^bP is the proportion of animals with carcinomas. D is the dose

^cP(D_a) - P(0) is the additional risk due to an added dose. D_a, in ppm, in the diet

Source: Food Safety Council. "Proposed Systems for Food Safety Assessment". Washington, D. C., 1980.

dence to support these particular distributions over others. In fact, all models, including those discussed above, may be interpreted as tolerance distributions.

Krewski et al. compare time-to-response functions with quantal models and find that when the multistage Weibull is compared with the multistage, the time-to-response information "... will not result in estimates of risk in the low dose region that are substantially more precise than those based on quantal data ..." (18). These authors examine the multistage Weibull, the multistage (nonparametric) and the Hartley-Sielken time-to-response functions. They also discuss the probit, Weibull, multistage, and linear-quadratic quantal functions. Their findings indicate that the three time-to-tumor models yield "point estimates of risk in the low dose region [that] were highly variable, with the actual risk at the [Virtually Safe Dose] often being a factor of 1000 or more greater than the target risk of 10^{-5} ..." Moreover, the difference in results between quantal and time-to-response models is variable. Others have concluded that for the risks estimated at low doses, a comparison of dose-response functions using 19 data sets in which these functions were convex showed that the "log normal < (log logistic, multihit) < multistage < single hit" (19).

Table 2 shows an example from Whittemore of different estimates re-

TABLE 2
Variability of risk estimates^a

Dose-response function	Nasal sinus cavity tumors per 10 ³ mice exposed
Multihit	395
Probit	551
Multistage	1

^aData from tests in which male mice and female rats inhaled EDB in concentrations from 10 ppm to 40 ppm (the OSHA standard is 20 ppm) indicate the substance is carcinogenic in those animals, although EDB was not determined carcinogenic in occupational studies. The California Occupational Safety and Health Administration proposed regulation of EDB by establishing an ambient air level at 0.015 ppm. This required extrapolation from the available data to 0.015 ppm (20)

sulting from three well-known dose-response functions: multihit, probit, and multistage (20). We now turn to the data used to estimate the coefficients of dose-response functions.

Epidemiology

Epidemiology can describe the circumstances under which a disease occurs within and between population groups. It can be used to discover an association between exposure to a chemical and the occurrence of cancer. Positive results from epidemiologic studies provide direct evidence of disease from human exposure. However,

epidemiologic results do not normally provide detailed biological information. In Table 3 the principal types of epidemiologic studies are described. The incidence rate is a good measure for studying diseases that have long periods of latency between exposure and the manifestation of the disease. The disease-specific mortality rate generally provides a good approximation of the incidence rate, particularly for cancer and other diseases that often are fatal within a relatively short time.

Interpretation of epidemiologic results can be affected by a sample's lack of representativeness, uncertainty about the actual exposure, extraneous or omitted factors, and poor records or diagnosis (22). The International Agency for Research on Cancer has determined that epidemiologic studies associate exposure to 36 substances—in addition to smoking, exposure to radiation, and consumption of alcohol—with various cancers.

Animal studies

Animal test data must be modified by an interspecies factor that relates carcinogenic potency in animals to cancer in humans. There are several ways to account for metabolic differences between species, including mg/m² body surface/day and mg/kg body weight lifetime (23-25). The correct choice is uncertain because these conversions are rough approximations of actual metabolic pathways (26, 27). EPA suggests

TABLE 3
Epidemiologic methods in risk assessment

Studies

Type	Unit of analysis	Disease measure	Remarks
Ecological correlations (spatial or temporal)	Groups of individuals	Prevalence, incidence, or mortality rates	Helpful in developing hypotheses between exposure and effect.
Cross sectional	Single individuals	Prevalence rates	Useful in the study of diseases with latency or that vary with time.
Case control	Single individuals	Proportion of cases to controls	Useful in forming and establishing etiological hypotheses. Exposure is difficult to establish; controls can be doubtful; cases may be unrepresentative.
Cohort (retrospective or prospective)	Groups with and without exposure are followed over time.	Incidence rate; frequency of disease in exposed to frequency in the unexposed ^a	Appropriate for testing causal hypotheses. Diseases are determined from initial development. Confounding can be avoided and rare diseases accounted for.

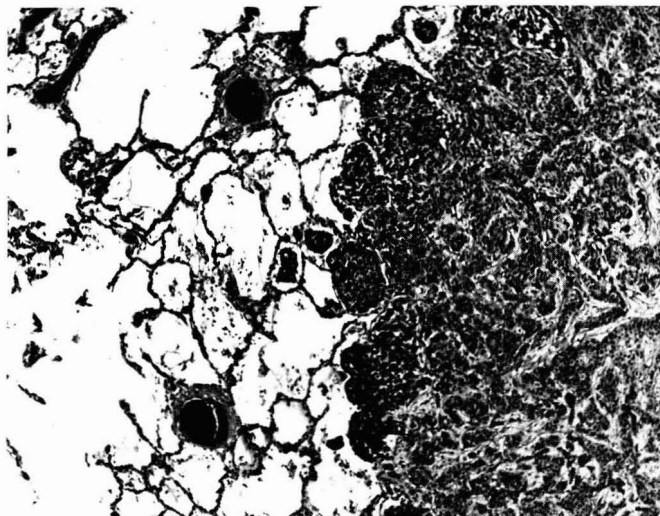
Disease measures

Rate ^b	Comment
Prevalence = (Cases in a specific population) _t ÷ (Population) _t	Measured at time t.
Incidence = (Nc.w cases in a specific population) _{Δt} ÷ (Population) _{Δt}	Measured over a period of time (Δt).
Mortality = (Total deaths in a specific population) _{Δt} ÷ (Unit of population) _{Δt}	Measured over a period of time (Δt).

^aCommonly used measure of excess risk is the "relative risk," which is defined as the ratio of observed cancers to expected cancers

^bFor a specific disease, alternative specifications of the denominator are feasible, as are adjustments for age (specificity and standardization), sex, race, and socioeconomic characteristics

Source: References 21 and 22



Healthy lung tissue (left) is invaded by cancer cells (right)

that without information on the process of cancer, the appropriate conversion is body weight to the 0.67 power (28).

The National Cancer Institute (NCI) uses benign and malignant tumors as end points in its rodent bioassays, although not all agencies do so. Generally, experiments involve two species (rats and mice) and examine the results for a no-exposure group and three dose levels (the maximum tolerated dose and two fractions of it). Fifty males and 50 females of each species are exposed at each dose level. The animals are sacrificed and examined externally and histopathologically.

The NCI National Toxicological Program bioassays of 190 chemicals found that 98 tested positive either in one or in both species, 44 were positive in both species, and 54 were positive either in rats or mice but not in both (29). IARC reviewed animal studies of 362 substances. It determined that those studies are sufficient to indicate that 121 substances are carcinogens. It reported that although additional data would be needed, the evidence was limited but strong that another 100 chemicals were carcinogens. Insufficient information exists for the remaining chemicals (29).

Animal bioassays normally are conducted with a small number of animals and thus suffer from small-sample bias. The interpretation of results often is difficult because some animal species may yield positive results with a chemical, whereas others do not.

Although this paper focuses on quantitative risk assessment, there are qualitative, short-term tests that often are relevant to quantitative assessments. Most of these are based on the assumption that mutagens will prove to be

carcinogenic. There are tests to detect mutations of genes, alterations to chromosomes, repair or lesions of DNA, and transformations of cells. For example, the Ames test detects a reverse mutation in a strain of a bacterium (30). Chromosomal alterations, such as translocations, have been associated with certain cancers, including Burkitt's lymphoma and chronic myelocytic leukemia. Those tests that look at DNA damage or repair can yield information on atypical synthesis of DNA (31). Finally, alteration to the morphology of certain cells has been studied by injecting these cells into live animals, thus causing tumors (32, 33).

Short-term tests also have been used to study tumor processes and to discriminate, to some extent, between those chemicals that affect DNA and those that do not appear to do so. Although most of these tests have been directed toward chemicals that affect DNA, some have attempted to detect promoters. Their low cost and the rapidity with which end points can be determined have made them desirable additions to the regulatory arsenal.

Evaluating data

Many federal agencies attempt to decide whether a given chemical is a carcinogen based on interpretation of the combined animal and human evidence. The results often are grouped—for the sake of comparison—into categories. Because agencies have limited resources, these rankings will decide which substances actually will be regulated. For example, EPA's current proposed regulations put chemicals into one of five categories: A, carcinogen; B, probable carcinogen; C, possible

carcinogen; D, inadequate evidence; and E, no evidence (28). If a chemical is in group E, the substance is considered not carcinogenic, based on evidence from human and animal studies or from animal studies of at least two species. When assigning potential carcinogens to a category, EPA gives the most weight to human studies, then to animal studies, and then to short-term tests.

Cancer policy

The first part of this review examined the basis for obtaining measures of health risk. We now consider how risk is regulated and how the law seeks to define the minimum safe level of exposure to toxicants. Our focus is on federal regulatory statutes, but we also must note that indirect methods of regulation exist as well. These include education efforts, taxation of alcohol and cigarettes, and strict liability for handlers of hazardous substances such as plutonium.

Federal regulation of health risk is widespread and varied in its approach; nearly 30 statutes affect exposure to carcinogens. Through agency interpretation and case law, policies have been created out of the vague language of sweeping statutes. The next sections present the alternative paradigms used to regulate risk.

There is no consistent guideline for the acceptability of carcinogen exposure, and laws enacted over the past 30 years reflect diverse regulatory philosophies. There are three reasons for this. First, our biological understanding of carcinogenesis and our ability to detect minuscule amounts of a substance and to observe its effects have improved dramatically. Next, our view as a society of how much of what risk is appropriate also has changed: Concern over cancer exploded in the 1960s; concern over maintaining our economic position and rate of innovation has increased during the past decade. Third, regulatory statutes originate with different committees in Congress, each responsive to the needs of diverse interest groups. All of these forces have been significant.

Prohibit exposure

The first paradigm for regulating risk is also the simplest approach: the prohibition of any exposure to a given carcinogen. Preventing exposure is preferred to any possible benefits the carcinogen might provide. The sections of the Clean Air Act (CAA) that require the establishment of primary air quality standards and emission limits for toxic pollutants are described as zero risk because they require the standard to be solely a function of health risk (34).

However, they do not eliminate emissions, so this is not really zero-risk legislation.

True mandates for zero risk appear in state laws that prohibit the transport and storage of nuclear waste and, most prominently, in the Delaney Clause of the Federal Food, Drug and Cosmetic Act. The Delaney Clause first appeared in the Food Additives Amendment of 1958 and the Color Additives Amendment of 1960. It states: "No additive shall be deemed to be safe if it is found to induce cancer when ingested by man or animal" (35).

This clause has been the subject of heated debate since the 1960s. It forces the hand of the Food and Drug Administration (FDA) no matter how overwhelming the benefits of a substance or how low the hazard estimated by a risk assessment. FDA usually has avoided using Delaney, but two battles of the 1970s illustrate its problems.

Animal studies on saccharin led FDA to announce in March 1977 that it intended to ban the sweetener. Faced with strong public pressure and evidence of a group for whom saccharin was medically recommended, Congress passed a law that November prohibiting FDA from taking action. The statute is still in force. In 1978, FDA formally received data showing that nitrites, which are added to smoked meats to prevent the growth of *Clostridium botulinum*, cause lymphomas in rats. After two years of study, FDA concluded that the rat data showed that nitrites did not induce cancer. The existence of serious methodological issues concerning diseased animals, nonrandomized subjects, and tumor classification gave the FDA an escape hatch. Had the evidence been less flawed, there would have been no legal alternative to a nitrite ban (36).

Quantify risk

If the expected lifetime risk is below a given level, the substance can remain in use. Examples include animal drugs and indirect food additives. This paradigm is based on FDA interpretation of the "DES proviso" to the Delaney Clause, first enacted in 1962. To allow new applications for the use of diethylstilbestrol (DES) as a growth promoter in cattle feed—a practice used in 90% of U.S. cattle at the time—the law was changed to permit carcinogenic animal drugs if "no residue of such drug will be found . . . in any edible portion of such animals." After a long battle, FDA banned DES in animal feed in 1979, based on a theory that "no residue" meant a residue that created no significant risk to human consumers (37).

During the 1960s and 1970s, the in-

troduction of the gas and liquid chromatography and radiotracer techniques enabled FDA to detect residues at levels as much as five orders of magnitude below previous capabilities. This made use of carcinogenic additives under any conditions practically impossible. Hence, FDA established a significant level of lifetime cancer risk of 10^{-6} . Using the linear no-threshold model, FDA determined what dose corresponded to this level of risk. Once FDA shows that a drug is carcinogenic, the burden shifts to the manufacturer to prove that the risk is insignificant. This is a nearly impossible burden, given the very cautious assumptions FDA uses.

Indirect food additives—those not intended to become part of the food—are now regulated similarly. Acrylonitrile copolymer, a substance used in beverage containers, migrates into beverages in trace amounts. Despite methods that reduced this migration substantially, FDA argued for a ban on acrylonitrile. In 1979, a court overturned the ban, finding that *de minimis* (very small) risks could be ignored (38). The court found that the additive must migrate in "more than insignificant" amounts to be recognized. Although quantification is not always required, this judicial view reflects an intuition that some risks are just too minor. More recently, FDA has given approval to hair dyes that pose a minimal risk even though the essential ingredient, lead acetate, is a carcinogen.

Comparative risk

A third paradigm is the risk-to-risk approach, where the health risk of not using a substance is compared with the risk of using it (39). This was applied in the decision to use chloroform, a potential carcinogen, to kill bacteria in drinking water. It also could have been used for evaluating nitrites or any other substance that attacks one risk by creating another. However, it is seldom used in the environmental area; its largest application is in the approval of new prescription drugs.

A matter of balance

The fourth paradigm is the "balancing" approach, in which an agency weighs the positive and negative effects of regulation to decide whether control is justified. The positive side is the reduction in health risk. This often is difficult to evaluate, owing to the substantial uncertainty in the number of cancers expected at both existing and proposed exposure levels. Because food, pesticides, and household products are not used uniformly, dose and response are difficult to measure. The negative side, costs, includes direct financial expenditure to reduce emis-

sions, reductions in employment or profitability, reductions in availability of a desirable product, and the expense of the regulatory process itself. The relative weight given to these factors varies among agencies and cases.

One balancing method is benefit-cost analysis; it compares the net present value of alternatives—including no regulation at all—and selects the one with the highest net benefits. Because all factors must be comparable on one scale, health benefits, such as the number of fewer cancers, must be quantified.

A recent example is provided by CAA. In August 1984, EPA proposed regulations to reduce the amount of lead in gasoline, and thus in the air, by 91% (40). This was supported by a full benefit-cost analysis showing \$1.374 billion in benefits and \$468 million in costs. Formal analysis of this type is rarely required by statute. CAA mandates it for comparison of auto emission control systems, but it does not appear in any of the broad statutes. Executive Order 12291 (Feb. 17, 1981), however, does require benefit-cost studies before agency decisions are made.

A less formal but similar approach is used in a few areas. The Consumer Product Safety Commission regulates hazardous products, including carcinogens, under the Federal Hazardous Substances Act and the Consumer Product Safety Act, which allow the commission to ban a product if it poses an unreasonable risk of injury or illness. This has been held to require a balancing of health benefits and economic costs. The formula used is borrowed from tort law. The burden of regulation on the price, availability, and utility of the product is compared with the probability of harm multiplied by the gravity of harm. If (probability \times gravity) predominates, regulation is appropriate (41).

Two other statutes, the Federal Insecticide, Fungicide and Rodenticide Act and the Toxic Substances Control Act, also contain language on unreasonable risk. These approaches weigh a health risk, such as $x\%$ rise in the incidence of leukemia, against dollars, jobs, and intangible benefits. They do not require that all factors be converted to a common unit (dollars, for example) for comparison.

The next approach also requires a balancing of benefit and cost. In contrast to the previous approach, cessation of exposure is not an option. When setting new source performance standards under CAA, EPA requires the best available technology, taking into consideration costs and energy requirements. FDA takes a similar approach in the regulation of unavoidable contami-

nants in food, such as contamination of food by PCBs and PBBs, which are synthetic, and the existence of the natural carcinogen aflatoxin in peanuts and corn (42).

In each case, FDA performs a risk assessment that calculates average food consumption, number of cancers expected at various exposure levels, and the value of destroyed food. It then selects a tolerance level. Often the amount of food that would be destroyed rises sharply as the tolerance level approaches zero, although the risk declines linearly. The level selected must be high enough to permit effective detection of residues below that level. This sort of assessment is subjective, and critics have pointed to the arbitrariness of agency conclusions. In contrast to the case with drugs or pesticides, however, no one is trying to sell these substances. Because there is little if any data on their adverse effects, FDA must rely on poorer evidence to set tolerances at some level as required by law.

Another balancing approach takes the economic costs into account but assigns them less weight than the health risks. Under the Clean Water Act provision for Phase I effluent standards, the total cost—including loss of jobs—must be considered, but the standard will be imposed unless the cost is “wholly out of proportion” to the benefit (43). Standards for nonattainment areas under the CAA require that cost be taken into account but be given less weight than under the new source performance standards.

The final balancing approach is that used by the Occupational Safety and Health Act. It requires that workplace exposure standards ensure “to the extent feasible” that no employee suffers material impairment of health. Costs play only a minor role. The Supreme Court has defined feasible as “capable of being done” and interpreted economic feasibility to include any cost short of destroying the profitability of an industry, including even the bankruptcy of individual firms (44).

Uncertainties remain

It cannot be proved that a given balancing process has reached a correct conclusion. There is much debate over such issues as which factors should be quantified, how to incorporate voluntariness of the risk, and how to maximize consumer choice. Scientists and policy makers alike must grapple with the inherent uncertainty of risk assessment; each group depends on the other.

Scientific choices about the appropriateness of test conditions and the nature of cancer are policy statements. They are not purely scientific decisions because they rest on unprovable assump-

tions. Legal decisions that define phrases such as “induce cancer” or “significant risk” must have scientific rationality behind their pronouncements. In the past decade, legal institutions have done a better job of reflecting current scientific thought (45). The continued meshing of scientific and legal approaches is necessary to sound risk assessment.

Acknowledgment

We acknowledge the extensive comments by Bob Golden, Paul Chrostowski, Steven Colome, Cary Young, and several anonymous reviewers. We thank Kenny S. Crump for his contribution to our understanding of the differences among dose-response functions. The views expressed in this article are the authors' and do not necessarily reflect those of EPRI.

Before publication, this article was reviewed for suitability as an *ES&T* feature by Richard L. Perrine, University of California, Los Angeles, Calif. 90024 and M. Granger Morgan, Carnegie-Mellon University, Pittsburgh, Pa. 15213.

References

- (1) Doll, R.; Peto, R. *J. Nat. Cancer Inst.* **1981**, *66*, 1191.
- (2) Epstein, S. S.; Swartz, J. B. *Nature* **1981**, *289*, 127-30.
- (3) Farber, E. *N. Engl. J. Med.* **1981**, *305*, 1379.
- (4) Slamon, D. J. et al. *Science* **1984**, *224*, 256.
- (5) Roberts, L. “Cancer Today: Origins, Prevention and Treatment”; National Academy Press: Washington, D.C., 1984.
- (6) Weinberg, R. A. *Technol. Rev.* **1983**, *53*, 47-55.
- (7) D'Eustachio, P. *Am. Sci.* **1984**, *72*, 32.
- (8) Land, H.; Pareda, L. F.; Weinberg, R. A. *Science* **1983**, *222*, 771.
- (9) Cairns, J. *Nature* **1981**, *289*, 353.
- (10) Miller, E. C.; Miller, J. A.; Brown, R. R. *Cancer Res.* **1952**, *12*, 282.
- (11) Conney, A. J.; Miller, E. C.; Miller, J. A. *Cancer Res.* **1956**, *16*, 450.
- (12) Cornfield, J. *Science* **1977**, *198*, 693.
- (13) Weisburger, J. H.; Williams, G. M. *Environ. Health Perspect.* **1983**, *50*, 233.
- (14) Office of Science and Technology Policy. “Chemical Carcinogens; Notice of Review of the Science and Its Associated Principles”; *Fed. Regist.* **1984**, *49*, 21594.
- (15) Land, C. *Science* **1980**, *209*, 1197.
- (16) Peto, R. In “Origins of Human Cancer,” Vol. 4; Kiah, H. H.; Watson, J. D.; Winston, J. A., Eds.; Cold Spring Harbor Laboratory: Cold Spring Harbor, N.Y., 1977; p. 1403.
- (17) Hartley, H. O.; Sielken, R. L. *Biometrics* **1977**, *33*, 1.
- (18) Krewski, D. et al. *Fund. Appl. Toxicol.* **1983**, *3*, 140.
- (19) Brown, C. C.; Koziol, J. A. *SIAM Rev.* **1983**, *25*, 151.
- (20) Whittemore, A. K. *Risk Analysis* **1983**, *3*, 23.
- (21) Kleinbaum, D. G.; Kupper, L. L.; Morgenstern, H. “Epidemiologic Research: Principles and Quantitative Methods”; Lifetime Learning Publications: Belmont, Calif., 1982.
- (22) MacMahon, B.; Pugh, T. F. “Epidemiology: Principles and Methods”; Little, Brown: Boston, Mass., 1970.
- (23) Crouch, E.; Wilson, R. J. *Toxicol. Environ. Health* **1979**, *5*, 1095.
- (24) Freireich, E. J. et al. *Cancer Chemother. Rep.* **1966**, *50*, 219.
- (25) Du Mouchel, W. H.; Harris, J. E. *J. Am. Stat. Assoc.* **1983**, *52*, 105.

- (26) Portier, C.; Hoel, D. J. *Toxicol. Environ. Health* **1983**, *12*, 1.
- (27) Hoel, D. G. *Environ. Health Perspect.* **1979**, *32*, 25.
- (28) U.S. EPA. “Proposed Guidelines for Carcinogenic Risk Assessment; Request for Comments”; *Fed. Regist.* **1984**, *49*, 46294-301.
- (29) Office of Technology Assessment. “Assessment of Technologies for Determining Cancer Risk from the Environment”; OTA: Washington, D.C., 1981.
- (30) Ames, B. N.; McCann, J.; Yamasaki, E. *Mutat. Res.* **1982**, *99*, 53.
- (31) Mitchell, A. D. et al. *Mutat. Res.* **1983**, *123*, 363.
- (32) Slaga, T. J. et al. *J. Am. Coll. Toxicol.* **1982**, *1*, 83.
- (33) Shimkin, M. B.; Stoner, G. D. *Adv. Cancer Res.* **1975**, *21*, 1.
- (34) Clean Air Act, 42 U.S.C. §7401 et seq. (P.L. 95-95).
- (35) The Delaney Clause appears in the Federal Food, Drug and Cosmetic Act of 1938 at 21 U.S.C. §348(c)(3)(A), 360b(d)(1)(H), and 376(b)(5)(B).
- (36) Marraro, C. H. In “Quantitative Risk Assessment in Regulation”; Lave, L. B., Ed.; Brookings Institution: Washington, D.C., 1982.
- (37) *Fed. Regist.* **1979**, *44*, 54851.
- (38) *Monsanto v. Kennedy*, 613 F.2d 947 (D.C. Cir. 1979).
- (39) Lave, L. In “The Strategy for Social Regulation: Decision Frameworks for Policy”; Lave, L., Ed.; Brookings Institution: Washington, D.C., 1981.
- (40) *Fed. Regist.* **1984**, *49*, 31032.
- (41) This calculus originated as “Learned Hand’s Algebra,” in the case of *U.S. v. Carroll Towing*, 159 F.2d 169 (2nd Cir. 1947).
- (42) Merrill, R. A.; Schewel, M. *University of Virginia Law Review* **1980**, *66*, 1357.
- (43) *EPA v. National Crushed Stone Association*, 449 U.S. 64 (1980).
- (44) Ricci, P. F.; Molton, L. *Science* **1981**, *214*, 1096.
- (45) Molton, L.; Ricci, P. F. In “Principles of Health Risk Assessment”; Ricci, P. F., Ed.; Prentice-Hall: Englewood Cliffs, N.J., 1984.

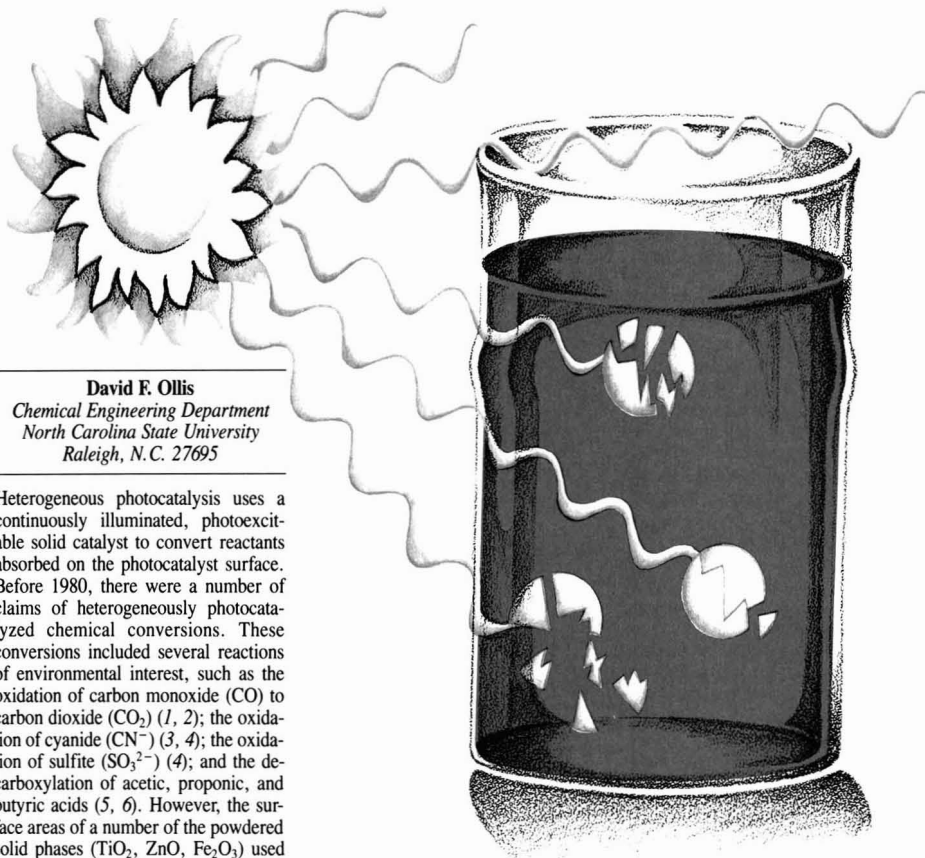


Paolo F. Ricci (l.) is a project manager of the Risk Assessment and Issue Analysis Program for the Energy Analysis and Environment Division of the Electric Power Research Institute in Palo Alto, Calif. He has a Ph.D. in environmental engineering and sciences and an M.S. in environmental health from Drexel University. He is the co-author of three books on risk assessment.

Lawrence S. Molton (r.) has an A.B. degree in political science from Stanford University and a J.D. from Stanford Law School. He is a member of the State Bar of California. He has worked for the Stanford Medical School's Division of Health Services Research and has served as a consultant to several research firms on issues of radiation exposure, groundwater management, and chemical carcinogen exposure.

Contaminant degradation in water

Heterogeneous photocatalysis degrades halogenated hydrocarbon contaminants



David F. Ollis
Chemical Engineering Department
North Carolina State University
Raleigh, N. C. 27695

Heterogeneous photocatalysis uses a continuously illuminated, photoexcitable solid catalyst to convert reactants absorbed on the photocatalyst surface. Before 1980, there were a number of claims of heterogeneously photocatalyzed chemical conversions. These conversions included several reactions of environmental interest, such as the oxidation of carbon monoxide (CO) to carbon dioxide (CO₂) (1, 2); the oxidation of cyanide (CN⁻) (3, 4); the oxidation of sulfite (SO₃²⁻) (4); and the decarboxylation of acetic, propionic, and butyric acids (5, 6). However, the surface areas of a number of the powdered solid phases (TiO₂, ZnO, Fe₂O₃) used in these studies left unanswered the question of whether the solids were functioning as photoactivated *reagents* or *catalysts*. A 1980 paper that summarized the previous results suggested that if conversion of more than 100 molecules per surface reaction site had been demonstrated—without changing the catalyst—then the observed process could reasonably be regarded as catalytic (7).

Photocatalyzed dehalogenations have been suggested previously in the literature. A report in 1976 noted the release of chloride ion upon illumination of a semiconductor oxide, titanium dioxide (TiO₂), in the presence of chlorinated

biphenyls (8). This intriguing result corresponded to the generation of only 10⁻³ monolayer equivalents of product on the solid surface, leaving open the photoreagent-vs.-photocatalyst question. Another paper reported disappearance of *p*-dichlorobenzene in water with illuminated TiO₂; again, chlorine mass balance and product identification were not reported (9).

Other processes mentioned include chloride transfer to ethane from carbon tetrachloride (CCl₄), fluorotrichloromethane (CFCl₃), and difluorodichloromethane (CF₂Cl₂) (10); and dechlorination of CF₂Cl₂ and CFCl₃ on illumi-

nated zinc oxide (ZnO) (11). The suggestion of dechlorination activity, and the general oxidation results for solutes led us to examine heterogeneous photocatalysis as a possible tool for water purification.

Photocatalytic dechlorination

The demonstration of catalysis and the measurement of reaction rates vs. reactant concentration are conveniently realized in a recirculating, differential conversion photoreactor (12). The quartz reactor wall allows entry of all near-UV light of 300 nm to <400 nm, which is generated by commercial

black-light fluorescent lamps. Wavelengths of < 360 nm are sufficient for TiO_2 photoexcitation (13).

In our reactor, a slurry of 0.1 wt% TiO_2 powder in water is continuously recirculated through the reactor, a temperature-controlled bath, and a vessel that holds chloride (or bromide) ion and reference electrodes for monitoring the progress of the reaction. The sample is injected through the septum of an orifice of the vessel. This system is used to study the degradation of chloromethanes and bromomethanes, chloroethanes, chloroethylenes and bromoethylenes, chlorobenzene, and chloroacetic acids in dilute aqueous solutions.

Mineralizations of chloromethane

During conventional water chlorination procedures, trichloromethane (CHCl_3) is the major chloroform produced from dissolved organic matter (14-16); it is a suspected carcinogen (17). When an aqueous solution of 122 ppm of chloroform is recirculated in the reactor, the data establish the photocatalyzed degradation of chloroform and the formation of chloride ion (Figure 1): With illumination and no catalyst (Region I), no trichloromethane conversion was noted, nor was any chloride ion detected in solution. With the lamp off, and 0.1 wt% TiO_2 catalyst in the recirculating system, no conversion was observed (Region II). The simultaneous presence of illumination and TiO_2 produced the chloride ion and caused the disappearance of chloroform (Region III) (18). Figure 1 demonstrates an absence of both homogeneous photochemical conversion (Region I) and heterogeneous catalysis (Region II); only the presence of a photoexcited catalyst (Region III) produces trichloromethane conversion.

With complete disappearance of trichloromethane to below a detection level of 1 ppm, the chlorine mass balances are demonstrated in three runs to be 100%, 102%, and 103% as chloride ion. Thus, no chlorinated hydrocarbon reactant or product remains; the chemical is degraded completely. Purging a reacted liquid with nitrogen gas and subsequently passing the purge stream through a saturated barium hydroxide solution produces a barium carbonate precipitate, which demonstrates complete oxidation of carbon to CO_2 (18). Separate experiments established a need for molecular oxygen, rather than water, as an oxidation source (19). Thus, an overall stoichiometry for complete photocatalyzed mineralization of chloroform to CO_2 and HCl can be written as follows:

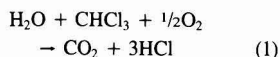
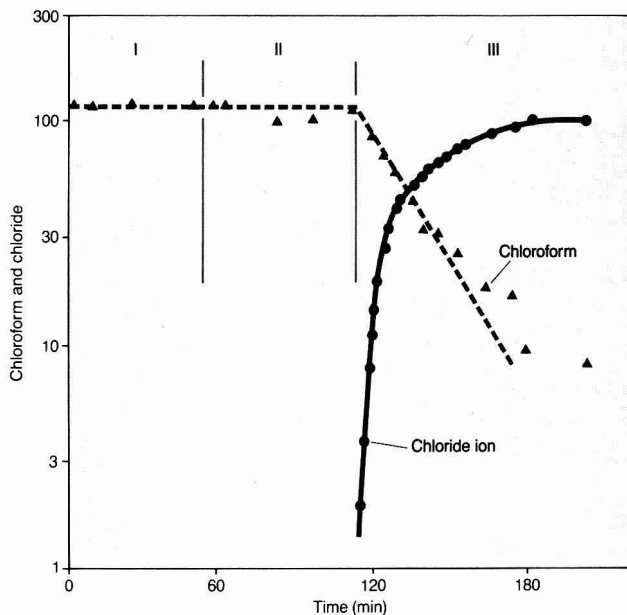


FIGURE 1
Photocatalyzed degradation of chloroform^a



^aInitial chloroform = 122 ppm; initial chloride = 2 ppm
Region I—illumination only; Region II—catalyst only; Region III—illumination plus catalyst

Subsequent study of dichloromethane and tetrachloromethane showed that these reactants also can be mineralized, that is, converted to CO_2 and HCl, but at a slower rate than that for CCl_4 (19).

Rate equations

For all 12 halogenated hydrocarbons examined, the initial rate of reaction vs. reactant concentration is satisfactorily shown by a Langmuirian surface with a slow surface reaction step. In this case, the rate of reaction is proportional to the coverage, θ_x , of the surface by an adsorbed intermediate, x:

$$\text{rate} = k \cdot \theta_x \quad (2)$$

where θ_x is given by a Langmuir isotherm:

$$\theta_x = \frac{K \cdot C}{1 + K \cdot C} \quad (3)$$

where C is the solution reactant concentration and K is the apparent binding constant of the intermediate on the illuminated catalyst. This rate form is validated if a plot of reciprocal rate vs. reciprocal initial concentration is linear, as shown in Equation 4:

$$\frac{1}{\text{rate}} = \frac{1}{k} + \frac{1}{kK} \cdot \frac{1}{C} \quad (4)$$

Such a plot for dichloromethane (Figure 2) is linear; a similar linear relationship was found for CFCl_3 and CCl_4 . From this result, the rate constant k and equilibrium constant K can be evaluated, as shown in Table 1.

Bromomethane conversions

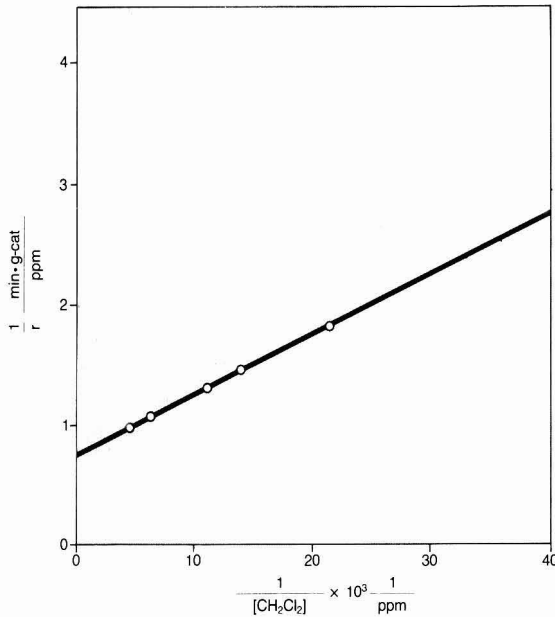
Trichloromethane is known to be convertible into chlorobromomethanes and, ultimately, tribromomethane in the presence of bromide ion. This reaction has been observed to occur in several rivers near populated areas. Dibromomethane and tribromomethane were easily and completely mineralized by heterogeneous photocatalysis to HBr and CO_2 . No intermediate was observed. The specific rate constant, k, and binding constant, K, are shown in Table 1 (20). The relative reactivities of halomethanes over near-UV illuminated TiO_2 are seen, from Table 1, by their respective rate constants, to be $\text{CHBr}_3 > \text{CHCl}_3 > \text{CH}_2\text{Br}_2 > \text{CH}_2\text{Cl}_2 \gg \text{CCl}_4$.

Chlorohydrocarbon degradation

Contamination of drinking water often is the result of one of two industrial solvents, trichloroethylene (TCE) and perchloroethylene (PCE) (21). Dichloroethanes have been found in drinking water (21, 22), as have chloroacetic acids (23). Complete photocatalyzed

FIGURE 2

Reciprocal initial rate vs. reciprocal initial concentration for dichloromethane (CH₂Cl₂)



Reprinted with permission from Reference 19. Copyright 1983, Academic Press

TABLE 1
Rate parameters from Equation 4 for halocarbon mineralization

Reactant	k ^a	K ^b
CH ₂ Cl ₂	1.6	0.02
CHCl ₃	4.4	0.003
CCl ₄	0.18	0.005
CH ₂ Br ₂	4.1	0.02
CHBr ₃	6.2	0.01
Cl ₂ C=CClH	830.0	0.01
Cl ₂ C=CCl ₂	6.8	0.02
H ₂ CICCClH ₂	1.1	0.01
CHBr ₂ CH ₃	3.9	0.02
CH ₂ BrCH ₂ Br	2.2	0.02
H ₂ CICCCOOH	5.5	0.002
HCl ₂ CCOOH	8.5	0.003
Cl ₃ CCOOH	~0	—

^appm/min-g (catalyst)

^bppm⁻¹

mineralizations of 1,2-dichloroethane, TCE, PCE, and mono- and dichloroacetic acids have been observed (24-26). However, trichloroacetic acid is unreactive.

Reciprocal rate vs. reciprocal concentration plots are linear for all of the reactants that are mineralized. Figure 3 presents data for 1,2-dichloroethane, two chloroacetic acids, and perchloroethylene. The corresponding rate constants and binding constants are pre-

Intermediates were noted in two instances. The conversion of TCE yielded an unstable intermediate identified by gas chromatography-mass spectrometry (GC/MS) as dichloroacetaldehyde. In turn, this intermediate completely decomposed to HCl and CO₂. Ultimately, approximately 100% of the chlorine was recovered as chloride ion (24). Degradation of 1,2-dichloroethane yielded trace vinyl chloride as an unstable intermediate that was rapidly degraded to HCl and CO₂ (26).

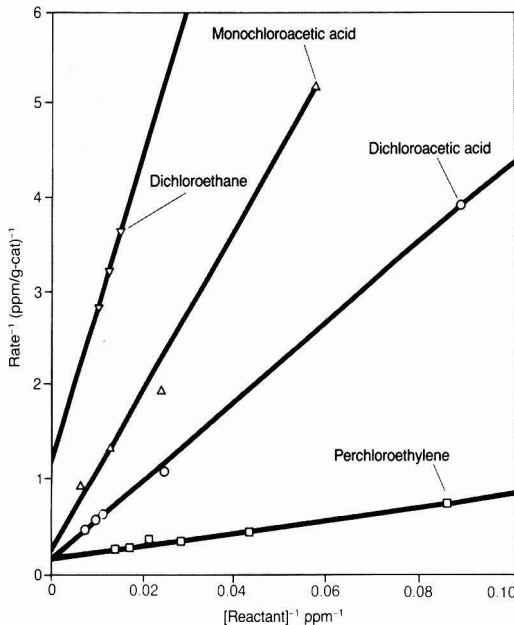
Ethylene dibromide

EDB (1,2-dibromoethane, or ethylene dibromide) has long been used as a scavenger for lead in gasoline, as a component of pesticides, and as a soil and crop fumigant. Recently, traces of EDB have been found in drinking-water wells in California and Florida (27). Because pesticide application was the suspected source of EDB contamination in water wells, the federal government has banned the use of EDB-containing pesticides.

Neither EDB nor its 1,1- isomer is converted by light or catalyst alone. In the presence of near-UV light and illuminated TiO₂, EDB dehalogenates rap-

FIGURE 3

Reciprocal rate vs. reciprocal reactant concentration

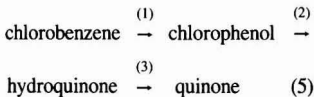


Reprinted with permission from Reference 25. Copyright 1984, Academic Press

idly and eventually mineralizes completely. Production and consumption of a trace organobromine intermediate have been observed (Figure 4). This unstable intermediate was identified as vinyl bromide by GC/MS. A 100% recovery of bromide ion was demonstrated when EDB and vinyl bromide levels became undetectable (28).

Chlorobenzene conversions

In contrast to the above results demonstrating complete mineralizations of a number of chlorinated alkanes and alkenes to CO₂ and HCl, the conversion of monochlorobenzene in dilute aqueous solutions produced no CO₂ (25). A characteristic result is shown in Figure 5. No degradation of the ring carbons was observed, and the results are presented as fractions of reactant and products found. The products formed correspond to the following sequence:



Step 1 is, and step 2 almost certainly is, photocatalyzed. The hydroquinone-to-quinone oxidation, step 3, has both a homogeneous photochemical and heterogeneous photocatalytic rate component.

Unusually long illumination times also produce trace amounts of condensed products such as 4,4'-dichloro-1,1'-biphenyl and 4,5'-dichloro-1,1'-biphenyl, which were identified using a GC/MS library. These products suggest a slow, homogeneous photochemical pathway, paralleling the heterogeneous photocatalysis results in Figure 5.

These data indicate that the photocatalytic treatment of chlorobenzenes produces a range of complex products. The products are relatively stable and include undesirable products, such as chlorophenols, that are easily tasted in water. However, a recent French report indicates that at higher dissolved oxygen levels, complete mineralization of chlorobenzenes is possible (29).

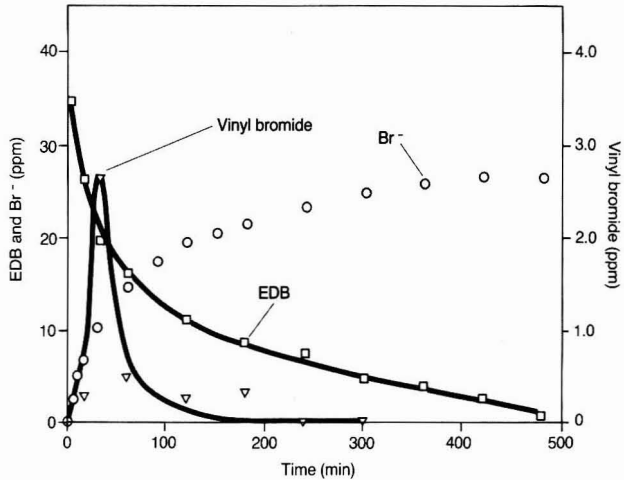
Reaction product inhibition

Characteristic products of these mineralization reactions are HCl and HBr. Each was established as a reaction inhibitor. On the other hand, CO₂ has been shown not to inhibit the rate of conversion. The competition by the inhibiting component for an adsorption site on a Langmuir surface leads to a modification of Equation 3:

$$\theta_x = \frac{KC}{1 + KC + K_1C_1} \quad (6)$$

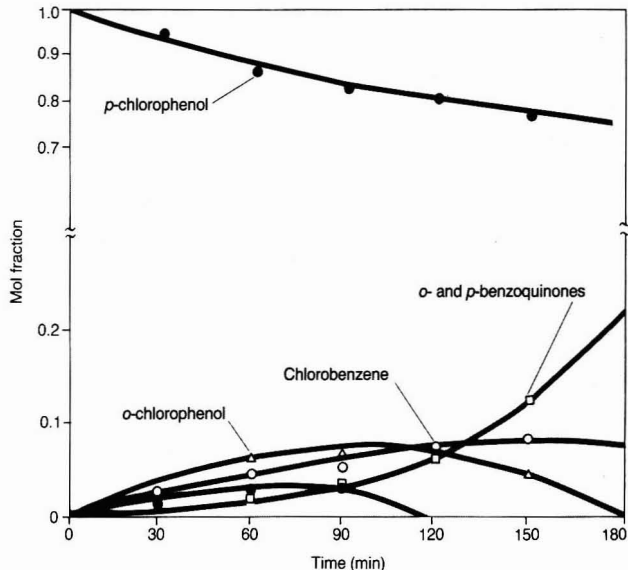
Substituting Equation 6 into Equation 2 results in a new reciprocal rate form,

FIGURE 4
Photocatalyzed degradation of EDB*



*EDB = 1,2-dibromomethane; Br⁻ = bromide ion
Reprinted with permission from Reference 28. Copyright 1984, American Chemical Society

FIGURE 5
Monochlorobenzene and single-ring products vs. time*



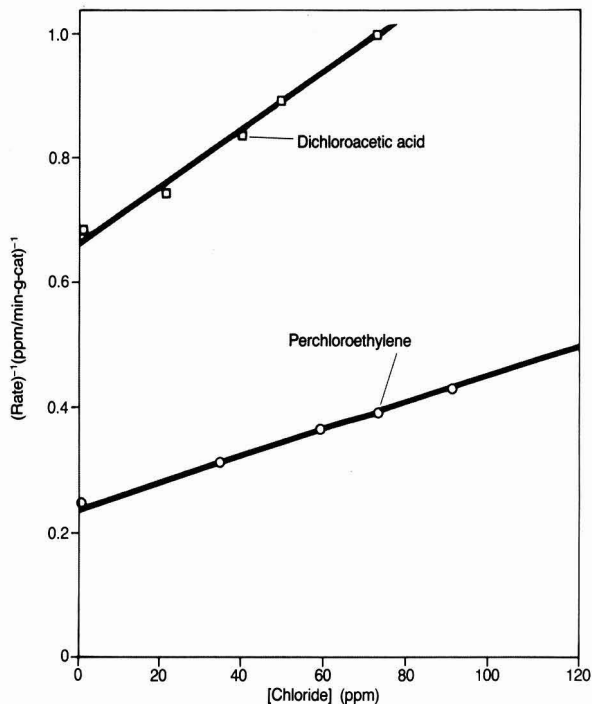
*Initial concentration 70 ppm
Reprinted with permission from Reference 25. Copyright 1984, Academic Press

which is linear in inhibitor concentration:

$$\frac{1}{r} = \frac{1}{k} \left[1 + \frac{1}{KC} + \frac{K_1}{KC} C_1 \right] \quad (7)$$

Figure 6 shows that HCl inhibition is adequately described by Equation 7 for conversions of perchloroethylene and dichloroacetic acid. Similarly, HBr inhibition is adequately described by Equation 7, up to a pH of 3.5 (18). For more acidic systems, a stronger inhibition becomes evident. These results

FIGURE 6
Inhibition by production of HCl*



*Inverse initial rate (ppm/min-g-cat)⁻¹ vs. initial chloride concentration (ppm). Initial reactant concentration = 67 ppm for dichloroacetic acid; 69 ppm for perchloroethylene
Reprinted with permission from Reference 25. Copyright 1984, Academic Press

suggest chloride ion (Cl⁻) or bromide ion (Br⁻) inhibition at neutral to slightly acidic pH values and a stronger inhibition by H⁺ at pH values near the pK_a of TiO₂ surfaces, that is, pH values from 3.5 to 4.5 (30).

Solar applications

The ground-level solar spectrum contains approximately 1% near-UV photons of sufficient energy to photoexcite the TiO₂ catalyst. The solar-driven, photocatalyzed decomposition of trichloromethane and trichloroethylene using TiO₂ catalysts has been demonstrated (31). An aqueous solution of 50 ppm halocarbon can be completely mineralized in two or three hours of illumination. An interesting result of this solar study was the finding that the reaction rate is nearly constant over much of the day, apparently indicating only a slight variation in near-UV illumination. The scattered solar "blue" flux varies only about 10% over this period (32).

Potential for purifying water

Drinking water standards typically concern halocarbon levels in the 1–50-

ppb range. At these low concentrations, the rate equation becomes pseudo-first-order, with an apparent first-order rate constant, k', a product of kK. In other words, rate ≈ kKC. The value of the parameters in Table 1 indicates that the order of ease of conversion is chloroolefins > chloroparaffins > chloroacetic acids. Thus, the common water contaminants, trichloroethylene and perchloroethylene, appear to be the strongest candidates for degradation by a potential photocatalytic process.

Acknowledgment

Before publication, this article was reviewed for suitability as an ES&T feature by Bruce E. Rittmann, Department of Civil Engineering, University of Illinois, Urbana, Ill. 61801 and R. Rhodes Trussell, James M. Montgomery Engineering, Pasadena, Calif. 91100.

References

- (1) Murphys, W. R.; Veerkamp, R. F.; Leland, T. W. *J. Catal.* **1976**, *43*, 304.
- (2) Julliet, F. et al. *Faraday Symp. Chem. Soc.* **1973**, *7*, 57.
- (3) Frank, S. W.; Bard, A. J. *Am. Chem. Soc.* **1977**, *99*, 303.
- (4) Frank, S. W.; Bard, A. J. *Phys. Chem.* **1977**, *81*, 1484.

- (5) Kraetler, B.; Bard, A. J. *J. Am. Chem. Soc.* **1978**, *100*, 2239.
- (6) Kraetler, B.; Bard, A. J. *J. Am. Chem. Soc.* **1978**, *100*, 5985.
- (7) Childs, L. P.; Ollis, D. F. *J. Catal.* **1980**, *66*, 383.
- (8) Corey, J. H.; Lawrence, J.; Tosine, H. M. *Bull. Environ. Contam. Toxicol.* **1976**, *16*, 697.
- (9) Oliver, B. G.; Cosgrove, E. G.; Carey, J. H. *Environ. Sci. Technol.* **1979**, *13*, 1075.
- (10) Ausloos, P.; Rebbert, R. F.; Glasgow, L. *J. Res. Nat. Bur. Stand.* **1977**, *82*, 1.
- (11) Filby, W. G.; Mintos, M.; Gusten, H. *Ber. Bunsenges. Phys. Chem.* **1981**, *85*, 189.
- (12) Childs, L. P. Ph.D. Dissertation, Princeton University, Princeton, N.J., 1981.
- (13) Herrman, J. M.; Pichat, P. *J. Chem. Soc. Eng. Trans.* **1980**, *176*, 1138.
- (14) Rook, J. *J. Water Treat. Exam.* **1974**, *23*, 234.
- (15) Bellar, T. A.; Lichtenberg, J. J.; Kroner, R. D. *J. Am. Water Works Assoc.* **1974**, *66*, 703.
- (16) Oliver, B. G.; Lawrence, J. *J. Am. Water Works Assoc.* **1979**, *71*, 161.
- (17) "Annual Report on Carcinogenesis Bioassay of Chloroform"; National Cancer Institute: Bethesda, Md., 1976.
- (18) Pruden, A. L.; Ollis, D. F. *Environ. Sci. Technol.* **1983**, *17*, 628.
- (19) Hsiao, C.-Y.; Lee, C.-L.; Ollis, D. F. *J. Catal.* **1983**, *82*, 418.
- (20) Nguyen, T.; Ollis, D. F., submitted for publication in *J. Catal.*
- (21) Brass, H. J. *J. Am. Water Works Assoc.* **1982**, *74*, 107.
- (22) Symons, J. M. et al. *J. Am. Water Works Assoc.* **1975**, *67*, 634.
- (23) Norwood, D. L. et al. *Environ. Sci. Technol.* **1980**, *14*, 187.
- (24) Pruden, A. L.; Ollis, D. F. *J. Catal.* **1983**, *82*, 404.
- (25) Ollis, D. F. et al. *J. Catal.* **1984**, *88*, 96.
- (26) Gauron, M. M.S. Thesis, University of California, Davis, Calif., 1983.
- (27) *Chem. Week*, Sept. 7, 1983, p. 13.
- (28) Nguyen, T.; Ollis, D. F. *J. Phys. Chem.* **1984**, *88*, 3386.
- (29) Barbeni, M. et al. *Nouv. J. Chim.* **1985**, *8*, 347.
- (30) Krylov, O. "Catalysis by Non-Metals"; Academic Press: New York, N.Y., 1972.
- (31) Ahmed, S.; Ollis, D. F. *Sol. Energy* **1984**, *32*, 1.
- (32) Meinel, A. B.; Meinel, M. P. "Applied Solar Energy"; Addison Wesley: Reading, Mass., 1976; p. 63.



David F. Ollis, distinguished professor of chemical engineering at North Carolina State University, has research interests in photocatalysis and biochemical engineering. Following his formal education in chemical engineering (B.S., Caltech, 1963; M.S., Northwestern, 1964; Ph.D., Stanford, 1969), Ollis taught for 11 years at Princeton and for four at the Davis campus of the University of California. His interest in photocatalysis was sparked by a sabbatical visit with Professors S. Teichner and J. E. Germain of the Université Claude Bernard, near the Beaujolais area of France.

Groundwater monitoring



Richard M. Dowd

Toxic and potentially toxic chemicals in groundwater continue to concern Congress, EPA, and the public. The House Investigations and Oversight Subcommittee recently released a survey of 1421 land disposal facilities' compliance with the 1981 Resource Conservation and Recovery Act (RCRA) groundwater monitoring requirements. Although most hazardous waste facilities had not been required to monitor groundwater quality until their permits were final, the 1984 RCRA amendments now require these and other new facilities to certify that they are in compliance by Nov. 8, 1985, or they will be required to close down. Of the 1246 facilities that were subject to groundwater monitoring requirements in the subcommittee's survey, only 40% were in compliance. Twenty-five percent had inadequate systems; 15% had no groundwater monitoring installations at all. An estimated 300 facilities may be contaminating groundwater resources. A separate General Accounting Office audit of 58 commercial facilities (some of which receive Superfund wastes) found 16 facilities currently out of compliance; five were reportedly leaking their contents.

EPA now estimates that about 50% of existing facilities will close or be closed rather than meet the November RCRA deadline. Case studies have been developed by EPA critics to illustrate the difficulties and counterproductive situations that have occurred as facility owners and operators attempt to com-

ply using rapidly developing monitoring technology and methods. To facilitate compliance in fiscal year 1986, EPA proposes to devote more resources to enforcement and to issuing technical guidelines for monitoring.

As awareness of groundwater problems increases, the need to determine the levels and locations of contamination becomes more evident. It is clear that developing this information, either within industry or the government, entails fairly extensive and expensive programs.

EPA's monitoring programs

In mid-April, EPA's Office of Groundwater Protection met with industrial, academic, and environmental representatives to forge a new overall EPA groundwater monitoring strategy. The Office of Solid Waste and the Hazardous Waste Task Force have been developing guidance and enforcement programs. The Office of Pesticides plans to issue guidelines on groundwater sampling and monitoring protocols for companies required to monitor groundwater as part of the pesticide registration process. The pesticides office is teaming with the Office of Drinking Water to conduct a \$5-\$6-million survey of about four dozen pesticides at 1500-2000 well sites.

Facility manager's view

In addition to meeting new requirements that stem from the 1984 RCRA amendments, facilities that were previously unregulated will now be required to monitor groundwater. Industry spokesmen suggest that RCRA-related monitoring often requires \$100,000-\$300,000 in capital and \$150,000 for annual operation and maintenance per facility. General hydrological investigations typically cost between \$25,000 and \$250,000. Chemical analysis using gas chromatography-mass spectrometry (which EPA favors for priority pollutants and which can be used for detecting other unknown substances)

costs about \$1000 per test. These costs are even higher for large-scale operations.

Congressional hearings also have focused attention on groundwater-supplied drinking water. An EPA survey of 48,000 public water supply systems that draw groundwater found synthetic chemicals in about one-third of the larger systems and in about one-fifth of all groundwater-supplied systems. The ability to detect many of these substances has been developing at a rapid pace. An ever-expanding list of chemicals to be concerned about is also forming. As the EPA adds substances to its lists of regulated wastes, the number of compounds considered for groundwater monitoring increases. The agency is currently considering nearly 350 compounds. One reason that evaluation of monitoring data is difficult is the federal government's establishment of only 25 enforceable maximum contaminant levels for drinking-water contamination. Many states also have promulgated their own standards.

At present, there is very little information on which to base a national assessment of groundwater contamination. The evidence to date has been anecdotal and subject to error as the testing procedures develop. The next steps—understanding how the data are to be evaluated and determining what actions to take—are only beginning to be investigated. The potential for alarm when concentrations of chemicals are found in groundwater at very low levels is obvious. Yet further scientific evaluation is absolutely essential to put the levels into perspective. Along with developing our abilities to judge when groundwater contamination levels are harmful, we need ways of determining when they are not.

Richard M. Dowd, Ph.D., is a Washington, D.C., consultant to Environmental Research & Technology, Inc.

Ocean incineration of hazardous wastes: An update

U.S. plans call for more research as Europe reaffirms its banning date

Fierce controversy characterized the annual meeting of the International Maritime Organization (IMO) Scientific Group on Dumping, which was convened in London in mid-March. The delegates were strongly polarized during plenary sessions and topic-spe-

cific group workshops on the ocean incineration of hazardous wastes. An EPA science advisory board (SAB) report was suppressed, and a working group on ocean incineration was unable to reach consensus on several issues.

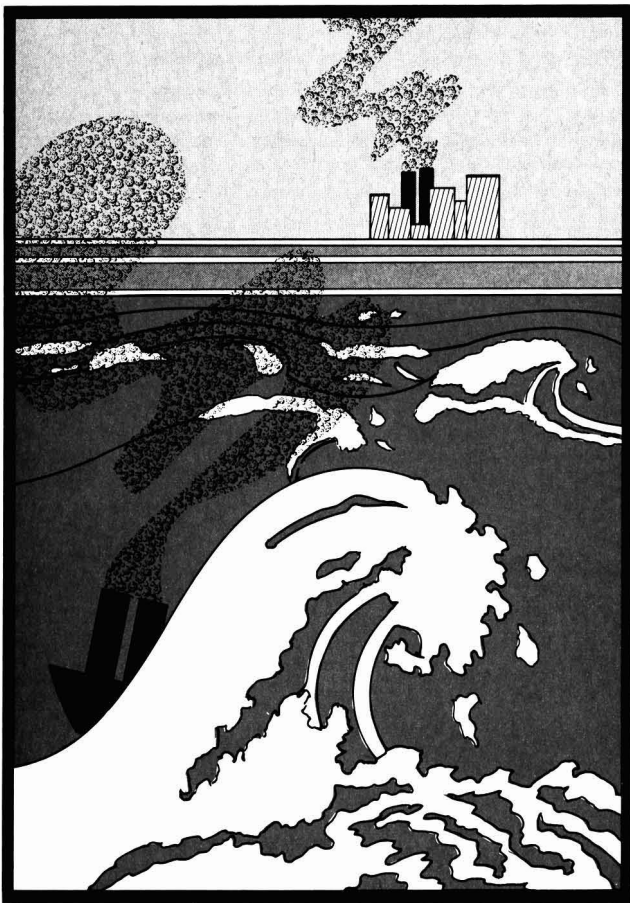
Given the makeup of the groups rep-

resented at the meeting, perhaps contention was unavoidable. Among them were Greenpeace representatives, with delegates from five countries. They received support from IMO representatives, particularly from Britain, the Netherlands, Sweden, and West Germany, who expressed many reservations concerning ocean incineration as a means of disposing of liquid hazardous wastes. In opposition were the U.S. delegation and the European Council of Chemical Manufacturers' Federation (CEFIC).

Those who led the opposing sides at the meeting are opponents in the same controversy in the U.S. On one side were Edward Kleppinger and myself. We attended the meeting as Greenpeace technical observers. Our purpose was to support a report we had provided to EPA in April 1983. It was the first comprehensive, critical analysis of ocean incineration (1). EPA had suggested that certain problems exist with the report.

On the other side of the debate was Donald Ackerman, who has reported extensively to EPA on burns of liquid hazardous wastes aboard the *Vulcanus* vessels. With funding from Chemical Waste Management (CWM, Oak Brook, Ill.), he had prepared a rebuttal (2) to the points made in our critique. CWM owns *Vulcanus I* and *Vulcanus II*. Ackerman attended as a member of the CEFIC delegation.

The analysis and its rebuttal were the basis for the discussion of the ocean incineration of liquid and hazardous wastes by the meeting's scientific group. Kleppinger and I attended to support the original analysis and to present an up-to-date expression of our uncertainties concerning ocean incineration (3). Support documents included an article from *ES&T* (4) on perceived shortcomings of the testing methods



aboard the *Vulcanus* and publicity documents on the *Vulcanus* vessels (5) by Ocean Combustion Services BV, a European subsidiary of CWM.

Report suppressed

The U.S. delegation, headed by Tudor Davies of the EPA, demanded the suppression of the SAB report on ocean incineration of liquid hazardous wastes (6). This report had expressed uncertainties about measurements and about the efficiency of incineration and destruction of the wastes, and its objections were similar to those we had presented previously (1, 2, 4). Despite the observation that the final draft of the SAB report, long available publicly, awaited only the EPA administrator's signature for final release, the insistence was that the report had not been made final. Hence, the scientific group was not permitted to apply the conclusions and recommendations of the SAB report at the 1985 meeting.

Motives for this and other actions on the part of the U.S. delegation are unclear. Perhaps one reason is EPA's intention to issue permits for the ocean incineration of liquid hazardous wastes later this year. Moreover, several delegates noted that the U.S. Maritime Administration provided a loan guarantee of about \$55 million (7) for the construction of *Apollo I* and *Apollo II*. These vessels are to be used for the ocean-based incineration of liquid hazardous wastes generated in the U.S. Some trade reports mention requirements for an additional \$15 million in guarantees. Several delegates believe that the loan guarantee could be in jeopardy if there is no U.S. ocean incineration program. Also, if the expected Eu-

ropean ban on ocean incineration goes into effect in 1990, the only significant market for the use of CWM's two vessels would be the U.S.

Jack E. Ravan, EPA's assistant administrator for water, has announced a 30-day extension of the comment period for proposed regulations on incineration at sea. The comment period will now close on June 28. Ravan is allowing the extension "to make sure that the public has ample time to review and comment on these very technical regulations." The proposed regulations were published in the *Federal Register* (Vol. 50, No. 40, Feb. 28, 1985, pp. 8222-88).

During the plenary session, Greenpeace representatives expressed concerns about the validity of various measurements that are said to be the basis for proof of the effectiveness of the incineration and destruction of hazardous wastes at sea. The study group then convened a working group on ocean incineration.

No consensus reached

The working group was unable to reach agreement on the issues. It did decide, however, that the matters it reviewed were serious enough to justify forming an intercessionary group of experts to consider them further.

Early in the meeting, it had been said that a voluminous quantity of ocean incineration data is available. Nevertheless, Davies and Alan Wastler of EPA said that additional data, to be gathered by EPA this year, should be examined before any intercessional meetings of experts are held or before any motions concerning ocean incineration of hazardous wastes are passed by IMO. Presumably, these additional data are to be gathered for EPA from burns aboard the *Vulcanus*. Other delegates, including the Greenpeace representatives, suggested that EPA's perspective was shortsighted and that if an intercessionary group of experts were to determine that EPA's methods were invalid, then EPA's latest research would be for naught.

European delegates noted that ocean incineration was only an "interim method of disposal of wastes" according to the London Dumping Convention (9). Many said that they plan to advise their governments to require review or action on the uncertainties that had been discussed at the meeting concerning the reliability of ocean incineration and disposal of hazardous wastes.

In addition, one delegate from West Germany pointed out that European countries may look toward beneficial uses of hazardous wastes. In that country, liquid hazardous wastes normally are processed for recycling and reuse

Working group impasse

The working group convened to study ocean incineration was unable to reach consensus on the following questions, which were subsequently referred to an intercessionary group of experts for examination:

- What is the relationship between destruction and combustion efficiencies over a wide range of operating conditions?
- What sampling procedure should be used to obtain a representative gas sample of the entire stack?
- What methodology should be used for collecting particulate material in the stack?
- What quality assurance requirements should be used for monitoring ocean incineration emissions?
- What new organic compounds may be synthesized during the incineration process?

or they are treated on site. This approach substantially reduces, if not eliminates, the need for ocean incineration. It is especially interesting to note that at the Oslo Commission meeting of 1981 (10), at which the U.S. was not represented, member countries unanimously resolved to ban the ocean incineration of liquid hazardous wastes by 1990. European delegates privately expressed the opinion that such a ban could take effect before that year.

—Desmond Bond

SAB report

The following statements are excerpted from the science advisory board report (6). All emphasis is as shown in the original.

"Conclusion 2: . . . the concept of destruction efficiency used by the Agency [EPA] was found to be incomplete and not useful for subsequent exposure assessments."

"Recommendation 2: THE EMISSIONS AND EFFLUENTS OF HAZARDOUS WASTE INCINERATORS NEED TO BE ANALYZED IN SUCH A WAY THAT THE IDENTITY AND QUANTITY OF THE CHEMICALS RELEASED INTO THE ENVIRONMENT, INCLUDING THEIR PHYSICAL FORM AND CHARACTERISTICS (PARTICLES, DROPLETS, GASES) CAN BE ESTIMATED."

References

- (1) Kleppinger, E.; Bond, D. "Ocean Incineration of Hazardous Waste: A Critique"; EWK Consultants: Washington, D.C., April 1983.
- (2) Ackerman, D. et al. "The Capability of Ocean Incineration—A Critical Review and Rebuttal of the Kleppinger Report," report by TRW to Chemical Waste Management; TRW: Redondo Beach, Calif., May 1983.
- (3) Kleppinger, E.; Bond, D. "Ocean Incineration of Hazardous Waste: A Revisit to the Controversy"; EWK Consultants: Washington, D.C., March 1985.
- (4) Bond, D. *Environ. Sci. Technol.* **1984**, *18*, 148-52A.
- (5) Ocean Incineration Services BV publicity brochure.
- (6) "Incineration of Hazardous Liquid Waste," draft report of Environmental Effects, Transport and Fate Committee, Science Advisory Board; EPA: Washington, D.C., December 1984.
- (7) "EPA Weighs Anchor on Long Feud"; *Washington Post*, March 26, 1985, p. D26.
- (8) International Maritime Organization. "Report of the 8th Meeting of the Scientific Group on Dumping," Document No. LDC/SG.8/WP.1; International Maritime Organization: London, U.K., March 1985.
- (9) Report of the Third Consultative Meeting of the London Dumping Convention, London, U.K., 1972.
- (10) 1981 Meeting of the Oslo Commission, Oslo, Norway, 1981.

Miami meeting report

Environmental activity highlights



M I A M I

The environmental component of the spring ACS meeting in Miami, Fla., consisted of three symposia, two awards, and general papers. The symposia were on aquatic photochemistry, environmental applications of chemodynamic models, and chlorinated dioxins and dibenzofurans in the environment. The awardees were Arthur Fontijn and Harold Johnston.

ACS awards

An award symposium was held in honor of Arthur Fontijn, the recipient

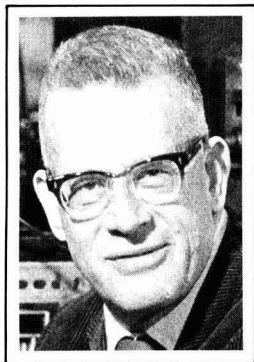
of the ACS Award for Creative Advances in Environmental Science and Technology, sponsored by Air Products & Chemicals, Incorporated. As a professor of chemical engineering and environmental engineering at Rensselaer Polytechnic Institute in Troy, N.Y., Fontijn has made far-reaching contributions to the measurement of trace atmospheric pollutants using chemiluminescent gas reactions. His work began as fundamental research and has culminated with the use of chemiluminescence as the instrumental method of

choice for measurement of NO, NO₂, and O₃ in air, as well as in many laboratory systems. He is widely recognized for his leadership in the field of gas-phase reactions and for his specific advances in NO_x monitoring.

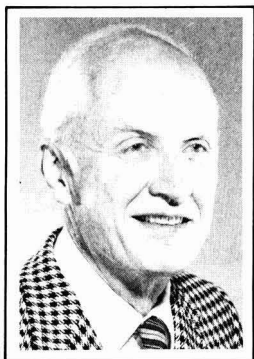
Fontijn's work has resulted in the most significant advance in monitoring atmospheric pollutants in the past two decades. His methods replace the slow, laborious, and rather insensitive wet-chemical method that was standard for the analysis of NO and NO₂ in tropospheric air. Fontijn and his colleagues have since made further advances in technique by developing an NO_x monitor based on the chemiluminescent reaction of NO and NO₂ with H atoms. This method eliminates the need for the NO₂-to-NO converters that are required with NO_x-O₃ detectors.

A simple NO₂ conversion technique permits the detection of NO_x measurements (NO + NO₂) and NO₂ by difference. By changing the reagent gas from excess O₃ to excess NO, Fontijn's instrument also serves as an excellent detector for atmospheric O₃. On the basis of these techniques, Fontijn has published more than 50 papers and holds seven patents.

Harold Johnston of the University of California at Berkeley is a world authority on gas-phase kinetics. He received the ACS Award in the Chemistry of Contemporary Technological Problems, sponsored by the Mobay Chemical Corporation. Johnston documented the fragility of the stratosphere in 1971 and was the first to alert the scientific community to the dangerous effects of NO_x in the ozone layer. He has been a leader in showing how contaminants introduced into the stratosphere reduce stratospheric ozone. Ozone, which is present in the stratosphere in parts per million, shields the



Arthur Fontijn



Harold Johnston

Earth from the damaging effects of the sun's ultraviolet radiation.

In his 1971 paper in *Science*, Johnston reported on the reduction of stratospheric ozone by NO_x catalysts present in exhaust from supersonic transport aircraft. This field of research has led to an understanding of the interactions of nitrogen oxides and other gas molecules in the atmosphere. The area has advanced from a primitive state—in 1970 there were only two balloon flight measurements of stratospheric NO_x —to present-day global coverage by satellite of upper atmospheric NO_x .

Johnston also pioneered the now-universal use of spectroscopic techniques for kinetic studies. He has made significant contributions to the theory of reaction kinetics, specifically as it applies to unimolecular reactions, activated complex theory, quantum mechanical tunneling, and kinetic isotope effects. He was elected to the National Academy of Sciences in 1965. His excellent monograph, "Gas Phase Reaction Rate Theory," which was published in 1966, is still quoted widely.

Dioxin symposium

Chlorinated dioxins and dibenzofurans are increasing in importance for

many segments of our society. Recent highly publicized incidents affecting large areas of our civilian population have captured the attention of environmentalists, lawyers, regulatory agencies, safety professionals, medical doctors, and the population at large.

In 1981, a series of symposia on the environmental problems of these compounds was organized by Lawrence H. Keith of Radian Corporation (Austin, Texas), Christoffer Rappe of the University of Umeå, Sweden, and Gangadhar Choudhary of the National Institute of Occupational Safety and Health (Cincinnati, Ohio). All three symposia were planned as continuations of ACS national meetings and sponsored by the Division of Environmental Chemistry. The first convened as part of the September 1982 meeting in Kansas City, Mo., the second at the September 1983 meeting in Washington, D.C., and the third this year at the meeting in Miami Beach, Fla.

Proceedings of the first two symposia have been published by Butterworth Publishers under the title "Chlorinated Dioxins and Dibenzofurans in the Total Environment I and II." Publication of the third symposium is expected in early 1986.

The symposium on chlorinated dioxins and dibenzofurans in the environment had seven sessions, which covered the topics of fate and transport, analytical chemistry, synthesis and destruction, emissions from incinerator sources, human exposure, epidemiology and bioassays, and soil contamination.

In a keynote address, Alvin L. Young of the president's Office of Science and Technology Policy said that extensive public attention has been devoted to these compounds, especially 2,3,7,8-TCDD, for more than a decade. He said that the science policy implications of the massive research and remedial programs under way on dioxin are disturbing. The federal government has committed hundreds of millions of dollars and thousands of staff-years to confirming that actual human exposure to dioxins is minimal and occurs primarily in "hot spots." Furthermore, the number of individuals exposed is very low, according to Young. Data collected to date do not associate chemical exposure with carcinogenesis, teratogenesis, or mutagenesis in humans. He also stated that data from combustion studies show that the production of dioxin is minimal and easily controlled with current technology. However, he said that fear of dioxin has paralyzed the development and application of incinerator technology.

In 1981, low levels of 2,3,7,8-TCDD were detected in Lake Ontario

fish. This discovery led to a study and monitoring activity by the Ontario Ministry of the Environment. In the session on fate and transport, ministry spokesman H. M. Tosine said that the analysis of PCDDs and PCDFs in drinking water at the parts-per-quadrillion level is an expensive and sensitive procedure. Analytical determination of PCDDs in water is very difficult, and some investigators use complex procedures for preconcentration to bring the concentrations of PCDD to the detection limit. Tosine indicated that this can lead to an unacceptable level of error in data from such studies.

EPA has proposed and published in the *Federal Register* a new method for the analysis of dioxins and dibenzofurans under the Resource Conservation and Recovery Act (RCRA), according to J. R. Donnelly of Lockheed Service and Management Service (Las Vegas, Nev.). This method is concerned with the total group of Cl_4 - Cl_6 homologues. Thus it includes 46 chlorinated dioxins and 82 chlorinated dibenzofurans.

Destruction session

Destruction and detoxification of these chemicals are important, of course, to reduce problems of environmental contamination.

In early 1985, a mobile rotary kiln incinerator was evaluated in Missouri for its effectiveness in destroying solid and liquid wastes that contain 2,3,7,8-TCDD and other RCRA-regulated chemicals. Robert D. Kleopfer of EPA's Kansas City, Mo., office stated that the test was designed to verify that stack emissions did not pose any unacceptable risk to the health and safety of residents in surrounding counties. Final results from the study were not available.

On July 10, 1976, there was a chemical accident in Seveso, Italy, during which chlorinated dioxins were released from the industrial plant of ICMESA, a subsidiary of Hoffmann-LaRoche. At this year's meeting, Sergio P. Ratti presented a mathematical explanation for interpreting data collected from 1976 to 1984.

The lesson from the Seveso episode was presented by Gustavo U. Fortunati, an official spokesman from the Lombardy region—scene of the episode. He said that only chemical dechlorination, specifically the method of SEA-MARCONI (Torino, Italy), proved successful for cleaning up equipment contaminated with trichlorophenol (TCP). He described the dismantling of the TCP plant at the ICMESA facility. The equipment was finally buried in a steel container and filled in place with bentonite mixed

with concrete inside a second basin. Fortunati welcomed suggestions and ideas on the use of this reclamation experience acquired since 1976. Deactivation of hazardous wastes by chemical methods has been discussed in this publication (see *ES&T*, March 1985, pp. 215-20).

Emissions from incinerator sources

The question of whether chlorinated dioxins and dibenzofurans are thermally stable is controversial and is being studied extensively.

In 1977-78, it was first reported that PCDDs and PCDFs could be identified in fly ash from municipal incinerators and industrial heating facilities in Europe. The levels reported were in the range of 0.1-0.6 $\mu\text{g/g}$. During the period 1978-84 a series of papers was published, confirming the original findings.

H. C. Thompson, Jr., of the Food and Drug Administration's National Center for Toxicological Research (Jefferson, Ark.) called for a multitiered sampling approach for such emissions because limited samples from different sources lead to unconvincing data. Thompson believes this approach is needed because of the large number of samples required in determining the extent of contamination. Another speaker, S. Markland of the University of Umeå, Sweden, noted that the sampling procedure in large incinerators is complex and expensive. Currently, there is no standard method for sampling and analysis of the complex combustion products.

R. M. Smith of the New York State Department of Health noted that capillary GC-multiple peak monitoring high-resolution mass spectrometry (HRMS) separates toxic 2,3,7,8-chlorinated dibenzodioxin from less toxic CDD and CDF isomers. Further, this analytical technique, which is useful for incinerator residues, separates and identifies interfering chlorinated biphenylenes and PCBs.

The most revealing comments on dioxins came from the session on emissions from incinerator residues. It has recently been reported by C. Rappe and colleagues at the University of Umeå, Sweden, that a series of 2,3,7,8-substituted PCDDs and PCDFs has been identified in samples of human adipose (fatty) tissue and mothers' milk from studies in Sweden as well as in a series of ecological samples taken from the Baltic Sea Gulf of Bothnia. The levels are in the ppt range, and the data strongly indicate a background for these chemicals in the general population and in the aquatic environment.

Dioxins also were found in emissions from an energy recovery municipal in-

cinerator in Canada in 1982. H. M. Tosine reported that stack emissions were performed using two Method 5 trains, modified to contain two florilic cartridges in series between the third and fourth impingers.

Research on incinerators is taking place in Italy. R. Bonaiuti of the CNR Progetto Finalizzato Energetica (Milan, Italy) said that to explore the problem of emissions from municipal waste incinerators the Italian Research Council financed the construction of an incinerating pilot plant equipped with a post-combustion chamber that will analyze effluents and test postcombustion efficiency. The plant is working discontinuously, burning about 2 t of wastes every 4 h at a temperature of 600 °C at the start of the combustion cycle, which rises to 950-1000 °C and then decreases to 750 °C at the cycle's end.

Human exposure

Knowledge of human exposure to chlorinated dioxins and dibenzofurans is necessary to evaluate their risks. John J. Ryan of the Food Directorate of the Canadian Health Protection Branch in Ottawa, Ont., said that tetrachlorodibenzo-*p*-dioxins and pentachlorodibenzofurans (specific isomers were not identified) are known to be present at the 5-15-ppt level in human adipose tissue from the general population. Earlier, little or no information was available on the levels and distribution of dioxins and furans other than in fatty tissue. But now 2,3,7,8-tetrachlorodioxin, other dioxins, and chlorinated dibenzofurans in the ppt range have been found in all tissue types assayed—abdominal, subcutaneous, adrenal, bone marrow, liver, muscle, and kidney. The results clearly show that a wide variety and concentration of dioxins and furans can be found not only in fat but in all other human tissues. The source of these contaminants and their toxicological significance is uncertain now but should be determined in the near future.

L. Hardell of the University Hospital at the University of Umeå presented an overview of the Swedish studies on the relationship between herbicide exposure and soft-tissue sarcoma and malignant lymphoma. In previous Swedish studies, exposure to phenoxyacetic acids or chlorophenols had been associated with an increased risk of soft-tissue sarcoma and malignant lymphoma, according to Hardell, who is a medical doctor. The validity of the assessment of exposure to phenoxy acids and chlorophenols in these studies was further analyzed by using a fairly common cancer type, colon cancer, for comparison. No association was found between exposure to phenoxy acids or chlorophe-

nols and colon cancer.

The objective of the newer study was to determine whether previous exposure to PCDDs and PCDFs as contaminants in phenoxy acids could be estimated by analyses of these substances in fat tissue. No conclusion has yet been drawn from this study.

Epidemiology and bioassays

Research studies are under way to learn the effects of human exposure to dioxins and dibenzofurans. P. A. Stehr of the Centers for Disease Control (Atlanta, Ga.) reminded the audience that in 1971 waste oil containing 2,3,7,8-TCDD was sprayed on various sites throughout the state of Missouri for dust control. By definition the areas in this study contained between 20 ppb and 100 ppb for a period of two years or more than 100 ppb for six months. Stehr's research involved a pilot study of a group of 122 persons, presumed to be at highest risk of exposure to environmental dioxins. Eighty-two of these individuals lived and worked in the contaminated areas or participated more than once each week in activities involving close contact with the soil, such as gardening or playing on the ground.

The results of the CDC study were largely inconclusive; no real link was drawn between exposure to dioxin and poor health. For example, there was no consistent diagnostic difference between the control and study groups for birth defects, no cases of chloracne in the study population, no difference in immune system function, and no trend or problem in the medical histories regarding hepatic (liver) function.

A report of the epidemiologic investigation of the health effects of Agent Orange was presented by Royce Moser, Jr., of the U.S. Air Force School of Aerospace Medicine (Brooks Air Force Base, Texas). The study's cohort consisted of military personnel who used Agent Orange in Vietnam in a well-publicized jungle defoliation operation called Ranch Hand. The purpose of the report was to present the baseline morbidity study.

A total of 2272 individuals were involved in the study. This included 87% of the Ranch Hand personnel and 72% of a comparison group of persons who served in Vietnam but who were never involved in the use of Agent Orange. Physical examination and questionnaire data were analyzed with respect to major organ systems. The questionnaire data showed that more Ranch Hand personnel perceived themselves to be in fair or poor health in general than did their counterparts. There was no significant difference in the occurrence of malignant or benign systemic tumors

between the two groups.

The baseline report concluded that currently there is insufficient evidence to support a cause-and-effect relationship between Agent Orange exposure and adverse health in the Ranch Hand group. The study disclosed numerous medical findings, mostly of a minor or undetermined nature, that require detailed follow-up, according to Moser.

J. F. Gierthy of the New York State Department of Health reported on an in vitro bioassay for dioxinlike compounds.

Soil contamination

The most alarming issue concerning the environment in the state of Missouri is the contamination of many sites with TCDD, according to Armon F. Yanders of the University of Missouri's Environmental Trace Substance Research Center. Forty sites in Missouri are known to be contaminated with 2,3,7,8-TCDD, the most toxic of the 75 possible dioxin isomers. The city of Times Beach, in eastern Missouri near St. Louis, has areas in which levels as high as 1500 ppb have been found. Dioxin concentration in soil under the asphalt averages about 300 ppb. EPA

and the state of Missouri are spending more than \$33 million to purchase all property in Times Beach and to relocate the 800 families living there. Two blocks in the most contaminated area have been set aside for research. Several studies of in situ degradation of dioxin in soil began in the summer of 1984; more are expected this year.

J. H. Exner of IT Corporation (Martinez, Calif.) discussed a sampling strategy for cleaning soil contaminated with 2,3,7,8-TCDD. R. A. Freeman of the Monsanto Company (St. Louis, Mo.) presented a model that describes the transport of this compound in a soil column. Freeman's mathematical model calculates the rate of movement of the compound through the soil by determining the dynamic material balance and energy balance around a section of soil. Using soil column concentration profiles, it is possible to estimate when the original contaminated waste oil loading was completed. The estimated time of loading is then used to define the behavior of the contaminant with time.

D. R. Jackson of Battelle Laboratories (Columbus, Ohio) is interested in the solubility of TCDD in contaminated

soils. He reported on the mechanisms that account for the solubility of the material in soil solution.

Aquatic photochemistry symposium

Some of the scientists who contributed to this symposium were present at a NATO-sponsored meeting on this subject at Woods Hole, Mass., in September 1983. Various significant species of ions, radicals, and the like were discussed, as well as their concentrations and half-life values in aquatic systems. A critical review of the research activities in this area was published in *ES&T's* December 1984 issue ("Photochemistry of natural waters," p. 358A).

Prognosis

It is questionable whether there will be another ACS symposium on the problems of chlorinated dioxins and dibenzofurans. A questionnaire was distributed to participants at the Miami Beach meeting asking if another symposium should be held. Responses, which were addressed to Larry Keith, will be considered in planning future meetings.

—Stanton Miller



People who make the news, read the News.

When you're sitting at the top, you need to get to the bottom of news that affects your business. That's why senior executives throughout industry read *Chemical & Engineering News* each week.

It's the only weekly chemical magazine that covers the news from three angles. Not just science. Not just technology. Not just business. But all three. So you not only know what's happening in chemistry, you know how it's going to affect your business.

Read the weekly the news-makers read. Call 800-424-6747 and ask about our offer of six complimentary issues.

BUSINESS
SCIENCE
TECHNOLOGY

The Chain Straighteners

Fruitful Innovation: The Discovery of Linear and Stereoregular Synthetic Polymers

by Frank M. McMillan

Presents the story of a key event in polymer science—the discovery of linear and stereoregular synthetic polymers. Karl Ziegler and Giulio Natta are the star players in this scientific drama, which has as its supporting cast the most renowned names in polymer science. Details the dynamic interplay of people and events that led to this fruitful innovation.

CONTENTS

The Stage is Set • The Shadows Before ("Prediscoveries") • Karl Ziegler and the Max Planck Institute • Giulio Natta and the Milan Polytechnic Institute • Fruitful Innovation—1. The Polyethylene Discovery • Harvesting the Fruits of Innovation—Polyethylene • Fruitful Innovation—2. Polypropylene • The Falling Out • Harvesting the Fruits of Innovation—Polypropylene • Fruitful Innovation—3. Synthetic Rubber • The Crest of the Wave—and the

Trough • Shadows of the Future • Interpretations
Published by The Macmillan Press Ltd.
206 pages (1979) Clothbound
ISBN 0-333-25929-7
US & Canada only \$31.95

Order from:
American Chemical Society
Distribution Office Dept. 17
1155 Sixteenth St., N.W.
Washington, DC 20036
or CALL TOLL FREE 800-424-6747
and use your VISA, MasterCard
or American Express credit card.

Attention: Chemical Scientists

Do you want to . . .

- Keep up to date?
- Increase professional contacts?
- Receive substantial discounts on publications?
- Present your latest research?
- Receive assistance in financial planning?
- Attend chemical expositions?
- Find a new position?
- Continue your chemical education?

If you can say "yes" to even one of these the **ACS** should be *your* Society!


Write or call today for information about these and many other benefits.

**Membership Development Office
American Chemical Society
1155 16th St., N.W.
Washington, D.C. 20036
202-872-4437**

INDEX TO THE ADVERTISERS IN THIS ISSUE

ADVERTISERS	PAGE NO.		
		Advertising Management for the American Chemical Society Publications	
		CENTCOM, LTD.	
		<i>President</i>	
		Thomas N. J. Koerwer	
		<i>Executive Vice President</i>	
		James A. Byrne	
		<i>Senior Vice President</i>	
		Benjamin W. Jones	
		<i>Vice President</i>	
		Alfred L. Gregory	
		<i>Vice President</i>	
		Clay S. Holden	
		<i>Vice President</i>	
		Robert L. Voepel	
		<i>Vice President</i>	
		Joseph P. Stenza	
		<i>Production Director</i>	
		25 Sylvan Road South P.O. Box 231 Westport, Connecticut 06881 (Area Code 203) 226-7131 Telex No. 643310	
		ADVERTISING SALES MANAGER	
		James A. Byrne, VP	
		ADVERTISING PRODUCTION MANAGER	
		Jay S. Francis	
		SALES REPRESENTATIVES	
		Philadelphia, Pa. . . . Patricia O'Donnell, CENTCOM, LTD., GSB Building, Suite 725, 1 Belmont Ave., Bala Cynwyd, Pa 19004 (Area Code 215) 667-9666	
		New York, N.Y. . . . Dean A. Baldwin, CENTCOM, LTD., 60 E. 42nd Street, New York 10165 (Area Code 212) 972-9660	
		Westport, Ct. . . . Edward M. Black, CENTCOM, LTD., 25 Sylvan Road South, P.O. Box 231, Westport, Ct 06881 (Area Code 203) 226-7131	
		Cleveland, Oh. . . . Bruce Poorman, CENTCOM, LTD., 325 Front St., Berea, OH 44017 (Area Code 216) 234-1333	
		Chicago, Ill. . . . Michael J. Pak, CENTCOM, LTD., 540 Frontage Rd., Northfield, Ill 60093 (Area Code 312) 441-6383	
		Houston, Tx. . . . Michael J. Pak, CENTCOM, LTD., (Area Code 312) 441-6383	
		San Francisco, Ca. . . . Paul M. Butts, CENTCOM, LTD., Suite 1070, 2672 Bayshore Frontage Road, Mountainview, CA 94043. (Area Code 415) 969-4604	
		Los Angeles, Ca. . . . Clay S. Holden, CENTCOM, LTD., 3142 Pacific Coast Highway, Suite 200, Torrance, CA 90505 (Area Code 213) 325-1903	
		Boston, Ma. . . . Edward M. Black, CENTCOM, LTD., (Area Code 203) 226-7131	
		Atlanta, Ga. . . . Edward M. Black, CENTCOM, LTD., (Area Code 203) 226-7131	
		Denver, Co. . . . Paul M. Butts, CENTCOM, LTD., (Area Code 415) 969-4604	
		United Kingdom:	
		Reading, England—Technomedia, Ltd. . . . Wood Cottage, Shurlock Row, Reading RG10 0QE, Berkshire, England 0734-343302	
		Lancashire, England—Technomedia, Ltd. . . . c/o Meconomics Ltd., Meconomics House, 31 Old Street, Ashton Under Lyne, Lancashire, England 061-308-3025	
		Continental Europe . . . Andre Jamar, Rue Mallard 1, 4800 Verviers, Belgium. Telephone (087) 22-53-85. Telex No. 49263	
		Tokyo, Japan . . . Shuji Tanaka, International Media Representatives Ltd., 2-29, Toranomon 1-Chrome, Minatoku, Tokyo 105 Japan. Telephone: 502-0656	
EG&G Ortec	468-469		
Charles Tombras Advertising			
Seastar Instruments Ltd.	IFC		
Stanford University Press	IFC		
Stock Brothers Corp.	IFC		
Alden Design Associates			

professional consulting services directory




TRADITIONAL SOURCE SAMPLING

- Air Emissions Testing and Compliance Determination for Particulate and Gases
- Control Device Evaluation
- Particle Sizing Studies
- Resistivity Studies
- Specialized Analysis
- Method 1 Alternative
- 3-D Air Flow Studies

D. James Grove, P.E., Director
 PO Box 12291, Research Triangle Park, NC 27709 (919) 781-3550 or 1-800-ENTROPY

ENTROPY
 ENVIRONMENTALISTS INC.




SPECIALIZED SAMPLING

- (RCRA) Incinerator Testing
- Volatile Organic Compound (VOC) Testing
- Vapor Recovery Unit Compliance/Performance Testing
- Specialized Hydrocarbons Testing
- Testing of High Temperature and Pressure Sources

Walter S. Smith, P.E. Director
 PO Box 12291, Research Triangle Park, NC 27709 (919) 781-3550 or 1-800-ENTROPY

ENTROPY
 ENVIRONMENTALISTS INC.



CONTINUOUS EMISSIONS MONITORING (CEM)/ENGINEERING

- Performance Specification Tests of Opacity, SO₂, NO_x, O₃, CO, CO₂ and TRS CEMS
- Stratification Tests (All Pollutants)
- CEM Performance Audits (RAA and CGA)
- Real-time Measurements Using Transportable CEM System — Boiler Tuning (NO_x) — FGD Performance Evaluation — Combustion Efficiency Studies
- Performance Tests of Gas Turbines (Method 20) — James W. Heiler, Director — William G. DeWies, Associate Director

PO Box 12291, Research Triangle Park, NC 27709 (919) 781-3550 or 1-800-ENTROPY

ENTROPY
 ENVIRONMENTALISTS INC.

Cenref Labs ENVIRONMENTAL TESTING

GC/MS • PSD • PCB'S
 RCRA • NPDES
 STACK TESTING

P.O. BOX 68, BRIGHTON, CO 80601
 (303) 659-0497



COMPLETE ANALYTICAL SERVICES GC/MS CAPABILITIES

- Screening & Analysis of Industrial & Hazardous Waste.
- Superfund & RCRA Requirements.
- Sampling to EPA Protocols.
- Toxicity Studies.


(516) 334-7770
 75 URBAN AVE, WESTBURY, NY 11590
NYTEST ENVIRONMENTAL INC.

HITTMAN EBASCO
 Analytical Laboratories

- EPA Priority Pollutants - GC/MS
- Water Monitoring
- Hazardous Waste Characterization
- Sampling Services
- NPDES and RCRA Services

—EPA Approved and State Certified—

HITTMAN EBASCO ASSOCIATES INC.
 A Subsidiary of EBASCO SERVICES INCORPORATED
 9151 Rumsey Road, Columbia, MD 21045
 (301) 730-8525



ENVIRODYNE ENGINEERS

a consulting engineering and sciences firm

- environmental engineering analytical chemistry priority pollutant analyses environmental monitoring and assessment hazardous waste monitoring hazardous waste management
- transportation engineering
- energy engineering
- construction management

12161 Lackland Road
 St. Louis, Missouri 63141
 (314) 434-6960
 Baltimore / Chicago / New York



COMPLETE ANALYTICAL SERVICES

- Gas Chromatography/ Mass Spectroscopy
- Trace Metal Analyses - ICAP, AA, GFAA
- Drinking Water Analyses
- Industrial Hygiene Services
- Research and Development
- Environmental Field Sampling
- EPA Priority Pollutant Analyses

Brochure and/or fee schedule available on request
BARRINGER MAGENTA LTD.
 304 Caringview Drive Rexdale Ont Canada (416) 675-3870
 US Office Denver CO 80401 (303) 232-8811

THE CONSULTANTS' DIRECTORY

UNIT	Six Issues	Twelve Issues
1" x 1 col.	\$55	\$50
1" x 2 col.	110	100
1" x 3 col.	160	140
2" x 1 col.	110	100
2" x 2 col.	200	180
4" x 1 col.	200	180

Jay Francis
 ENVIRONMENTAL SCIENCE & TECHNOLOGY
 25 Sylvan Road South
 P.O. Box 231
 Westport, CT 06881
 Or call him at (203) 226-7131


nai
NORMANDEAU ASSOCIATES, INC.

ENVIRONMENTAL SCIENTISTS, ENGINEERS & PLANNERS

FULL SERVICE ENVIRONMENTAL CONSULTANTS

- SOLID/HAZARDOUS WASTE MANAGEMENT
- IMPACT ASSESSMENTS
- AIR QUALITY MONITORING & MODELING
- PERMIT ASSISTANCE
- FACILITY AUDITS
- BIOLOGICAL/WATER QUALITY MONITORING

25 NASHUA ROAD, BEDFORD, N.H. 03102
 (603) 472-5191



Dunn Geoscience

ALBANY NY 518/782-0102
 BUFFALO NY 716/884-1500
 NEW YORK CITY 212/712-0661
 LACONIA NH 603/528-4205
 HARRISBURG PA 717/781-6710

Geologic and Hydrologic Consultants
 • Ground Water Assessment & Supply
 • Solid & Hazardous Waste Site Design

CLASSIFIED SECTION

SENIOR CHEMICAL ENGINEER

Degreed Chemical Engineer with 5-10 years experience in responsible charge of plant or corporate environmental management in the process industry.

Resource Engineering is an engineering management contractor for major hazardous waste projects.

Position is Senior Level Engineering Management of hazardous waste projects for the chemical and hydrocarbon processing industries. Send resume and salary requirements to:

Resource Engineering
3000 Richmond Avenue
Houston, Texas 77098

Environmental consulting firm has immediate opening for a self-motivated individual to supervise an organics laboratory. Must be experienced with GC procedures for pesticide, herbicide and volatile organics analyses according to EPA, APHA and ASTM protocols. LC experience desirable. Send resume and salary requirements to: Dr. Henry J. Kania, Environmental & Chemical Sciences, Inc., P.O. Box 1393, Aiken, SC 29802.

CLASSIFIED ADVERTISING RATES

Rate based on number of insertions used within 12 months from date of first insertion and not on the number of inches used. Space in classified advertising cannot be combined for frequency with ROP advertising. Classified advertising accepted in inch multiples only.

Unit	1-T	3-T	6-T	12-T	24-T
1 inch	\$100	\$95	\$90	\$85	\$80

(Check Classified Advertising Department for rates if advertisement is larger than 10".)

SHIPPING INSTRUCTIONS: Send all material to

Environmental Science & Technology
Classified Advertising Department
25 Sylvan Rd. South
Westport, CT. 06881
(203) 226-7131

ENVIRONMENTAL CHEMISTS & ENGINEERS

Battelle Columbus Laboratories has openings for environmental professionals to contribute to current contract research programs in solid and hazardous waste, toxicology, environmental and preventative health, and environmental control technology. Specific opportunities exist for:

ENVIRONMENTAL ENGINEER with graduate training and a minimum of 10 years experience in the design, analysis, and management of solid and hazardous waste treatment systems.

APPLIED CHEMIST with graduate training and significant experience in environmental or water chemistry to work in the area of contaminant behavior in aquatic systems. Ability to integrate field and lab measurements into mathematical fate models is desirable. Experience in project management is required.

These assignments involve extensive contact with research sponsors, and candidates must have excellent writing and speaking ability.

Battelle offers a professional research environment, competitive salaries, and opportunities for professional growth. Please submit resume to: **Virginia Tyler, Employment, Department S-2, BATTELLE COLUMBUS LABORATORIES, 505 King Avenue, Columbus, Ohio 43201.**



An Equal Opportunity Affirmative Action Employer M/F/H

Environmental Engineer

If you want a high-technology environment, unlimited opportunity, long-range stability and a convenient location. You owe it to yourself to take a closer look at General Dynamics Pomona Division, a leading supplier of advanced tactical defense systems.

We currently have an opportunity available for an individual to develop division-wide surveys to implement hazardous material handling practices. The primary functions of the position will be to perform audits of on-site and off-site procedures in order to evaluate overall compliance; and to investigate applicability of new or emergent technology to Pomona Division issues. The individual will serve as the primary interface to regulatory agencies. Five years' industry experience in an environmental field and a B.S. degree are required. Science degree preferred.

Technology. Opportunity. Stability. Location. We have them all. If you're looking for a way to join us, you can start by sending your resume to: **Director of Production Administration, General Dynamics Pomona Division, P.O. Box 3011, Drawer E-293, Pomona, CA 91769.**

**We're looking forward
to meeting you.**

GENERAL DYNAMICS
Pomona Division

Equal Opportunity Employer/U.S. Citizenship Required.

Pay only
one half year's dues
if you join now

ACS Membership Application 1985

American Chemical Society • 1155 Sixteenth Street, N.W., Washington, D.C. 20036
(202) 872-4600 TDD: (202) 872-8733

Applicant

Mr., Mrs. (Name) _____
Dr., Miss, Ms. (Please type or print) Family Name First Middle
Mailing Address _____
Number and Street
City State Zip Code/Country Telephone _____
Area Code

Academic Training

Name of College or University (Including current enrollment)	City and State	Curriculum Major	Years of Attendance	Title of Degree(s) Received or Expected	Date Degree Received or Expected
_____	_____	_____	_____	_____	_____
_____	_____	_____	_____	_____	_____
_____	_____	_____	_____	_____	_____

Courses Completed

Please list completed courses (by title) in the chemical sciences (Attach separate sheet or transcript if more space is needed.)
Not required of those with a bachelor's, master's or doctor's degree in a chemical science or those with a doctor's degree in a science closely related to chemistry with demonstrated significant experience in the practice of a chemical science.

Quarter hour credits should be multiplied by two-thirds. If school did not use a credit hour system, please estimate credits on basis of 15 lecture clock hours or 45 laboratory clock hours as equivalent to one semester hour credit.

Course Title	Semester Hours	Course Title	Semester Hours	Course Title	Semester Hours
_____	_____	_____	_____	_____	_____
_____	_____	_____	_____	_____	_____
_____	_____	_____	_____	_____	_____

Nomination

Nomination by two ACS members (not necessary for former members, student affiliation does not constitute former membership). If this presents difficulty, please contact the Washington office.

We recommend _____ for membership in the American Chemical Society.
(Name of Applicant)

ACS Member: _____
(Signature) (Printed Name)

ACS Member: _____
(Signature) (Printed Name)

This space for use of:
ADMISSIONS COMMITTEE

1 2 3 4 6 N

Local Section/Division Commission Claim

Statistical Information

Mr., Mrs. (Name) _____
Dr., Miss, Ms. (Please type or print) Family Name First Middle

Mailing Address _____
Number and Street

City State Zip Code/Country

Date of Birth _____ Sex F M
(Information needed for statistical purposes)

Previous Membership

I have have not previously been a member.
I have have not previously been a student affiliate.

Office Use Only

AMC _____
MJR _____
DEL _____
MED _____
CSD _____
PNI **8140S** _____
CLD _____
CNS _____
CNR _____
TEC _____
WTD _____

Professional Experience

Employer	Job Title	Functions	% Time on Chemical Work	Inclusive Dates of Employment (Mo. & Yr.)

Dues/Subscriptions/Divisions

There are four start dates for membership: 1 January, 1 April, 1 July and 1 October. We are anxious to begin your membership as soon as possible and will therefore enroll you immediately upon approval by the Admissions Committee. Dues for 1985 are \$67.00. Your membership will begin at the nearest quarter and you will be billed accordingly. *Please send no money now.*

Student Dues

If you are a student majoring in the chemical sciences a 50% reduction on membership is available. To apply you must be registered for at least six credit hours as an undergraduate or be enrolled as a full-time graduate student.

I am an undergraduate student enrolled as described above.
 a graduate student enrolled as described above.

Name of College or University

National Affiliation

National affiliates pay three-quarters dues (i.e. \$50.25) and likewise will receive a prorated bill based on the quarter national affiliation begins.

Husband/Wife Dues

If you are the spouse of a member receiving C&EN, 23% (or the prorated amount) will be deducted from your bill. This is the portion that is allotted for C&EN. If you are eligible, please give the name of your spouse and his/her membership number.

Spouse's Name

Membership Number

As an introduction to ACS divisions, they are pleased to offer free membership in one division of your choice (subject to certain limitations) for one year. If your ACS membership begins January 1st or April 1st, 1985, your free division membership will be for 1985. If your ACS membership begins July 1st or October 1st, 1985, your free division membership will be for 1986. Select the division of your choice for your introductory free membership. You may join more than one division, but only one membership will be free. This offer is limited to those joining the Society, for the first time, in 1985. If you wish to subscribe to an ACS publication or join an ACS division, please list the publication(s)/division(s) below.

Remember, send no money now.

Agreement

I agree to restrict for my own personal use all publications to which I subscribe at member rates. I understand that membership dues are payable annually unless my signed resignation is received by the Executive Director before January 1 of the year for which the resignation is to take effect.

(Date)

(Signature of Applicant)



All forward thinking environmental scientists depend on ES&T. They get the most authoritative technical and scientific information on environmental issues—and so can you! Have your own

subscription delivered directly to you each month!

YES! Enter my own subscription to ENVIRONMENTAL SCIENCE & TECHNOLOGY at the rate I've checked below:

One Year	U.S.	Mexico & Canada	Europe	All Other Countries
ACS Members*	<input type="checkbox"/> \$ 26	<input type="checkbox"/> \$ 34	<input type="checkbox"/> \$ 40	<input type="checkbox"/> \$ 49
Nonmembers—Personal*	<input type="checkbox"/> \$ 35	<input type="checkbox"/> \$ 43	<input type="checkbox"/> \$ 49	<input type="checkbox"/> \$ 58
Nonmembers—Institutional	<input type="checkbox"/> \$149	<input type="checkbox"/> \$157	<input type="checkbox"/> \$163	<input type="checkbox"/> \$172

Payment Enclosed (Payable to American Chemical Society)
 Bill Me Bill Company Charge my: VISA MasterCard

Card No. _____

Exp. Date _____ Interbank # _____ (Mastercard Only)

Signature _____

Name _____

Title _____ Employer _____

Address _____

City, State, Zip _____

Employer's Business: Manufacturing, type _____

Academic Government Other _____

*Subscriptions at these rates are for personal use only.

All foreign subscriptions are now fulfilled by air delivery. Foreign payment must be made in U.S. currency by international money order, UNESCO coupons, U.S. bank draft, or order through your subscription agency. For nonmember subscription rates in Japan, contact Maruzen Co., Ltd.

Please allow 45 days for your first copy to be mailed. Redeem until December 31, 1985.



All forward thinking environmental scientists depend on ES&T. They get the most authoritative technical and scientific information on environmental issues—and so can you! Have your own

subscription delivered directly to you each month!

YES! Enter my own subscription to ENVIRONMENTAL SCIENCE & TECHNOLOGY at the rate I've checked below:

One Year	U.S.	Mexico & Canada	Europe	All Other Countries
ACS Members*	<input type="checkbox"/> \$ 26	<input type="checkbox"/> \$ 34	<input type="checkbox"/> \$ 40	<input type="checkbox"/> \$ 49
Nonmembers—Personal*	<input type="checkbox"/> \$ 35	<input type="checkbox"/> \$ 43	<input type="checkbox"/> \$ 49	<input type="checkbox"/> \$ 58
Nonmembers—Institutional	<input type="checkbox"/> \$149	<input type="checkbox"/> \$157	<input type="checkbox"/> \$163	<input type="checkbox"/> \$172

Payment Enclosed (Payable to American Chemical Society)
 Bill Me Bill Company Charge my: VISA MasterCard

Card No. _____

Exp. Date _____ Interbank # _____ (Mastercard Only)

Signature _____

Name _____

Title _____ Employer _____

Address _____

City, State, Zip _____

Employer's Business: Manufacturing, type _____

Academic Government Other _____

*Subscriptions at these rates are for personal use only.

All foreign subscriptions are now fulfilled by air delivery. Foreign payment must be made in U.S. currency by international money order, UNESCO coupons, U.S. bank draft, or order through your subscription agency. For nonmember subscription rates in Japan, contact Maruzen Co., Ltd.

Please allow 45 days for your first copy to be mailed. Redeem until December 31, 1985.



(800) 424-6747 (U.S. only)



NO POSTAGE
NECESSARY
IF MAILED
IN THE
UNITED STATES

BUSINESS REPLY CARD

FIRST CLASS PERMIT NO. 10094 WASHINGTON, D.C.

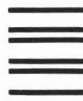
POSTAGE WILL BE PAID BY ADDRESSEE

American Chemical Society

Periodicals Marketing Dept.
1155 Sixteenth Street, N.W.
Washington, D.C. 20036



(800) 424-6747 (U.S. only)



NO POSTAGE
NECESSARY
IF MAILED
IN THE
UNITED STATES

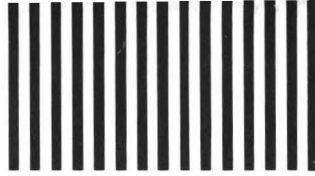
BUSINESS REPLY CARD

FIRST CLASS PERMIT NO. 10094 WASHINGTON, D.C.

POSTAGE WILL BE PAID BY ADDRESSEE

American Chemical Society

Periodicals Marketing Dept.
1155 Sixteenth Street, N.W.
Washington, D.C. 20036



New Conceptual Formulation for Predicting Filter Performance

Vinod Tare* and C. Venkobachar

Environmental Engineering Division, Department of Civil Engineering, Indian Institute of Technology, Kanpur 208016, India

■ This paper describes the development of a new conceptual model for predicting head loss buildup and removal efficiency during filtration by packed beds based on the postulate that some retained particles can act as collectors and thereby improve the filtration efficiency. The concept of Unit Bed Element (UBE) and of the unit collector is used for the quantitative description of the various processes of interest which occur in the porous medium. The filtration efficiency is described by a set of three interdependent equations for monosized particles in suspension assuming the porosity of the bed to remain constant as filtration progresses. The first equation computes the single collector removal efficiency related to clean grain efficiency and retained particles acting as collectors. The second equation estimates the number of retained particles acting as collectors as a function of depth, time, and local particle concentration in suspension. The third equation predicts suspended particle concentration with time over the entire filter depth. The head loss buildup is predicted by modifying the classical head loss equation for clean beds incorporating change in the surface area to volume ratio of the filter grains. The model is calibrated and verified with a set of laboratory data obtained from literature under varying conditions of operating and system variables. The results show strong agreement between model predictions and experimental observations as indicated by low values of standard error of estimate associated with coefficient of correlation values approaching unity.

Introduction

Filtration, a physicochemical process, is one of the most important unit operations employed for the final clarification of water and wastewater in treatment plants. Despite its wide application, the filtration process is not well understood. This is because conceptual mathematical formulations do not exist that can quantitatively describe the complete dynamics of deep bed filtration, taking into account the complex interaction between filter grains and liquid solution particles to be removed as well as the effects of operating and system variables. Only recently, O'Melia and Ali (1) proposed a model for the development of head loss and removal efficiency during filtration by packed beds based on the postulate that some retained particles can act as collectors and thereby improve the filtration efficiency. Though the concept seems to be appropriate and the mathematical model very well agrees within the certain limits of experimental data, the estimated coefficients may not reflect or may not have any correlation with the actual properties of the suspension and filter media responsible for filtration. This is because the aforementioned model

does not incorporate a few important factors such as surface coverage of the filter media grains and that of retained particles acting as collectors, variation of retained particles acting as collectors along the filter depth, etc., which would influence the filter performance to a large extent.

The present research attempts to modify the model proposed by previous workers (1) for predicting filter performance by incorporating the above-mentioned factors. The model is calibrated with a set of laboratory experimental data and tested with other experimental data.

Model Formulation

According to O'Melia and Ali (1) the single collector removal efficiency (η_r) of a filter grain and its associated retained particles can be written as

$$\eta_r = \eta\alpha + N\eta_p\alpha_p(d_p/d_c)^2 \quad (1)$$

Here, η is the single collector efficiency of a clean collector, η_p is the collision efficiency of a retained particle, N is the number of retained particles acting as collectors, d_c and d_p are the diameters of media grain and suspended particles, respectively, and α and α_p are the particle-to-filter grain and particle-to-particle attachment coefficients that can range from 0 to 1.

The prediction of filter performance is dependent on estimation of the number of retained particles acting as collectors. O'Melia and Ali (1) have proposed the equation for estimating N , neglecting the change in surface coverage that must occur with time. The present study takes into consideration the surface coverage of media grain and retained particles acting as collectors along with variation of N with time and depth. The development of a modified equation is described subsequently.

Considering the number of retained particles that can act as collectors (N), which can vary with time and with location in the bed, the removal efficiency of a clean filter grain is $\eta\alpha$. Consequently, the rate of removal of suspended particles by the clean grain is $\eta\alpha n v_{0dc}^2 (\pi/4)$. As the filtration progresses, the single collector removal efficiency increases by N times the rate at which particles are removed by the retained particles acting as collectors; at the same time there is a decrease in the single collector removal efficiency because of the decreased effective area of the media grain and retained particles acting as collectors (N) as a result of surface coverage. The reduction in effective area of the media grain will be proportional to the number of retained particles acting as collectors (N), while the reduction in effective area of the retained par-

ticles acting as collectors would be proportional to the square of the number of retained particles acting as collectors (N^2). This is based on a simple logic as follows. Suppose that on a retained particle two particles can be deposited at any instance. Then the surface coverage of this particle would depend on the particles deposited on these two particles which are 4, i.e., 2^2 . If we suppose that on a retained particle three particles can be deposited at any instance, then the surface coverage of this particle would depend on the particles deposited on these three particles which are 9, i.e., 3^2 . Similarly, if N particles are deposited at any instance, then the surface coverage would depend on the particles deposited on these N particles which are $N \times N$, i.e., N^2 .

Thus, the change in the number of collector particles on a single filter grain can be expressed as follows: rate of change of the number of collector particles on a single filter grain equals rate of removal of particles by a single filter grain plus N times rate of removal of particles by retained particles on a filter grain acting as collectors minus N^2 times rate of particles removed which would contribute to the reduction in effective area of the retained particles acting as collectors.

$$\text{rate of change} = \eta\alpha v_0 n \pi (d_c^2/4) + N\eta_p \alpha_p v_0 n \pi (d_p^2/4) - N\eta_p \alpha_p v_0 n \pi (d_p^2/4) \beta_c - N^2 \eta_p \alpha_p v_0 n \pi (d_p^2/4) \beta_p$$

$$\text{rate of change} = (C_1 + C_2 N - C_3 N - C_4 N^2) n \quad (2)$$

where β_c is the fraction of removed particles which contributes to the reduction in effective area of filter grain and β_p is the fraction of removed particles which contributes to the reduction in effective area of the retained particles acting as collectors.

$$C_1 = \eta\alpha v_0 (\pi/4) d_c^2 \quad (3)$$

$$C_2 = \eta_p \alpha_p v_0 (\pi/4) d_p^2 \quad (4)$$

$$C_3 = \eta_p \alpha_p v_0 (\pi/4) d_p^2 \beta_c \quad (5)$$

$$C_4 = \eta_p \alpha_p v_0 (\pi/4) d_p^2 \beta_p \quad (6)$$

Considering an extremely thin layer of thickness " ΔL " of the filter bed and making the mass balance for N , the following equation can be obtained:

$$\frac{\partial N}{\partial t} + v_0 \frac{\partial N}{\partial L} = [C_1 + (C_2 - C_3)N - C_4 N^2] n \quad (7)$$

The removal efficiency of a single filter grain is related to the removal accomplished by a packed bed through a mass balance about a differential volume element of the filter. For the case considered here, in which retained particles act as collectors so that removal varies with time, the result of such a mass balance is given as follows:

$$\frac{\partial n}{\partial t} + v_0 \frac{\partial n}{\partial L} + \frac{3(1-F)}{2d_c} v_0 n \eta_r = 0 \quad (8)$$

Here, F is the bed porosity.

Equations 1, 7, and 8 comprise a mathematical model to describe the removal efficiency of a filter bed in time and space. Their solution results in the removal efficiency of a filter bed. The exact solution of the above equations is not possible. Simplifying techniques are used to obtain a reasonably accurate solution. In this η_r and n are considered as step functions rather than continuous functions of time and depth. A new algorithm is developed to solve

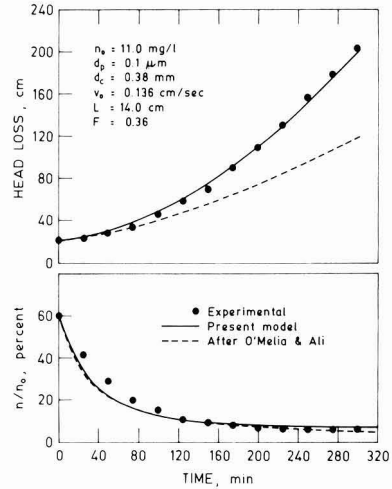


Figure 1. Model calibration.

these equations by making use of numerical methods.

The development of head loss (h_f) is based on the Carman-Kozeny (2) equation modified for change in surface area to volume ratio of the media due to deposition as filter run advances. The equation is as follows:

$$\frac{h_f}{L} = \frac{36}{d_c^2} K \frac{\mu v_0 (1-F)^2}{\rho g F^3} \left[\left[1 + \beta' \frac{N_p}{N_c} \left(\frac{d_p}{d_c} \right)^2 \right] \right] / \left[1 + \frac{N_p}{N_c} \left(\frac{d_p}{d_c} \right)^3 \right]^2 \quad (9)$$

Here, K is an empirical coefficient, μ and ρ are the dynamic viscosity and density of fluid, g is the acceleration due to gravity, v_0 is the undisturbed superficial velocity above the filter bed, N_c is the number of filter grains, N_p is the number of retained particles in the filter bed estimated by using the modified equation (eq 8), and β' is an empirical coefficient that represents the fraction of retained particles that is exposed to the flowing fluid and contributes to the additional surface area.

Model Calibration

Use of eq 1 and 7-9 to describe filter performance requires evaluation of the terms η , η_p , α , α_p , β_c , β_p , and β' . Data obtained by Habibian (3) have been used to estimate certain of these coefficients in calibrating the model (Figure 1). The model is calibrated by using the procedure adopted by O'Melia and Ali (1).

In calibrating the model, the single collector removal efficiency ($\eta\alpha$) is calculated from the experimental data for a "clean" filter. For example, n/n_0 is 0.6 for the filters in Figure 1. Hence, by use of eq 8 at $t = 0$, $\eta\alpha = 1.44298 \times 10^{-3}$. With this initial condition established, the constants $\eta_p \alpha_p$, β_c , and β_p are determined by using nonlinear curve-fitting techniques. Morquardt (BSOLVE regression algorithm) is used to solve for the coefficients in multivariable nonlinear regression equations (4). The values of $\eta_p \alpha_p$, β_c , and β_p were found to be 0.4897×10^{-2} , 0.7582, and 0.2437×10^{-7} , respectively. The values of η and η_p calculated by using Happel's flow model (5-7) for packed beds are 8.4192×10^{-3} and 1.0, respectively. Thus, α and α_p can now be computed as 0.17139 and 0.4897×10^{-2} . In a similar manner, β' was estimated by using eq 9. Calcu-

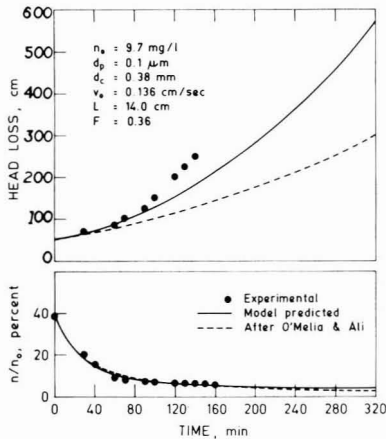


Figure 2. Model verification.

lations of head loss as a function of time were compared with experimental results (Figure 1). A value of $\beta' = 0.193$ is obtained as a result of curve fitting. Very good correlation is obtained for the experimental and model predicted values of removal efficiency and head loss. Removal efficiency and head loss as predicted by O'Melia and Ali (1) are also shown in Figure 1.

Model Verification

The model is tested by using data from other experiments by Habibian (3) and Tare (8) in which one or more filtration variables were significantly different from conditions in the runs used for calibration. Observed values of the particle removal by the clean filters were used to calculate $\eta\alpha$ for each run. Coefficients β_c , β_p , and β' are kept constant as they are not expected to vary with surface properties of media and particle and concentration of particles. The value of $\eta_p\alpha_p$ was estimated for the best fit of the experimental results as it would vary with the surface properties of the media, suspended particles, and size of the suspended particles. Only the typical data from two other filtration experiments by Habibian (3), which is also used by O'Melia and Ali (1), employing different suspended particle sizes ($d_p = 0.1$ and $1 \mu\text{m}$) and influent concentrations ($n_0 = 9.7$ and 37.2 mg/L) are presented in Figures 2 and 3. Proposed model predicted values along with those of O'Melia and Ali (1) are also plotted. The model values are in better agreement with the experimental data than those predicted by using the previous model.

Conclusions

The following conclusions may be drawn on the basis of the present work.

(1) The model presented here has better agreement with results of laboratory experiments compared to the model proposed by previous researchers. This clearly shows that the surface coverage of media grains and retained particles acting as collectors and the variation of retained particles with depth are the important factors.

(2) High values (≈ 0.758) for the surface coverage coefficient for media grains indicate that as the filtration progresses, surface properties of media grains are not important, while particle to particle interaction dominates the filter performance.

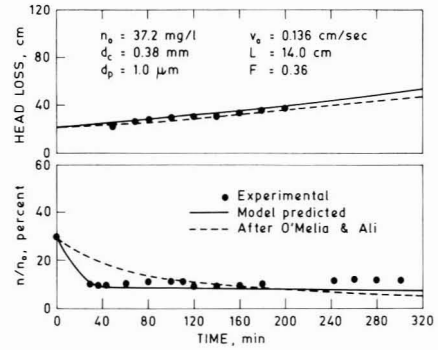


Figure 3. Model verification.

Glossary

C_1	$\eta\alpha v_0(\pi/4)d_c^2$
C_2	$\eta_p\alpha_p v_0(\pi/4)d_p^2$
C_3	$\eta_p\alpha_p v_0(\pi/4)d_p^2\beta_c$
C_4	$\eta_p\alpha_p v_0(\pi/4)d_p^2\beta_p$
d_c	diameter of media grain
d_p	diameter of suspended particle
F	bed porosity
g	acceleration due to gravity
h_f	head loss
K	empirical coefficient
L	depth
N	number of retained particles acting as collectors
N_c	number of filter grains
N_p	number of retained particles
n	undisturbed or bulk particle concentration
n_0	influent particle concentration
t	time
v_0	fluid velocity
α	particle-to-filter grain attachment coefficient
α_p	particle-to-particle attachment coefficient
β'	fraction of retained particles that is exposed to the flowing fluid and contributes to the additional surface area
β_c	fraction of removed particles which contributes for reduction in the effective area of filter grain
β_p	fraction of removed particles which contributes for reduction in the effective area of retained particles acting as collectors
η	single collector efficiency of clean collector
η_p	contact efficiency of a retained particle
η_r	single collector removal efficiency
ρ	density of fluid
μ	dynamic viscosity

Literature Cited

- O'Melia, C. R.; Ali, W. *Prog. Water Technol.* **1978**, *10*, 167-182.
- Carman, P. C. *Trans. Inst. Chem. Eng.* **1937**, *15*, 150-166.
- Habibian, M. T. Ph.D. Dissertation, University of North Carolina, Chapel Hill, NC, 1971.
- Kuester, J. L.; Mize, J. H. *Optimization Techniques with Fortran*, McGraw-Hill: New York, NY, 1973.
- Eliassen, R. J.—*Am. Water Works Assoc.* **1941**, *33*, 128-134.
- Spielman, L. A.; Friedlander, S. K. *J. Colloid Interface Sci.* **1974**, *46*, 22-31.
- Spielman, L. A.; Goren, S. L. *Environ. Sci. Technol.* **1970**, *4*, 135-140.
- Tare, V. Ph.D. Dissertation, Indian Institute of Technology Kanpur, India, 1981.

Received for review April 4, 1983. Revised manuscript received October 25, 1984. Accepted December 28, 1984.

Estimation of Vapor Pressures for Polychlorinated Biphenyls: A Comparison of Eleven Predictive Methods

Lawrence P. Burkhard,[†] Anders W. Andren, and David E. Armstrong*

Water Chemistry Program, University of Wisconsin, Madison, Wisconsin 53706

■ Eleven methods were used to predict vapor pressures at 25.0 °C for 15 polychlorinated biphenyls with experimental values. These results permitted an assessment of the predictive ability of these methods for compounds with low vapor pressures (<1.0 Pa) and one or less experimental determinations. The error for theoretically based methods was high and increased with decreasing vapor pressure. The correlative methods, based on a set of compounds with known vapor pressures, had much better predictive power. The best correlative method was based on a relationship between ΔG_v and gas-liquid chromatographic retention indexes. The predictive error for this method was estimated to be a factor of 1.75. Vapor pressures obtained by using the three best correlative methods for all polychlorinated biphenyls are reported.

Introduction

Vapor pressures are necessary for predicting the behavior of organic microcontaminants in the environment. Calculation of Henry's law constants requires vapor pressure data, since Henry's law constant for a solute with a low aqueous solubility is the ratio of the vapor pressure to the aqueous solubility. In turn, Henry's law constants are used to predict vapor exchange rates across air/water interfaces and fugacity potentials for aqueous systems. Vapor pressure data are also used in the chemical industry and in assessing volatility rates of chemicals used in the workplace.

Vapor pressure data are often scarce for chemicals of environmental concern. In part, data are limited especially for substances with low vapor pressures (<1.0 Pa), due to analytical difficulties. Also, chemical products of environmental concern are often mixtures of many compounds. Vapor pressure determinations for each component in the mixture are often difficult because individual components may not be available in pure form. Thus, physical-chemical property estimation techniques are often used.

When vapor pressures are estimated for a compound of interest, one of two predictive cases is encountered. In the first case, enough experimental data exists to determine a vapor pressure-temperature relationship. In most instances, at least two experimental values must be available. Consequently, vapor pressures can be estimated by interpolation or extrapolation. Problems involved with interpolation have been indirectly examined by many investigators, and equations for correlating measured vapor pressure data with temperature have been derived on either an empirical or theoretical basis. Equations such as those of Clapeyron (1), Antoine (1), Gomez-Nieto-Thodos (2), Kirchoff (1), Riedel-Plank-Miller (1), and Wagner (3) are among an ever expanding list of equations. When interpolating, almost any of these equations may be used if the experimental data are fit well. However, investigations comparing the fitting error of different vapor pressure-temperature relationships reveal that some equations are slightly better than others (1, 4, 5). Usually,

these equations exhibit mathematical behavior that mimics the curvature of vapor pressure-temperature relationships.

For estimation via extrapolation, unacceptable amounts of error must not be introduced into the predictions. This problem can be minimized by requiring the predictive equation to have mathematical behavior characteristic of the vapor pressure-temperature relationship. Ambrose et al. (6) and Scott and Osborn (7) have demonstrated that the Wagner (3) and Cox (8) equations have poorer extrapolation properties when mathematical constraints are not included in the development of the relationships.

In the second predictive case, one or less experimental values exist, and a vapor pressure-temperature relationship cannot be formulated. Estimation of vapor pressures is usually performed with one of two approaches in this situation. These approaches are (1) using vapor pressure-temperature equations derived from a theoretical basis or (2) using equations and parameters derived from molecular topology.

The methods based on theory are derived from the Clausius-Clapeyron equation, and a variety of assumptions are made in their derivation. These assumptions specify the relationships between the enthalpy of vaporization and temperature and the compressibility term and temperature. Some of these methods are described by Lee-Kessler (1), Mackay et al. (9), Riedel (1), Rechsteiner (10), Frost-Kalkwarf-Thodos (1), and Thek-Stiel (1). Most theoretically based equations were developed by using reduced variables and included a reduced boiling point. Consequently, boiling point, critical pressure, and critical temperature must be known or estimated prior to performing the predictions.

The methods based on molecular topology are also theoretically based. However, these methods use chemical theory to develop relationships and chemical parameters from other compounds with known physical-chemical properties. These relationships and chemical parameters are then used in making predictions about the compound of interest. Included in this group are UNIFAC (11), AMP (12), SWAP (13), and comparison (14) methods. These methods have widely different foundations and require knowledge of molecular structure. The SWAP and comparison methods require one or two known vapor pressures for the compound of interest.

When vapor pressures are predicted for chemicals of environmental concern, the predictive problem frequently falls into the second case. Often, the only chemical information known is the molecular structure and, possibly, the melting point of the compound.

Almost all of the predictive methods previously cited are for liquids with vapor pressures of 100 Pa or greater. When these predictive methods are used, difficulties occur for many environmental contaminants because these compounds are often solids at ambient temperatures and have very low vapor pressures (<1.0 Pa). If the compound is a solid, the problem of different states can be avoided by transforming the solid into a subcooled liquid. However, even with this transformation, these methods are extended beyond their predictive limits. The accuracy of such predictions is unknown.

[†]Present address: Center for Lake Superior Environmental Studies, University of Wisconsin—Superior, Superior, WI 55880.

Table I. Experimental Vapor Pressures for Polychlorinated Biphenyls

PCB congener	melting point, °C	vapor pressure at 25.0 °C, Pa	vapor pressure calculation method ^a	temperature range, °C (source of data)
biphenyl	71.0	1.01	In	4.0–40.0 (19–23)
2-	34.0	1.53	ExMP	89.3–267.3 (24)
3-	16.5	7.23×10^{-1}	Ex	152.0 (17), 284.0 (16)
4-	77.7	1.75×10^{-1}	Ex	4.2–24.9 (23)
2,2'-	61.0	1.34×10^{-1}	Ex	37.12–54.92 (25)
3,3'-	29.0	2.58×10^{-2}	ExGC	60.0–130.0 (15)
4,4'-	149.0	2.63×10^{-3}	Ex	59.0–87.0 (25)
2,5-	23.0	7.75×10^{-2}	Ex	100.0–157.0 (17)
2',3,4-	60.0	1.38×10^{-2}	Ex	30.0–40.0 (18)
			ExGC	60.0–130.0 (15)
2,4,6-	62.0	1.24×10^{-2}	ExMP	124.0–172.0 (17)
2,2',5,5'-	87.0	4.97×10^{-3}	Ex	30.0–40.0 (18)
			ExGC	60.0–130.0 (15)
2,2',4,5,5'-	77.0	1.11×10^{-3}	Ex	30.0–40.0 (18)
			ExGC	60.0–130.0 (15)
2,2',4,4',6,6'-	114.0	1.73×10^{-3}	ExGC	60.0–130.0 (15)
2,2',3,3',5,5',6,6'-	162.0	2.89×10^{-5}	Ex	29.0–61.2 (23)
2,2',3,3',4,4',5,5',6,6'-	305.0	5.30×10^{-8}	Ex	50.7–89.8 (23)

^a In = interpolated; ExMP = extrapolated from liquid state vapor pressures and then corrected for subcooled liquid- to solid-state transition; Ex = extrapolated; ExGC = extrapolated by using a gas-liquid chromatographic technique.

The purpose of this investigation is to examine this problem for compounds with very low vapor pressures by using 11 predictive methods. The polychlorinated biphenyls (PCBs) are used as a test case. Vapor pressure data exists for 15 of 210 PCB congeners (15–25). These 15 congeners represent nine different molecular weights and are rather evenly distributed among the molecular weight classes.

Results and conclusions from this investigation have two direct applications. First, since different methods of estimating vapor pressures are compared and evaluated, the results should be directly applicable to other chemical mixtures. Some of the molecular topology estimation methods examined may be applicable to other physical-chemical properties. Second, the best estimation methods will be used to predict vapor pressures for all PCB congeners. These predictions should enable environmental chemists to study and model the physical behavior of PCBs in the environment more accurately.

Methods of Estimation and Correlative Equations

This analysis proceeds from estimation methods requiring the least to those requiring increasing amounts of chemical information. In general, predictive ability should increase with increasing amounts of chemical information.

Several predictive methods require a set of compounds with known vapor pressures. The compounds used in this investigation are listed in Table I, and these values are accepted as being "correct". In general, we believe the error to be less than 20%. However, for the values obtained by large extrapolation (>50 °C), the errors may be much larger and could range up to a factor of 3 or more. Although comparisons are predicated on the assumption that these values (Table I) are correct, some of the error observed in all of the predictive methods is associated with this uncertainty.

Several correlative estimation methods are based on Gibbs' free energy of vaporization, ΔG_v . Basing estimates on ΔG_v eliminates the Gibbs free energy of fusion, ΔG_f , for compounds that are solids at the temperature of interest and permits vapor pressure data of solids and liquids to be included in a correlation.

The thermodynamic cycle and Gibbs' free energies employed by the correlative methods are displayed in Figure 1. From basic chemical thermodynamics (26), Gibbs' free

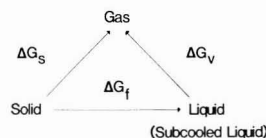


Figure 1. Thermodynamic cycle and Gibbs' free energies.

energies of sublimation, ΔG_s , and vaporization may be determined by using

$$\Delta G_s = -RT \ln P_s \quad (1)$$

$$\Delta G_v = -RT \ln P_l \quad (2)$$

where R is the ideal gas constant, T is the temperature of interest, and P_s and P_l are the vapor pressures of the pure solid and liquid at temperature T .

From equilibrium thermodynamics (27), the ΔG_f can be approximated by eq 3 where ΔS_f is the entropy of fusion

$$\Delta G_f = \Delta S_f(T_m - T) \quad (3)$$

of the solid and T_m is the melting point of the solid. ΔS_f was assumed to be constant for all compounds and equal to 13.1 cal/(mol·K), the average of 16 individual PCB values obtained by Miller et al. (28). For liquids, ΔG_f is equal to zero. Gibbs' free energy for the transformation between the subcooled liquid and vapor states for a solid is calculated as follows:

$$\Delta G_v = \Delta G_s - \Delta G_f \quad (4)$$

From the thermodynamic cycle, the relationship between the vapor pressure of the subcooled liquid and solid states is

$$\ln P_l = \ln P_s + \Delta S_f(T_m - T)/(RT) \quad (5)$$

Method A. This method, presented by Rechsteiner (10), requires no chemical measurements and does not differentiate between isomers. It is based on the Clausius-Clapeyron equation, the modified Watson correlation (10), and Fishtine's method (10). In equation form, the vapor pressure is calculated by using the following relationship:

$$\ln P = \frac{\Delta H_{vb}}{\Delta Z_b RT_b} \times [1 - (3 - 2T_{pb})^m / T_{pb} - 2m(3 - 2T_{pb})^{m-1} \ln T_{pb}] \quad (6)$$

$$\Delta H_{vb}/T_b = K_f(8.75 + R \ln T_b) \quad (7)$$

where P is the vapor pressure of the substance of interest, ΔH_{vb} is the heat of vaporization at the normal boiling point, ΔZ_b is the compressibility factor at the normal boiling point, T_b is the normal boiling point, T_{pb} is T/T_b , and m and K_F are empirical constants. ΔZ_b is assumed to equal 0.97, and m and K_f are tabulated by Rechsteiner (10). Vapor pressures for the PCB congeners were calculated by using boiling points estimated by the method of Meissner (10). No melting points are used in this method.

Method B. This method was recently presented by Mackay et al. (9). Vapor pressures are calculated with a modified Clausius-Clapeyron equation using a linear relationship between the enthalpy of vaporization and temperature, Kistiakowsky's constant, and a fugacity correction ratio between the subcooled liquid and solid states. One empirical constant (0.803) was determined by using 72 compounds in a nonlinear regression analysis. The predictive relationship for a solid is

$$\ln P_s = -(4.4 + \ln T_b)[1.803(T_b/T - 1) - 0.803 \ln (T_b/T)] - 6.8(T_m/T - 1) \quad (8)$$

If the compound of interest is a liquid, the final term in the above equation is ignored. Vapor pressures were predicted by using boiling points estimated by the method of Meissner (10) and the 15 melting points from Table I.

Method C. Originally developed by Miller (29), this method is called the Riedel-Plank-Miller vapor pressure equation by Reid et al. (1). It was derived from the empirical equation

$$\log P = A + B/T + CT + DT^3 \quad (9)$$

by using reduced variables, the Riedel-Plank condition, and known properties of liquids. The Riedel-Plank-Miller relationship is

$$\log P_r = -G/T_r [1 - T_r^2 + k(3 + T_r)(1 - T_r)^3] \quad (10)$$

$$G = 0.210 + 0.200a \quad (11)$$

$$k = [(a/LG) - (1 + T_{rb})]/[(3 + T_{rb})(1 - T_{rb})^2] \quad (12)$$

$$a = (T_{rb} \ln P_c)/(1 - T_{rb}) \quad (13)$$

where P_r , T_r , and T_{rb} are reduced pressure, temperature, and normal boiling point, respectively, a , k , and G are constants defined above, P_c is the critical pressure, and L is a constant equal to 2.3026.

The required input variables, boiling points, critical temperatures, and critical pressures, were estimated by using the methods of Meissner (10), Lydersen (1), and Lydersen (1), respectively. Vapor pressures for the subcooled liquid state were predicted by using the estimated parameters. The vapor pressures for the solid state were derived by using melting points from Table I and eq 5. This method was designed for the liquid state and for vapor pressures ranging from 1.33 to 200.0 kPa.

Method D. This group contribution method was developed by Macknick and Prausnitz (12) from an equation derived from the kinetic theory of Moelwyn-Hughes (30) for liquids by Abrams et al. (31, 32). The vapor pressure-temperature relationship (31, 32) is

$$\ln P_1 = A + B/T + C \ln T + DT + ET^2 \quad (14)$$

where

$$A = \ln (R/V_w) + (s - 1/2) \ln (E_0/R) - \ln [(s - 1)!] + \ln \alpha \quad (15)$$

$$B = E_0/R \quad (16)$$

$$C = 3/2 - s \quad (17)$$

$$D = (s - 1)/(E_0/R) \quad (18)$$

$$E = (s - 3)(s - 1)/[2(E_0/R)^2] \quad (19)$$

where V_w is the van der Waals volume, E_0 is the enthalpy of vaporization at $T = 0$, s is the number of equivalent oscillators per molecule, and α is 0.0966. The parameters s , E_0/R , and V_w are calculated by using eq 20-22 where

$$s = \sum_i v_i s_i \quad (20)$$

$$E_0/R = \sum_i v_i (\epsilon_{0i}/R) \quad (21)$$

$$V_w = \sum_i v_i v_{wi} \quad (22)$$

v_i is the number of carbon atoms of type i in the molecule and s_i , ϵ_{0i} , and v_{wi} are the individual group contribution values. These group contribution values are tabulated in Macknick and Prausnitz (12), Edwards and Prausnitz (33), Ruzicka (34), and Burkhard (35) for s_i and ϵ_{0i}/R and in Bondi (36) for v_{wi} .

Vapor pressures for the liquid or subcooled liquid state are predicted by using the sums of the group contributions in the equation of Abrams et al. (31, 32). If the substance is a solid at the temperature of interest, the solid-state vapor pressure can be estimated from the vapor pressure of the subcooled liquid by using the melting point of the compound and eq 5. This method was designed for the liquid state and for vapor pressures ranging from 1.33 to 200.0 kPa. For the PCB congeners, the melting points from Table I were employed.

Method E. This group contribution method, presented by Jensen et al. (11), is an application of UNIFAC (37) to predicting pure component physical-chemical properties. The basic predictive equation for this method is

$$RT \ln (\rho^s P_1) = \sum_k V_k \Delta g_k + RT \sum_k V_k \ln \Gamma_k \quad (23)$$

$$k = 1, 2, \dots, N$$

where ρ^s is the fugacity coefficient at temperature T and saturation pressure P_1 , N is the number of different groups, V_k is the number of groups of type k , Γ_k is the residual UNIFAC group activity coefficient for a "solution" of the pure compound, and Δg_k is the Gibbs free energy function for group k .

The only term not known in eq 23 is Δg_k . Consequently, Jensen et al. (11) redefined the first term on the right-hand side of equation (23) to be

$$\sum_k V_k \Delta g_k = \sum_k V_k \Delta g_k' + \Delta G'' \quad (24)$$

$$\Delta g_k' = A_k/T + B_k + C_k T + D_k \ln (T) \quad (25)$$

$$\Delta G'' = \sum_{kj} V_{kj} \Delta g_{kj}'' \quad (26)$$

$$\Delta g_{kj}'' = E_k + F_k T \quad (27)$$

Here $\Delta g_k'$ is the structure-independent group contribution, $\Delta G''$ is the structure-dependent group contribution, $\Delta g_{kj}''$ is the structure-dependent group contribution for the interaction of groups j and k , and $A-F$ are empirically derived constants. Constants $A-F$ are tabulated in Jensen et al. (11), and the residual UNIFAC group activity coefficients can be determined by using the data of Magnussen et al. (38). Fugacity coefficients, when required, can be determined by using the method of Hayden and O'Connell (39).

Jensen et al. (11) did not calculate aromatic carbon-chlorine group contributions. We have calculated a value using the method of Jensen et al. (11), and vapor pressure data for chlorobenzene and 1,2-, 1,3-, and 1,4-dichlorobenzenes. Fugacity coefficients were calculated by using the technique of Hayden and O'Connell (39), and input data for these calculations were taken from Reid et al. (1). Group parameters were estimated by performing a least-squares analysis with a pseudo-Gauss-Newton algorithm contained in the BMDP statistical software package (40). The group parameters obtained for the aromatic carbon-chlorine group are for the structure-independent contribution ($\Delta g_k'$) $\Delta g_{Cl}' = -1603.42 + 3.55905T$ and for the structure-dependent contribution ($\Delta G''$) $\Delta g_{Cl}'' = 0$.

For the PCB congeners, subcooled liquid vapor pressures were calculated by using the method of Jensen et al. (11) and the above carbon-chlorine group contribution values. These vapor pressures were calculated by using a fugacity coefficient of 1.00. If the compound of interest was a solid, the subcooled liquid vapor pressure was corrected by using eq 5 and the melting points from Table I. This application is an extrapolation beyond the previously tested range of the UNIFAC method, 1.33 to 266.6 kPa.

Method F. This method is based on a correlation between the ΔG_v and molecular weight. The correlative equation is developed from a set of compounds with known vapor pressures prior to making the predictions.

For the PCB congeners, the correlative equation was determined by regressing ΔG_v vs. chlorine number, N_{Cl} . The equation

$$\Delta G_v = 604.5N_{Cl} + 6717.0 \quad r^2 = 0.898 \quad (28)$$

was found best to represent the experimental data (Table I). r^2 is the correlation coefficient of the regression.

Liquid or subcooled liquid vapor pressures were calculated from the predicted ΔG_v . These values were then corrected to the solid state by using eq 5 and the experimental melting points (Table I).

Method G. This correlative method was presented by Amidon and Anik (41). A relationship between ΔG_v and the molecular surface area is constructed by using a set of compounds with known vapor pressures. Predictions for ΔG_v are made from the derived equation, and these values are used in calculating vapor pressures for the compounds of interest.

For the PCBs, the experimental data (Table I) were best represented by the regression equation

$$\Delta G_v = 39.1(\text{area}) - 761.3 \quad r^2 = 0.899 \quad (29)$$

where area is the molecular surface area of the compound of interest. Vapor pressures were calculated by using the predicted ΔG_v and experimental melting points (Table I).

Molecular surface areas for all PCB congeners were calculated by using the numerical method of Pearlman (42) obtained in program form from the Indiana Quantum Exchange Program, Indiana University, Bloomington, IN. Input data to the program consisted of atomic coordinates, a solvent radius of 0.0, and van der Waal radii. Atomic coordinates were created in-house by using a Fortran program (43). Atomic bond distances and angles for the biphenyl structures were taken from the work of Trotter (44). van der Waal radii for all atoms and bond lengths for chlorine were obtained from Bondi (36) and Weast (12). On the basis of the gas-phase electron diffraction data of Bastiansen (45), the angle between the two benzene rings for each congener was set at the smallest angle where no overlap occurs between the adjacent ortho substituent atoms. These angles were 39°, 57°, 57° or 123°, and 73°

for zero, one, two, three, and four ortho chlorines, respectively.

Method H. This correlative method creates a relationship between the ΔG_v and gas-liquid chromatographic retention indexes. With a set of compounds with known vapor pressures, the correlative relationship can be determined, and hence, the predictions can be made.

Predictions for the PCB congeners were made by using the equation

$$\Delta G_v = 5.44(\text{RI}) - 1711.9 \quad r^2 = 0.955 \quad (30)$$

where RI is the gas-liquid chromatographic retention index and ΔG_v values are for 25.0 °C. Other forms of the correlative equation were evaluated but did not improve the fit of the data (Table I). With the predicted ΔG_v 's, vapor pressures were estimated by using the melting points in Table I.

Retention indexes were obtained from Albro et al. (46) for a Apiezon L stationary phase column. For compounds not measured by these investigators, retention indexes were derived by using the method of Sisson and Welti (47) as described by Albro et al. (46).

Method I. This method is the same as method H, except that a different source of retention data was used (48), viz., relative retention times (RRT) from a 30-m SE-54 fused silica capillary column temperature programmed over the length of the run. The experimental data were best represented by the equation

$$\Delta G_v = 5202.1(\text{RRT}) + 5320.4 \quad r^2 = 0.917 \quad (31)$$

Subcooled liquid-state vapor pressures were determined by using the derived equation and the retention times. Solid-state vapor pressures were then calculated with the melting points (Table I) and eq 5.

Method J. This correlative method is based on molecular connectivity indexes (MCI), the molecular topological indexes of Kier and Hall (49). In this procedure, a stepwise or all-possible-subset regression analysis of a physical property against the MCIs is performed. Consequently, a set of compounds with known vapor pressures is required before predictions can be made. With the derived relationship, the desired physical property can be estimated.

For the PCB congeners, a stepwise linear regression was performed by using the logarithm of the vapor pressure (Table I) as the dependent variable and the MCIs as the independent variables. The final regression equation selected contained the largest number of coefficients in ascending order which were all significantly different from 0.0 at a 95% confidence level. In equation form, the final regression equation used is

$$\log(P) = 2.781 - 0.413(\text{NP10}) \quad r^2 = 0.953 \quad (32)$$

where P is the saturation vapor pressure (for the standard state at the temperature of interest) and NP10 is the number of paths of order 10 MCI. Vapor pressures can be calculated by using the derived equation with a knowledge of the MCI.

For a brief discussion of the MCI theory and computational techniques, the reader is referred to ref 50. If further details are required, the reader is referred to ref 49 and 51.

Method K. This correlative method is an extension of the MCI approach as presented by Burkhard et al. (50). In this method, new variables are derived from a principal component analysis of the MCIs. These new variables are regressed against the physical property of interest to obtain a predictive relationship. This method requires a set of

Table II. Factor of Error in Predicting Vapor Pressures for PCB Congeners^a

PCB congener	method of prediction										
	A	B	C	D	E	F	G	H	I	J	K
biphenyl	-2.01	1.79	1.83	1.99	10.79	-2.39	-2.10	-1.44		-1.70	-1.62
2-	-19.46	1.00	-1.32	-2.26	1.84	-4.31	-3.68	-2.03	-3.63	-5.88	-7.44
3-	-9.20	2.61	1.97	1.15	4.79	-1.66	-1.67	-1.97	-4.69	-2.78	-3.13
4-	-2.23	3.24	2.45	1.43	5.96	-1.34	-1.36	-1.79	-1.82	-1.54	1.28
2,2'-	-7.98	2.22	1.16	-2.55	1.49	-1.94	-1.59	1.41	-1.25	-1.18	-2.20
2,5'-	-4.61	8.72	4.56	1.54	5.87	2.03	2.08	2.60	2.33	1.47	-1.06
3,3'-	-1.54	23.90	12.50	4.22	16.09	5.55	4.84	2.37	3.19	4.42	3.19
4,4'-	6.39	15.19	7.96	2.69	10.25	3.54	3.00	1.19	1.71	8.31	29.58
2',3,4-	-2.88	8.71	2.90	-1.70	2.48	1.96	2.07	3.39	1.22	1.76	1.49
2,4,6-	-3.21	8.19	2.72	-1.80	2.34	1.85	1.85	-1.20	3.10	1.05	1.59
2,2',5,5'-	-33.15	4.75	-1.09	-8.49	-1.47	-1.00	-1.07	-1.01	1.22	1.93	1.31
2,2',4,5,5'-	-34.66	10.79	1.10	-10.70	-1.06	2.03	1.85	1.06	1.90	-1.38	1.54
2,2',4,4',6,6'-	-261.02	1.19	-17.40	-275.54	-11.56	-4.96	-7.33	-2.76	-1.69	-2.15	-5.21
2,2',3,3',5,5',6,6'-	-101.11	3.91	-31.54	-701.37	-1.43	-1.90	-1.81	-1.10	-1.04	1.02	-3.32
2,2',3,3',4,4',5,5',6,6'-	-1.27	14.49	-71.07	-1744.21	195.36	1.43	1.87	1.01	-1.63	-1.32	2.62
average absolute error	32.71	7.38	10.77	184.11	18.18	2.53	2.55	1.75	2.17	2.53	4.44

^aFactor of error is defined as the ratio of the predicted to experimental vapor pressures. However, if this ratio is less than 1.0, the negative reciprocal of this ratio is reported.

compounds with known vapor pressures. With the derived relationship and the new variables, the desired property can be estimated.

For the PCB congeners, the predictive equation was found as described in method I. The predictive equation was

$$\log(P) = -6.792 - 2.649(\text{PCA1}) \quad r^2 = 0.910 \quad (33)$$

where PCA1 is the first principal component variable.

Results and Discussion

Comparison and Evaluation of the Methods. Predictions were made by using each method for the 15 compounds in Table I. Individual and average absolute errors for each method are presented in Table II. The error (factor of error) is defined as the ratio of the predicted to experimental values. However, if this ratio is less than 1.0, the negative reciprocal of this value is reported.

The noncorrelative methods (A-E) have large average errors and poorer predictive ability with increasing molecular weight (Table II). Methods C-E were designed for liquids and pressures ranging from 1.33 to ca. 200.0 kPa. These methods are inaccurate when vapor pressures well below 1.33 kPa (>3 orders of magnitude) are predicted. Methods A and B were designed for compounds with very low vapor pressures. Of the noncorrelative methods (A-E), B is the best. However, vapor pressures predicted by this method are always too high. Structure information is required by all methods, and only method A does not require melting points.

For the correlative methods (F-K), the predictive ability is better. This improvement was expected because the compounds used in developing the correlative equation were also used in evaluating the method. These errors should be viewed as representing best-case predictive ability. Even so, there are noticeable differences in the average errors.

Methods F and G have almost identical overall errors. This was initially unexpected, but comparison of the chlorine number and surface area values revealed an almost perfect correlation between these variables. For other classes of compounds, this relationship may or may not exist.

The correlative methods using gas-liquid chromatographic retention data, H and I, yielded strikingly different average errors. Method H, which used retention indexes obtained from isothermal column conditions, yielded much

better predictions than did method I, which used relative retention times from temperature-programmed column conditions. We were somewhat surprised by the predictive ability of both methods since ΔG_c values at 25.0 °C were correlated with retention data for much higher temperatures, ca. 200 °C. If ΔG_c data existed at higher temperatures, the correlation would probably be much better. Attempts to extrapolate to these temperatures for the compounds in Table I were made, but unacceptable amounts of error were introduced into the ΔG_c values. Consequently, this approach was not considered further.

In addition to the retention indexes for the Apiezon L stationary phase, Albro et al. (46) report retention indexes for 12 additional phases. Their AFEs when used in method H ranged from 1.79 to 2.05. Phases with polarities closest to the SE-54 column used in method I were OV-101 and OV-3, and their AFEs were 1.89 and 1.90. These results suggest that the poor agreement between methods H and I are caused by differences in temperature conditions for the column and retention data type and not by differences in polarity of the stationary phases.

The two methods using MCIs, J and K, also have quite different predictive errors. This difference may be caused by the arbitrary selection of a 95% confidence level for the coefficients in the final predictive equations. However, a higher error was expected for method K based on previous work (50). This study demonstrated that the variables derived from the MCIs employed in method K have increased physical meaning over the MCIs used by method J but have less specificity for each compound. With method K, predictive ability has been sacrificed for an increase in the physical meaning of the derived relationship. For the PCB congeners, the loss of predictive ability is large (Table II).

Correlations were also developed for methods J and K by using ΔG_c instead of log (vapor pressure) as the dependent variable. Because these correlations always showed less predictive ability, they are not reported.

Of the six correlative methods, H and I have the lowest errors. These methods require melting points, gas-liquid chromatographic retention indexes, and a set of compounds with known vapor pressures. Different chemical information is required by methods F, G, and J which have larger but similar errors, ca. 2.50. These methods require parameters calculable for each molecule and a set of compounds with known vapor pressures. Also, methods F and G require melting points. For all of these methods, as-

Table III. Vapor Pressures Calculated from the Product of Average Henry's Law Constants and Average Experimental Aqueous Solubilities and the Predictive Errors for Methods F, H, and J

PCB congener	calculated vapor pressure, Pa	factor of error ^a			exptl
		method F	method H	method J	
biphenyl	1.80	-4.26	-2.57	-3.04	1.79
4-	1.14×10^{-1}	-1.66	1.65	-1.00	-1.17
2,4'-	2.79×10^{-1}	-2.68	-2.79	-5.58	
4,4'-	8.99×10^{-3}	1.03	-2.87	2.44	3.42
2,2',5-	8.97×10^{-2}	-2.44	-1.48	-2.72	
2',3,4-	4.60×10^{-3}	5.54	2.50	3.15	-3.00
2,2',4,4'-	1.01×10^{-2}	1.40	1.10	-2.42	
2,2',4,5'-	1.13×10^{-3}	7.06	6.24	2.45	
2,2',5,5'-	4.27×10^{-3}	1.17	1.16	2.24	-1.17
2,3',4',5-	7.69×10^{-3}	-2.28	-8.37	-2.77	
2,2',3,4,5'-	1.41×10^{-3}	-1.39	-3.59	-1.75	
2,2',3,3',4,4'-	5.08×10^{-5}	3.03	-2.20	1.33	
2,2',3,3',5,6-	1.46×10^{-4}	3.29	3.31	5.51	
2,2',4,4',5,5'-	4.57×10^{-4}	-1.02	-3.69	-6.76	
average absolute error		2.73	3.11	3.08	2.11

^a Factor of error is defined in Table II.

sembling a set of compounds with known vapor pressures will be the most difficult step in the analysis. The retention indexes, molecular weights, surface areas, and MCIs can be readily determined in most laboratories today.

Evaluation of the Predictive Error. To examine the correlative methods further, vapor pressures were predicted for all PCB congeners by using methods F, H, and J [Table I, supplementary material (see paragraph at end of paper regarding supplementary material)]. Included in this listing are the known melting points for PCBs. Where melting points are not known, vapor pressures for the subcooled liquid state are reported for methods F and H.

Where melting point data exist, the average absolute error (factor of error) between the predicted values are 3.0, 4.0, and 5.8 for methods F and H, F and J, and H and J, respectively. Methods F and H are in closest agreement. Of the three predictive techniques, method F, the correlation of chlorine number against ΔG_v , uses the simplest and least descriptive independent variable. The other two methods, H and J, use independent variables that are more descriptive and have similar specificity for each PCB congener. We expected that methods H and J, because of their similar power in differentiating between the PCB congeners, would have the lowest comparative error. Since the comparative error for methods F and H was lower, method J apparently does not have the predictive abilities of method H. This poorer predictive ability of method J may be caused by the MCIs used in constructing the correlative relationship. These MCIs may not have the same intrinsic meaning for the unknown compounds. This problem might be eliminated if a larger set of compounds with known vapor pressures were used when constructing the correlation. Use of method K would also eliminate this problem if MCIs were employed (50).

One additional evaluation was performed on these methods. Vapor pressures were calculated from Henry's law constants (52-55) and experimental aqueous solubilities (28, 56) for 14 PCB congeners. Vapor pressures were determined by calculating the product of the average Henry's law constant and average experimental aqueous solubility. (This relationship is a good approximation for compounds with low aqueous solubilities and vapor pressures.) These vapor pressures, the errors between the calculated and experimental values, and the errors between the calculated and predicted values for methods F, H, and J are reported in Table III.

The amount of uncertainty associated with the calculated vapor pressures is unknown. This uncertainty is in

part caused by the experimental error in Henry's law constants and aqueous solubilities. We can estimate the uncertainty for these values by comparing the calculated and experimental vapor pressures (Table III). For the five compounds with known vapor pressures, an average error of 2.11 was observed for the calculated values.

For methods F, H, and J, the total uncertainties reported in Table III are a combination of errors in the calculated and predicted vapor pressures. When it is assumed that the average errors are approximately equal to their standard deviations, total uncertainties for methods F, H, and J after correction for the predictive error are 1.0, 2.6, and 1.8, respectively. Since none of the corrected uncertainties are significantly larger than the error observed for the calculated values, 2.11, we suggest that uncertainties (average absolute errors) in Table II are representative for these methods.

One important difference between methods B-I and methods A, J, and K is the assumption that the entropy of fusion is 13.1 cal/(mol·K) for all PCB congeners. Methods B-I use this assumption, and methods A, J, and K do not. On the basis of the work of Miller et al. (28), the entropy of fusion varies between 9.8 and 16.6 for the PCB congeners. The absolute factor of error introduced by this assumption ranges from 1.0 to 1.3. However, for decachlorobiphenyl, which has a high melting point, this error rises to 4.8. The magnitude of this error could explain some of the error observed for the methods using this assumption. However, this error appears to be a minor part of the overall error for these methods.

Summary

Eleven methods were used in predicting the vapor pressures at 25 °C for 15 PCB congeners, and these results were compared to the experimental values. This exercise permitted an examination of our current state-of-the-art ability to predict values for compounds with low vapor pressures (<1.0 Pa) which have one or less experimental values. Three general conclusions can be drawn from this investigation. First, noncorrelative methods have poor predictive ability, and error increases with decreasing vapor pressure. Method B, the vapor pressure equation derived by Mackay et al. (9), is the best of these methods and requires the boiling and melting points of the compound. Second, correlative methods that require a set of compounds with known vapor pressures have much better predictive ability than noncorrelative methods. Third, the best predictive method is H, a correlative method using

G_v vs. gas-liquid chromatographic retention indexes. The predictive error was estimated to be ca. 1.75, the error in deriving the correlation.

Acknowledgments

We thank Helen Grogan and Jean Schneider for typing the manuscript and John Harkin for his critical review.

Supplementary Material Available

One table of vapor pressures calculated by using methods F, H, and J for the PCB congeners (5 pages) will appear following these pages in the microfilm edition of this volume of the journal. Photocopies of the supplementary material from this paper or microfiche (105 × 148 mm, 24× reduction, negatives) may be obtained from Microforms Office, American Chemical Society, 1155 16th St., N.W., Washington, DC 20036. Full bibliographic citation (journal, title of article, author, page number) and prepayment, check or money order for \$9.00 for photocopy (\$11.00 foreign) or \$6.00 for microfiche (\$7.00 foreign), are required.

Registry No. Biphenyl, 92-52-4; 2-chlorobiphenyl, 2051-60-7; 3-chlorobiphenyl, 2051-61-8; 4-chlorobiphenyl, 2051-62-9; 2,2'-dichlorobiphenyl, 13029-08-8; 3,3'-dichlorobiphenyl, 2050-67-1; 4,4'-dichlorobiphenyl, 2050-68-2; 2,5'-dichlorobiphenyl, 34883-39-1; 2,3',4'-trichlorobiphenyl, 38444-86-9; 2,4,6-trichlorobiphenyl, 35693-92-6; 2,2',5,5'-tetrachlorobiphenyl, 35693-99-3; 2,2',4,5,5'-pentachlorobiphenyl, 37680-73-2; 2,2',4,4',6,6'-hexachlorobiphenyl, 33979-03-2; 2,2',3,3',5,5',6,6'-octachlorobiphenyl, 2136-99-4; deca-chlorobiphenyl, 2051-24-3.

Literature Cited

- Reid, R. C.; Prausnitz, J. M.; Sherwood, T. K. "The Properties of Gases and Liquids", 3rd ed.; McGraw-Hill: New York, 1977.
- Gomez-Nieto, M.; Thodos, G. *Ind. Eng. Chem. Fundam.* **1977**, *16*, 254-259.
- Wagner, W. *Cryogenics* **1973**, *13*, 470-482.
- Ambrose, D. *J. Chem. Thermodyn.* **1978**, *10*, 765-769.
- McGarry, J. *Ind. Eng. Chem. Process Des. Dev.* **1983**, *22*, 313-322.
- Ambrose, D.; Counsell, J. F.; Hicks, C. P. *J. Chem. Thermodyn.* **1978**, *10*, 771-778.
- Scott, D. W.; Osborn, A. G. *J. Phys. Chem.* **1979**, *83*, 2714-2723.
- Cox, E. R. *Ind. Eng. Chem.* **1936**, *28*, 613-616.
- Mackay, D.; Bobra, A.; Chan, D. W.; Shiu, W. Y. *Environ. Sci. Technol.* **1982**, *16*, 645-649.
- Lyman, W. J.; Reehl, W. F.; Rosenblatt, D. H. "Handbook of Chemical Property Estimation Methods"; McGraw-Hill: New York, 1982.
- Jensen, T.; Fredenslund, A.; Rasmussen, P. *Ind. Eng. Chem. Fundam.* **1981**, *20*, 239-246.
- Macknick, A. B.; Prausnitz, J. M. *Ind. Eng. Chem. Fundam.* **1979**, *18*, 348-351.
- Smith, G.; Winnick, J.; Abrams, D. S.; Prausnitz, J. M. *Can. J. Chem. Eng.* **1976**, *54*, 337-343.
- Othmer, D. F.; Yu, E. *Ind. Eng. Chem.* **1968**, *60*, 22-35.
- Westcott, J. W.; Bidleman, T. F. *J. Chromatogr.* **1981**, *26*, 331-336.
- Weast, R. C. "Handbook of Chemistry and Physics"; CRC Press: Cleveland, OH, 1981.
- Augood, D. R.; Hey, D. H.; Williams, G. H. *J. Chem. Soc.* **1953**, 44-50.
- Westcott, J. W.; Simon, C. G.; Bidleman, T. F. *Environ. Sci. Technol.* **1981**, *15*, 1375-1378.
- Aihara, A. *Bull. Chem. Soc. Jpn.* **1959**, *32*, 1242-1248.
- Bradley, R. S.; Cleasby, T. G. *J. Chem. Soc.* **1953**, 1690-1692.
- Bright, N. F. H. *J. Chem. Soc.* **1951**, 624-625.
- Seki, S.; Suzuki, K. *Bull. Chem. Soc. Jpn.* **1953**, *26*, 209-213.
- Burkhard, L. P.; Armstrong, D. E.; Andren, A. W. *J. Chem. Eng. Data* **1984**, *29*, 248-250.
- Stull, D. R. *Ind. Eng. Chem.* **1947**, *39*, 517-540.
- Smith, N. K.; Gorin, G.; Good, W. D.; McCullough, J. P. *J. Phys. Chem.* **1964**, *68*, 940-946.
- Lewis, G. N.; Randall, M.; Pitzer, K. S.; Brewer, L. "Thermodynamics"; McGraw-Hill: New York, 1961.
- Prausnitz, J. M. "Molecular Thermodynamics of Fluid-Phase Equilibria"; Prentice Hall: Englewood Cliffs, NJ, 1969.
- Miller, M. M.; Ghodbane, S.; Wasik, S. P.; Tewari, Y. B.; Martire, D. E. *J. Chem. Eng. Data* **1984**, *29*, 184-190.
- Miller, D. G. *J. Phys. Chem.* **1965**, *69*, 3209-3212.
- Moelwyn-Hughes, E. A. "Physical Chemistry", 2nd ed.; Pergamon Press: Oxford, 1961.
- Abrams, D. S.; Massaldi, H. A.; Prausnitz, J. M. *Ind. Eng. Chem. Fundam.* **1974**, *13*, 259-262.
- Abrams, D. S.; Massaldi, H. A.; Prausnitz, J. M. *Ind. Eng. Chem. Fundam.* **1977**, *16*, 392.
- Edwards, D. R.; Prausnitz, J. M. *Ind. Eng. Chem. Fundam.* **1981**, *20*, 280-283.
- Ruzicka, V., Jr. *Ind. Eng. Chem. Fundam.* **1983**, *22*, 266-267.
- Burkhard, L. P. *Ind. Eng. Chem. Fundam.* **1984**, *24*, 119-120.
- Bondi, A. "Physical Properties of Molecular Crystals, Liquids, and Gases"; Wiley: New York, 1968; Chapter 14.
- Fredenslund, A.; Gmehling, J.; Rasmussen, P. "Vapor-Liquid Equilibria using UNIFAC"; Elsevier: Amsterdam, 1977.
- Magnussen, T.; Rasmussen, R.; Fredenslund, A. *Ind. Eng. Chem. Process Des. Dev.* **1981**, *20*, 331-339.
- Hayden, J. G.; O'Connell, J. P. *Ind. Eng. Chem. Process Des. Dev.* **1975**, *14*, 209-216.
- Ralston, M. In "BMDP-79. Biomedical Computer Programs P-Series"; Dixon, W. J.; Crown, M. B., Eds.; University of California Press: Los Angeles, 1979; pp 484-498.
- Amidon, G. L.; Anik, S. T. *J. Chem. Eng. Data* **1981**, *26*, 28-33.
- Pearlman, R. S. In "Physical Chemical Properties of Drugs"; Yalkowsky, S. Y.; Sikula, A. A.; Valvani, S. C., Eds.; Marcel Dekker: New York, 1980; Medicinal Research Series 10, pp 321-347.
- Loux, N. University of Wisconsin—Madison, Madison, WI, unpublished program, 1984.
- Trotter, J. *Acta Crystallogr.* **1961**, *14*, 1135-2240.
- Bastiansen, O. *Acta Chem. Scand.* **1949**, *3*, 408-414.
- Albro, P. W.; Haseman, J. K.; Chemmer, T. A.; Corbett, B. J. *J. Chromatogr.* **1977**, *136*, 147-153.
- Sissons, D.; Welti, D. *J. Chromatogr.* **1971**, *60*, 15-32.
- Doucette, W. J. University of Wisconsin—Madison, Madison, WI, personal communication, 1984.
- Kier, L. B.; Hall, L. H. "Molecular Connectivity in Chemistry and Drug Research"; Academic Press: New York, 1976.
- Burkhard, L. P.; Andren, A. W.; Armstrong, D. E. *Chemosphere* **1983**, *12*, 935-943.
- Kier, L. B. In "Physical Chemical Properties of Drugs"; Yalkowsky, S. H.; Sikula, A. A. P.; Valvani, S. C., Eds.; Marcel Dekker: New York, 1980; Medicinal Research Series 10, pp 277-320.
- Mackay, D.; Shiu, W. Y.; Sutherland, R. P. *Environ. Sci. Technol.* **1979**, *13*, 333-337.
- Atlas, E.; Foster, R.; Giam, C. S. *Environ. Sci. Technol.* **1982**, *16*, 283-286.

- (54) Murphy, T. J.; Pkojowczyk, J. C.; Mullin, M. D. In "Physical Behavior of PCBs in the Great Lakes"; Mackay, D.; Patterson, S.; Eisenreich, S. J.; Simmons, M. S., Eds.; Ann Arbor Science: Ann Arbor, MI, 1983; pp 49-58.
- (55) Neely, W. B. In "Physical Behavior of PCBs in the Great Lakes"; Mackay, D.; Patterson, S.; Eisenreich, S. J.; Simmons, M. S., Eds.; Ann Arbor Science: Ann Arbor, MI, 1983; pp 71-88.
- (56) Mackay, D.; Mascarenhas, R.; Shiu, W. Y.; Valvani, S. C.; Yalkowsky, S. H. *Chemosphere* 1980, 9, 257-264.
- (57) Ballschmiter, K.; Zell, M. *Fresenius' Z. Anal. Chem.* 1980, 302, 20-31.

Received for review March 30, 1984. Accepted November 28, 1984. This work was funded by the University of Wisconsin Sea Grant College Program under grants from the Office of Sea Grant, National Oceanic and Atmospheric Administration, U. S. Department of Commerce, and from the State of Wisconsin. Federal Grant NA800-AA-D-00086, Project R/MW-21.

Phase-Transfer-Catalyzed Methylation of Hydroxyaromatic Acids, Hydroxyaromatic Aldehydes, and Aromatic Polycarboxylic Acids

Sowmianarayanan Ramaswamy and Murugan Malaiyandi*

Bureau of Chemical Hazards, Environmental Health Directorate, HPB, Health and Welfare Canada, Tunney's Pasture, Ottawa, Canada K1A 0L2

Gerald W. Buchanan

Ottawa—Carleton Institute for Research and Graduate Studies in Chemistry, Department of Chemistry, Carleton University, Ottawa, Canada K1S 5B6

■ The phase-transfer-catalyzed methylation of hydroxyaromatic acids, hydroxyaromatic aldehydes, and aromatic polycarboxylic acids with iodomethane or dimethyl sulfate in dichloromethane-water solvent system at room temperature using tetra-*n*-butylammonium hydroxide provided moderate (68%) to near quantitative yields of O-methylation products. It was observed that iodomethane tends to give more ring methylation products than dimethyl sulfate under identical conditions. The methylation products were identified by their spectral characteristics. The ¹³C nuclear magnetic resonance spectra of the methyl derivatives are discussed in detail.

Introduction

It has been reported (1, 2) that the possible oxidation products of fulvic acids from different sources were hydroxyaromatic acids, hydroxyaromatic aldehydes, and aromatic polycarboxylic acids. Gas chromatographic analysis of these oxidation products in the underivatized form are prone to strong adsorption and decomposition on gas chromatographic columns and at the injection ports. In order to avoid loss of the above compounds, sometimes found in trace amounts in the oxidized mixture, it is necessary to prepare suitable derivatives of these compounds to quantitate by the gas chromatographic technique. Phenols and carboxylic acids are most often transformed into their corresponding methyl derivatives prior to gas chromatographic analysis. There are several reagents to effect this transformation. Diazomethane is often used as the reagent for the methylation of the oxidation products of fulvic materials (1, 3). However, the use of diazomethane has been reported to lead to significant side reactions in the case of unsaturated acids (4, 5) although this reagent afforded quantitative yields of methylated products with saturated systems. In addition, diazomethane is potentially hazardous and explosive in high concentrations.

Silver oxide catalyzed methylation using iodomethane has been frequently employed for the methylation of phenols and carboxylic acids (6). This method involves a mixed solid-liquid-phase reaction and requires prolonged reaction periods (sometimes several days) (7), often re-

sulting in poor yields of products (see below). The use of dimethyl sulfate and potassium carbonate in acetone (2) provides high yields of methylation products but requires refluxing conditions for the reaction to occur and is not adaptable to the methylation of aqueous solutions containing phenols and carboxylic acids.

A mild procedure involving the use of phase-transfer catalysis with benzyltri-*n*-butylammonium salts in the alkylation of phenoxide ion with alkyl halide or sulfate in a dichloromethane-water system was employed by McKillop et al. (8) to prepare the ethers of phenols in excellent yields. Tivert and co-workers (9) have studied the kinetics of methylation of several substituted phenols by this procedure. However, methylation of carboxylic acids, hydroxyaromatic aldehydes, using phase-transfer catalysis have not been reported in the literature. Since some of these compounds have been reported as products of oxidation of fulvic acid, the present investigation details conditions and procedures using the phase-transfer technique involving tetra-*n*-butylammonium hydroxide as the catalyst with either iodomethane or dimethyl sulfate for the methylation of these compounds.

Materials and Methods

Reagents and Chemicals. Baker-analyzed reagent silver oxide was purchased through Canadian Laboratory Supplies Ltd., Ottawa. All other reagents and candidate acids and aldehydes were purchased from Aldrich Chemical Co., Inc., Montreal, and were used without further purification. Glass-distilled dichloromethane and ethyl acetate were obtained from Caledon Laboratories, Mississauga, and redistilled prior to use. Glass-distilled hexane purchased from Caledon Laboratories was purified according to the method of Malaiyandi and Benoit (10). Merck precoated TLC sheets of silica gel 60/F-254 were used for analytical thin-layer chromatography (TLC). Analtech Uniplate (preparative silica gel GF plates) purchased from Fisher Scientific Co. Ottawa, were used for preparative thin-layer chromatography.

Methods and Instruments. Melting points were determined on a Büchi Model M-50 melting point apparatus. Infrared spectra were recorded on a Perkin-Elmer Model 221 spectrometer using KBr pellets in the case of crys-

talline products and as thin films in the case of liquids and were calibrated with the bands at 3027.1, 2850.7, 1601.4, 906.7, and 698.7 cm^{-1} of polystyrene. The ^{13}C and ^1H nuclear magnetic resonance (NMR) spectra were recorded on a Varian Model XL-200 spectrometer, as solutions in CDCl_3 with tetramethylsilane as the internal standard. Chemical shifts are reported on the δ scale. The multiplicity, integrated peak area and coupling constants in hertz (Hz), wherever observed, are indicated in parentheses after each signal. The following abbreviations are used in the description of the multiplicity of each signal in the ^1H NMR spectrum: s = singlet, d = doublet, m = multiplet, dd = doublet of doublets, dm = doublet of multiplets, and ddd = doublet of doublet of doublets.

The ^{13}C spectra were obtained routinely in the presence of complete ^1H noise decoupling. Spectral width was 10 000 Hz, 32K data points, pulse width = 7.0 μs (45°), acquisition time = 1.6 s, and repetition rate = 1.0 s. Normally 1000 scans were sufficient for adequate signal to noise ratios.

The mass spectra were recorded on a Finnigan Model 4000 automated gas chromatography/mass spectrometry (GC/MS) system coupled to an Inco Data System.

Mass Spectrometric Conditions. The ionization energy was 70 eV; the electron multiplier was at 1200 V.

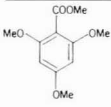
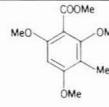
Gas Chromatography Conditions. The following were the conditions: Column DB-5 15m \times 0.25 cm (i.d.); temperature of injection, port 250 $^\circ\text{C}$; column initial temperature 50 $^\circ\text{C}$; initial hold 0.1 min; programmed to 150 $^\circ\text{C}$ at 15 $^\circ\text{C}/\text{min}$ and then to 270 $^\circ\text{C}$ at 5 $^\circ\text{C}/\text{min}$; carrier gas helium; head pressure 5 psi; sample size 3 μL .

The gas chromatographic analyses for identification were carried out on a Varian Vista 6000 gas chromatograph coupled to a dedicated Varian Vista 401 data processor and fitted with flame ionization detector and a 1.8 m \times 2 mm (i.d.) coiled glass column packed with Chromosorb WHP (100–120 mesh) coated with 3% OV-17. The analyses of the derivatives were carried out under the following instrumental operating conditions: column temperature initial 50 $^\circ\text{C}$ programmed to 100 $^\circ\text{C}$ at 10 $^\circ\text{C}/\text{min}$ followed by increasing the rate at 15 $^\circ\text{C}/\text{min}$ to 225 $^\circ\text{C}$; final hold 12.0 min; injection port temperature 250 $^\circ\text{C}$; detector temperature 300 $^\circ\text{C}$; N_2 flow 30.75 mL/min; H_2 flow 29.25 mL/min; air flow 286 mL/min; attenuation 16 \times 1; current 10^{-12} A; chart speed 0.5 cm/min; sample size 3 μL . H_2 flow was adjusted for maximum sensitivity by injecting solution of methyl 2-methoxybenzoate.

The gas chromatographic response factors and retention times for these derivatives were also obtained as an average of three to five injections of hexane solutions of the samples. The products were characterized by infrared, ^1H , and ^{13}C nuclear magnetic resonance spectra.

Standard Procedure for the Methylation of Hydroxyaromatic Acids, Hydroxyaromatic Aldehydes, and Benzene Polycarboxylic Acids. A mixture of 1 mmol of the substrate in 2 mL of dichloromethane, 1.5 equiv of dimethyl sulfate or iodomethane, and 1.5 equiv of tetra-*n*-butylammonium hydroxide (aqueous 1.5 M solution) was stirred vigorously at room temperature, for 18 h (overnight). The reaction mixture was extracted with 40 mL of ethyl acetate, and the extract was washed 3 times with 10-mL portions of water and dried over purified Na_2SO_4 (10), and the solvents were evaporated. The residue, if solid, was purified by recrystallization or, if liquid, by thin-layer chromatography on silica gel plates with 25% ethyl acetate in hexane (V/V) as the developing solvent, and the products were identified by GC/MS. (Note, when dimethyl sulfate was used as an alkylating

Table I. Methylation of 2,4,6-Trihydroxybenzoic Acid

reagents, solvent conditions ^a	yields of products, %	
		
CH_3I , Ag_2O , acetone, 25 $^\circ\text{C}$	19	4 ^c
CH_2Cl_2 , 22–25 $^\circ\text{C}$ ^b	40–60	
CH_3I , $\text{N}(n\text{-C}_4\text{H}_9)_3\text{OH}$, $\text{CH}_2\text{Cl}_2\text{-H}_2\text{O}$, 22–25 $^\circ\text{C}$	20	18
$(\text{CH}_3\text{O})_2\text{SO}_2$, $\text{N}(n\text{-C}_4\text{H}_9)_3\text{OH}$, $\text{CH}_2\text{Cl}_2\text{-H}_2\text{O}$, 22–25 $^\circ\text{C}$	68	7
$(\text{CH}_3\text{O})_2\text{SO}_2$, anhydrous K_2CO_3 , acetone, 56 $^\circ\text{C}$	90–100	0

^a All reactions were allowed to stir at the indicated temperatures, overnight. ^b We are thankful to Dr. V. Paramasigamani for this result. ^c The compound was identified by ^1H NMR resonances at δ (CDCl_3) 6.243 (s, 1), 3.883 (s, 3), 3.821 (s, 3), 3.804 (s, 3), 3.749 (s, 3), and 2.054 (s, 3), by ^{13}C NMR resonances at δ 167.2, 160.3, 157.0, 156.0, 111.9, 110.5, 91.3, 61.8, 56.0, 55.7, 52.3, and 8.3, and by GC/MS peak at m/z 240 consistent with the molecular formula $\text{C}_{12}\text{H}_{16}\text{O}_5$ of the parent ion. The corresponding product derived from methylation reaction with CD_3I showed a peak at m/z 255 by GC/MS analysis in agreement with the formula $\text{C}_{12}\text{H}_{15}\text{O}_5$. This establishes the fact that the nuclear methylation product results from direct ring methylation reaction and not from a nuclear methylated precursor originally present in the starting material.

agent, the reaction mixture was stirred with excess of 1 M aqueous ammonium hydroxide for ca. 1 h to destroy the unreacted reagent prior to extraction with ethyl acetate.)

Results and Discussion

Our preliminary investigation using different alkylating agents and hindered 2,4,6-trihydroxybenzoic acid is summarized in Table I.

The silver oxide-iodomethane route was not pursued due to poor and varying yields of products whereas the dimethyl sulfate-potassium carbonate method is not amenable to the methylation of aqueous solutions of the oxidation products of fulvic acid (see above) since anhydrous conditions are absolutely essential for the reaction to go to completion. Investigations of phase-transfer-catalyzed methylation of hydroxyaromatic acids and aldehydes in aqueous media were therefore carried out by using both iodomethane and dimethyl sulfate (entries 1–10, Table II). Methylation of aromatic polycarboxylic acids were also studied by using the latter reagent alone (entries 11–16, Table II). When ethyl acetate was used as the extracting solvent for the methyl derivatives, better yields were obtained compared to extraction with 25% ethyl acetate in hexane (v/v).

In a typical experiment 1.5 equiv of the alkylating agent was added to a two-phase system consisting of 1.5 equiv of a 40% (1.5 M) aqueous solution of tetra-*n*-butylammonium hydroxide and a dichloromethane solution of the hydroxyaromatic acid, hydroxyaromatic aldehyde, or benzene polycarboxylic acid. The reactions were complete in 12–18 h. The competing dimethyl sulfate hydrolysis, as evidenced by the reaction mixture becoming acidic, and consequent consumption of the base warranted the use of excess of base and dimethyl sulfate.

Although, with simple hydroxyaromatic acids, both iodomethane and dimethyl sulfate gave good yields of methylation products (entries 1 and 2, Table II), iodomethane gave varying amounts of ring methylation products with polyphenolic acids and aldehydes containing hydroxyl in the 1,3-positions (entries 3, 6, and 9 Table II). For example, in the case of 2,4,6-trihydroxybenzoic acid (entry 5),

1985

Environmental Science & Technology

ES&T

Order *your own* subscription to ES&T and be among the first to get the most authoritative technical and scientific information on environmental issues.

Yes, I want my own subscription to ENVIRONMENTAL SCIENCE & TECHNOLOGY at the rate I've checked:

One Year	ACS Members	Nonmembers Personal	Nonmembers Institutional
U.S.	<input type="checkbox"/> \$ 26	<input type="checkbox"/> \$ 35	<input type="checkbox"/> \$149
Mexico & Canada	<input type="checkbox"/> \$ 34	<input type="checkbox"/> \$ 43	<input type="checkbox"/> \$157
Europe	<input type="checkbox"/> \$ 40	<input type="checkbox"/> \$ 49	<input type="checkbox"/> \$163
All Other Countries	<input type="checkbox"/> \$ 49	<input type="checkbox"/> \$ 58	<input type="checkbox"/> \$172

- Payment Enclosed (Payable to American Chemical Society)
 Bill Me Bill Company Charge my: VISA MasterCard

Card No. _____

Exp. Date _____ Interbank # _____
 (Mastercard Only)

Signature _____

Name _____

Title _____

Employer _____

Address _____

City, State, Zip _____

Employer's Business: Manufacturing, type _____

Academic Government Other _____

*Subscriptions at these rates are for personal use only.

All foreign subscriptions are now fulfilled by air delivery. Foreign payment must be made in U.S. currency by international money order, UNESCO coupons, U.S. bank draft, or order through your subscription agency. For nonmember subscription rates in Japan, contact Maruzen Co., Ltd. Please allow 45 days for your first copy to be mailed. Redeem until December 31, 1985.

MAIL THIS POSTAGE-PAID CARD TODAY!

3145H



**CALL
TOLL
FREE**

(800) 424-6747 (U.S. only)



NO POSTAGE
NECESSARY
IF MAILED
IN THE
UNITED STATES

BUSINESS REPLY CARD

FIRST CLASS PERMIT NO. 10094 WASHINGTON D.C.

POSTAGE WILL BE PAID BY ADDRESSEE

American Chemical Society

Periodicals Marketing Dept.
1155 Sixteenth Street, N.W.
Washington, D.C. 20036

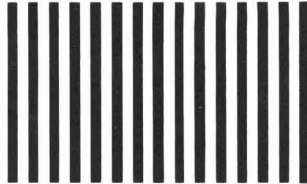
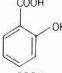
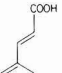
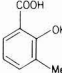
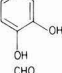
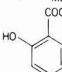
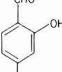
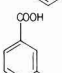
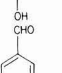
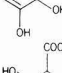
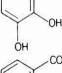
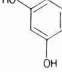
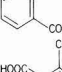
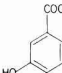
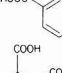
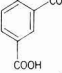
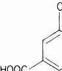


Table II. Methylation of Hydroxyaromatic Acids, Hydroxyaromatic Aldehydes, and Aromatic Polycarboxylic Acids

no.	substrate	product yields, % ^a		no.	substrate	product yields, % ^a	
		CH ₃ I, N(<i>n</i> -C ₄ H ₉) ₄ OH, CH ₂ Cl ₂ -H ₂ O	(CH ₃ O) ₂ SO ₂ , N(<i>n</i> -C ₄ H ₉) ₄ OH, CH ₂ Cl ₂ -H ₂ O			CH ₃ I, N(<i>n</i> -C ₄ H ₉) ₄ OH, CH ₂ Cl ₂ -H ₂ O	(CH ₃ O) ₂ SO ₂ , N(<i>n</i> -C ₄ H ₉) ₄ OH, CH ₂ Cl ₂ -H ₂ O
1		~100	~100	8		~100	~100
2		~98	~100	9		35+ (37)	~100
3		60+ (10)	~100	10			~100
4		95	~100	11			85
5		20+ (18)	68+ (6.6)	12			~100
6		64+ (6.4)	89	13			81
7		98	100	14			98
				15			86
				16			84

^aThe yields were calculated on the basis of isolated material. The numbers in parentheses refer to the yields of ring methylation products.

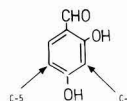
a mixture of the O-methylated and ring-methylated products were obtained in the ratio of 10:9, when iodomethane was used as the methylating agent. The ratio of the two products increased in favor of the O-methylated product (10:1) when dimethyl sulfate was used in lieu of iodomethane. This tendency to give rise to ring methylation product in going to iodomethane from dimethyl sulfate can be explained in terms of hard and soft acids and bases concept (11). The strongly electron-withdrawing sulfate group tends to concentrate more positive charge on the carbon attached to the sulfate, making it a harder acid than does the iodide group. Therefore, dimethyl sulfate tends to alkylate the harder nucleophilic center, viz., oxygen, whereas the carbon attached to iodide, being a softer acid, alkylates on the softer nucleophilic center, viz., carbon.

The pronounced carbon reactivity of compounds containing hydroxyl groups in the 1,3-position may be ascribed to the enhanced activation of the aromatic ring by the electron-releasing +M effect of the two phenolic oxygen atoms which reinforces the effects of one another.



Apparently, this reinforcing activation must be present for ring methylation to occur under these conditions. Compounds containing only one OH or two OH's in 1,2-positions do not give rise to any observable quantities of ring methylation. Interestingly enough, no noticeable amount of second methylation takes place in any of these compounds. This may be due to the fact that once methylation has occurred on the ring, activation of the ring by the oxygen is prevented by steric inhibition of resonance. The steric compression due to the 1,2,3 substituents forces the C-2 oxygen atom out of the plane of the benzene ring. This effectively suppresses the overlap of the p orbital of the oxygen atom with the π system of the benzene ring. Poorer yields of ring methylation products formed in the case of 3,4,5-trihydroxybenzoic acid (entry 6, Table II) as compared with 2,4,6-trihydroxybenzoic acid (entry 5, Table II) lends support to the above view.

In the case of 2,4-dihydroxybenzaldehyde which can give



rise to two regioisomeric ring methylated products, methylation occurred only at C-3, and no observable amount

of C-5 methylated product was obtained, although resonance participation can be expected to equally stabilize these two positions. This may be attributed to the stabilization of the C-3 anion by an internal coordination of the adjacent oxygen atoms with the tetraalkylammonium ion.



High yields of methylation product were obtained even with the hindered phenolic acid 3-methylsalicylic acid (entry 2, Table II). Further, the polycarboxylic acids (entries 11–16, Table II) in aqueous media also gave excellent yields (85–100%) by this procedure.

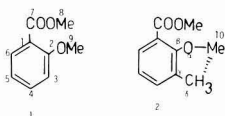
A summary of the melting points (for solid derivatives), the relative retention time, and the relative response factor per nanogram of the derivatives with reference to methyl 2-methoxybenzoate is available as supplementary material (see paragraph at end of paper regarding supplementary material).

It can be seen that isomeric pairs of methyl 2,4,6-trimethoxybenzoate and methyl 3,4,5-trimethoxybenzoate and 2,4- and 3,4-dimethoxybenzaldehydes are easily resolved by the OV-17 packing. Under the experimental conditions, there is a slight overlap of peaks of the isomeric pairs of methyl 2,6-dimethoxybenzoate and methyl 3,4-dimethoxybenzoate. Further in the case of trimethyl benzenetricarboxylates the 1,3,5-tricarboxylate (entry 14 Table A, available in the supplementary material) is easily separated from the other two isomers.

The relative response factor of the isomeric mixtures are quite different for the dimethoxybenzaldehydes (3,4 > 2,4) and only slightly different for methyl dimethoxybenzoates (3,4 > 2,6) whereas in the case of methyl trimethoxybenzoates the 3,4,5 isomer is far greater than the 2,4,6 isomer. It would seem that 3,4-dimethoxy derivatives have a higher response factor than the 2,4- or 2,6-dimethoxy derivatives. However, a similar correlation on the relative response factor was not observed among the benzenetricarboxylic acid esters, except that the 1,3,5 isomer has a better response than the 1,2,3 or the 1,2,4 isomers even though their carbon:oxygen ratios are identical.

The spectroscopic data of the methylation products are also available as supplementary material. The infrared spectra of these compounds did not show any hydroxyl group. All the compounds showed peaks due to the parent ions in the GC/MS. Assignment of ^1H NMR signals was straightforward and hence will not be elaborated here. Since the ^{13}C NMR spectra of many of these compounds are not available in the literature and since the substituent-induced chemical shifts are significantly larger with ^{13}C nucleus than those observed with ^1H nucleus, the ^{13}C NMR spectra of these compounds are discussed in detail.

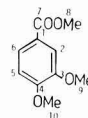
The ^{13}C assignments were made via a variety of techniques. For cases in which the ^1H assignment was unambiguous, selective ^1H decoupling identified the directly bonded carbons. Single frequency off-resonance decoupling (SFORD) methods were used to distinguish between carbons bearing zero, one, or three directly bonded protons. Occasionally, chemical shifts of model compounds (12) were employed. For example, in the case of 1, the ^{13}C



chemical shifts (Table B, available in the supplementary material) can be assigned, except for C-4 and C-6, on the basis of SFORD experiments and by using methylbenzoate (13) and anisole (14) as model compounds. In the ^1H spectrum, the aromatic proton on C-6 appears at δ_{H} 7.781. Selective irradiation at this site sharpens the ^{13}C resonance at δ_{C} 131.6, thus identifying C-6. Subsequently, the resonance at δ_{C} 133.5 is assigned to C-4 by elimination.

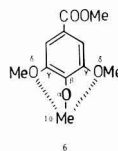
For 2, similar methods were employed for signal assignment. Interestingly, the C-10 carbon of 2 is deshielded by 5.6 ppm relative to its counterpart in 1. This appears to be another example of the deshielding "δ" effect (15) which is now well documented, since C-10 of 2 experiences an additional δ steric interaction (above) which is not present at C-9 of 1.

Assignments for 3 are straightforward by consideration of symmetry and SFORD experiment results. In the case of 4, the major assignment problem lies in the distinction of resonance for C-2 vs. C-5. This was accomplished, however, by consideration of the totally ^1H -coupled ^{13}C spectrum. It is known (16) that *C–C–C–H couplings (i.e., vicinal or three-bond J 's) are in the range of 5–12 Hz for substituted benzenes, whereas C–C–H couplings (i.e., geminal or two-bond J 's) are smaller (0.3–3.5 Hz). Also,



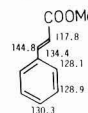
it is evident for 4 that the proton on C-6 is vicinal to C-2, but there are *no* aromatic protons vicinal to C-5. In the ^1H coupled spectrum, the resonance centered at δ_{C} 111.9 shows a splitting of 7.2 Hz, in addition to the large $^1J_{\text{CH}}$, whereas the resonance at δ_{C} 110.2 shows only a large $^1J_{\text{CH}}$. Thus, C-2 is assigned to the 111.9 ppm line, and C-5 resonates at 110.2 ppm.

For compounds 5 and 6, symmetry considerations and

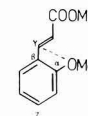


SFORD results led to straightforward resonance assignments. Again, the OCH_3 carbon (C-10) of 6 shows a marked deshielding effect (ca. 5 ppm) relative to C-10 of 4. Apparently when *both* *ortho* sites are occupied, as in 2 and 6, the O–CH₃ group cannot escape (by rotation) the steric influence of the δ groups adjacent to it, and a deshielding trend is noted.

In the case of methyl *o*-methoxycinnamate 7, cinnamic acid was used as a model compound (14), and we also recorded the ^{13}C spectrum of methyl cinnamate (with assignments as depicted).

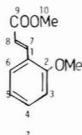


These data, as well as those for anisole, and SFORD results permitted assignments for 7. Interestingly, the *ortho*



OCH₃ group of **7** causes a 4.5 ppm shielding effect at C-7 of **7** vs. the corresponding carbon of methyl cinnamate, a consequence of the well-known (11) "γ" steric shift.

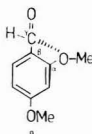
There is a concomitant *deshielding* of 2.9 ppm at C-8 of **7** vs. methyl cinnamate. This cannot be attributed to δ steric shifts, however, since there could be bond rotation about the C-1-C-7 bond of **7** to generate other conformers,



which lack δ steric interactions.

Compound **8** has the same orientation of aromatic substituents as compound **4**. Again, distinction between C-2 and C-5 was made on the basis of results from the completely ¹H-coupled ¹³C spectrum. Other assignments were made by using anisole and methyl cinnamate as model compounds, as well as by considering SFORD experiment results.

In the case of aldehyde **9**, results for benzaldehyde itself



(13) and anisole were used in conjunction with SFORD results to make signal assignments. The aldehyde resonance of **9** is shielded by 2.4 ppm relative to benzaldehyde, due to the γ effect of the ortho oxygen atom.

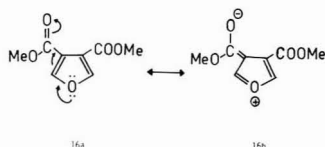
For **10**, in which the ortho oxygen is not present, the aldehyde carbon resonance is within 0.5 ppm of that for benzaldehyde. Again, the ¹H-coupled ¹³C spectrum was employed to distinguish between resonances for C-2 and C-5, as was done for **8** and **4**.

Resonances for compound **11** were assigned by using SFORD results and selective ¹H decoupling. The protons on C-3,6 are deshielded by 0.28 ppm relative to those on C-4,5. It is well-known that CO₂Me groups deshield ortho H's relative to meta or para hydrogens (17). Accordingly, selective ¹H irradiation was used to identify the carbon resonances for C-3,6 vs. those for C-4,5.

Symmetry considerations and SFORD results led directly to assignments for **12**. Interestingly, the central carbonyl group (C-8) is deshielded relative to C-7 and C-9. This effect may be caused by steric inhibition to conjugative electron release by the aromatic ring into the central carbonyl function, due to the presence of ester functions at each ortho site. Notably, two ortho OCH₃ groups do not cause a similar deshielding at the central carbonyl carbon (i.e., compare **2** and **3** results).

Compound **13** presented the most difficult case for making reliable ¹³C signal assignments. The aromatic proton on C-3 is the most deshielded, resonating at δ_H 8.42. Selective ¹H decoupling identified the ¹³C resonance at δ 126.8 as being due to C-3. Subsequently, distinction between C-5 and C-6 was made on the basis of the totally ¹H-coupled ¹³C spectrum, since C-5 has a vicinal proton (at C-3), whereas C-6 has no vicinal proton.

For **14-16**, the ¹³C signal assignments were made directly on the basis of SFORD results. Interestingly in **16**, the



carbonyl carbon is appreciably shielded relative to carbonyl carbons bonded to benzene ring systems. This may be a consequence of resonance contributions from forms such as **16b**.

Acknowledgments

We express our indebtedness to F. M. Benoit for mass spectral analysis, and we thank D. T. Williams and H. Morita for critically reviewing the manuscript and Barbara Goldhamer for word processing.

Supplementary Material Available

Tables of physical constants, retention parameters (Table A), and spectroscopic data of the methylation products (Table B) (6 pages) will appear following these pages in the microfilm edition of this volume of the journal. Photocopies of the supplementary material from this paper or microfiche (105 × 148 mm, 24× reduction, negatives) may be obtained from Microforms Office, American Chemical Society, 1155 16th St., N.W., Washington, DC 20036. Full bibliographic citation (journal, title of article, author, page number) and prepayment, check or money order for \$10.50 for photocopy (\$12.50 foreign) or \$6.00 for microfiche (\$7.00 foreign), are required.

Registry No. 1, 69-72-7; 1 (SM), 606-45-1; 2, 83-40-9; 2 (SM), 52239-62-0; 3, 303-07-1; 3 (SM), 2065-27-2; 4, 99-50-3; 4 (SM), 2150-38-1; 5, 83-30-7; 5 (SM), 29723-28-2; 6, 149-91-7; 6 (SM), 1916-07-0; 7, 583-17-5; 7 (SM), 15854-58-7; 8, 331-39-5; 8 (SM), 5396-64-5; 9, 95-01-2; 9 (SM), 613-45-6; 10, 139-85-5; 10 (SM), 120-14-9; 11, 88-99-3; 11 (SM), 131-11-3; 12, 569-51-7; 12 (SM), 2672-57-3; 13, 528-44-9; 13 (SM), 2459-10-1; 14, 554-95-0; 14 (SM), 2672-58-4; 15, 89-05-4; 15 (SM), 635-10-9; 16, 3387-26-6; 16 (SM), 4282-33-1; methyl-2,6-dihydroxybenzoic acid, 95124-64-4; 3-methyl-2,4,6-trihydroxybenzoic acid, 95124-62-2; 2-methyl-3,4,5-trihydroxybenzoic acid, 95124-63-3; 3-methyl-2,3-dihydroxybenzaldehyde, 6248-20-0; methyl sulfate, 77-78-1; iodomethane, 74-88-4.

Literature Cited

- (1) Liao, W.; Christman, R. F.; Johnson, J. D.; Millington, D. *S. Environ. Sci. Technol.* **1982**, *16*, 403-410.
- (2) Schnitzer, M. *Soil Sci* **1974**, *117*, 94-102.
- (3) Lawrence, J.; Tosine, H.; Onuska, F. I.; Comba, M. E. *Ozone: Sci. Eng.* **1980**, *2*, 55-64.
- (4) Schlenk, H.; Gallerman, J. L. *Anal. Chem.* **1960**, *32*, 1412-1414.
- (5) Mlejnek, O. *J. Chromatogr.* **1972**, *70*, 59-65.
- (6) Purdie, T.; Irwine, J. C. *J. Chem. Soc., Trans.* **1903**, *83*, 1021-1037.
- (7) Barton, D. H. R.; Schnitzer, M. *Nature (London)* **1963**, *198*, 217-218.
- (8) McKillop, A.; Fiaud, J. C.; Hug, R. P. *Tetrahedron* **1974**, *30*, 1379-1382.
- (9) Tivert, A. M.; Lillieborg, S., *Acta. Pharm. Suc.* **1981**, *18*, 331-338, and references cited therein.
- (10) Malaiyandi, M.; Benoit, F. M. *J. Environ. Sci. Health, Part A* **1981**, *A16*, 215-250.
- (11) Ho, T. L. "Hard and Soft Acids and Bases Principle in Organic Chemistry"; Academic Press: New York, NY, 1977.
- (12) Stothers, J. B. "Carbon-13 NMR Spectroscopy"; Academic Press: New York, NY, 1972.
- (13) Levy, G. C.; Nelson, G. L. "Carbon-13 Nuclear Magnetic Resonance for Organic Chemists"; Wiley-Interscience: New York, NY, 1972.

- (14) Breitmaier, E.; Voelter, W. ¹³C NMR Spectroscopy, 2nd ed.; Verlag Chemie: New York, NY, 1978.
- (15) Grover, S. H.; Guthrie, J. P.; Stothers, J. B.; Tan, C. T. *J. Magn. Reson.* 1973, 10, 227-230.
- (16) Wehli, F. W.; Wirthlin, T. "Interpretation of Carbon-13 NMR Spectra"; Heyden: New York, NY, 1976; p 55.
- (17) Lambert, J. B.; Shurvell, H. F.; Verbit, L.; Cooks, R. G.;

Stout, G. H. "Organic Structural Analysis"; Macmillan: New York, NY, 1976; p 43.

Received for review April 23, 1984. Revised manuscript received September 28, 1984. Accepted December 11, 1984. This work was partially supported by a NSERC Visiting Fellowship (to S.R.).

Identification of Intermediates Leading to Chloroform and C-4 Diacids in the Chlorination of Humic Acid

Ed W. B. de Leer,* Jaap S. Sinnighe Damsté, Corrie Erkelens, and Leo de Galan

Laboratory for Analytical Chemistry, Delft University of Technology, 2628 BX Delft, The Netherlands

■ The chlorination of terrestrial humic acid was studied at pH 7.2 with varying chlorine to carbon ratios. The principal products are chloroform, di- and trichloroacetic acid, and chlorinated C-4 diacids. At a high chlorine dose many new chlorination products were detected, among them chlorinated aromatic acids. At a low chlorine dose a class of chlorinated compounds was found, which contained a trichloromethyl group. These compounds may be converted into chloroform and in most cases C-4 diacids by oxidation and hydrolysis reactions. Because these compounds are found mainly at low chlorine dosage, they may be regarded as intermediates in the reactions that give chloroform. The intermediates support the hypothesis of Rook that *m*-dihydroxybenzene moieties in humic acid are responsible for the formation of chloroform. A reaction scheme is proposed that explains the formation of the intermediates.

Introduction

In 1974 Rook (1) described that superchlorination of water from the rivers Rhine and Meuse produced trihalomethanes as undesirable side products. Because a good correlation was found between the chloroform formation and the color intensity of the water, he suggested that humic substances are the precursors for the trihalomethanes. This hypothesis was supported by the observation that an aqueous extract of peat gave the four trihalomethanes CHCl_3 , CHBrCl_2 , CHBr_2Cl , and CHBr_3 upon chlorination in the presence of bromide ions. Since then, the presence of trihalomethanes has been demonstrated in many drinking waters (2, 3), and generally, the reaction between chlorine and humic material is regarded as the main source for these products (4).

Detailed investigations of the reaction between chlorine and humic material have clearly established that chloroform is the major volatile chlorination product but that a large number of other halogenated and nonhalogenated products are also formed. The formation of volatile chlorination products like chloral and chlorinated acetones (5), 2-chloropropenal (6), and chlorinated isoprenoid alcohols (7) was demonstrated by gas chromatography/mass spectrometry (GC/MS). However, total organic halogen formed in the chlorination of water or solutions of humic materials is much greater than can be accounted for by the amount of volatile products (8, 9). Many nonvolatile products can be converted into volatile products by methylation with diazomethane, which makes them amenable to analysis by GC/MS or other special techniques.

Quimby et al. (10) found by gas chromatography with microwave emission detection that trichloroacetic acid was a major product and identified several chlorinated acids

and phenols on the basis of their retention times. Later, Uden and Miller (11, 12) and Christman et al. (13) showed that trichloroacetic acid is formed in a molar yield comparable to that of chloroform. More systematic studies, aimed at the identification of a large number of nonvolatile products, were conducted by Christman and co-workers (13-15). Over 100 products were identified and many structures were assigned by GC/MS. Di- and trichloroacetic acid and 2,2-dichlorobutanedioic acid were the main products, which, together with chloroform, accounted for 53% of the total organic halogen. Other chlorinated products included 2,2-dichloropropanoic acid, 2-chlorobutanedioic acid, 2-chlorobutenedioic acid, 2,3-dichlorobutenedioic acid, dichloropropanedioic acid, and various other less abundant compounds.

No chlorinated aromatics were found. Most of the nonchlorinated products are aliphatic and aromatic carboxylic acids, demonstrating that chlorine acted not only through substitution and addition but also through oxidation reactions.

To establish a reaction pathway for the production of chloroform and the chlorinated acids, knowledge of the structure of humic material is necessary. Humic materials are geopolymers formed from lignin, carbohydrates, proteins, and fatty acids by microbiological degradation and enzymatic or autooxidative coupling reactions (16). Although humic materials obviously are not well-defined organic compounds, several structures (17-20) have been proposed, which contain fragments that may be converted into chloroform by chlorine in aqueous medium at pH 7-8. 1,3-Dihydroxybenzenes (1, 5, 21), 1,3-diketo compounds (22), natural acids like citric acid (23), and compounds with activated C-H bonds like indoles (24) were shown to give chloroform in high yield on chlorination in aqueous medium. For humic acid, 1,3-dihydroxybenzenes seem to be the more likely candidates as 3,5-dihydroxybenzoic acid is formed in the degradation of humic material with $\text{CuSO}_4\text{-NaOH}$ at 175-180 °C (20). From the work of Cheshire et al. (25) it appears, however, that the products of KOH fusion may be of no diagnostic value for the structure of humic substances, and in recent KMnO_4 degradation studies of humic and fulvic acids (26, 27) no 1,3-dihydroxybenzene structures were detected, possibly as a result of complete oxidation of these structures (28).

Although the possibility of 1,3-dihydroxybenzene structures as the precursor fragment for chloroform formation from humic material remains to be proven, Rook (5, 21) proposed a mechanism based on the chemistry of the reaction between chlorine and resorcinol. For a better understanding of this mechanism and for the identification of the structural fragments in humic material that are converted into chloroform and chlorinated acids, the

identification of intermediates is necessary (29).

We report here the identification and structural assignment of such intermediates in the reaction between terrestrial humic acid and chlorine in aqueous medium at pH 7.2. We propose structural assignments for a large number of products analyzed by gas chromatography/mass spectrometry and compared the products with the chlorination products of 3,5-dihydroxybenzoic acid. Suggestions are given for the mechanism of the reactions leading to chloroform and chlorinated acids.

Experimental Section

Separation of Humic Acid. Humic acid was isolated from peat (Liesselse Peel, O-Brabant) following the procedure described by Stevenson (30). This involved treatment with 0.1 M HCl, extraction with 0.5 M NaOH, removal of residual solids, acidification to pH 1 with precipitation of humic acid, purification by redissolution/precipitation, washing with deionized water, and freeze-drying. To minimize chemical changes caused by oxidation, all steps (if possible) were carried out in an atmosphere of nitrogen.

The elementary composition of the final humic acid was the following: C, 50.7%; H, 5.1%; N, 1.5%; O, 39.4%; ash, 1.5%.

Chlorination Procedure. For the *identification studies*, 250 mg of humic acid was dissolved in 40 mL of 0.1 M NaOH. A total of 100 mL of 1 M KH_2PO_4 buffer (pH 7.2) and aqueous hypochlorite was added, and the volume was adjusted to 200 mL with deionized water. Two chlorine concentrations were chosen with Cl_2/C molar ratios of 0.39 and 3.35, respectively. After 24 h the possible excess of chlorine was removed by adding solid sodium arsenite, and the pH was lowered to 1 with HCl. The solution was then extracted with 50 mL of freshly distilled diethyl ether and 50 mL of freshly distilled ethyl acetate. The extracts were dried with sodium sulfate, concentrated in a Kuderna Danish apparatus to about 5 mL, methylated by passing a stream of diazomethane gas through the solution, and finally concentrated to 100 μL by passing a gentle stream of nitrogen.

For the *quantitation studies* this procedure was slightly modified. To 25 mL of humic acid solution (960 mg/L in 0.01 M NaOH) was added 25 mL of KH_2PO_4 buffer (1 M, pH 7.2) and aqueous hypochlorite to various Cl_2/C molar ratios (0.12–2.96). After adjustment of the volume to 100 mL, the bottle was capped head space free and allowed to react for 24 h.

The chlorination of 3,5-dihydroxybenzoic acid was carried out at pH 7.2 in a 0.16 M phosphate buffer. A total of 250 mL of a solution of 3,5-dihydroxybenzoic acid (2×10^{-3} mol/L) and sodium hypochlorite (20×10^{-3} mol/L) was allowed to react in the dark without head space for 2 h. After the given reaction times the excess of chlorine was removed by adding solid sodium arsenite. The solution was acidified to pH 1 with concentrated sulfuric acid and extracted 3 times with 25 mL of freshly distilled diethyl ether.

The concentration and methylation procedure was as described above.

Chlorine Consumption. Chlorine concentrations before and after chlorination were measured iodometrically (31).

Quantitation of Chloroform Production. A total of 25 mL of the reaction mixture was extracted with 25 mL of pentane after destruction of the excess of chlorine with solid sodium arsenite.

The extraction yield was >95%. After proper dilution the extract was analyzed by gas chromatography using a

glass column (ϕ 2.5 mm \times 1.8 m) packed with 13% OV-101 on Chromosorb W HP (100–200 mesh) and an electron capture detector: injector 120 °C; column 70 °C; detector 300 °C; carrier gas N_2 ; flow 30 mL/min. The quantitation was carried out with external standards.

Quantitation of Dichloroacetic Acid (DCA) and Trichloroacetic Acid (TCA) Production. The extraction procedure described by Quimby et al. (10) was used. To 25 mL of reaction mixture were added some solid sodium arsenite and 5 g of sodium chloride. After acidification to pH 0.5 with concentrated H_2SO_4 the solution was extracted with 25 mL of diethyl ether. The extract was methylated with diazomethane gas, and the volume was adjusted to 50 mL. The final solutions were analyzed by gas chromatography with a glass column (ϕ 2.5 mm \times 1.8 m) packed with 15% OV-225 on Chromosorb W-HP (100–200 mesh) and an electron capture detector: injector 200 °C; column 120 °C; detector 300 °C; carrier gas N_2 ; flow 30 mL/min. The quantitation was carried out with external standards: calibration range for DCA, 38–66 $\mu\text{g}/\text{L}$, and TCA, 14–24 $\mu\text{g}/\text{L}$. If necessary, the sample solutions were diluted to an appropriate volume, to obtain a signal in the linear range of the detector.

Determination of Extraction Yields. (1) Chloroform. A total of 25 mL of the type of water under investigation was equilibrated with 25 mL of a series of standard solutions of chloroform in pentane (147–588 $\mu\text{g}/\text{L}$). The extraction yield was calculated from the slope of a graph of the chloroform concentrations in pentane before and after the equilibration. The yield was >95%. Experiments with a 10/1 volume ratio of water to pentane gave a distribution coefficient $K = 56$ (extraction yield = 82%), from which an extraction yield of 98% for a 1/1 volume ratio can be calculated.

(2) DCA and TCA. A solution of 5 g of NaCl in 25 mL of water acidified to pH 0.5 was equilibrated with 25 mL of a solution of DCA and TCA in diethyl ether (66 and 24 $\mu\text{g}/\text{L}$, respectively). DCA and TCA concentrations before and after equilibration were determined as described above. Duplicate experiments gave yields of 98 and 100% for DCA and TCA, respectively.

The quantitative extraction was also checked on actual reaction mixtures, by spiking with known amounts of DCA and TCA.

Retention Index Determination. The retention indexes were measured by mixing a portion of the methylated extract with an *n*-alkane standard (*n*- C_6 –*n*- C_{27}) and analyzing on a fused silica capillary column (ϕ 0.23 mm \times 25 m), CP-SIL-5 (Chrompack, Middelburg): injector 280 °C; column 35 °C (5 min) programmed to 300 °C (15 min), program rate 6 °C/min; detector FID 300 °C; carrier gas N_2 ; flow rate 0.8 mL/min. The retention indexes were calculated by linear interpolation of the retention time of the compound of interest with the retention times of the two neighboring *n*-alkanes.

The same GC conditions were used for the analysis of the chlorination products of humic acid and 3,5-dihydroxybenzoic acid.

Apparatus. The gas chromatograph was a Varian 3700, equipped with a packed and a capillary column, a flame ionization detector, and a ^{63}Ni electron capture detector.

The GC/MS combination was a Varian MAT 44 capillary GC–quadrupole MS with a computerized data system of own design.

The fused silica capillary column (CP-SIL-5) was connected to the mass spectrometer by an open atmospheric split. GC conditions used were as above, except that helium was used as the carrier gas. Electron impact spectra

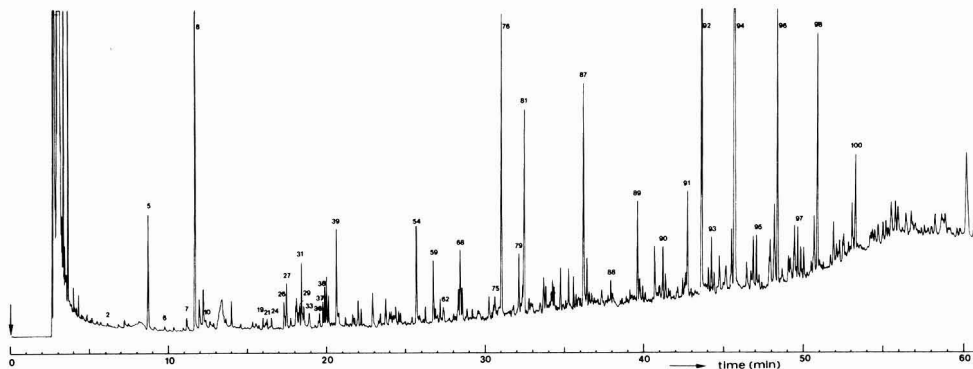


Figure 1. Humic acid chlorination products at a chlorine to carbon ratio of 0.39. Methylated ether extract on a capillary CP-Sil-5 column (FID). Peak numbers refer to the numbers given in Table I.

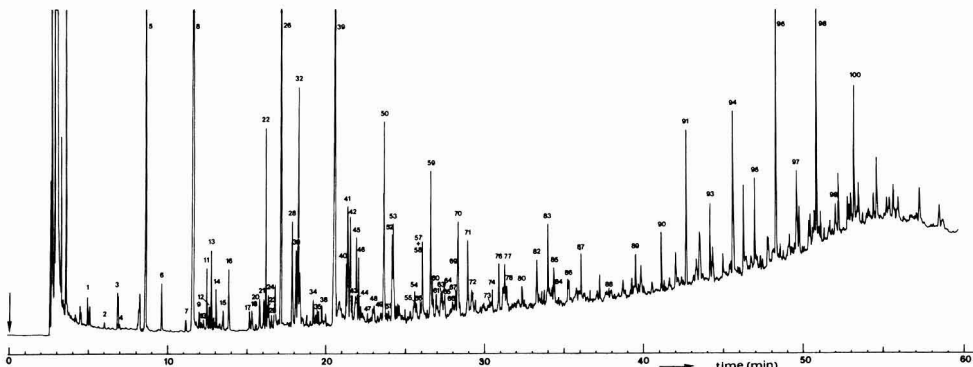


Figure 2. Humic acid chlorination products at a chlorine to carbon ratio of 3.35. Methylated ether extract on a capillary CP-Sil-5 column. The high chlorine dose produces more low molecular weight compounds, while at a low chlorine dose (Figure 1) more high molecular weight compounds are detected.

were obtained at 80 eV and chemical ionization spectra at 160 eV with isobutane as the reagent gas. Ionization current was 700 and 200 μA , respectively. Cyclic scanning from m/z 50 up to 500 was used with a cycle time of 2 s.

Structural Assignments. The confidence level of the structural assignments is given as confirmed (level 3), confident (level 2), tentative (level 1), and very tentative according to Christman (32–34).

For level 3 and level 2 identifications we strictly followed the proposed definitions (34). All level 1 identifications are based on a priori interpretation of the EI spectrum and are supported by the CI spectrum. An identification is given as very tentative if based on the a priori interpretation of the EI spectrum only.

Reference spectra were taken from the literature as indicated or from a mass spectra data base from the Mass Spectrometry Data Centre (England).

Results and Discussion

The chlorination of humic acid was carried out at two chlorine to carbon molar ratios of 0.39 and 3.35, respectively, in a pH 7.2 buffer system. A ratio of 0.39 represents the normal chlorination practice for drinking water, and the 3.35 ratio is used to obtain a high yield of chlorination products. As shown by the chromatograms for the ether extracts (Figures 1 and 2), the composition of the product mixture was quite different in the two experiments. The ether and ethyl acetate extracts differed mainly in the fact that ethyl acetate is more effective in extracting aromatic acids. The identified products are presented in Table I.

With the low chlorine dose more high molecular weight chlorinated products are formed, while at a high chlorine dose more low molecular weight chlorinated products and aromatic acids are formed.

The structural assignments for more than 100 different reaction products was accomplished by the combined use of GC/MS with electron impact and chemical ionization. At the high chlorine dose, the products identified agree very well with the compounds identified by Christman et al. (13, 14) after chlorination of aquatic humic and fulvic acid. This shows that the differences in the nature of the chlorination products from terrestrial or aquatic humic material are small and that differences may be reflected only in the product distribution and product yield.

The main products were identified as chloroform and trichloroacetic acid (TCA), which were quantified together with dichloroacetic acid (DCA) and the chlorine consumption as a function of the chlorine to carbon ratio. The results are presented in Figure 3.

The analytical procedure for the quantitation of DCA and TCA used a simple packed GC column and an electron capture detector. This compares favorably in speed and/or simplicity with the microwave plasma emission detection used by Miller et al. (35) and the isotope dilution GC/MS method with trichloro[^{13}C]acetic acid used by Christman et al. (13). The extraction/methylation procedure proceeded quantitatively, as demonstrated by external calibration and spiking of the reaction mixture. Drying of the ether extract on Na_2SO_4 was omitted in this procedure, because then losses of 10–15% were observed. The water

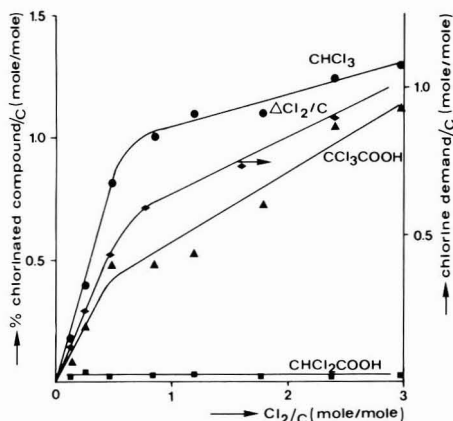


Figure 3. Production of chloroform, dichloroacetic acid, and trichloroacetic acid and chlorine consumption as a function of chlorine dose in humic acid chlorination.

content of the extract apparently did not influence the methylation step.

At the highest chlorine dose, 1.3% of the carbon content is converted into chloroform, 2.2% into TCA, and 0.1% in DCA. These values for terrestrial humic acid agree with results obtained in the chlorination of other humic materials, for which yields of 0.3–1.6% for chloroform (5, 9, 11–13, 36), 1.8–3.0% for TCA (12, 13), and 0.4–0.7% for DCA (12, 13) have been reported.

When we consider that a very favorable chloroform precursor like resorcinol gives a yield of 14.2% mol of CHCl_3 /mol of C (5), the yields for chloroform and TCA are quite high. Indeed, if only resorcinol structures are responsible for the chloroform production in the chlorination of humic acid, about 10% of the organic carbon must be present as free or fused 1,3-dihydroxybenzene structures. This is within the possibilities for Suwannee River fulvic acid, which was shown (37) to have a molecular formula of approximately $\text{C}_{74}\text{H}_{72}\text{N}_{0.7}\text{O}_{46}$ and a total of 20 aromatic plus phenolic carbon atoms (28% aromatic carbon).

Apart from the three quantified products, many other compounds were detected which are discussed below in two groups: nonchlorinated and chlorinated compounds.

Nonchlorinated Compounds. The nonchlorinated reaction products were similar to the KMnO_4 oxidation products of humic and fulvic acid (26, 27). Aliphatic carboxylic acids were observed from *n*-heptanoic acid up to *n*-octacosanoic acid. The strong even predominance is typical for the terrestrial origin of the humic acid (38). It indicates that the aliphatic carboxylic acids are formed by hydrolysis of ester groups, and in this case not by oxidation of alkylarenes (26). Aliphatic dicarboxylic acids and aromatic carboxylic acids were found mainly at the high chlorine dose, indicating that they are end products in the oxidation process.

Two cyano-substituted carboxylic acids were detected for the first time and identified as 3-cyanopropanoic acid (level 2) and 4-cyanobutanoic acid (level 1). The EI and CI spectra for the methyl esters of both compounds are given in Figures 4 and 5.

The spectrum assigned to methyl 3-cyanopropanoate showed a good match with a reference spectrum (39), while the possibility of methyl 2-cyanopropanoate could be ruled out as this compound shows fragments at m/z 59 and 68 as the dominant peaks.

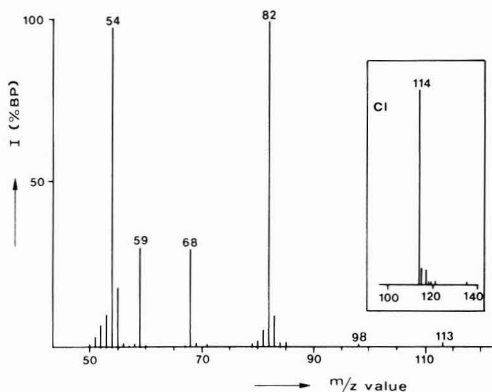


Figure 4. EI and CI mass spectrum of the methyl ester of 3-cyanopropanoic acid. m/z 82 ($-\text{OCH}_3$); m/z 54 ($-\text{COOCH}_3$); m/z 59 ($=\text{COOCH}_3^+$).

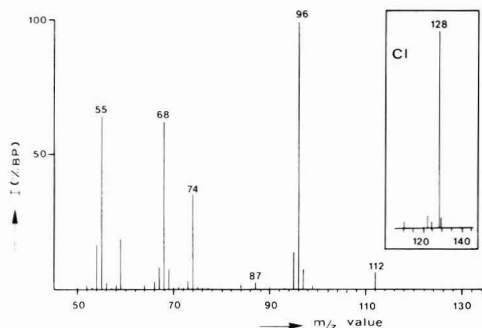
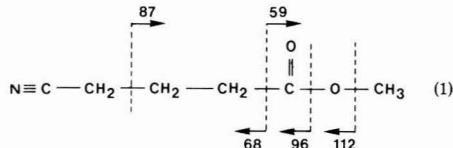
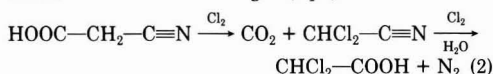


Figure 5. EI and CI mass spectrum of the methyl ester of 4-cyanobutanoic acid. m/z 112 ($-\text{CH}_3$); m/z 96 ($-\text{OCH}_3$); m/z 74, McLafferty rearrangement product; m/z 68 ($-\text{COOCH}_3$).

The spectrum of the cyanobutanoic acid is assigned to methyl 4-cyanobutanoate on the basis of the formation of the m/z 74 ion, which is the normal McLafferty rearrangement product for unbranched methyl alkanates with γ -H atoms, and the m/z 87 ion, which indicates the 4-position of the cyano group (eq 1).



Cyano acids are of interest in the formation of dihaloacetonitriles after chlorination of water. The two cyano-substituted acids may be formed from some protein material containing glutamic acid and 2-aminoadipic acid, according to a mechanism proposed by Bieber and Trehy (40). No cyanoethanoic acid was detected, possibly because of a rapid conversion into dichloroacetonitrile followed by oxidation to DCA and nitrogen (eq 2).



Chlorinated Compounds. Chloroform, chloral, and tetrachloromethane were the only volatile chlorinated products detected. Chloral appeared at different places in the chromatogram due to artifact formation by reaction

Table I. Products Found in the Chlorination of Humic Acid

	no. ^a	RI	structural assignment ^b	low Cl ₂ dose ^c		high Cl ₂ dose ^c	
				Et ₂ O ^d	EtOAc ^e	Et ₂ O	EtOAc
Nonchlorinated Products							
aliphatic monobasic acids							
2-methylpropanoic acid	1		C			+	
2-methylbutanoic acid	3		C			+	
2-methylpentanoic acid		962	C				+
heptanoic acid	18	1009	C			+	
octanoic acid		1109	C			+	
nonanoic acid	40	1209	C			+	
decanoic acid	49	1309	C			+	
undecanoic acid	56	1409	C			+	
dodecanoic acid	67	1509	SC			+	
tridecanoic acid	73	1608	SC			+	
tetradecanoic acid	80	1710	SC			+	
pentadecanoic acid	84	1810	SC			+	
hexadecanoic acid	87	1910	SC	++++	+++	+	+
heptadecanoic acid	88	2011	SC	+		+	
octadecanoic acid	89	2111	SC	+++	+++	++	+
nonadecanoic acid	90	2212	SC	++	+	++	
eicosanoic acid	91	2312	C	+++	++	+++	+
heneicosanoic acid	93	2414	C	+++	++	++	+
docosanoic acid	94	2514	C	++++	+++	+++	+
tricosanoic acid	95	2614	C	+++	+	++	+
tetracosanoic acid	96		C	++++	+++	+++	+
pentacosanoic acid	97		C	+++	+	++	
hexacosanoic acid	98		C	++++	++	+++	+
heptacosanoic acid	99		C	++		++	
octacosanoic acid	100		C	+++	++	++	+
aliphatic dibasic acids							
ethanedioic acid		804	SC		++		+
butanedioic acid	17	1004	SC	+	++	+	++
pentanedioic acid		1110	SC				+
hexanedioic acid		1214	SC				+
heptanedioic acid		1315	SC				+
octanedioic acid	57	1416	SC			+	++
nonanedioic acid	70	1516	SC			++	+
decanedioic acid	74	1617	SC			+	
cyano-substituted monobasic acids							
3-cyanopropanoic acid		940	C				++
4-cyanobutanoic acid		1036	T				+
aromatic carboxylic acids							
benzoic acid	26	1070	SC	++		++++	+
phenylacetic acid	36	1149	SC	++			
1,2-benzenedicarboxylic acid	58	1416	SC		+++	++	++
1,4-benzenedicarboxylic acid	63	1471	SC			+	+
1,3-benzenedicarboxylic acid	65	1478	SC			+	+
toluenedicarboxylic acid			T				+
1,2,3-benzenetricarboxylic acid		1772	SC				++
1,2,4-benzenetricarboxylic acid	83	1797	SC			++	+++
1,3,5-benzenetricarboxylic acid	86	1872	SC			+	+
benzenetetracarboxylic acid		2068	C				+
1,2,4,5-benzenecarboxylic acid		2102	SC				+++
benzenetetracarboxylic acid		2136	C				++
benzenepentacarboxylic acid		2363	C				+
heterocyclic acids							
5-methyl-2-furancarboxylic acid	24	1045	C	+		+	++
methylfurandicarboxylic acid	54	1393	T	+++	++	+	++
miscellaneous							
trimethyl phosphate	9	911	C	+	++	+	+++
benzaldehyde	12	930	SC			+	
indole	28	1094	C			++	
unknown (<i>M</i> , 242)	81	1711	VT	++++			
branched fatty acid	82	1759	VT			++	
unknown (<i>M</i> , 398)	92	2371	VT	++++			
unknown (<i>M</i> , 278)			VT				+
Chlorinated Products							
aliphatic monobasic acids							
α-monochlorinated							
chloroethanoic acid	2	733	SC	+	+	+	+
2-chloropropanoic acid	4	765	SC			+	
2-chlorobutanoic acid			T			+	
2-chloropentanoic acid	11	924	T			++	
2-chlorohexanoic acid	25	1051	T			+	
2-chloroheptanoic acid	35	1149	T			+	

Table I (Continued)

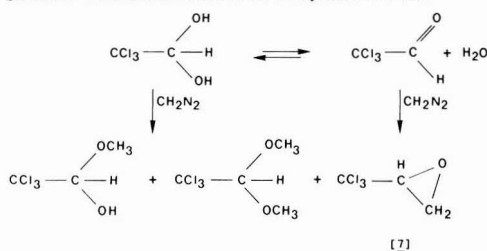
	no. ^a	RI	structural assignment ^b	low Cl ₂ dose ^c		high Cl ₂ dose ^c	
				Et ₂ O ^d	EtOAc ^e	Et ₂ O	EtOAc
<i>α,α</i> -dichlorinated							
dichloroethanoic acid	5	816	SC	+++	++++	++++	++
2,2-dichloropropanoic acid	6	838	SC	+		++	+
2,2-dichlorobutanoic acid	15	955	C			+	
2,2-dichloropentanoic acid	22	1039	T			+++	
2,2-dichlorohexanoic acid	34	1142	T			+	
2,2-dichloro-3-hydroxypropanoic acid	20	1027	T			+	++
unspecified substitution							
trichloroethanoic acid	8	898	SC	+++++	+++++	+++++	++
3,3,3-trichloropropanoic acid	16	965	T			++	+++
C ₂ H ₂ Cl ₃ COOH	19	1027	T	+			
C ₄ H ₇ Cl ₂ COOH	27	1075	T	++			
C ₄ H ₇ Cl ₂ COOH (isomer)		1093	T		++		+
C ₅ H ₉ Cl ₂ COOH	29	1100	T	+			
C ₅ H ₉ Cl ₂ COOH (isomer)		1175	T				++
CCl ₃ C ₃ H ₅ COOH		1209	T		++		+
C ₆ H ₁₁ Cl ₂ COOH		1255	T		++		++
unsaturated							
3,3-dichloropropenoic acid	10	918	T	++		+	
2,3-dichloropropenoic acid	13	933	T			++	
2,3-dichloropropenoic acid	14	942	SC			+	
2,3,3-trichloropropenoic acid	21	1034	SC	++		+	
C ₃ H ₄ ClCOOH			T		+		+
C ₃ H ₃ Cl ₂ COOH	33	1126	T	++			
C ₃ HCl ₄ COOH	46	1248	T			++	
aliphatic dibasic acids							
<i>α</i> -monochlorinated							
chlorobutanedioic acid	30	1104	SC		+++	++	+++
2-chloroheptanedioic acid	61	1453	T			+	
2-chlorooctanedioic acid	72	1557	T			+	
2-chlorononanedioic acid	78	1662	T			+	
<i>α,α</i> -dichlorinated							
2,2-dichloropropanedioic acid	32	1108	T			+++	+++
2,2-dichlorobutanedioic acid	39	1190	T	+++	++++	++++	+++++
2,2-dichloropentanedioic acid	53	1336	T		+++	++	++
2,2-dichlorohexanedioic acid	60	1442	T			+	+
2,2-dichlorooctanedioic acid	77	1655	T			++	
unspecified substitution							
HOOC ₂ H ₃ ClCOOH	23	1045	T			+	++
HOOC ₃ H ₄ Cl ₂ COOH	47	1271	T			+	+
trichlorobutanedioic acid	48	1286	T			+	
HOOC ₄ H ₇ ClCOOH		1311	T				+
HOOC ₄ H ₇ Cl ₂ COOH	71	1545	T			++	++
HOOC ₃ H ₄ OCl ₂ COOH			VT				++
unsaturated							
chlorobutenedioic acid		1170	SC				+
dichlorobutenedioic acid	41	1221	SC		++++	+++	++
dichlorobutenedioic acid	42	1227	SC		+++	++	++
HOOC ₃ H ₃ ClCOOH			T		++		
HOOC ₃ H ₃ ClCOOH			T			+	
HOOC ₃ H ₃ ClCOOH			T			+	
HOOC ₃ H ₃ ClCOOH			T		+		+
HOOC ₃ H ₂ Cl ₂ COOH	51	1324	T		++	+	+
HOOC ₃ HCl ₃ COOH	59	1439	T	+++	+++	+++	++
tetrachloropentanedioic acid	69	1516	T			++	
aromatic carboxylic acids							
4-chlorobenzoic acid	43	1228	SC			+	
2-chlorobenzoic acid	44	1239	SC			+	
2-chlorophenylacetic acid	50	1312	SC			+++	
4-chlorophenylacetic acid	52	1333	SC			++	
2,6-dichlorophenylacetic acid	64	1476	T			+	
2,4-dichlorophenylacetic acid	66	1500	T			+	
chloroform precursors							
3,3,3-trichloro-2-hydroxypropanoic acid	31	1107	T	+++	+++		
2,4-dichloro-3-hydroxybutanoic acid		1142	T				+
3,3,3-trichloro-2-methyl-2-hydroxypropanoic acid	37	1157	T	++			
4,4,4-trichloro-3-hydroxybutanoic acid	38	1160	T	++		+	+
3,5,5-tetrachloro-4-oxopentenoic acid		1420	VT			+	
3,5,5-tetrachloro-4-oxo-2-methylpentenoic acid	62	1466	T	++		+	
3,5,5-tetrachloro-4-oxo-2-methylpentenoic acid		1475	T			+	
3,3,5,5-pentachloro-4-hydroxypentanoic acid	68	1514	T	+++			
2-chloro-3-(trichloroacetyl)butenedioic acid	75	1618	T	++	++		
2,3,3,5,5-hexachloro-4-hydroxypentanoic acid	76	1639	T	++++	+++	++	
2-carboxy-3,5,5,5-tetrachloro-4-oxopentenoic acid	79	1693	T	++	++	+	
heptachloro-5-oxohexenoic acid	85	1816	VT			++	

Table I (Continued)

	no. ^a	RI	structural assignment ^b	low Cl ₂ dose ^c		high Cl ₂ dose ^c	
				Et ₂ O ^d	EtOAc ^e	Et ₂ O	EtOAc
miscellaneous							
tetrachloromethane			C			+	
chloral			T	+		+	
1,1,1-trichloro-2,3-epoxypropane	7	887	T	+		+	+
dichlorinated acid (<i>M_r</i> 196)	45	1241	VT			++	++
C ₂ H ₂ O ₃ CCl ₂ COOH		1307	T				+
chloroethenetetracarboxylic acid	55	1398	T			+	
trichlorinated acid (<i>M_r</i> 374)			VT				++

^aNo numbers are given if the product was detected in the ethyl acetate extracts only. ^bSC = standard confirmed; C = confident; T = tentative; VT = very tentative. ^c(+++++) most abundant peak (MAP); (+++++) 30-100% MAP; (++++) 10-30% MAP; (++) 3-10% MAP; (+) <3% MAP. ^dEt₂O = diethyl ether extract. ^eEtOAc = ethyl acetate extract.

Scheme I. Artifact Formation in the Methylation of Chloral



with diazomethane in the methylation step (41-44) (Scheme I).

The monomethyl and dimethyl acetal, resulting from methylation of one or two hydroxyl groups in the hydrate, and 1,1,1-trichloro-2,3-epoxypropane (7), resulting from methylene insertion into the carbonyl group, were repeatedly found in chlorination experiments with humic acid and model compounds. The EI spectrum of 7 which shows an interesting fragmentation pattern is given in Figure 6. Other volatile chlorinated products such as chlorinated acetones or 3-chloropropenal were not detected.

The principal nonvolatile reaction products were chlorinated aliphatic monobasic and dibasic acids and one tribasic acid. At a low chlorine dose in particular, a large number of chlorinated acids containing a trichloromethyl group were detected. Because these compounds may be converted into chloroform by further chlorination and/or hydrolysis, they will be denoted as "chloroform precursors". At a high chlorine dose several chlorine-substituted benzoic acids and phenylacetic acids were detected for the first time.

The chlorinated saturated aliphatic acids comprised a series of α -chlorinated acids from 2-chloroethanoic acid up to 2-chloroheptanoic acid and a series of α,α -dichlorinated acids from 2,2-dichloroethanoic acid up to 2,2-dichlorohexanoic acid.

The identification of the unsaturated 3,3-dichloropropenoic acid has been reported earlier by Christman (13, 14), but at a high chlorine dose we found larger amounts of the two *Z/E* isomers of 2,3-dichloropropenoic acid.

2,2-Dichlorobutanedioic acid was the major representative of the class of chlorinated aliphatic dibasic acids. Saturated and unsaturated C-4 diacids were the dominant products, but C-3, C-5, C-6, and C-7 diacids were also found. C-4 diacids are also formed in the chlorination of resorcinol and resorcinol derivatives, where 2-chlorobutanedioic acid has been detected with a yield of 60% (22, 45). The C-4 diacids found in this study, therefore,

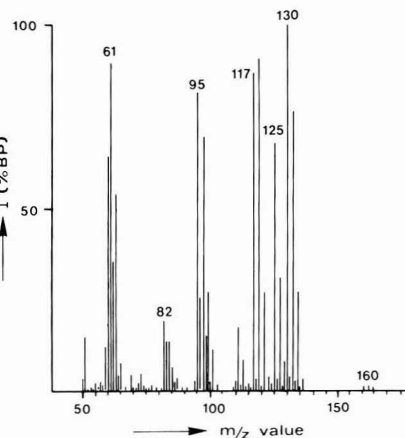


Figure 6. EI mass spectrum of 1,1,1-trichloro-2,3-epoxypropane (7). *m/z* 130 (-CH₂=O), 125 (-Cl), 117 (-CCl₃⁺), and 95 (130 - Cl).

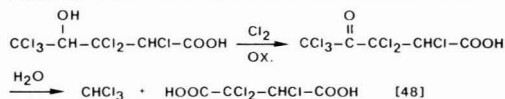
may reflect 1,3-dihydroxybenzene structures as a part of the humic acid structure.

Several aryl-chlorinated aromatic acids were detected and standard confirmed, although only at high chlorine dose and most of them in low yield. Direct chlorination of the aryl group in the phenylacetic acid derivatives seems possible, and the substitution pattern found follows the normal substitution rules. Direct chlorination of benzoic acid does not seem very likely and would yield meta-substituted products. A better explanation for the formation of chlorinated benzoic acids may be given by the assumption that first an alkyl-substituted aromatic ring is chlorinated, followed by an oxidative breakdown of the alkyl side chain. The 2,4-substitution pattern is in accordance with this explanation.

Chloroform Precursors. From a mechanistic point of view, the identification of a large number of compounds containing a trichloromethyl group is the most important result of this study. Upon further chlorination, decarboxylation, oxidation, and/or substitution, these compounds may be converted into chloroform and, in most cases, C-4 diacids. These chloroform precursors were detected mainly in the low chlorine dose experiment, which demonstrates that they are converted into other products at the high chlorine dose.

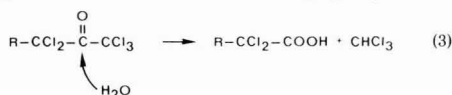
Not all products containing a trichloromethyl group may be converted into chloroform in aqueous medium at pH 7-8. For example, chloral could be converted into chloroform by a simple hydrolysis, and this reaction has been

Scheme II. Conversion of HCHPA into Chloroform and TCBDA



observed on injection of aqueous solutions in the heated injection port of a gas chromatograph (46). However, at neutral pH and room temperature the conversion is very slow, and chloral is detected as an important product, even at a high chlorine dose when oxidation to trichloroacetic acids seems a more plausible reaction.

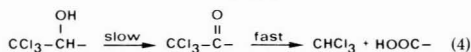
If conversion of a trichloroacetyl group into chloroform is to be achieved at neutral pH and normal temperatures (eq 3), further activation of the carbonyl group for nu-



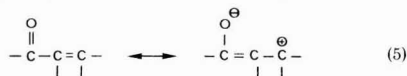
cleophilic substitution is required (22, 47). This may be accomplished by chlorine substitution on the carbon adjacent to the trichloroacetyl group. The most abundant chloroform precursor identified after chlorination of humic acid at a low chlorine dose fulfills this requirement. The hydroxy group in 2,3,3,5,5-hexachloro-4-hydroxypentanoic acid (HCHPA) (76) may be oxidized to a carbonyl group by the action of chlorine, which makes the compound susceptible to hydrolysis, which gives chloroform and trichlorobutanedioic acid (TCBDA) (48) (Scheme II).

In a similar way, the 3,3,5,5,5-pentachloro-4-hydroxypentanoic acid (68) may be converted into chloroform and the most abundant C-4 diacid, 2,2-dichlorobutanedioic acid (39).

Six of the 12 chloroform precursors listed in Table I contain a hydroxyl group, presumably adjacent to the trichloromethyl group, indicating that oxidation of the hydroxyl group may become the rate-determining step in the conversion to chloroform (eq 4). The other six chloro-



form precursors contain a trichloroacetyl group, bound to a carbon-carbon double bond. In these cases the carbonyl group is part of a conjugated double bond system (eq 5). Hydrolysis to chloroform is hampered now by



resonance stabilization which makes these compounds rather stable under the chlorination conditions applied.

The two unsaturated diacids found in this group (75 and 79) are very interesting because 79 was found as the major reaction product in the chlorination of 3,5-dihydroxybenzoic acid. Hydrolysis of both compounds produces chloroform and the only tricarboxylic acid (55) detected. The tricarboxylic acid may be converted into 2-chlorobutenedioic acid by a decarboxylation reaction (Scheme III).

Model Studies. An explanation for the formation of the chloroform precursors on the basis of the structure of humic acid is still speculative, but resorcinol structures play an important role. Chlorination of 3,5-dihydroxybenzoic acid gave chloroform in a yield of 74%, but after extraction and methylation, GC/MS revealed the presence of a large number of other chlorinated compounds. The

Scheme III. Conversion of 2-Chloro-3-(trichloroacetyl)butenedioic Acid into Chloroform and 2-Chlorobutenedioic Acid

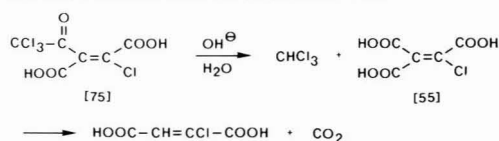


Table II. Identical Products Found in the Chlorination of Humic Acid and 3,5-Dihydroxybenzoic Acid^a

CHCl ₃
CCl ₃ CHO
CHCl ₂ COOH (5)
CCl ₃ COOH (8)
CHCl=CClCOOH (14)
CCl ₂ CH ₂ COOH (16)
CCl ₃ CHOHCOOH (31)
C ₃ H ₂ Cl ₃ COOH (33)
HOOC-C≡C-CClCOOH (41, 42)
C ₃ HCl ₄ COOH (46)
HOOC-C ₂ H ₂ Cl ₂ COOH (51)
HOOC-C≡C-(COOH) ₂ (55)
CCl ₃ CHOHCCl ₂ CHClCOOH (76)
CCl ₃ COCCl=C(COOH) ₂ (79)

^a Numbers in parentheses indicate the peak numbers in Figures 1 and 2 and numbers in Table I.

major product was 2-carboxy-3,5,5,5-tetrachloro-4-oxo-2-pentenoic acid (79), indicating that humic acid and 3,5-dihydroxybenzoic acid may give identical products on chlorination. Other identical products are summarized in Table II, which includes three chloroform precursors (31, 76, and 79) in Table I.

The two isomers of 3,5,5,5-tetrachloro-4-oxo-2-methyl-2-pentenoic acid (62) have also been found in the chlorination of 3,5-dihydroxytoluene, which again indicates the crucial role of resorcinol structures in the formation of chloroform and chloroform precursors on chlorination of humic acid.

Boyce and Hornig (48) studied the chlorination of various resorcinol derivatives and tentatively identified several trichloromethyl-substituted products. In all cases the trichloromethyl group was part of a trichloroacetyl group conjugated with a C=C bond, in accordance with our proposal of a retardation of the hydrolysis reaction.

The mechanism for the chlorination of resorcinol was proposed originally by Rook (5, 21) and later extended by Boyce and Hornig (48). This mechanism may explain the formation of the precursor (79) when additional hydrolysis and decarboxylation reactions are included and is given in Scheme IV. Supporting evidence for these steps was found in the identification of the intermediate dicarboxylic acid and in the formation of 1 mol of CO₂/mol of 3,5-dihydroxybenzoic acid.

Structural Assignments. The identification of the chloroform precursors is based on a priori interpretations of the EI and CI spectra. In those cases, where the spectra did not provide sufficient information to allow a complete structural assignment, the proposed structures are also based on the information that identical products are formed in the chlorination of resorcinol and resorcinol derivatives.

The structural assignments will be exemplified by the identification of two hydroxyl-type precursors, 31 and 76, and one acetyl-type precursor, 79.

The EI and CI spectra of 31 are given in Figure 7. The CI spectrum shows the protonated molecular ion (M + 1)⁺ at m/z 207, and the chlorine isotope distribution pattern

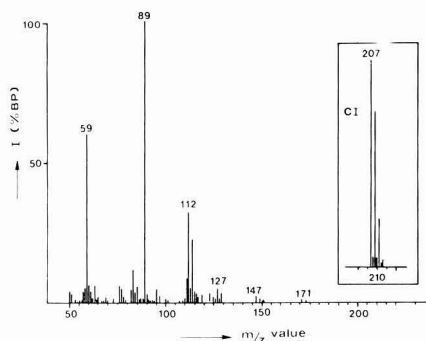
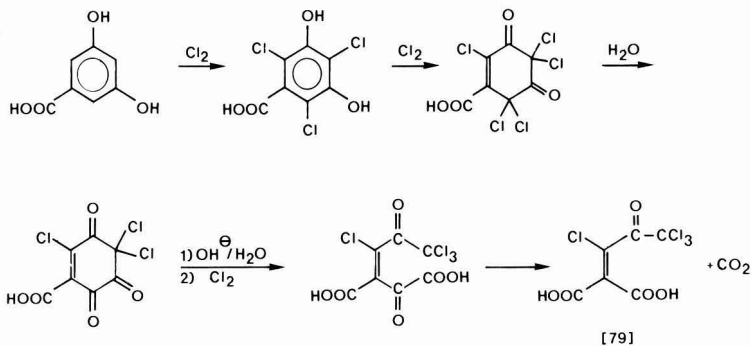


Figure 7. EI and CI mass spectrum of the methyl ester of 3,3,3-trichloro-2-hydroxypropanoic acid (3).

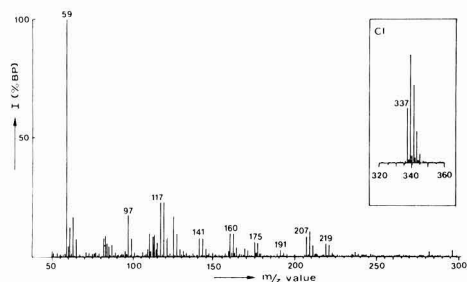


Figure 8. EI and CI mass spectrum of the methyl ester of 2,3,3,5,5,5-hexachloro-4-hydroxypentanoic acid (76).

indicates the presence of three chlorine atoms. The three chlorine atoms must be bound to the same carbon atom, as the fragment at m/z 89 in the EI spectrum does not contain chlorine and therefore must be formed by elimination of a CCl_3 group ($206 - 117 = 89$). The presence of a COOCH_3 group is evident from the m/z 59 ion, which leaves $-\text{CH}_2\text{O}-$ for the rest of the molecule.

Methyl 3,3,3-trichloro-2-hydroxypropanoate is the only plausible structure, which explains the fragments at m/z = 89 and 147 by a simple α -cleavage mechanism (eq 6).

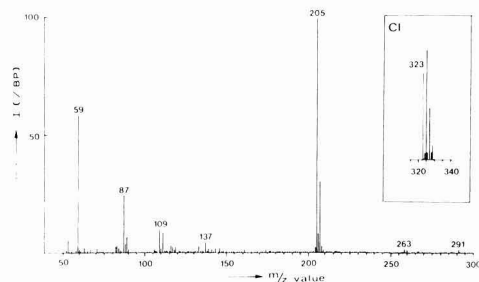
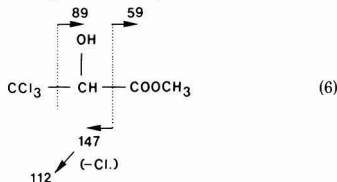
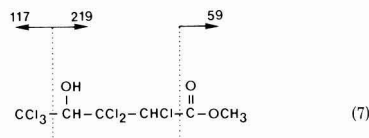


Figure 9. EI and CI mass spectrum of the dimethyl ester of 2-carboxy-3,5,5,5-tetrachloro-4-oxo-2-pentenoic acid (79).

The structure of the more complicated precursor 76 cannot be deduced conclusively from the EI and CI spectrum (Figure 8) alone. The CI spectrum gives the protonated molecular ion at m/z 337 and indicates the presence of six chlorine atoms.

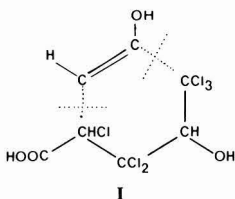
The EI spectrum shows many fragments up to m/z 235, most of which contain chlorine. The fragments at m/z 59, 117, and 219 can be explained by simple bond fission processes (eq 7). Because the central part of the molecule



is saturated, the O atom must be part of an ether or a hydroxyl group. As there is only evidence for the elimination of a CCl_3 group and not for C_2 and C_3 fragments, we propose that the CCl_3 group is bound to a $-\text{CHOH}-$ group. The formation and stability of the m/z 219 ion are then explained by the α -type cleavage of alcohols.

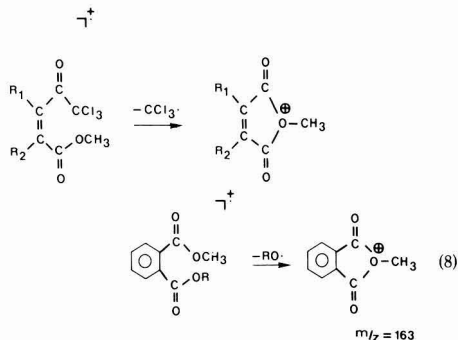
Most of the other fragments in the EI spectrum can be explained by successive eliminations of CO , CO_2 , Cl_2 , etc., which, however, do not provide information about the structure of the central part of the molecule. We propose methyl 2,3,3,5,5,5-hexachloro-4-hydroxypentanoate to be the final structure because the same product was found in the chlorination of 3,5-dihydroxybenzoic acid. This structure gives relevance to the structure of the starting compound and the possible mechanism of the chlorination of resorcinol derivatives (I).

All chloroform precursors of the acetyl type show only one important fragment which is caused by the loss of a CCl_3 group from the molecule. As further fragmentations are observed only to a minor extent (Figure 9), the ion



formed apparently must have a very stable structure.

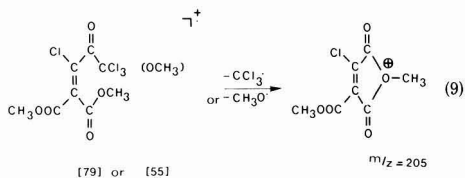
We propose a methylated cyclic anhydride structure for this ion, in analogy with the m/z 163 ion which is the most abundant fragment in the mass spectra of methyl phthalates (eq 8). We observed this ion for $R_1 = \text{Cl}$ and $R_2 =$



H (m/z 147), CH_3 (m/z 161), and COOCH_3 (m/z 205). With $R_2 = \text{CH}_3$ or COOCH_3 , structural isomers with identical EI/CI spectra were found, which may be caused by the reversal of R_1 and R_2 or by Z/E isomerism.

It must be noted that the spectrum of the dimethyl ester of 2-carboxy-3,5,5,5-tetrachloro-4-oxo-2-pentenoic acid (79) showed a very strong resemblance with the spectrum of the trimethyl ester of chloroethenetricarboxylic acid (55) (15).

In the last case the ion at m/z 205 is formed by the elimination of a CH_3O group instead of a CCl_3 group (eq 9). The difference between 55 and 79 was detected only



by the combined use of EI and CI mass spectrometry.

Conclusion

It has been shown that chlorination of terrestrial humic acid at a chlorine to carbon ratio commonly used in the production of drinking water produces several compounds that can be regarded as precursors for chloroform and C-4 diacids. Whether these precursors form the only source of chloroform cannot be concluded, but they point strongly to the important role of 1,3-dihydroxybenzene structures as the primary source. It remains to be demonstrated, however, that these structures form a significant part of the humic acid frame.

Because conversion of the precursors into chloroform is slow, they may account for the slow formation of chloroform at high chlorine to carbon doses and long reaction times (49). The fast initial formation of chloroform may proceed through other mechanisms starting with the same

1,3-dihydroxybenzene structures.

The other chlorination and oxidation products closely agree with the compounds identified by Christman and co-workers (13-15), who worked mostly with aqueous humic material. Many new chlorination and oxidation products have been detected, i.e., the cyano-substituted carboxylic acids, the chlorinated aromatic acids, and several α -monochloro and α,α -dichloroaliphatic mono- and dibasic acids.

Registry No. 1, 79-31-2; 2, 79-11-8; 3, 116-53-0; 4, 598-78-7; 6, 75-99-0; 9, 512-56-1; 12, 100-52-7; 14, 13167-36-7; 15, 13023-00-2; 17, 110-15-6; 18, 111-14-8; 21, 2257-35-4; 24, 1917-15-3; 26, 65-85-0; 28, 120-72-9; 30, 16045-92-4; 36, 103-82-2; 40, 112-05-0; 43, 74-11-3; 44, 118-91-2; 49, 334-48-5; 50, 2444-36-2; 52, 1878-66-6; 56, 112-37-8; 57, 505-48-6; 58, 88-99-3; 63, 100-21-0; 65, 121-91-5; 67, 143-07-7; 70, 123-99-9; 73, 638-53-9; 74, 111-20-6; 80, 544-63-8; 83, 528-44-9; 84, 1002-84-2; 86, 554-95-0; 87, 57-10-3; 88, 506-12-7; 89, 57-11-4; 90, 646-30-0; 91, 506-30-9; 93, 2363-71-5; 94, 112-85-6; 95, 2433-96-7; 96, 557-59-5; 97, 506-38-7; 98, 506-46-7; 99, 7138-40-1; 100, 506-48-9; TCA, 76-03-9; DCA, 79-43-6; chloroform, 67-66-3; 2-methylpentanoic acid, 97-61-0; octanoic acid, 124-07-2; ethanedioic acid, 144-62-7; pentanedioic acid, 110-94-1; hexanedioic acid, 124-04-9; heptanedioic acid, 111-16-0; 3-cyanopropanoic acid, 16051-87-9; 1,2,3-benzenetricarboxylic acid, 569-51-7; 1,2,4,5-benzenetetracarboxylic acid, 89-05-4; benzenepentacarboxylic acid, 1585-40-6; 2-chlorobutenedioic acid, 19071-21-7; (E)-2,3-dichlorobutenedioic acid, 25144-43-8; (Z)-2,3-dichlorobutenedioic acid, 608-42-4; tetrachloromethane, 56-23-5.

Literature Cited

- Rook, J. J. *Water Treat. Exam.* 1974, 23, 234-243.
- Symons, J. M.; Bellar, T. A.; Carswell, J. K.; De Marco, J.; Kropp, K. L.; Robeck, G. G.; Seeger, D. R.; Slocum, C. J.; Smith, B. L.; Stevens, A. A. *J.-Am. Water Works Assoc.* 1975, 67, 634-647.
- Zoeteman, B. C. J. Ph.D. Thesis, University of Utrecht, The Netherlands, 1978.
- Stevens, A. A.; Slocum, C. J.; Seeger, D. R.; Robeck, G. G. *J.-Am. Water Works Assoc.* 1976, 68, 615.
- Rook, J. J. *Environ. Sci. Technol.* 1977, 11, 478-482.
- Kringstad, K. P.; Ljungquist, P. O.; De Sousa, F.; Strömberg, L. M. *Environ. Sci. Technol.* 1983, 17, 555-559.
- Havlicek, S. C.; Reuter, J. H.; Ingols, R. S.; Lupton, J. D.; Ghosal, M.; Ralls, J. W.; El-Barbary, I.; Stratton, L. W.; Cotruvo, J. H.; Trichilo, C. *Prepr. Pap. Natl. Meet.-Am. Chem. Soc. Div. Environ. Chem.* 1979, 19.
- Sander, R.; Kühn, W.; Sontheimer, H. Z. *Wasser Abwasser Forsch.* 1977, 10, 155-160.
- Oliver, B. G. *Can. Res.* 1978, 21-22.
- Quimby, B. D.; Delaney, M. F.; Uden, P. C.; Barnes, R. M. *Anal. Chem.* 1980, 52, 259-263.
- Uden, P. C.; Miller, J. W. *J.-Am. Water Works Assoc.* 1983, 75, 524-527.
- Miller, J. W.; Uden, P. C. *Environ. Sci. Technol.* 1983, 17, 150-157.
- Christman, R. F.; Norwood, D. L.; Millington, D. S.; Johnson, J. D.; Stevens, A. A. *Environ. Sci. Technol.* 1983, 17, 625-628.
- Johnson, J. D.; Christman, R. F.; Norwood, D. L.; Millington, D. S. *Environ. Health Perspect.* 1982, 46, 63-71.
- Christman, R. F.; Johnson, J. D.; Norwood, D. L.; Liao, W. T.; Hass, J. R.; Pfaender, F. K.; Webb, M. R.; Bobenrieth, M. J. "Chlorination of Aquatic Humic Substances". 1981, U.S. Environmental Protection Agency Report EPA-600/2-81-016.
- Gjessing, E. T. "Physical and Chemical Characteristics of Aquatic Humus"; Ann Arbor Science: Ann Arbor, MI, 1976.
- Schnitzer, M.; Khan, S. U. "Humic Substances in the Environment"; Marcel Dekker: New York, 1972; p 196.
- Kleinhenkel, D. *Albrecht-Thaer-Arch.* 1970, 14, 3.
- Dragunov, S. In "Soil Organic Matter"; Kononova, M. M., Ed.; Pergamon Press: New York, 1961; p 65.
- Christman, R. F.; Ghassemi, M. J. *-Am. Water Works Assoc.* 1966, 58, 723-741.

- (21) Rook, J. J. In "Water Chlorination: Environmental Impact and Health Effects"; Jolley, R. L., et al., Eds.; Ann Arbor Science: Ann Arbor, MI, 1980; Vol. 3, pp 85-98.
- (22) De Laat, J.; Merlet, N.; Dore, M. *Water Res.* 1982, 16, 1437-1450.
- (23) Larson, R. A.; Rockwell, A. L. *Environ. Sci. Technol.* 1979, 13, 325-329.
- (24) Morris, J. C.; Baum, B. In "Water Chlorination: Environmental Impact and Health Effects"; Jolley, R. L., et al., Eds.; Ann Arbor Science: Ann Arbor, MI, 1978; Vol. 2, pp 29-48.
- (25) Cheshire, M. V.; Cranwell, P. A.; Haworth, R. D. *Tetrahedron* 1968, 24, 5155-5167.
- (26) Liao, W.; Christman, R. F.; Johnson, J. D.; Millington, D. S.; Hass, J. R. *Environ. Sci. Technol.* 1982, 16, 403-410.
- (27) Reuter, J. H.; Ghosal, M.; Chian, E. S. K.; Giabbi, M. In "Aquatic and Terrestrial Humic Materials"; Christman, R. F.; Gjessing, E., Eds.; Ann Arbor Science: Ann Arbor, MI, 1983; pp 107-125.
- (28) Randall, R. B.; Bengner, M.; Grocock, C. M. *Proc. Soc. London, Ser. A* 1938, 165, 432-452.
- (29) Christman, R. F.; Gjessing, E. In "Aquatic and Terrestrial Humic Materials"; Christman, R. F.; Gjessing, E., Eds.; Ann Arbor Science: Ann Arbor, MI, 1983; pp 517-528.
- (30) Stevenson, F. J. "Humus Chemistry, Genesis, Composition, Reactions"; Wiley: New York, 1982.
- (31) American Public Health Association "Standard Methods for Examination of Water and Wastewater" APHA: Chicago, 1980; p 408A.
- (32) Christman, R. F. *Environ. Sci. Technol.* 1982, 16, 143A.
- (33) Christman, R. F. *Environ. Sci. Technol.* 1982, 16, 594A.
- (34) Christman, R. F. *Environ. Sci. Technol.* 1984, 18, 203A.
- (35) Miller, J. W.; Uden, P. C.; Barnes, R. M. *Anal. Chem.* 1982, 54, 485-488.
- (36) Babcock, D. B.; Singer, P. C. *J. Am. Water Works Assoc.* 1979, 71, 149-152.
- (37) Thurman, E. M.; Malcolm, R. L. In "Aquatic and Terrestrial Humic Materials"; Christman, R. F.; Gjessing, E. T., Eds.; Ann Arbor Science: Ann Arbor, MI, 1983; pp 1-23.
- (38) Schnitzer, M.; Ogner, G. *Isr. J. Chem.* 1970, 8, 505-512.
- (39) Del'Nik, V. B.; Kagna, S. Sh.; Katsnel'son, M. G.; Rabinovich, A. S.; Skop, S. L. *J. Gen. Chem. USSR (Engl. Transl.)* 1982, 51, 1623-1626.
- (40) Bieber, T. I.; Trehy, M. L. In "Water Chlorination: Environmental Impact and Health Effects"; Jolley, R. L., et al., Eds.; Ann Arbor Science: Ann Arbor, MI, 1983; Vol. 4, pp 85-96.
- (41) Schlotterbeck, F. *Chem. Ber.* 1909, 42, 2559-2564.
- (42) Arndt, F.; Eistert, B. *Chem. Ber.* 1928, 61, 1118-1122.
- (43) Meerwein, H.; Bersin, T.; Burneleit, W. *Chem. Ber.* 1929, 62, 999-1009.
- (44) Bowman, R. E.; Campbell, A.; Williamson, W. R. N. *J. Chem. Soc.* 1964, 3846-3856.
- (45) Norwood, D. L.; Johnson, J. D.; Christman, R. F.; Hass, J. R.; Bobenrieth, M. J. *Environ. Sci. Technol.* 1980, 14, 187-190.
- (46) Boyce, S. D.; Hornig, J. F. *Water Res.* 1983, 17, 685-697.
- (47) Gurol, M. D.; Wowk, A.; Myers, S.; Suffet, I. H. In "Water Chlorination: Environmental Impact and Health Effects"; Jolley, R. L., et al., Eds.; Ann Arbor Science: Ann Arbor, MI, 1983; Vol. 4, pp 269-284.
- (48) Boyce, S. D.; Hornig, J. F. *Environ. Sci. Technol.* 1983, 17, 202-211.
- (49) Peters, C. J.; Young, R. J.; Perry, R. *Environ. Sci. Technol.* 1980, 14, 1391-1395.

Received for review May 22, 1984. Revised manuscript received November 14, 1984. Accepted January 8, 1985.

Relationships between Octanol-Water Partition Coefficient and Aqueous Solubility

Michele M. Miller and Stanley P. Wasik

Chemical Thermodynamics Division, Center for Chemical Physics, National Bureau of Standards, Washington, DC 20234

Guo-Lan Huang,[†] Wan-Ying Shiu, and Donald Mackay*

Department of Chemical Engineering and Applied Chemistry, University of Toronto, Toronto, Ontario, Canada M5S 1A4

■ The thermodynamic relationship between octanol-water partition coefficient and aqueous solubility is discussed in the light of recently measured data for highly hydrophobic chemicals. Experimental data indicate that the presence of dissolved octanol in water has little effect on the solubility of chemicals in water and that the presence of dissolved water in octanol has little effect on the solubility of chemicals in octanol. The activity coefficients of hydrophobic chemicals in aqueous solution and in octanol solution both increase with increased chemical molar volume. An approximately linear relationship between log activity coefficient and molar volume is suggested in both phases, a consequence of which is that a plot of log octanol-water partition coefficient vs. log liquid or subcooled liquid solubility has a slope of approximately -0.8. A molecular thermodynamic interpretation of the data is presented, and some environmental implications are discussed.

Introduction

Two physical chemical properties, aqueous solubility (C^s , mol/m³) and octanol-water partition coefficient (K_{OW}),

play an important role in determining the partitioning behavior of chemicals in the environment, especially bio-concentration factor and organic carbon partition coefficients. Of particular concern are stable, hydrophobic chemicals such as benzene, the polynuclear aromatic hydrocarbons, biphenyl, dibenzodioxin, and dibenzofuran, and their chlorinated and brominated congeners which have low solubilities and high K_{OW} values and thus partition appreciably into biota and organic matter in soils and sediments. It is experimentally difficult to measure very low solubilities and high K_{OW} values; thus, few accurate measurements are available for chemicals with K_{OW} values exceeding 10^6 or, correspondingly, solubilities below 50 mg/m³ (i.e., 50 µg/L). It is clear that reliable assessment of environmental fate requires accurate values for both properties; thus, there is an incentive to ensure that reported values are accurate and, since the properties are related, consistent.

Hansch et al. (1) first proposed a linear relationship between aqueous solubility and K_{OW} . Later Chiou et al. (2) developed this relationship more quantitatively for environmental chemicals, and several subsequent correlations have been proposed, notably by Yalkowsky and Valvani (3), Mackay et al. (4), Amidon et al. (5), Chiou et al. (6), Tewari et al. (7), Banerjee et al. (8), and Bowman

[†]Present address: Department of Chemistry, Nankai University, Trientsin, China.

and Sans (9). Since K_{OW} and C^S vary over approximately 8 orders of magnitude, it is logical that most correlations seek a relationship between $\log K_{OW}$ and $\log C^S$ since this avoids distortion of the results in favor of the high K_{OW} or high C^S values by assuming that the errors are normally distributed about the logarithmic quantities and are thus errors of a constant factor (e.g., \pm a factor of 2) rather than of constant absolute magnitude (e.g., ± 10 $\mu\text{g/L}$). This approach, although logical, justifiable, and convenient, can be criticized in that there has been no demonstrated fundamental thermodynamic reason that a log-log plot should be linear. As is shown later there is thermodynamic justification for suggesting that the product ($K_{OW}C^S$) should display relative constancy or at least should vary systematically with molecular structure or some other parameter. This is equivalent to forcing a slope of -1 on a $\log K_{OW}$ vs. $\log C^S$ plot. But, as Chiou et al. (6) and Bowman and Sans (9) have convincingly demonstrated, the available experimental data display a consistently lower slope.

Recently, accurate values of C^S and K_{OW} have become available (10) for a wide range of chemicals which enable these two correlation approaches to be explored with more reliability than has been previously possible. In this work we examine this issue and report some experimental data that help to elucidate the fundamental thermodynamic relationships between K_{OW} and C^S and thus the preferred method of correlation. It is shown that there is a thermodynamic basis for a slope of approximately -0.8 on the $\log K_{OW}$ - $\log C^S$ plot. Further, we discuss some implications regarding environmental partitioning, especially bioconcentration.

Thermodynamic Basis

The thermodynamic relationships between C^S and K_{OW} have been reviewed recently by Chiou et al. (6); thus, only a brief summary is presented here. It can be shown that K_{OW} is given by eq 1 where γ_{WO} is the activity coefficient

$$K_{OW} = (\gamma_{WO}v_{WO})/(\gamma_{OW}v_{OW}) \quad (1)$$

of the chemical in water saturated with octanol, γ_{OW} is its activity coefficient in octanol saturated with water, v_{WO} is the molar volume (m^3/mol) of water saturated with octanol, and v_{OW} is the molar volume of octanol saturated with water.

For liquid chemicals the solubility C^S_L is given by eq 2

$$C^S_L = 1/(\gamma_{Ww}) \quad (2)$$

in which v_w is the molar volume of water saturated with the chemical and γ_w is the activity coefficient of the chemical in water. It is assumed that the solubility of water in the liquid chemical is negligible; thus, the activity coefficient of the chemical in the chemical phase is unity. These equations contain the implicit assumption that the chemical is present at high dilution; thus, its presence does not significantly affect the molar volumes.

For a solid chemical of melting point T_M (K), the solubility C^S_S is reduced by a factor F , the fugacity ratio, which is given approximately at temperature T by

$$F = \exp[\Delta S(1 - T_M/T)/R] = C^S_S/C^S_L \quad (3)$$

where ΔS is the entropy of fusion and R is the gas constant. ΔS can be calculated from experimentally measured enthalpies of fusion as discussed by Miller et al. (10), or for approximate purposes, it can be estimated from Walden's rule as discussed by Yalkowsky (11) in which case $\Delta S/R$ is approximately 6.8 ± 1.0 . Another method of estimating

$\Delta S/R$ is to measure the solubility of the solid in a solvent in which the chemical is believed to form an ideal solution. C^S_S is then F/v_S where v_S is the solvent molar volume. For the substances of interest here benzene is probably the most suitable solvent. It follows that for liquid chemicals

$$K_{OW}C^S_L = (\gamma_{WO}/\gamma_w)(v_{WO}/v_w)/(\gamma_{OW}v_{OW}) = Q \quad (4)$$

while for solid chemicals

$$K_{OW}C^S_S/F = (\gamma_{WO}/\gamma_w)(v_{WO}/v_w)/(\gamma_{OW}v_{OW}) = Q \quad (5)$$

The quantity Q has dimensions of concentration (mol/m^3). It can be viewed as the "pseudosolubility" of the liquid chemical (or the subcooled liquid chemical in the case of a solid) in octanol saturated with water. This view is justified by noting that a partition coefficient can be regarded not only as a ratio of two concentrations but also as a ratio of the two saturation concentrations or solubilities. The prefix "pseudo" is necessary because in many cases the chemical and octanol are fully miscible; thus, a real solubility limit does not exist.

The use of the product Q has been previously discussed by Banerjee et al. (8) and Mackay et al. (4). Our approach is thus to examine the values, determinants, and constancy of Q in the hope that it can be estimated from molecular structure or from some other property, including solubility and K_{OW} . If successful, this leads to a relationship between solubility and K_{OW} . It is first instructive to examine the various groups which comprise Q and discuss their likely variability.

First, γ_{WO}/γ_w is the ratio of the activity coefficient of the chemical in water saturated with octanol, to that in pure water. It will deviate from unity only if octanol interacts appreciably with the chemical in aqueous solution. Now the octanol concentration in water is low ($4.5 \text{ mol}/\text{m}^3$) (12, 13) as is that of the chemical; thus, no strong interaction is expected. If there is such an interaction it will be detectable as a difference in solubility between that of the chemical in water and that in water saturated with octanol. Chiou et al. (6) have suggested that there may be a significant difference; i.e., γ_{WO}/γ_w deviates from unity due to a "solubilizing" effect of octanol. Specifically, they suggest that the ratio may be 2.6 for DDT and 1.8 for hexachlorobenzene. To investigate this, we have conducted, and later report, some experimental determinations of these solubilities.

Second, v_{WO}/v_w , the ratio of molar volumes, can be calculated from the solubility of octanol in water. Assuming no volume change on mixing, 1 m^3 of a saturated solution of octanol in water of concentration $4.5 \text{ mol}/\text{m}^3$ contains only 4.5 mol of octanol and some 55000 mol of water; thus, the molar volume of the solution is essentially that of water, and v_{WO}/v_w differs negligibly from unity.

Third, v_{OW} , the molar volume of octanol saturated with water, has been measured as $126.6 \times 10^{-6} \text{ m}^3/\text{mol}$ (9) and is likely to vary only when the chemical is at high enough concentration in the octanol solution to alter the miscibility of water and octanol. It can thus be taken as constant.

Finally, γ_{OW} , the activity coefficient of the substance in octanol saturated with water, is likely to depend on the chemical nature of the substance, but in an as yet unpredictable way. It is possible to invoke theories of the Regular Solution or Flory-Huggins type to explain any variation in γ_{OW} , but there is no a priori method of estimating the magnitude of γ_{OW} or its constancy. In their previous study Mackay et al. (4) noted that γ_{OW} is fairly constant and certainly varies much less than γ_{WO} . The only method of estimating γ_{OW} is to measure a property of a solution of the chemical in octanol saturated with

water such as solubility or partial vapor pressure. To investigate this term, we have measured the solubilities of selected chemicals in octanol saturated with water. This is possibly only for solids that also have a F value which influences solubility; thus, to estimate γ_{OW} directly requires an accurate value of F .

Finally, it is interesting to measure solubilities in octanol alone, i.e., with no water present, in order to determine the extent to which the presence of water influences the behavior of the chemical in octanol solution.

Experimental Section

Chemicals. The polynuclear aromatic hydrocarbons were obtained from Aldrich, K & K Rare and Fine Chemicals, and Eastman Kodak Co. The polychlorinated biphenyls were obtained from Aldrich and Foxboro/Analab, and some were kindly supplied by Dr. S. Safe. All chemicals received were of the highest available commercial quality and were used for analysis without further purification. Octanol of 99+ % purity was also obtained from Aldrich. Methanol and acetonitrile (high-performance liquid chromatography grade) were obtained from Caledon Laboratory Ltd. Milli-Q Water and retreated Milli-Q water using a Norganic system were used for all experiments.

(a) Determination of Solubility in Water. The apparatus and experimental procedure used were the dynamic-coupled-column liquid chromatography method previously described by May et al. (14, 15). Saturated aqueous solutions were prepared by passage of water through a generator column which was packed with glass beads coated with the chemical. The saturated solution was then pumped through an extractor column packed with 37–50 μ Bondapak/Corasil (Waters Associates). By switching of the eight-port Valco valve the absorbed chemical was extracted by the mobile phase and directly injected onto the analytical column. The instrument was a Waters Associates Model ALC/GPC liquid chromatograph consisting of a Model 6000 solvent delivery system, a Model 660 solvent flow programmer, a Model M45 solvent delivery system, a Model 440 UV absorbance detector with 254- and 280-nm kits, and a Model 420-E fluorescence detector with excitation filter 340 nm. The analytical column was a 3.9 mm OD \times 300 mm long μ Bondapak C₁₈ column. Integration of the peak area was done by a Hewlett-Packard Model 3380A integrator recorder.

(b) Determination of Solubility in Water Saturated with Octanol. To determine the solubility of PNAs or PCBs in water saturated with octanol, the general procedure was the same as described above. Water saturated with octanol was prepared by equilibrating octanol and water by gentle stirring and then prolonged settling. This solution was pumped through the generator column and extractor column instead of pure water. Methanol was used to purge the extractor and analytical columns after each run to prevent deposition of octanol on the columns.

(c) Determination of the Solubilities of PNAs and PCBs in Pure Octanol and Water-Saturated Octanol. Saturated solutions were prepared in dry octanol by adding an excess amount of the PNAs and PCBs to approximately 2 mL of solvent in a 7-mL sample vial, capped with a screw top with a Teflon septum. The vials were clamped onto a wrist-action shaker, shaken gently for 24 h, and left to settle for at least 48 h before analysis. The second method for preparation of saturated solutions was by gently stirring a layer of octanol on water in a flask. To prepare solutions in octanol saturated with water, approximately 20 mL of double-distilled water was added to a 50-mL flask with a ground-glass stopper, and approximately 10 mL of octanol together with an excess amount of the compound of in-

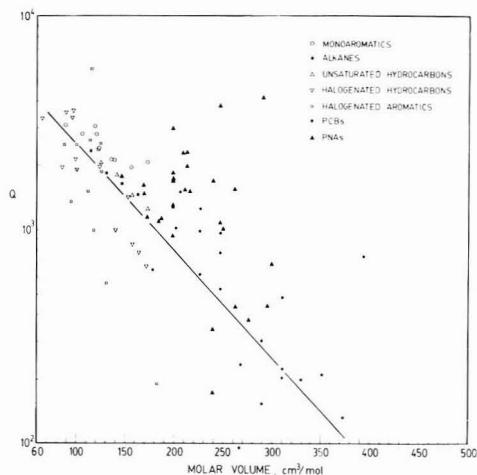


Figure 1. Plot of $\log Q$ vs. molar volume using data from Table I.

terest was also added to the flask. This solution was stirred gently for at least 24 h with a Teflon-coated magnetic stirrer without breaking up the octanol–water interface. In the case of solids, the mixture was shaken gently. The solution was then allowed to settle for 48 h before analysis, with no emulsion formation being observed.

GC Analysis. A Hewlett-Packard Model 5750 GC equipped with a flame ionization detector was used for the analysis of the octanol solutions. A pair of 3 m long \times 3.2 mm OD stainless steel columns packed with 10% SE30 ultraphase coated on Chromasorb P [dimethylchlorosilane (DMCS) treated, acid washed, 60/80 mesh] was used. The injection port temperature was set at 300 °C, the detector was set at 320 °C, and the oven was in the isothermal mode (set between 200 and 260 °C depending on the boiling point of the compound being analyzed). Peak areas corresponding to 0.5 μ L of the octanol solution were determined on a Hewlett-Packard Model 3371B electronic integrator. Calibration standards were prepared by weighing known amounts of the chemical and dissolving in benzene.

Results and Discussion

Experimental C^S_S , C^S_L , and K_{OW} data were gathered for hydrophobic organic chemicals, chlorinated benzenes, chlorinated biphenyls, and polynuclear aromatics. The data given in Table I are C^S_S , C^S_L , K_{OW} , and the group Q as defined by eq 4 or 5. The molar volumes V were obtained from density data or calculated by the Le Bas method (16), which is a simple additive method for estimating molar volume at the normal boiling point. It should be noted that the chlorobenzene and chlorobiphenyl data are taken from the recent accurate work of Miller et al. (10). There is a definite trend illustrated in Figure 1 for Q to become smaller as molar volume increases, an equation being indicated by the form

$$\log Q = A - BV \quad (6)$$

There is a considerable scatter in the data due, it is believed, to a combination of errors in K_{OW} and C^S_L determinations. Regression of all the data gave a correlation coefficient of only 0.67. Examination of the data indicates that A has a value of 3.9 ± 0.2 and B a value of 0.005 ± 0.001 when V has units of cubic centimeter per mole. Such an equation could be used in combination with eq 4 for

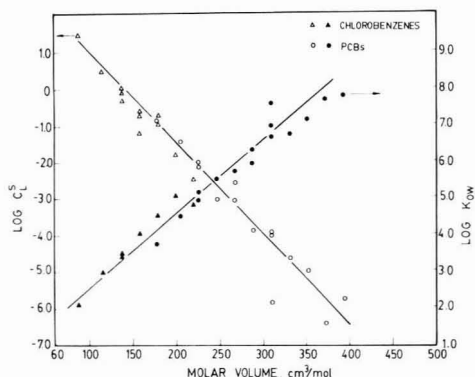


Figure 2. Plots of $\log C^S_L$ and $\log K_{OW}$ data (10) vs. molar volume for chlorobenzenes and PCBs.

liquids or eq 5 and 3 for solids to provide a solubility-octanol-water partition coefficient correlation, namely

$$(\log K_{OW} + \log C^S_L) \text{ or } (\log K_{OW} + \log C^S_L - \log F) = \log Q = A - BV \quad (7)$$

where

$$F \approx \exp[6.8(1 - T_M/T)] \quad (8)$$

It is preferable to use measured entropy of fusion data when available in place of 6.8, which is $\Delta S/R$. Table I contains some measured and estimated values of $\Delta S/R$ as indicated. In their previous correlation, Mackay et al. (4) suggested that Q was constant with a value of 1795 mol/m³. The reason for failing to recognize the variability in Q was that the data used to generate that conclusion were for substances with molar volumes primarily restricted to the range 100–200 cm³/mol. Further, there was a tendency to use overestimated, calculated values of K_{OW} for substances of high K_{OW} . The new data for high molar volume PCBs indicate that Q is substantially reduced for highly hydrophobic substances. A consistent experimental error of a factor of 10 would be required to account for this variation.

It is important to emphasize that these solubility and K_{OW} data extend over 8 orders of magnitude; thus, combining them in the term Q , which varies only by a factor of 28, is a considerable initial accomplishment which is almost certainly the correct "first-order" correlating step. The characterization of the variation in Q can thus be regarded as a "second-order" correlating step to further refine the accuracy of the solubility- K_{OW} relationship. We use these terms in the same sense that the ideal gas law is a first-order correlation and expressions for compressibility are second order.

We can now address the question of the source of the Q variation. This information may be valuable in suggesting suitable correlating equations.

First, it is useful to explore how the Q variation arises from the solubility and K_{OW} terms. Figure 2 is a plot of $\log C^S_L$ and $\log K_{OW}$ vs. molar volume for the PCBs and chlorobenzenes. Since $\log Q$ is the sum of these terms, it is clear that the fall in Q arises because the slope of the $\log K_{OW}$ line is less than that of $\log C^S_L$. A molar volume increase of 100 cm³/mol causes C^S_L to decrease by a factor of 224, while K_{OW} increases by a factor of 71; thus, Q decreases by a factor of 3.15.

The term γ_{WO}/γ_W which equals the ratio of the solubility in water S_W to that in water saturated with octanol S_{WO} can be evaluated from the data in Table II. There is no

significant variation from unity for these substances. Unfortunately these measurements are difficult to make because if the presence of the chemical, or some other effect such as temperature variation, causes the octanol to become supersaturated and form a second, possibly micelle phase, this phase will dissolve the chemical and may coat the solid chemical surface with a layer of octanol. The most likely effect, a "solubilization" of the chemical due to the presence of octanol, is possible only if there is appreciable octanol-chemical interaction in the aqueous solution. There is at present little evidence for such an effect at the high dilutions discussed here, although the effect is well-known for concentrations of the order of a few percent. The magnitude of the "solubilizing" effect is often overestimated, as discussed by Herzl and Murty (17). Chiou et al. (6) suggest an effect of the order of a factor of 2.6 for DDT which has a molar volume of 341 cm³/mol calculated by the Le Bas method (16). This factor is small compared to the factor required to explain the variation in Q or with the factor required to "correct" the DDT solubility to the "ideal line value" presented by Chiou et al. (6). We thus conclude that the group γ_{WO}/γ_W is probably not the primary source of the variation in Q , but we do not rule out the possibility that it has some effect. Determining the magnitude of the effect experimentally will be very difficult. As we discuss later, this effect, even if present, may be of little environmental relevance.

Table II also presents the data for the solubility of selected chemicals in octanol, S_O , and in octanol saturated with water, S_{OW} . It is clear that the presence of water has very little effect on the solubility of chemicals in octanol. This is remarkable considering that water is soluble in octanol to the extent of 1.7 mol/L, i.e., a water to octanol mole ratio of approximately 1/3.5. Apparently the solubility of a chemical in octanol saturated with water is almost totally dominated by the interactions between the chemical and octanol and not the chemical with water. This suggests that the hydrophobic chemical is surrounded by the aliphatic octanol chain and does not experience appreciable contact with water. The molar volume of octanol is 157 cm³/mol; thus, when the solute molar volume greatly exceeds this value, it is possible that complete segregation of hydrophilic groups from the chemical becomes less feasible. The result is onset of a decreased compatibility or solubility between the chemical and the now partially hydrophilic medium because hydrophobic-hydrophilic interactions become more prevalent. This may be manifested as a decrease in the pseudosolubility or in Q . We therefore suggest that the decrease in Q with increased molar volume is the result of decreased solubility of the chemical in octanol saturated with water, which in turn may be attributable to an increased interaction between hydrophobic and hydrophilic parts of the molecules. Other effects such as restricted rotation may also be important (18).

If it is accepted that γ_{WO}/γ_W and v_{WO}/v_W are unity, then eq 4 can be used to derive a fundamental correlation for γ_{OW} , while eq 2 can be used to give a correlation for γ_W , in both cases a suitable correlating parameter being chemical molar volume V . It can be shown that for the chlorobenzene and PCB data in Figure 2

$$\log C^S_L = 3.40 - 0.0248V \quad r = 0.92 \quad (9)$$

$$\log K_{OW} = 0.49 + 0.0200V \quad r = 0.97 \quad (10)$$

where r is the correlation coefficient; hence, by addition a version of eq 4 is obtained.

$$\log Q = 3.89 - 0.0048V \quad (11)$$

Table I. Physical-Chemical Properties of Selected Hydrophobic Organic Chemicals at 25 °C^a

compounds	<i>M_r</i>	mp, K	molar volume, cm ³ /mol	solubility, mol/m ³		log <i>K_{OW}</i>	<i>Q</i>
				<i>C^S</i> (measd)	<i>C^S_L</i> (calcd)		
Saturated Hydrocarbons							
<i>n</i> -pentane	72.15	143.3	115.3	0.565		3.62	2355
<i>n</i> -hexane	86.17	178	126.7	0.143		4.11	1842
<i>n</i> -heptane	100.21	182.4	146.5	0.0305		4.66	1394
<i>n</i> -octane	114.23	216.8	162.5	0.00597		5.18	903
Unsaturated Hydrocarbons							
1-hexene	84.16	121.6	125	0.828		3.39	2032
1-heptene	98.19	154	140.8	0.185		3.99	1808
1-octene	112.2	171.3	157	0.0365		4.57	1356
1-nonene	126.24	192	173	0.00885		5.15	1250
1-pentyne	68.13	183	98.7	11.54		2.12	1521
1-hexyne	82.15	141.1	114.8	8.37		2.73	4602
Halogenated Hydrocarbons							
1-chlorobutane	92.57	150	66.04	9.43		2.55	3346
1-chloroheptane	134.65	204	94.5	0.101		4.15	1427
1-bromobutane	137.03	161	95.23	6.34		2.75	3565
1-bromopentane	151.05	178	104.6	0.838		3.37	1964
1-bromohexane	165.08	188	114.0	0.156		3.80	984
1-bromoheptane	179.11	215	123.5	0.0371		4.36	850
1-bromooctane	193.13	218	133	0.00865		4.89	671
bromochloromethane	129.4	185	87.25	129.0		1.41	3316
1-bromo-3-chloropropane	157.44		106.01	14.2		2.18	2149
1-iodoheptane	226.10	225	151.74	0.0155		4.70	777
trichloroethylene	131.39	186	89.02	10.4		2.53	3524
4-bromo-1-butane	135.01		92.42	5.66		2.53	1918
allyl bromide	120.98	223	82.36	31.7		1.79	1955
Halogenated Aromatics							
chlorobenzene (CB)	112.56	22.74	116.9 ^b	2.62		2.98	2502
1,2-CB	147.01	156	137.8 ^b	0.628		3.38	1506
1,3-CB	147.01	248.3	137.8 ^b	0.847		3.48	2627
1,4-CB	147.01	326.1	137.8 ^b	0.210	0.407	3.38	976
1,2,3-CB	181.45	325.8	158.7 ^b	0.0676	0.157	4.04	1721
1,2,4-CB	181.45	290	158.7 ^b	0.254		3.98	2426
1,3,5-CB	181.45	337	158.7 ^b	0.0227	0.054	4.02	565
1,2,3,4-CB	215.9	320	179.6 ^b	0.0565	0.092	4.55	3264
1,2,3,5-CB	215.9	323.9	179.6 ^b	0.0134	0.0247	4.65	1103
1,2,4,5-CB	215.9	412.2	179.6 ^b	0.0109	0.164	4.51	5307
penta-CB	250.3	357.7	200.5 ^b	0.00332	0.0133	5.03	1425
hexa-CB	284.8	501.5	221.4 ^b	1.65 × 10 ⁻⁵	6.47 × 10 ⁻⁴	5.47	191
iodobenzene	241.79	242	126.0	0.984		3.28	1875
<i>o</i> -fluorobenzyl chloride	144.58		95.43	2.88		2.67	1347
<i>m</i> -fluorobenzyl chloride	144.58		121.1	2.86		2.77	1684
Aromatic Hydrocarbons							
benzene	78.11	278.5	88.7	22.90		2.13	3089
toluene	92.13	178	106.3	6.28		2.65	2805
ethylbenzene	106.2	178	122.5	1.76		3.13	2374
<i>o</i> -xylene	106.2	247.8	120.6	2.08		3.13	2806
<i>m</i> -xylene	106.2	225.1	123.2	1.51		3.20	2393
<i>p</i> -xylene	106.2	286.2	119.8	2.02		3.18	3057
<i>n</i> -propylbenzene	120.2	171.4	139.4	0.434		3.69	2126
<i>n</i> -butylbenzene	134.2	185	156.1	0.103		4.28	1963
<i>n</i> -pentylbenzene	148.65	198	172.7	0.0259		4.90	2057
<i>n</i> -hexylbenzene	162.28	211		0.00627		5.52	2076
1,2,3-trimethylbenzene	120.2	247.6		0.545		3.55	1934
1-ethyl-2-methylbenzene	120.2	192.2	136.5	0.621		3.53	2104
PNAs							
naphthalene	128.2	353.2	148 ^b	0.239	0.797	3.35	1784
1-methylnaphthalene	142.2	251	170 ^b	0.200		3.87	1483
2-methylnaphthalene	142.2	307.6	170 ^b	0.18	0.224	3.86	1622
1,3-dimethylnaphthalene	156.2		199 ^b	0.0512		4.42	1315
1,4-dimethylnaphthalene	156.2	280.7	199 ^b	0.073		4.37	1711
1,5-dimethylnaphthalene	156.2	354	199 ^b	0.0216	0.0771	4.38	1850
2,3-dimethylnaphthalene	156.2	378	199 ^b	0.0192	0.12	4.40	3014
2,6-dimethylnaphthalene	156.2	381	199 ^b	0.0128	0.0853	4.31	1742
1-ethylnaphthalene	156.2	259.1	199 ^b	0.0685		4.39	1681
1,4,5-trimethylnaphthalene	176.2	337	214 ^b	0.0119	0.029	4.90	2304
biphenyl	154.21	344	185 ^b	0.0454	0.126	3.95	1123
acenaphthene	154.21	369.2	173 ^b	0.0255	0.140	3.92	1164
fluorene	154.21	389	188 ^b	0.0119	0.0753	4.18	1140
phenanthrene	178.2	374	199 ^b	6.62 × 10 ⁻³	0.0252	4.57	936

Table I (Continued)

compounds	M_r	mp, K	molar volume, cm^3/mol	solubility, mol/m^3		$\log K_{OW}$	Q
				C^S (measd)	C^S_L (calcd)		
anthracene	178.2	489.2	197 ^b	4.10×10^{-3}	0.0398	4.54	1380
9-methylanthracene	196.3	354.5	219 ^b	1.33×10^{-3}	1.32×10^{-2c}	5.07 ^d	1551
9,10-dimethylanthracene	206.3	455	241 ^b	2.7×10^{-4}	9.68×10^{-3c}	5.25 ^d	1720
pyrene	202.3	429	214 ^b	6.67×10^{-4}	1.32×10^{-2c}	5.18	1998
fluoranthene	202.3	384	217 ^b	1.3×10^{-3}	9.15×10^{-3c}	5.22 ^d	1519
1,2-benzofluorene	216.28	460	240 ^b	2.1×10^{-4}	8.35×10^{-3c}	5.32 ^d	174
2,3-benzofluorene	216.28	482	240 ^b	9.25×10^{-6}	6.12×10^{-4c}	5.75 ^d	344
1-methylfluorene	180	358	210 ^b	6.06×10^{-3}	0.0237 ^c	4.97	2211
chrysene	228.3	528	251 ^b	8.76×10^{-6}	1.66×10^{-3c}	5.79 ^d	1023
1,2-benzoanthracene	228.3	433	248 ^b	6.13×10^{-5}	1.33×10^{-3c}	5.91 ^d	1081
2,3-benzanthracene	228.3	630	248 ^b	2.5×10^{-6}	4.82×10^{-3c}	5.90 ^d	3828
3,4-benzopyrene	252.3	448	263 ^b	1.5×10^{-5}	4.59×10^{-4}	5.98	438
perylene	252.3	550	263 ^b	1.6×10^{-6}	4.95×10^{-4c}	6.50 ^d	1565
3-methylcholanthrene	268.36	451	296 ^b	1.1×10^{-5}	3.43×10^{-4c}	7.11 ^d	441
benzo[ghi]perylene	276.34	550	277 ^b	9.4×10^{-7}	3.02×10^{-4c}	7.10 ^d	380
1,2,3,4-dibenzanthracene	278.35	479	300 ^b			7.19 ^d	
1,2,5,6-dibenzanthracene	278.35	539	300 ^b	1.80×10^{-6}	4.46×10^{-4c}	7.19 ^d	690
2,3,6,7-dibenzanthracene	278.35	543	300 ^b			7.19 ^d	
coronene	300.36	633	292 ^b	4.66×10^{-7}	9.63×10^{-4c}	7.64 ^d	4203
PCBs							
biphenyl	154.21	342.6	178.3 ^b	0.0435	0.109	3.76	645
2-	188.7	305.3	205.5 ^b	0.0268	0.0315	4.50	1015
2,5-	223.1	295	226.4 ^b	0.0087		5.16	1258
2,6-	223.1	307.9	226.4 ^b	0.00623	0.00733	4.93	624
2,4,5-	257.5	349.5	247.3 ^b	6.32×10^{-4}	2.45×10^{-3}	5.51	793
2,4,6-	257.5	334.3	247.3 ^b	8.76×10^{-4}	1.80×10^{-3}	5.47	531
2,3,4,5-	292	363.9	268.2 ^b	7.17×10^{-5}	4.51×10^{-4}	5.72	237
2,2',4,5-	292	339.1	268.2 ^b	5.63×10^{-5}	1.77×10^{-4}	5.73	95
2,3,4,5,6-	326.4	347.6	287.1 ^b	1.68×10^{-5}	1.53×10^{-4}	6.30	305
2,2',4,5,5'-	326.4	350.1	287.1 ^b	5.92×10^{-5}	1.83×10^{-4}	5.92	152
2,2',3,3',6,6'-	360.9	385.2	310 ^b	1.67×10^{-5}	1.14×10^{-4}	6.63	486
2,2',3,3',4,4'-	360.9	424.9	310 ^b	7.84×10^{-7}	2.65×10^{-5}	6.93	226
2,2',4,4',6,6'-	360.9	386.7	310 ^b	1.13×10^{-6}	5.71×10^{-6}	7.55	203
2,2',3,3',4,4',6-	395.3	395.4	330.9 ^b	5.49×10^{-6}	4.13×10^{-5}	6.68	198
2,2',3,3',5,5',6,6'-	429.8	433.8	351.8 ^b	9.15×10^{-7}	1.63×10^{-5}	7.11	210
2,2',3,3',4,5,5',6,6'-	464.2	455.8	372.7 ^b	3.88×10^{-8}	9.13×10^{-7}	8.16	132
deca-	487.7	578.9	393.6 ^b	1.49×10^{-8}	4.12×10^{-6}	8.26	7.49

^a Solubilities and octanol-water partition coefficients were obtained from ref 7 and 10 except for PNAs which were obtained from ref 4, 19, and 20. ^b Le Bas method. ^c Calculated from fugacity ratio using $\Delta S = 13.5$ eu. ^d Calculated $\log K_{OW}$ values.

The molar volume V has units of cubic centimeter per mole. If the ratio γ_{OW}/γ_W differs from unity, the magnitude of the effect can be regarded as being subsumed in the correlation for γ_{OW} which is then $\gamma_{OW}\gamma_W/\gamma_{OW}$. Thus, since v_W is 18×10^{-6} and v_{OW} is 126×10^{-6} m^3/mol , then

$$\log \gamma_W = -\log C^S_L - \log v_W = 1.34 + 0.0248V \quad (12)$$

$$\log \gamma_{OW} = -\log Q - \log v_{OW} = 0.01 + 0.0048V \quad (13)$$

It is striking that when V is small, γ_{OW} as correlated by eq 13 is close to unity, implying an ideal solution, which is expected for similar chemicals. As molar volume increases, the nonideality in the water phase increases very rapidly because of the high value of the coefficient 0.0248 in eq 9 and 12, and the solubility drops correspondingly. There is a similar tendency in octanol as indicated in the equations for γ_{OW} and Q , but its magnitude is less, corresponding to the coefficient 0.0048. This can be interpreted as a drop in the solubility of the chemical in the octanol phase. The net effect on K_{OW} , which is the ratio of these solubilities, is a coefficient of 0.020. The advantage of this correlating approach over the simple $\log C^S_L - \log K_{OW}$ approach is that it can be traced to fundamental activity coefficient—molar volume relationships.

In general, for a homologous series we suggest that C^S_L and Q can be correlated with molar volume (or other

molecular descriptors such as surface area) by equations of the form of 9 and 10 containing four adjustable constants $X_1, X_2, Y_1,$ and Y_2 namely

$$\log C^S_L = X_1 - Y_1V \quad (14)$$

$$\log Q = X_2 - Y_2V \quad (15)$$

thus

$$\log K_{OW} = \log Q - \log C^S_L = (X_2 - X_1) + (Y_1 - Y_2)V \quad (16)$$

Eliminating V from eq 14 and 16 gives

$$\log K_{OW} = [(Y_1 - Y_2)/Y_1] \log C^S_L + (X_2 - X_1Y_2/Y_1) \quad (17)$$

which is the correlating form used by Chiou et al. (6).

If fundamental relationships between activity coefficients or solubility and molar volumes (or another descriptor) apply of the form of eq 12 and 13 or eq 14 and 15, a consequence is that a plot of $\log K_{OW}$ vs. $\log C^S_L$ will be linear and will have a slope of $(Y_1 - Y_2)/Y_1$. Since Y_1 and Y_2 are both likely to be positive (higher molar volume leading to greater nonideality) and Y_2 is much smaller than Y_1 (because octanol is a more ideal solvent), then $(Y_1 - Y_2)/Y_1$ will tend to have a value somewhat less than 1.0 and apparently in the range 0.79–0.86. The correlating approach adopted by Chiou et al. (6) and others has thus a fundamental thermodynamic basis, if log activity coef-

Table II. Solubilities at 25 °C of Chemicals in Water (S_w), in Water Saturated with Octanol (S_{wo}), in Octanol (S_o), and in Octanol Saturated with Water (S_{ow})

compounds	S_w , g/m ³	S_{wo} , g/m ³	S_o , kg/m ³	S_{ow} , kg/m ³
naphthalene	31.7	28.9	122.9	126.5
biphenyl	7.5	6.85	106.6	106.9
acenaphthene	3.9		39.5	37.4
fluorene	1.9		34.6	35.9
1-methylfluorene	1.09	1.05	50.1	39.9
anthracene	0.075		2.11	2.37
	0.046	0.031		
phenanthrene	1.18		71.5	71.6
fluoranthene	0.26		34.9	36.1
pyrene	0.135		28.3	29.4
chrysene	0.0012	0.0066	0.457	0.425
2,3-benzofluorene	0.04	0.037	3.83	3.83
perylene	0.0004		0.768	0.738
2,3-benzanthracene	0.00057		1.21	1.35
1,2,5,6-dibenzanthracene	0.0005		0.261	0.261
coronene	0.00014		0.116	0.112
4-chlorobiphenyl (CBP)	1.17	1.11	114.7	110.3
4,4'-diCBP	0.062	0.0343	15.9	14.8
2,4,5-triCBP	0.163		45.37	39.9
2,2',5,5'-tetraCBP	0.0265		68.41	64.85
2,3,4,5-tetraCBP	0.0209		40.8	37.23
decaCBP	7.43×10^{-6}		0.826	0.546

ficient vs. linear descriptor equations apply in both water and octanol phases.

Correlating Approaches. The preferred correlations depend on the quality and quantity of the available data. We suggest several methods of decreasing rigor.

If reliable solubility and K_{OW} data are available for a homologous series, any solid solubilities should be "corrected" to the subcooled liquid values C_{SL}^S , with correlations sought of the form of eq 14–16 for C_{SL}^S , K_{OW} , and their product Q as a function of molar volume. These can be used to derive the fundamental activity coefficient equations of the form of 12 and 13. It is likely that X_2 will be close to zero and X_1 will have a large value close to 3.0. Y_1 will probably be in the range 0.02–0.03 and Y_2 in the range 0.004–0.005 such that $(Y_2 - Y_1)/Y_1$ has a value of -0.79 to -0.86 . Correlations can then be established for C_{SL}^S , Q , and K_{OW} and between K_{OW} and C_{SL}^S . A second simpler method is to use the two constants to establish the linear relationship between $\log K_{OW}$ and $\log C_{SL}^S$ for a homologous series, but this does not enable either to be calculated individually from molar volume. It may be difficult to determine whether the source of error in "outliers" originates in K_{OW} or C_{SL}^S .

A third approach is to acknowledge that although different homologous series will have different $\log K_{OW} - \log C_{SL}^S$ constants, it may be possible to extrapolate from series to series if there is some assurance that similar values apply. The correlations of Chiou et al. (6) and Bowman and Sans (9) include differing series; thus, it is expected that their accuracy suffers although the convenience and utility increase.

The correlation of Mackay et al. (4) is equivalent to forcing Y_2 to be zero; thus, $(Y_2 - Y_1)/Y_1$ is -1 .

It is hoped that as more accurate data become available for solubility and K_{OW} , they can be subjected to correlation and thermodynamic interpretation and thus build up a reliable data base from which modest predictions can be made.

Environmental Implications. The constants X_2 and Y_2 which characterize the octanol-phase nonideality presumably have magnitudes which are specific to the nature of the octanol–water–chemical interactions in the octanol phase and possibly to octanol–chemical interactions in the

aqueous phase. The following question must then be addressed: do the magnitudes of these constants describe interactions between the chemical and lipid phases as occur in organisms or organic carbon phases as occur in soils and sediments? It can be argued that biological lipid and natural organic carbon phases are sufficiently different from octanol that the nature of the interactions may be quite different; thus, there may be little environmental merit in pursuing in much further detail the nature of octanol–water–chemical interactions. Certainly natural lipid or organic carbon phases are not water soluble to the same extent as octanol; thus, the study of the "solubilizing" effect of octanol on chemicals in aqueous solution is largely irrelevant to environmental concerns. Likewise, there may be little merit in examining in detail the solubility of chemicals in octanol, with or without water, unless there is some assurance that the results have some significance for elucidating the solubility of chemicals in natural organic phases. Until such significance can be justified, a strong case can be made that most effort should be devoted to measuring, explaining, and correlating partitioning between aqueous phases and naturally occurring organic phases such as lipids, sediments, or soils. The success of correlations between K_{OW} or solubility and bioconcentration factor or organic carbon partition coefficient may be due largely to their mutual dependence on γ_w which is the quantity which varies over the widest range. It is not known if γ_{OW} provides a reliable estimate of activity coefficients of chemicals in lipids or natural organic phases. Further refinement of the relationship between solubility and octanol–water partition coefficient is probably not justified for environmental purposes because the magnitude of any further "correction" is probably less than the doubt surrounding the differences between octanol and naturally occurring environmental organic phases which octanol purports to simulate.

Acknowledgments

We are grateful to the Ontario Ministry of Environment for financial support and to S. Safe of Texas A&M University for kindly providing some pure PCBs.

Registry No. 4-CBP, 2051-62-9; 4,4'-diCBP, 2050-68-2; 2,4,5-triCBP, 15862-07-4; 2,2',5,5'-tetraCBP, 35693-99-3; 2,3,4,5-tetraCBP, 33284-53-6; decaCBP, 2051-24-3; naphthalene, 91-20-3; biphenyl, 92-52-4; acenaphthene, 83-32-9; fluorene, 86-73-7; 1-methylfluorene, 1730-37-6; anthracene, 120-12-7; phenanthrene, 85-01-8; fluoranthene, 206-44-0; pyrene, 129-00-0; chrysene, 218-01-9; 2,3-benzofluorene, 243-17-4; perylene, 198-55-0; 2,3-benzanthracene, 92-24-0; 1,2,5,6-dibenzanthracene, 53-70-3; coronene, 191-07-1; octanol, 111-87-5.

Literature Cited

- Hansch, C.; Quinlan, J. E.; Lawrence, C. L. *J. Org. Chem.* **1968**, *33*, 347.
- Chiou, C. T.; Freed, V. H.; Schmedding, D. W.; Kohmert, R. L. *Environ. Sci. Technol.* **1977**, *11*, 475–478.
- Yalkowsky, S. H.; Valvani, S. C. *J. Pharm. Sci.* **1980**, *69*, 912–922.
- Mackay, D.; Bobra, A. M.; Shiu, W. Y.; Yalkowsky, S. H. *Chemosphere* **1980**, *9*, 701–711.
- Amidon, G. L.; Yalkowsky, S. H.; Leung, S. *J. Pharm. Sci.* **1974**, *63*, 1858–1866.
- Chiou, C. T.; Schmedding, D. W.; Manes, M. *Environ. Sci. Technol.* **1982**, *16*, 4–10.
- Tewari, Y. B.; Miller, M. M.; Wasik, S. P.; Martire, D. E. *J. Chem. Eng. Data* **1982**, *27*, 451–454.
- Banerjee, S.; Yalkowsky, S. H.; Valvani, S. C. *Environ. Sci. Technol.* **1980**, *14*, 1227–1229.
- Bowman, B. T.; Sans, W. W. *J. Environ. Sci. Health, Part B* **1983**, *B18*, 67–83.

- (10) Miller, M. M.; Ghodbane, S.; Wasik, S. P.; Tewari, Y. B.; Martire, D. E. *J. Chem. Eng. Data* 1983, 29, 184-190.
- (11) Yalkowsky, S. H. *Ind. Eng. Chem. Fundam.* 1979, 18, 108-111.
- (12) Lyman, W. J.; Reehl, W. F.; Rosenblatt, D. H. "Handbook of Chemical Property Estimation Methods"; McGraw-Hill: New York, 1982.
- (13) Chiou, C. T.; Schmedding, D. W.; Block, J. H. *J. Pharm. Sci.* 1981, 70, 1176-1177.
- (14) May, W. E.; Wasik, S. P.; Freeman, D. H. *Anal. Chem.* 1978, 50, 175-179.
- (15) May, W. E.; Wasik, S. P.; Freeman, D. H. *Anal. Chem.* 1978, 50, 997-1000.
- (16) Reid, R. C.; Prausnitz, J. M.; Sherwood, T. K. "The Properties of Gases and Liquids", 3rd ed.; McGraw-Hill: New York, 1977.
- (17) Herzel, F.; Murty, A. S. *Bull. Environ. Contam. Toxicol.* 1984, 32, 53-58.
- (18) Osinga, M. *J. Am. Chem. Soc.* 1979, 101, 1621-1622.
- (19) Mackay, D.; Shiu, W. Y. *J. Chem. Eng. Data* 1977, 22, 399-401.
- (20) Yalkowsky, S. H.; Valvani, S. C.; Mackay, D. *Residue Rev.* 1983, 85, 43-55.

Received for review June 18, 1984. Accepted December 14, 1984.

Composition of Fine Particle Regional Sulfate Component in Shenandoah Valley

Semra G. Tuncel, Ilhan Olmez, Josef R. Parrington,[†] and Glen E. Gordon*

Department of Chemistry, University of Maryland, College Park, Maryland 20742

Robert K. Stevens

Environmental Science Research Laboratory, U.S. Environmental Research Agency, Research Triangle Park, North Carolina 27711

■ Fine fractions of atmospheric particulate samples collected over 3 weeks in July/Aug 1980 in Shenandoah Valley, VA, and previously analyzed by X-ray fluorescence were reanalyzed by instrumental neutron activation analysis to provide data for many additional elements. Modified factor analysis of the combined data yielded a regional sulfate component containing S, NH₄⁺, V, Mn, Zn, Se, As, In, Sb, and Pb. If the component originates mainly from coal combustion, there is modification of the elemental composition pattern during transport from distant power plants to the receptors, even in the <2.5-μm fraction. The regional sulfate component should be used in receptor-model treatments of areas strongly affected by sulfate from distant sources, as it may account for substantial fractions of several airborne elements, especially Se and Mn. Particulate S/Se mass ratios from this and other work are usually in the vicinity of 3300 in areas not immediately affected by fresh SO₂ sources, but drop significantly near such sources.

Introduction

Receptor modeling is used to determine origins of airborne particles, the basic idea being the resolution of observed concentration patterns of particles at sampling sites, "receptors", into contributions from several sources (1). Most receptor modeling has been done on an urban scale, but attempts are being made to extend the approach to regional scale problems, i.e., to determine types of sources or source areas contributing to the aerosol at distances up to about 1500 km away. Macias et al. (2) used gas and particle compositions and air-mass trajectories to assign light scattering associated with regional haze in the desert Southwest mainly to secondary particles from photochemical smog in southern California, 750 km away, and smaller contributions from forest fires. To assess the impact of coal-fired power plants upon air quality in the Ohio

River Valley (ORV), Shaw and Paur (3) collected particles for 16 months at three rural sites in Kentucky, Indiana, and Ohio with dichotomous samplers. They performed factor analyses of the fine particle (<2.5-μm diameter) compositions to identify particulate species besides sulfate (from slow conversion of SO₂ gas) associated with emissions from coal combustion. Among elements observed by X-ray fluorescence (XRF), only Se was strongly loaded on the sulfate factor. High levels of fine K were observed during a period of forest fires and high Cl concentrations during an incursion of marine aerosol (4). Stevens et al. (5) performed similar measurements, plus chemical analyses for C, SO₄²⁻, NO₃⁻, NH₄⁺, and H⁺, in the Smokey Mountains and the Shenandoah Valley in the U.S. and at Abastumani Mountain in the U.S.S.R. Factor analysis of fine fractions from Shenandoah Valley yielded a factor 1 strongly loaded with S, SO₄²⁻, H⁺, NH₄⁺, NO₃⁻, and Se, which they attributed to coal-fired power plants.

Rahn and Lowenthal (6) have devised an alternate approach, an empirical tracer system to identify particles from large regions with dimensions of the order of 1000 km on a side. They characterize particles from such regions by ratios of concentrations of As, Zn, Sb, In, and noncrustal Mn and V to that of Se. [Noncrustal concentrations are obtained by subtracting crustal contributions based on observed Al concentrations and the Mn/Al and V/Al ratios of Mason's crustal abundances (7).] For example, in samples collected in New England, particles transported from the interior of the U.S. (INT) were distinguished from those from the East (ECOAST) by higher ratios of As/Se and lower ratios of the other five elements.

Despite these advances, many questions must be answered before regional scale receptor modeling can be established on a firm basis. Do particles from a large source region, e.g., the INT region, have a narrow range of compositions, at least for selected tracer species, as implied by Rahn and Lowenthal's treatment? Or is the composition modified when air masses pass over certain

[†]Present address: General Electric Co., Schenectady, NY.

cities, industrial areas, or power-generating complexes within the region? Particles with a diameter greater than about 5 μm travel short distances before settling, but if we consider only particles of diameter < 2.5 μm , is the composition retained over several hundred kilometers, or is there fractionation? If these questions are answered successfully, regional scale receptor modeling may allow one to determine distant sources of particles which bear acid and/or sulfate, cause visibility degradation, or are related to acid deposition.

To help answer these questions, the fine fractions of samples collected in Shenandoah Valley by Stevens et al. (5) were reanalyzed by instrumental neutron activation analysis (INAA), by which many trace elements are measured more reliably than with XRF. Back-trajectories of air masses for each sampling period were calculated to associate concentration patterns with prior histories of the air masses, and the combined XRF, INAA, and chemical data were interpreted by factor analysis and other methods.

Experimental Methods

Samples were collected 0.5 km east of U.S. Highway 340 by using dichotomous samplers which separated particles into two size fractions with a cut point at 2.5- μm diameter (5). Sampling periods were 12 h, and other samples were taken concurrently for analysis for chemical species such as SO_4^{2-} , NO_3^- , NH_4^+ , and elemental and total carbon. Details of the collection and original analyses are given in ref 5. The fine particle fractions, along with blank filters and flux monitors, were irradiated in the National Bureau of Standards (NBS) reactor at a thermal neutron flux of $5 \times 10^{13} \text{ n}/(\text{cm}^2\text{-s})$. γ -ray spectra of the irradiation products were observed with lithium-drifted germanium [Ge(Li)] γ -ray detectors coupled to a 4096-channel analyzer and the amounts of observed elements calculated by procedures described in ref 8-11.

Results and Discussion

Arithmetic and geometric mean concentrations and standard deviations (for all observations above blanks) are listed in Table I. Data for elements are from INAA except for Br, S, Si, and Pb, which are from XRF. Concentrations measured in five or more samples for Ti, Ga, Sr, Mo, In, Ba, Yb, and Au by INAA are not listed.

These results show the value of analyses of samples by more than one technique. INAA is more expensive and time consuming than XRF but sensitive enough for precise determination of some critical trace elements, e.g., As, Se, Sb, In, and rare earths, which are good markers of certain areas or sources. Ratios of concentrations of eight elements observed in the same samples by XRF and INAA are listed in Table II. Agreement between techniques is good for Cl, K, Ca, and Fe. Zinc is measured more accurately by INAA than by XRF. The INAA measurements of Se have much greater precision, but the greater fluctuation of XRF results is centered on the correct average. Bromine is accurately measured by both methods, so the lower values obtained by INAA may have resulted from vaporization of Br from the samples during the 3-year storage between XRF and INAA measurements (perhaps a result of reactions on the filter).

Concentrations for Various Wind Trajectories. Concentrations of several elements are shown in Figure 1, which shows several episodes. Sulfur peaks, accompanied by Se, occur on July 23, 25-27, and 29-31 and Aug 2 and 3, with Mn tracking these elements fairly closely. Several elements including As, Sb, Zn, Pb, and V have elevated concentrations during the July 29-31 major S

Table I. Average Concentrations and Standard Deviations of Elements and Species Observed in Fine Fractions of Shenandoah Samples

species	anal method ^a	no. of samples detected	concentration, ng/m ³	
			arithmetic, $\bar{x} \pm \sigma$	geometric, $x_g (\sigma_g)$
Na	INAA	33	51 \pm 27	46 (1.6)
Al	INAA	32	69 \pm 77	45 (2.5)
Si	XRF	32	133 \pm 160	87 (2.4)
S	XRF	32	4400 \pm 3300	3300 (2.2)
Cl	INAA	33	13 \pm 14	8.6 (2.4)
K	INAA	32	66 \pm 32	59 (1.7)
Ca	INAA	32	40 \pm 28	33 (1.9)
Sc	INAA	30	0.012 \pm 0.015	0.0080 (2.5)
V	INAA	32	1.54 \pm 1.04	1.26 (1.9)
Cr	INAA	30	0.6 \pm 0.6	0.40 (2.6)
Mn	INAA	31	2.5 \pm 1.8	2.0 (2.0)
Fe	INAA	31	53 \pm 58	43 (1.9)
Co	INAA	32	0.06 \pm 0.07	0.047 (2.0)
Cu	INAA	24	7.1 \pm 4.1	6.2 (1.7)
Zn	INAA	32	9 \pm 7	7.4 (1.9)
As	INAA	30	0.40 \pm 0.31	0.27 (2.6)
Se	INAA	32	1.3 \pm 0.94	1.05 (2.0)
Br	XRF	33	7.5 \pm 2.3	7.0 (1.5)
Cd	INAA	24	2.4 \pm 7.4	0.93 (2.6)
Sb	INAA	32	0.30 \pm 0.14	0.26 (1.8)
I	INAA	21	0.48 \pm 0.30	0.43 (1.6)
Cs	INAA	21	0.028 \pm 0.021	0.022 (2.0)
La	INAA	27	0.09 \pm 0.09	0.056 (3.6)
Ce	INAA	32	0.23 \pm 0.21	0.18 (2.1)
Sm	INAA	25	0.008 \pm 0.005	0.0063 (2.1)
W	INAA	19	0.06 \pm 0.04	0.045 (2.0)
Pb	XRF	32	51 \pm 18	47 (1.5)
Th	INAA	17	0.024 \pm 0.031	0.014 (2.6)
SO ₄ ²⁻	IC	28	13600 \pm 10100	10500 (2.1)
NO ₃ ⁻	IC	15	600 \pm 1100	340 (2.5)
H ⁺	chem	26	96 \pm 128	40 (4.4)
C (total)	chem	25	1750 \pm 970	1420 (2.1)
C (org)	chem	21	540 \pm 460	375 (2.4)
C (elem)	chem	25	1300 \pm 760	990 (2.4)
NH ₄ ⁺	IC	26	3400 \pm 2000	2900 (1.8)
N (total)	chem	26	1270 \pm 730	1100 (1.7)
mass	β	32	42000 \pm 29000	33000 (2.1)

^a XRF = X-ray fluorescence; INAA = instrumental neutron activation analysis; IC = ion chromatography; chem = other chemical methods; β = β gauge.

Table II. Summary of Ratios of XRF/INAA Concentration Ratios for the Shenandoah Valley Samples

element	ratio \pm σ	no. of samples
Al	0.94 \pm 0.27	7
Cl	0.96 \pm 0.09	13
K	1.1 \pm 0.4	30
Ca	0.93 \pm 0.40	13
Fe	1.2 \pm 0.3	30
Zn	1.4 \pm 0.8	29
Se	1.1 \pm 0.7	18
Br	2.3 \pm 0.9	30

peak, but all of these have higher concentrations at earlier times, especially during the smaller sulfate episode centered on July 26. The high V concentrations of July 27 and 28 are not accompanied by maxima for other elements.

Back-trajectories were calculated for each sampling period by using the Air Resources Laboratory (ARL) Branching Atmospheric Trajectory (BAT) model (12) using a NAMER-WINDTEMP data base, which contains continental U.S. upper air meteorological data of the U.S. Air Force. Branching trajectories of 3-day duration from any origin can be calculated for every 6-h period moving either forward or backward in time. Three layers in the lower troposphere are defined as "surface", "boundary", and

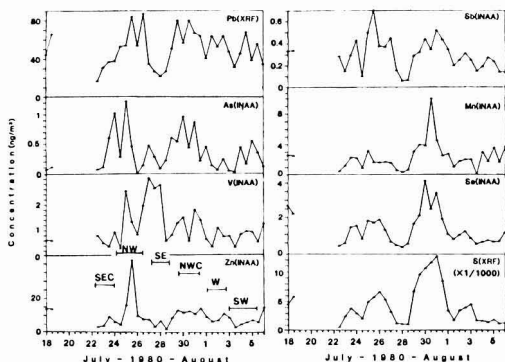


Figure 1. Concentrations of several elements vs. time at Shenandoah Valley. Horizontal bars in the bottom panel on the left side of the figure indicate the class of wind trajectories existing during the indicated periods.

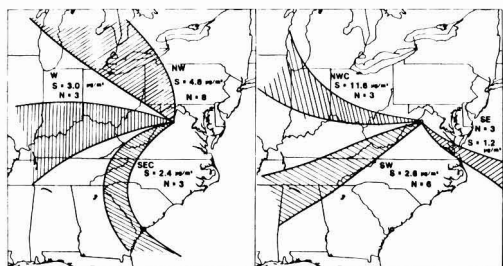


Figure 2. Envelopes of the six classes of back-trajectories observed during the Shenandoah Valley study. The trajectory groups are classified according to the general direction from which the air masses came: W = west; NW = northwest; NWC = northwest, curved; SW = southwest; SWC = southwest curved; SE = southeast. Average sulfur concentrations and the number of cases, *N*, are shown with each group.

"upper" according to whether it is day or night and from the vertical temperature profile at each rawinsonde station. The surface layer has a constant height of 300 m above the surface and is a nighttime layer. The boundary layer has a variable height determined from a critical inversion and extends from the top of the surface layer at night or from the surface during the day to the bottom of critical inversion layer. The upper layer extends from the top of critical inversion to a fixed height of 3000 m. If no inversion found, the model assumes a 3000-m height for the boundary layer. The trajectory calculation is based on the average wind in a particular layer as interpolated from surrounding stations.

We classified trajectories into six categories according to their directions. Envelopes of patterns of each category are shown in Figure 2. We do not show individual trajectories, as they imply an accuracy better than that with which they are known. Furthermore, the maps become very complicated because each trajectory branches into three parts for different altitudes. Eventually more detailed interpretations can be obtained from the vertical information, but we have not done so because of the small number of samples present in the trajectory groups. The periods classified are shown in Figure 1. There are gaps in the classification because trajectories were mixed during transitional periods, so seven sampling periods were not placed in a trajectory group. Transport shown by the back-trajectory envelopes of Figure 2 are largely determined by wind circulations around high and low pressure

cells and their locations relative to the Shenandoah site. West trajectories (NW, W, NWC, and SW) are the dominant type. Typically, these are associated with high pressure southwest of the sampling site. When this high pressure shifted east off the coast of Virginia, back-trajectories became characteristic of the SEC group of Figure 2. A low pressure system off the Carolina coast is apparently responsible for the SE trajectories between July 27 and July 29, 1980.

The NWC and NW trajectory groups had high S and Se loadings, as expected, because of heavy industrial and power-generation activities in these regions. Although we refer to S concentrations from XRF in this discussion, the ionic analyses (7) showed that most S was present as sulfate. Surprisingly, the W trajectory group had lower sulfate loadings than the NWC and NW groups. The SE group had the lowest sulfate loading. High V concentrations were associated with the SE component, as expected, because of oil-burning power plants in the East. Manganese and Se have their highest peaks associated with the highest S peak of the NWC trajectories, but many trace elements (e.g., Zn, Sb, and As) are more concentrated during the earlier NW period. The NW trajectories traverse heavier industrial areas of western Pennsylvania, northern Ohio, and much of Michigan.

Average concentrations for different wind directions are shown for some species in Figure 3. Within limits of error, concentrations of H^+ plus NH_4^+ (in nequiv/L) balance those of SO_4^{2-} for all trajectory groups. (Data for NO_3^- are available for less than half of the samples.) The highest ratio of H^+/NH_4^+ , 1.1 (approximately the stoichiometry of NH_4HSO_4) is observed for the NWC group, which also has the highest sulfate concentrations. The ratio and concentrations suggest that these are the most recently formed sulfate particles. Those from other directions are largely neutralized by NH_4^+ . The tendency for high SO_4^{2-} to be accompanied by higher ratios of H^+ to SO_4^{2-} agrees with observations by Pierson et al. (13) at Allegheny Mt. during July/Aug 1977. Again, we see that concentrations of S, SO_4 , Mn, and Se are highest for NWC trajectories, whereas that of Zn is highest for NW trajectories; averages for As and Sb are comparable for NWC and NW. Clearly, the V concentration is highest for SE trajectories. Concentrations of Al and Si, probably indicating soil, are highest for SW trajectories, perhaps because of more uncovered ground in that direction.

Comparison with Rahn-Lowenthal Tracer System.

Ratios of concentrations of ncr-Mn, ncr-V, Zn, As, Sb, and S to that of Se for the six groups of samples are shown in Figure 4. Note the near constancy of the S/Se ratio for various trajectories (discussed below). Ratios for V and As are much greater for the SE groups than those that come in from the west (including SEC). There are factor of 2 or greater variations of each ratio for the different westerly trajectory groups, showing that the ratios are more variable than implied by Rahn and Lowenthal.

In Figure 5 we compare our average ratios with those recommended by Rahn and Lowenthal (6). Data from all samples in the NW, NWC, W, and SW groups have been included in our westerly group (WES). Rahn and Lowenthal also used the In/Se ratio, but we measured too few values to make valid comparisons. Except for As/Se, our SE ratios are smaller than the ECOAST ratios of Rahn and Lowenthal. However, theirs refer mainly to the Washington-Boston regions, whereas ours are for trajectories from near Norfolk, VA, which has fewer pollution sources. The more serious disagreement is for particles from the West as, except for Sb/Se, our WES ratios are

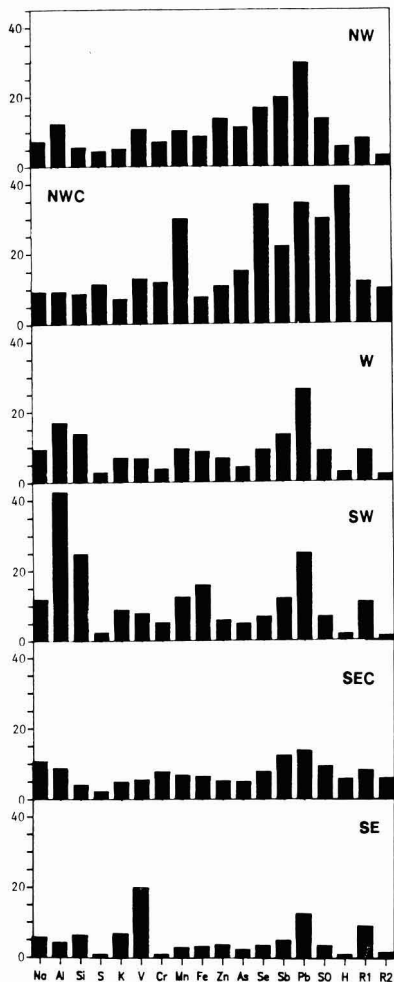


Figure 3. Average concentrations (ng/m^3) observed at Shenandoah Valley site (fine fraction) for six wind-trajectory groups. Concentrations were multiplied by the following scale factors: Na (0.2), Al (0.5), Si (0.1), S (0.001), K (0.1), V (10), Cr (10), Mn (5), Fe (0.2), As (20), Se (10), Br (2), Pb (0.05), SO_4 (0.001), H^+ (0.1), and R1 and R2 (10). R1 and R2 are the molar ratios ($\text{H}^+ + \text{NH}_4^+/\text{SO}_4^{2-}$ and $\text{H}^+/\text{SO}_4^{2-}$, respectively).

consistently lower than the INT ratios of Rahn and Lowenthal. Results obtained by Rahn and Lowenthal (14) at Allegheny Mt., PA (ALG), are also shown. These ratios agree much better with our WES ratios than their original INT ratios, which were based on samples collected at Underhill, VT. These results suggest that either the composition of particles changes considerably during transit from Pennsylvania and Virginia to Underhill or that the ratios vary significantly, depending on the areas of the Midwest through which an air mass passes. Note, especially, that the air masses appear to collect V during transit from Pennsylvania to Underhill.

Factor Analysis. To examine the interelement relationships in more detail, we performed factor analysis using the Bio-Medical Data (BMD) Program Package BMDP-P4M (15). Factor analysis is just the first step in receptor modeling. It can provide a guide to the interpretation of large data sets, but to obtain quantitative results, one needs

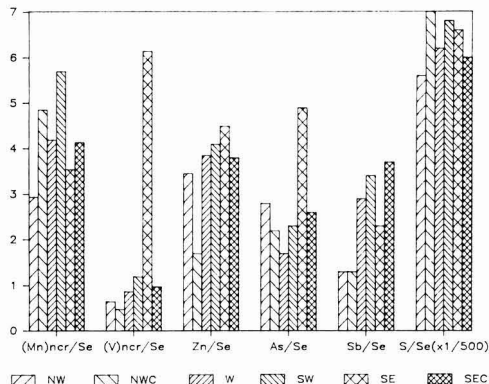


Figure 4. Geometric mean ratios of several trace element concentrations (fine fraction) to Se as observed at Shenandoah Valley for six wind-trajectory groups. Ratios have been multiplied by the following scale factors: $(\text{Mn})_{\text{ncr}}/\text{Se}$ (4), Zn/Se (0.5), As/Se (10), and Sb/Se (10).

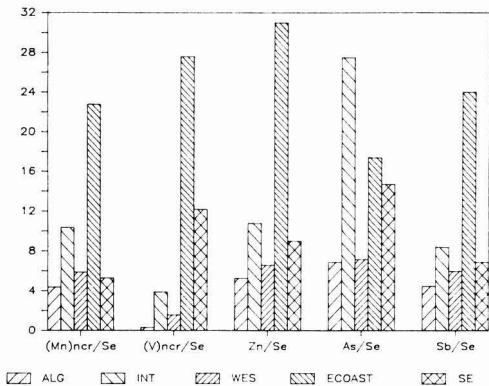


Figure 5. Comparison of ratios of several trace elements to Se as observed in this work to those reported by Rahn and Lowenthal (8, 14). The SE and WES are trajectory groups observed at Shenandoah Valley in this work, the WES group made up from all westerly trajectory groups (W, NWC, NW, and SW). ALG was obtained at Allegheny Mt. by Rahn and Lowenthal. INT and ECOAST were published in ref 6. Scale factors are $(\text{V})_{\text{ncr}}/\text{Se}(2)$, $(\text{Mn})_{\text{ncr}}/\text{Se}(4)$, As/Se , and Sb/Se (30).

to perform CMBs, multiple regressions, or other receptor-model calculations; however, factor analysis can help suggest the types of components to be used in CMB calculations. To obtain directional associations of the factors, we determined the angle of each back-trajectory at a distance of about 500 km from the sampling site, referred to as θ (0–360 deg) with $N = 0$ deg. Because of the discontinuity of θ at 360 = 0 deg, we assigned east-west (EW) and north-south (NS) as follows:

$$0 \leq \theta \leq 90, \text{EW} = \theta/90 \quad \text{NS} = 1 - \theta/90$$

$$90 \leq \theta \leq 180, \text{EW} = 2 - \theta/90$$

$$180 \leq \theta \leq 270, \text{EW} = 2 - \theta/90 \quad \text{NS} = \theta/90 - 3$$

$$270 \leq \theta \leq 360, \text{EW} = \theta/90 - 4$$

These variables are proportional to θ within each quadrant, and the absolute values of $d(\text{EW})/d\theta$ and $d(\text{NS})/d\theta$ are constant, so there is no distortion of the wind-frequency distribution. The NS variable indicates the strength of the northerly or southerly transport to the receptor, with +1 indicating a trajectory from 0 deg and -1 a trajectory originating directly from the south. Likewise, the EW

Table III. Factor Analysis of Concentrations of Species and Wind Trajectories Observed at Shenandoah Valley, July/Aug 1980 (30 Samples)

parameter	factor loading ($\times 100$) ^a					communality, %
	factor 1/ crustal	factor 2/ regional sulfate	factor 3/ anthropogenic	factor 4/ motor vehicle	factor 5/ oil	
Sc	96	0	0	0	0	96
Al	96	0	0	0	0	95
Si	95	0	0	0	0	95
Fe	94	0	0	0	0	93
Ca	85	0	0	0	0	77
Na	83	0	0	0	0	71
K	72	0	0	0	0	57
SO ₄ ²⁻	0	94	0	0	0	97
H ⁺	0	91	0	0	0	91
mass	0	89	32	0	0	96
NH ₄ ⁺	0	87	0	0	0	84
Mn	31	76	0	0	0	75
Se	0	64	62	0	0	81
As	0	30	83	0	0	84
NS ^b	0	0	82 (N)	0	0	79
Sb	0	33	66	52	0	85
Cr	0	0	56	0	0	34
Br	0	0	-29	84	0	84
Pb	0	53	0	76	0	90
Zn	0	0	46	69	0	72
V	0	0	0	0	94	90
EW ^b	-27 (W)	-37 (W)	0	-44 (W)	56 (E)	76
variance explained	5.9	5.0	3.2	2.4	1.5	18.0 (82%)

^a Factor loadings less than 0.25 suppressed. ^b NS and EW indicate components of wind trajectory in north-south and east-west directions (see text). Parentheses indicate predominant direction from which the air mass came.

variable represents the strength of easterly or westerly transport of air (+1 = east; -1 = west).

The five factors (Table III) account for 82% of the total variance. Several FA solutions with different numbers of factors and variables were tried. Compositions and loadings of the first two factors stayed nearly constant, but the others were not as stable. More samples are needed to support complete factor analysis for all variables measured. Factor analyses run without the NS and EW variables did not change the nature of the factors.

Factor 1, heavily loaded with crustal elements, is clearly the crustal factor. Factor 2 shows heavy loadings of mass, Se, SO₄²⁻, H⁺, NH₄⁺, and Mn. As expected, this sulfate factor is associated with winds from the west and contains NH₄⁺ and H⁺ associated with the sulfate. We did not include NO₃⁻ in the analyses because of missing values, but Stevens et al. (5) found it associated with this factor. Stevens et al. (5) called this the "coal-fired power plant" factor, as coal-fired plants are the dominant source of SO₂ west of the site. Although factor 2 is surely heavily influenced by coal combustion, we prefer to designate it in a more general way the "regional sulfate" factor.

The light loading of As on the second factor is surprising. The CMB treatment of Washington, DC (8), indicated that most As results from coal combustion, but the Shenandoah Valley results suggest that there are other important sources of the As. The modest loading of Pb does not necessarily indicate much association of it with coal combustion. As the closest highway (Route 340) was west of the site and the highest SO₄²⁻ concentrations were associated with air masses from that direction, there may have been inadvertent correlation of Pb with SO₄²⁻. Factor analysis often "smears" components that are partially correlated by wind direction. Arguing against this interpretation is the lack of Br on factor 2, suggesting nonautomotive Pb, perhaps from smelters.

The strong loading of Mn on factor 2 is unexpected, as Mn is depleted in coal relative to other crustal elements.

However, it is not clear if the Mn in Shenandoah Valley is associated with particles from coal-fired plants or simply with air masses from the west. The third factor is composed of pollution-derived elements such as Cr, Se As, Zn, and Sb. This factor probably indicates industrial emissions, as these elements have high concentrations in the NW trajectory group. The strong northerly association suggests Pittsburgh as a possible source region. The fourth factor indicates motor-vehicle contribution with high loadings of Pb and Br. The inclusion of Zn and Sb is surprising, as they are normally associated with incinerators (8). The westerly direction might simply be the result of Highway 340 west of the site. Factor 5, with a high loading of only V, is surely associated with oil-fired power plants, also indicated by the easterly direction.

Regional Sulfate Component. Sulfate has long been recognized as a regional pollutant. As it is formed slowly from SO₂ over travel distances of hundreds of kilometers, its ambient levels are not much affected by local sources. Concentrations are only slightly greater in urban areas than in surrounding rural areas (16). Until recently, we have had little knowledge of other elements associated with the sulfate. If a regional sulfate component can be resolved from data taken at Shenandoah Valley, is it a "universal" component for the Eastern U.S., or does its composition vary depending on the site at which it is observed?

We determined the composition of the regional sulfate component at Shenandoah Valley by the method advanced by Thurston and Spengler (17). One performs a multiple linear regression of the concentration of each element vs. the absolute scores of the factors. The latter were calculated by subtracting "absolute zero" factor scores from the factor scores. Absolute zero factor scores were determined by scoring an extra day in which all concentrations are set equal to zero. This method could not be used for In, as there were too many missing In concentration values, so the In/S ratio was calculated from a multiple linear regression of its measured concentrations vs. those of ele-

Table IV. Regional Sulfate Components

species	normalized concentrations				
	this work (33 samples)	Rahn and Lowenthal		Pierson et al., ^c Allegheny	Thurston/Spengler, ^d Watertown, MA
		INT ^a	Allegheny ^b		
S	1.00 ± 0.05	1.00		1.00 ± 0.03	1.00
NH ₄ ⁺	0.64 ± 0.06			0.21 ± 0.02	
V (×10 ⁵)	2.1 ± 1.7	48 ± 14	2.7 ± 1.1	16 ± 20	270
Mn (×10 ⁴)	4.7 ± 0.6	6.0 ± 3.2	1.9 ± 1.2	6.9 ± 2.1	9.7
Zn (×10 ³)	0.33 ± 0.27	2.7 ± 1.3	0.9 ± 0.15	1.7 ± 0.7	9.9
Se (×10 ⁴)	2.1 ± 0.3	2.6 ± 1.1	1.7 ± 0.4	1.7 ± 0.4	7.2
As (×10 ⁵)	3.3 ± 0.9	2.2 ± 0.6	3.9 ± 0.8		
In (×10 ⁶)	1.4 ± 0.5 ^e	0.9 ± 0.1	0.17 ± 0.17		
Sb (×10 ⁵)	1.6 ± 0.4	7.7 ± 2.8	2.5 ± 0.7	3 ± 6	
Pb (×10 ³)	3.5 ± 0.4			2.9 ± 1.2	59

^aRef 6. ^bRef 14. S/Se ratio based on Pierson et al. Allegheny component. ^cBased on our analysis of data from ref 12. ^dRef 17. ^eBased on In observed in only nine samples.

ments strongly associated with factors 1-5: Al, SO₄²⁻, As, Br, and V. This technique is similar to that used by Kleinman et al. (18) and discussed by Henry et al. (19). Results of these calculations for factor 2, normalized to S, are shown in Table IV. Uncertainties are large for elements weakly correlated with sulfate. In addition to the elements loaded on factor 2, we found weak correlations for Zn, V, and In.

A component can also be constructed from Rahn and Lowenthal's INT ratios to Se by use of the average S/Se ratio they observed for the INT group. We also extracted a regional sulfate component from the data of Pierson et al. (13) collected at Allegheny Mt. in 1977 using the same approach as on our Shenandoah Valley data. These data were taken with air filters and, thus, include both fine and coarse particles. However, our treatment of the data should extract only the fractions of elements which accompany sulfate, presumably the fine fractions of elements such as Mn and V. The S/Se ratio based on the Pierson et al. data was used to construct a regional sulfate based on the Allegheny Mt. data of Rahn and Lowenthal (14) for the summer of 1982. A component obtained by Thurston and Spengler (17) by principal component analysis of fine particle data from Watertown, MA, is also included.

Table IV contains virtually all existing data on the composition of regional sulfate components. Is there a single regional sulfate component which has the same composition wherever observed in or downwind from the coal-combustion region of the Midwest, or does its composition vary, depending on location, season, and other variables? When the data of Table IV are considered carefully, we see that we are not really in a position to answer the question. Errors resulting from extraction of concentrations of several elements are quite large. Furthermore, some data were taken with filters, whereas others represent only fine particles, and a variety of analytical methods were used. Because of the strong correlation of Se with S at most locations, errors for Se are reasonably small and there is good agreement among the first four values. The value from Thurston and Spengler is much larger, perhaps because their Watertown site is much less rural than the others. Also, the three values for As agree well with each other. Errors for some Sb values are quite large, but there is good agreement except for the INT value, which may have been affected by transport to Underhill, VT. Although errors for Zn and Mn are large, there may be some real variation of the Zn concentration among the sites, but Mn may be almost constant. Errors for V are also quite large, but there are probably real differences, with the Watertown and Underhill sites being influenced

Table V. Comparison of Composition of Fine Particles from Coal Combustion with That of the Regional Sulfate Component

element	relative concentration	
	regional sulfate (this work)	six Eastern coal-fired plants ^a
Al		880 ± 90 (6)
V	0.14 ± 0.11	1.9 ± 0.9 (6)
Mn	2.2 ± 0.3	1.9 ± 0.5 (6)
Fe		390 ± 140 (6)
Zn	1.6 ± 1.3	2.8 ± 0.7 (6)
As	0.16 ± 0.04	3.9 ± 1.5 (6)
Se	1.00 ± 0.14	1.00 ± 0.69 (6)
In	(6.7 ± 2.3) × 10 ⁻³	(4.5 ± 0.5) × 10 ⁻³ (2)
Sb	0.08 ± 0.02	0.34 ± 0.05 (2)
Pb	17 ± 2	2.4 ± 0.8 (4)

^aBased on compilation by Gordon and Sheffield (20). Average composition of fine particles emitted from six Eastern U.S. coal-fired power plants equipped with electrostatic precipitators. The number of individual measurements included in each average is shown in parentheses.

by oil combustion in the East. Despite its very small concentration, measurements of In are reasonably in agreement. The Watertown value for Pb is surely influenced by heavy traffic around the site. The data from Pierson et al. and this work may have also been affected by local traffic, but much less than in Watertown. The good agreement of the two Pb values is gratifying.

More data from samples collected in rural areas in and downwind from the Midwest are needed before we can answer these questions definitively. Samples should be collected with size segregation to permit analysis of the fine fraction free of coarse particles, which confuse the interpretation. Samples should be analyzed with high accuracy to provide data of such high quality that they can be treated statistically to obtain a regional sulfate component with small uncertainties for associated trace element concentrations.

Is Regional Sulfate from Coal Combustion? Because of the dominance of coal combustion as a source of SO₂ in Northeast U.S., most sulfate is surely secondary material from coal-fired plants. Selenium is so closely associated with S that most Se can also be safely assumed to originate from coal combustion, but what about the other trace elements associated with regional sulfate? Stevens et al. (5) referred to their sulfate factor as coal-fired power plants, but Se was the only trace element on it. Thurston and Spengler (17) called their component a "coal-related factor". But is its composition congruent with

that of particles released by coal combustion, with addition of secondary materials such as SO_4^{2-} , NO_3^- , and NH_4^{+} ?

In Table V we compare the composition of the regional sulfate component from this work with the average composition of fine particles from six power plants burning eastern coal and equipped with electrostatic precipitators, the predominant kind of plant that affects the Shenandoah Valley (20). Compositions are normalized to that of Se because SO_4^{2-} is secondary and Se is the species next most strongly associated with coal combustion. This choice is not without problems, as major fractions of the Se in coal leave the stack in the gas phase (21), but in ambient air, comparable amounts of Se are in the gas and particulate phases (22, 23). Thus, it appears that much of the gas-phase Se in the stack later becomes associated with particles; therefore, relative concentrations of other elements in the coal component of Table V may be overestimates. In defense of the validity of coal component, one plant included was studied by dilution source sampling, in which the stack gases are cooled and diluted with about 20 parts of ambient air before collection of particles (24). The relative amount of Se observed in that study was comparable with those of the other five. Also, the relative amount of Se in our component is comparable with that measured by Wengen in the plume at about 8 km downward of the Four Corners plant (25).

For Mn, Zn, and In, there is acceptable agreement between the regional sulfate and coal components. Lead is more concentrated in the regional sulfate, but as discussed above, excess Pb from other sources may have been smeared into the component. Vanadium is deficient in regional sulfate, but both values are quite uncertain and most other components in Table IV contain more V than ours. Also, Sb is somewhat deficient in regional sulfate. Arsenic presents a major problem, as it is deficient by a factor of nearly 30 in regional sulfate relative to the coal component! The As/Se ratio for the coal component may have been overestimated because of gas-phase Se which later attaches to particles, but this error could at most be a factor of 5 on the basis of dilution source sampling (24) and Wengen's plume study (25). Furthermore, it is unlikely that other Se sources are more dominant than coal-fired plants in this area. If the As/Se value were too high in regional sulfate, it could be explained by additional sources of As, but the low value is difficult to explain.

If coal-fired power plants are the dominant source of Se in regional sulfate, then major portions of As are lost during transport of particles to the Shenandoah site. Note that Al and Fe are also included in Table V, although no statistically significant amounts of these elements were observed in the regional sulfate component. If regional sulfate were simply fine particles from coal combustion with added secondary material, the data of Table V indicate that 860 units of Al and 400 units of Fe should be present. However, Table I shows that these amounts of Al and Fe would greatly exceed the total amounts observed, and factor analysis indicates that both elements are associated with crustal material. What happened to these elements and other lithophiles that should be present? A similar problem was encountered by Gordon et al. (26) when they compared enrichment factors (with respect to crustal material) of many elements on $<2.5\text{-}\mu\text{m}$ diameter particles from coal-fired plants with those of $<2.5\text{-}\mu\text{m}$ diameter particles from ambient air from cities. Even in Charleston, WV, which is dominated by coal-fired plants, enrichments for many elements, including As and Se, on ambient fine particles were much greater than for coal-fired plants, meaning that nonenriched elements, such

as Al and Fe, have been selectively lost from particles.

Particles of diameter $<2.5\text{ }\mu\text{m}$ from coal-fired plants are not uniform in composition vs. diameter. Ondov et al. (27), for example, observed three size groups below $10\text{-}\mu\text{m}$ diameter centered at about 7, 2, and $0.1\text{ }\mu\text{m}$, which have quite different compositions. Concentrations of lithophile elements such as Al and Sc drop off more rapidly with decreasing size than those of more volatile elements such as Se and As. Quann et al. (28) observed large enrichments of many elements relative to lithophiles in submicron fume released by coal in a laboratory combustor. According to most studies of deposition, one would not expect fractionation simply on the basis of size in the range of diameters between 0.1 and $2.5\text{ }\mu\text{m}$ (29). The fractionation, which apparently occurs, may result from other factors such as impaction on vegetation and processing of particles by fogs and clouds, which will depend on their sizes and solubilities, the finer particles being generally more soluble than the larger, lithophile-bearing particles.

This interpretation has many implications for receptor modeling on a regional scale. We cannot assume that particles, even with diameter $<2.5\text{ }\mu\text{m}$, retain their compositions during transit for many hours or days. This observation raises questions about Rahn and Lowenthal's (6) use of ratios of elements to Se as indicators of particles from large regions. Because of its volatility, Se is probably borne by particles of smaller diameters than those of trace elements in the numerators of their ratios, so the ratios may change with distance. In future collections of particles (both source and ambient), it would be desirable to use devices that subdivide the $<2.5\text{-}\mu\text{m}$ group into several subgroups and to analyze these groups for many species.

The regional sulfate component also has implications for urban-scale receptor modeling. Being a regional pollutant, much of the sulfate, even in urban centers, originates from sources hundreds of kilometers away (e.g., see ref 16). Regional sulfate has not been handled properly by CMB models, which are designed for primary particles, whose compositions are assumed constant between sources and receptors (1). Some modelers have used a CMB component that is simply sulfate or $(\text{NH}_4)_2\text{SO}_4$ (e.g., see ref 30), but without trace elements. The results listed in Table IV give a more complete composition of this component. In CMBs of the Washington, DC, area, Kowalczyk et al. (8) failed to account for substantial amounts of fine Mn and Se. Unexplained Mn was attributed to an unknown source, and the Se was thought to arise mainly from Se that left coal-fired plants in the gas phase (and, thus, was not included in the primary coal component) and later condensed on particles. Now we see that portions of the urban ambient concentrations of these and other elements in Table IV could be contributed by regional sulfate. Indeed, Thurston and Spengler's (17) "coal-related" factor accounts for much of the observed fine Se and some fine Mn in Watertown, MA. Our group has modified the Washington, DC CMB calculations by addition of the regional sulfate component of Table V to the original seven components. In work to be presented elsewhere (31), inclusion of regional sulfate often improves fits to observed elemental concentrations, especially that of Se. Substantial amounts of Se and a few percent of fine Mn regional arise from regional sulfate.

S/Se Ratios and the Hybrid Receptor Model. The buildup of sulfate on particles vs. distance from large SO_2 sources is difficult to observe via absolute concentrations because of dilution and deposition. To overcome this problem Lewis and Stevens (32) constructed a hybrid receptor model for the ratio of particulate sulfate to fine

Table VI. Sulfur/Selenium Ratios of Various Source Materials and As Observed on Ambient Particles

source or site	ratio	rural sites	ratio
sources			
Earth's crust ^a	4000	rural sites	
Eastern U.S. coals (23 samples) ^b	2500 ± 2000	Shenandoah Valley (fine fract) (32 samples) ^h	3400 ± 1400
Arizona Cu smelters (5 samples) ^c	1700	Ohio River Valley (fine fract) ⁱ	
urban sites			
coal using		Kentucky site (400 samples)	1700 ± 1100
St. Louis (fine fract) (36 samples) ^d	1500 ± 1700	Indiana site (400 samples)	1700 ± 1200
Charleston, WV (fine fract) (21 samples) ^e	480	Ohio site (400 samples)	1700 ± 1200
Steubenville, OH (fine fract) ^f	890	Allegheny Mt. ^j	
Washington, DC (37 samples) ^g	900 ± 900	West trajectories (15 samples)	2900
Harriman, TN (fine fract) ^f	1600	North trajectories (4 samples)	530
using little or no coal			
Topeka, KS (fine fract) ^f	2600		
Watertown, MA (fine fract) ^f	3000		

^a Ref 34. ^b Ref 35. ^c Ref 36. ^d S from ref 37; Se in the same samples by INAA in this laboratory. ^e Ref 38. ^f Ref 39. ^g Ref 8. ^h This work. ⁱ Ref 3. ^j Ref 13.

primary particles vs. time after release into ambient air. Use of the ratio allows them to cancel many poorly known terms, the major exception being the deposition rate of SO₂ gas, which is probably different from that of particles. Two major problems hinder the application of the model: (1) identification of particle-borne species that come almost entirely from large SO₂ sources and (2) tracking a plume over long distances without fresh injection of emissions from other strong sources.

No isolated sources of SO₂ exist in Eastern U.S., so the second limitation could be handled only by expanding the model to include subsequent additions. With regard to point 1, Se is a candidate for tracing fine particles from SO₂ sources, especially coal-fired power plants. From many studies of coal-fired power plants [references given by Gordon et al. (25)], we conclude that a large fraction, perhaps 50%, of the Se in coal is released to the atmosphere. Germani (33) found that 60% of the Se in the stack of a coal-fired power plant was in the gas phase and Andren et al. (20) reported about 90% at a different plant. Some gas-phase Se probably becomes attached to particles after cooling in ambient air, but few measurements have been made. Pillay and Thomas (22) found 57±7% of Se in the air of Buffalo in the gas phase, whereas Mosher and Duce (23) found 21 and 24% in the gas phase in Providence and Narragansett, RI, respectively. Thus, Se apparently condenses on particles after release from combustion sources, but it surely occurs more rapidly than conversion of SO₂ to particulate sulfate. Comparison of ratios of Se to other elements in conventional stack sampling suggests that the ratio from coal-fired plants is increased about four-fold by dilution source sampling (24) or collecting the particles 8 km downwind in the plume (25).

If this picture is correct, low S/Se particulate ratios should be observed near large sources, increasing with distance as SO₂ is converted to particulate sulfate. When additional SO₂ sources are encountered, the ratio should drop as fresh particulate Se is added without particulate sulfate. Gradually the S/Se ratio should build up until the next source is encountered. However, the S/Se ratio is surprisingly similar for all wind-trajectory groups (see Figure 4), despite the fact that some wind groups, e.g., NW and NWC, surely bring fresher emissions from coal-fired plants than others. If conversion of SO₂ to sulfate requires about 30 h, as indicated by most models, the typical distance involved in conversion would be about 200 km, assuming a wind velocity of 15 km/h.

Many S/Se ratios of source materials and ambient samples are listed in Table VI. At most rural sites in

Northeast U.S., the ratio is about the same as for eastern coals. Evidently, the Se remaining in the plant plus that remaining in the gas phase is almost exactly compensated by the faster deposition of SO₂ gas prior to conversion to sulfate (vs. the slower deposition of Se-bearing particles) plus the SO₂ remaining in the gas phase. In areas not strongly influenced by nearby power plants, the S/Se ratio has a value of about 3000. But in areas of local coal emissions, e.g., Charleston, WV, and Washington, DC, the ratio drops because of injection of Se without much sulfate. The high density of coal-fired plants along the Ohio River Valley never allows the ratio to attain its steady-state value of about 3000. Even in summer, when SO₂ conversion is faster, the ratio at ORV sites is only about 2000. A surprising result is the apparently short distance needed for the ratio to achieve its steady-state value. Measurements of the vapor/particle ratio of Se in rural areas would provide valuable insight on this question. Note that the apparent short distance required to reestablish the steady-state ratio could be confused by vertical mixing, which might bring down particles that have a ratio of about 3000.

The S/Se ratio at Allegheny Mt. is quite low when SO₄²⁻ concentrations are <5 µg/m³ and the trajectories come down from Canada (40). The explanation seems to be that there are three large (>1000 MW) coal-fired plants almost exactly upwind of the plant at distances of 50–88 km for these sampling periods (W. R. Pierson, private communication).

Conclusions

A regional sulfate component that carries with it several other elements, including Se, Mn, and small amounts of V, In, Pb, Zn, As, and Sb, was observed. Other elements may be associated with the component, but the amounts are too small relative to those of other sources such as the crust to be distinguished. Contributions of some elements borne by the component to the air of eastern cities are probably significant relative to those of local sources.

The absence of the predicted amounts of As, Al, and Fe in the regional sulfate component relative to other elements released by coal-fired plants indicates fractionation of particles of diameter < 2.5 µm during long-range transport. Fractionation may result from size differences or other factors such as differences in solubility. This result has serious implications for the development of regional scale receptor modeling indicating, among other things, the need for measurements of subdivisions of the <2.5-µm diameter particles. Also, it raises questions about the use of trace element ratios to Se as regional signatures

by Rahn and Lowenthal (6), as size distributions and solubilities of particles bearing Se may be different from those bearing the other elements. While we find some agreement with their regional signatures, e.g., high V/Se for particles from the east coast, we do not agree quantitatively with most of their ratios. Their more recent data from Allegheny Mt., agree better with our Shenandoah results than their INT ratios based on Underhill, VT, samples. More samples must be collected and analyzed for many species and the associated back-trajectories calculated before definitive patterns characteristic of sources and regions can be established.

Factor analysis was used a first step toward determining the nature of components present in the Shenandoah Valley. More definitive interpretations should be made by other techniques, especially CMBs, when reliable components for regional scale problems are developed.

The particulate S/Se ratio is nearly constant under many circumstances. In most rural areas of the Midwest and East, the ratio ranges from about 2000 to 3500, but drops to about 1000 or less in areas of strong SO₂ sources because of addition of particulate Se before the added SO₂ has converted to sulfate. Measurements of the gas/particle ratio of Se in SO₂ plumes and urban and rural areas are needed, as the results could provide tools for determining rates of SO₂ conversion. The S/Se ratio apparently reaches a steady-state value within a short distance from SO₂ sources.

Acknowledgments

We are grateful to Thomas Dzubay, Charles Lewis, and Robert Shaw, Jr., for help on the original Shenandoah Valley study and advice during this study. We thank Jerome Heffter of NOAA for advice on the trajectory calculations, Denise DeLozier, Sue Guise, and Wendy Linthicum for help in preparing samples, and the staff of the NBS reactor for help with irradiations. Computer time was in part provided by the Maryland Computer Center. This work will be included in the dissertation of S.G.T. to be submitted as a requirement for the Ph.D. degree from the University of Maryland.

Registry No. NH₄⁺, 14798-03-9; H⁺, 12408-02-5; S, 7704-34-9; V, 7440-62-2; Mn, 7439-96-5; Zn, 7440-66-6; Se, 7782-49-2; As, 7440-38-2; In, 7440-74-6; Sb, 7440-36-0; Pb, 7439-92-1; Na, 7440-23-5; Al, 7429-90-5; Si, 7440-21-3; Cl₂, 7782-50-5; K, 7440-09-7; Ca, 7440-70-2; Sc, 7440-20-2; Cr, 7440-47-3; Fe, 7439-89-6; Co, 7440-48-4; Cu, 7440-50-8; Br₂, 7726-95-6; Cd, 7440-43-9; I₂, 7553-56-2; Cs, 7440-46-2; La, 7439-91-0; Ce, 7440-45-1; Sm, 7440-19-9; W, 7440-33-7; Th, 7440-29-1; C, 7440-44-0; N₂, 7727-37-9.

Literature Cited

- Gordon, G. E. *Environ. Sci. Technol.* **1980**, *14*, 292.
- Macias, E. S.; Zwicker, J. O., White, W. H. *Atmos. Environ.* **1981**, *15*, 1987.
- Shaw, R. W., Jr.; Paur, R. J. *Atmos. Environ.* **1983**, *17*, 2031.
- Shaw, R. W.; Binkowski, F. S.; Courtney, W. J. *Nature (London)* **1982**, *296*, 229.
- Stevens, R. K.; Dzubay, T. G.; Lewis, C. W.; Shaw, R. W., Jr. *Atmos. Environ.* **1984**, *18*, 261.
- Rahn, K. A.; Lowenthal, D. H. *Science (Washington, D.C.)* **1983**, *223*, 132.
- Mason, B. "Principles of Geochemistry", 3rd ed.; Wiley: New York, 1966.
- Kowalczyk, G. S.; Gordon, G. E.; Rheingrover, S. W. *Environ. Sci. Technol.* **1982**, *16*, 79.
- Germani, M. A.; Gokmen, I.; Sigleo, A. C.; Kowalczyk, G. S.; Olmez, I.; Small, A.; Anderson, D. L.; Failey, M. P.; Guloval, M. C.; Choquette, C. E.; Lepel, E. A.; Gordon, G. E.; Zoller, W. H. *Anal. Chem.* **1980**, *52*, 240.
- Ondov, J. M.; Zoller, W. H.; Olmez, I.; Aras, N. K.; Gordon, G. E.; Rancitelli, L. A.; Abel, K. H.; Filby, R. H.; Shah, K. R.; Ragaini, R. C. *Anal. Chem.* **1975**, *47*, 1102.
- Zoller, W. H.; Gordon, G. E. *Anal. Chem.* **1970**, *42*, 257.
- Heffter, J. L. 1983, Branching Trajectory (BAT) Model, NOAA Technical Memorandum, ERL ARL-121.
- Pierson, W. R.; Brachaczek, W. W.; Truex, T. J.; Butter, J. W.; Korniski, T. J. *Ann. N.Y. Acad. Sci.* **1980**, *338*, 145.
- Lowenthal, D. H., private communication, 1984.
- Dixon, W. J.; Brown, M. B., Eds. "Biomedical Computer Program P-Series"; University of California Press: Berkeley, CA, 1979.
- Althuller, A. P. *Environ. Sci. Technol.* **1980**, *14*, 1337.
- Thurston, G. D.; Spengler, J. D. *Atmos. Environ.* **1985**, *19*, 9.
- Kleinman, M. T.; Pasternack, B. S.; Eisenbud, M.; Kneip, T. J. *Environ. Sci. Technol.* **1980**, *14*, 62.
- Henry, R. C.; Lewis, C. W.; Hopke, P. K.; Williamson, H. J. *Atmos. Environ.* **1984**, *18*, 1507.
- Gordon, G. E.; Sheffield, A. E. to be presented at the Symposium on Environmental Science of Fossil Fuels, Division of Fuel Chemistry, 189th National Meeting of the American Chemical Society, Miami FL, April 1985.
- Andren, A. W.; Klein, D. H.; Talmi, Y. *Environ. Sci. Technol.* **1975**, *9*, 856.
- Pillay, K. K. S.; Thomas, C. C. J. *Radioanal. Chem.* **1971**, *7*, 107.
- Mosher, B. W.; Duce, R. A. J. *Geophys. Res.* **1983**, *88*, 6761.
- Howes, J. E.; Cooper, J. A.; Houck, J. E. "Sampling and Analysis to Determine Source Signatures in the Philadelphia Area". 1984, draft report to U.S. EPA.
- Wangen, L. E. *Environ. Sci. Technol.* **1981**, *15*, 1080.
- Gordon, G. E.; Zoller, W. H.; Kowalczyk, G. S.; Rheingrover S. W. *ACS Symp. Ser.* **1981**, *No. 167*, 51-74.
- Ondov, J. M.; Biermann, A. H.; Heft, R. E.; Koszykowski, R. F. *ACS Symp. Ser.* **1981**, *No. 167*, 173-186.
- Quann, R. J.; Neville, M.; Janghorbani, M.; Minns, C. A.; Sarofim, A. F. *Environ. Sci. Technol.* **1982**, *16*, 776.
- National Research Council "Acid Deposition: Atmospheric Processes in Eastern North America"; National Academy of Sciences: Washington, DC, 1983; Appendix C.
- Dzubay, T. G. *Ann. N.Y. Acad. Sci.* **1980**, *338*, 126.
- Sheffield, A. E., private communication, 1985.
- Lewis, C. W.; Stevens, R. K. *Atmos. Environ.*, in press.
- Germani, M. S. Ph.D. Thesis, University of Maryland, College Park, 1980.
- Wedepohl, K. H. In "Origin and Distribution of the Elements"; Ahrens, L., Ed.; Pergamon Press: London, 1968; pp 999-1016.
- Gluskoter, J. J.; Ruch, R. R.; Miller, W. G.; Cahill, R. A.; Dreher, G. B.; Kuhn, J. R. "Trace Elements in Coal: Occurrence and Distribution". 1977, Illinois State Geology Survey Circular 499.
- Germani, M. S.; Small, M.; Zoller, W. H.; Moyers, J. L. *Environ. Sci. Technol.* **1981**, *15*, 299.
- Loo, B. W.; French, W. R.; Gatti, R. C.; Goulding, F. S.; Jaklevic, J. M.; Llacer, J.; Thompson, A. C. *Atmos. Environ.* **1978**, *12*, 566.
- Lewis, C. W.; Macias, E. S. *Atmos. Environ.* **1980**, *14*, 185.
- Spengler, J. D.; Thurston, G. D. submitted for publication in *J. Air Pollut. Control Assoc.*
- Samson, P. J. *J. Appl. Meteorol.* **1980**, *19*, 1382.

Received for review June 7, 1984. Revised manuscript received December 17, 1984. Accepted December 27, 1984. This work was in part supported by U.S. EPA Grant R810403-01-0 and EPA Purchase Order 2D5411NAEX. Although the research described in this article was funded in part by the U.S. Environmental Protection Agency, it has not been subjected to Agency review and, therefore, does not necessarily reflect the views of the Agency, and no official endorsement should be inferred.

Removal of Arsenic from Geothermal Fluids by Adsorptive Bubble Flotation with Colloidal Ferric Hydroxide

Eric Heinen De Carlo* and Donald M. Thomas

University of Hawaii and Hawaii Institute of Geophysics, Honolulu, Hawaii 96822

■ A method is described for the separation of arsenic species from high ionic strength geothermal fluids produced by the Hawaii Geothermal Project well-A (HGP-A). The oxyanions of As(III) and As(V), which are present at a concentration level of $100 \pm 10 \mu\text{g/L}$ total arsenic, are concentrated by adsorbing colloid flotation (ACF) onto, or precipitate flotation with, colloidal ferric hydroxide, depending on the pH. The anionic surfactant sodium lauryl sulfate (SLS) and the cationic surfactant laurylammonium chloride (LA) are used as collectors below and above the isoelectric point (IEP), respectively. Efficiency of recovery of the trivalent arsenic oxyanion is pH and method dependent whereas that of the pentavalent arsenic is independent of the flotation method employed. Quantitative removal of total arsenic in solution is achieved above pH 6.5 by coprecipitation with ferric hydroxide; LA is used as the collector, and the air flow rate is $17 \pm 3 \text{ mL/min}$. ζ potentials of flocs are greatly affected by a variety of species in the geothermal fluids and the source of iron.

Introduction

Discharge waters from the Hawaii Geothermal Project well-A (HGP-A) on the island of Hawaii represent a mixture of meteoric water and seawater that has reacted at depth under high pressure and temperature (350°C) with basalts of the Kilauea East Rift Zone (1). The well, which was completed in 1976 to a depth of 1966 m at a drill site located 182 m above sea level, penetrates 1784 m of basalt below sea level (1-3). The bottom hole temperature of the well was measured at 358°C under static conditions. The well is capable of producing approximately 49 000 kg/h geothermal fluid mixture composed of approximately 43% steam and 57% liquid. The separated brine produced is nearly 0.22 M in NaCl and is highly enriched over its seawater component in Li, K, and Ca as well as $\text{SiO}_{2(\text{aq})}$ (4). A variety of potentially toxic species such as H_2S , HS^- , AsO_4^{3-} , AsO_3^{3-} , SeO_3^{2-} , Pb^{2+} , and Cd^{2+} are also present at various concentrations in the fluids and steam components of the geothermal discharge (4). The arsenic content of the brine currently being produced ranges from 1.2×10^{-6} to 1.5×10^{-6} M (90-110 ng/mL); this concentration represents a significant increase from the $(0.67 \pm 0.11) \times 10^{-6}$ M (50 \pm 8 ng/mL) present when the well was first brought into production in 1981 (4). Although the seawater fraction of the recharge component in the well is increasing progressively, as evidenced by nearly an order of magnitude increase in the total dissolved solids content of the brine over 3 years of production, the $\text{SiO}_{2(\text{aq})}$ content has not significantly changed with time as have the other brine constituents (Table I). Data indicate that the geothermal fluid chemistry of HGP-A is strongly governed by seawater intrusion into the reservoir and the temperature and steam quality of the resource, as well as by other production-related parameters such as operating pressure and duration of production (1).

Presently, well production results in the generation of 3 MW or approximately 5% of the electricity consumed on the island of Hawaii (1). Other test wells in the vicinity of HGP-A are being evaluated and may be brought into

production. Commercial-scale production of geothermal fluids from other wells in this geothermal area will necessitate the inception of appropriate disposal methods for the spent geothermal fluids. The present method used at HGP-A involves dumping the brine flow into an atmospheric flash tank, after which it percolates into the ground. Although such a method is environmentally satisfactory on the small scale of the plant, a larger operation will have to deal with the disposal of fluids in a manner that will ensure protection of future drinking water supplies in the area. Potential wastewater disposal techniques under consideration include reinjection at depth under pressure, discharge into surface waters after treatment, ponding and evaporation, and secondary use of effluents. Because the recommended limit for arsenic in drinking waters is 0.67×10^{-6} M (50 ng/mL) (5), some form of arsenic removal will have to be applied to the geothermal effluents before the latter options can be considered. Because of convection problems (6), conventional wastewater treatment methods for arsenic removal such as coagulation with alum or iron sulfate and subsequent clarification by settling have been found to be inappropriate for the high temperatures encountered with geothermal discharges.

In this paper we investigate a method for the removal of arsenic from separated geothermal brine by adsorption onto, or coprecipitation with, ferric hydroxide flocs and subsequent flotation with long-chain alkyl surfactants. A survey of the literature indicates that flotation methods have been applied to geothermal systems in only one other instance, and the scheme utilized differs substantially from that presented here (6, 7). No other methods that employ adsorptive bubble techniques for removal of arsenic from wastewaters have been described (8). Previous related analytical uses of flotation methods for As include the preconcentration and determination of arsenate and phosphate in seawater, and the preconcentration of arsenic and several other oxyanion-forming elements from acidic solutions of transition metals (9, 10).

Adsorptive bubble separations have been in use since the early 1900s and have been extensively employed in the mineral processing industry for ore beneficiation (11-13). Recently, flotation methods have been successfully applied to the removal of heavy metals from wastewaters (14 and references cited therein). Modern analytical applications of the methods were pioneered by Zeitlin and co-workers a few years after the advent of adsorbing colloid flotation (ACF) was first described by Sebba (15). Other applications of flotation technology have been extensively reviewed (13, 16-18).

Adsorptive bubble techniques are based on interactions between (ionic) surface-active agents and (residually charged) non-surface-active species in liquid suspensions. Concentration of the non-surface-active species of interest at the air/water interface of gas bubbles rising through the water column, and their subsequent removal from solution, is achieved because of the hydrophobic nature of the uncharged hydrocarbon tails of surfactant/floc entities. The effectiveness of these methods, which make use of the properties of the electrical double layer, is the function of a number of parameters such as ionic strength, pH, analyte

Table I. Elemental Composition of HGP-A Geothermal Brines

date	element ^a							SiO ₂
	Li	Na	K	Ca	Mg	As	Cl	
6/20/81	0.38	1280	220	30	0.008	0.057	2320	
8/3/81	0.49	1710	265	55	0.027	0.053	2940	844
12/22/81 ^b	0.58	1820	295	56	0.016	0.061	3210	
6/7/82	0.94	3120	525	122	0.051	0.081	5670	832
10/18/82	1.03	3650	610	182	0.084	0.080	6660	802
6/9/83	1.16	4480	660	269	0.140	0.104	8275	745
1/12/84	1.26	4930	930	358	0.260	0.095	8970	825

^aAll concentrations expressed as milligrams per liter. ^bWell started up again after shutdown from Sept to Dec 1981.

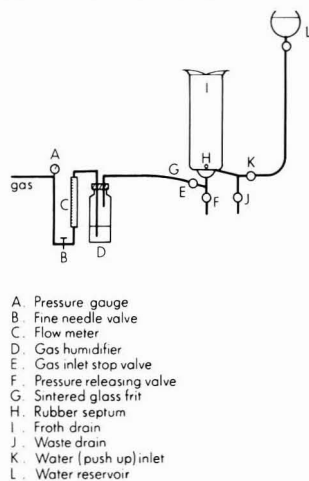


Figure 1. Flotation cell and associated apparatus. After De Carlo et al. (10).

concentration range, type and concentration of surfactant, and precipitating agent (11, 12, 14, 16). Physical characteristics of the cell, gas bubble size, and flow rate can also affect flotation behavior (10, 12, 14, 19).

Experimental Section

Apparatus and Equipment. The experimental setup is shown in Figure 1. The flotation cell employed in these studies was the same as that previously described by De Carlo et al. (10). All arsenic analyses were by atomic absorption spectrophotometry (AAS) on a Perkin-Elmer Model 603 spectrophotometer using the method of hydride generation. The pH of solutions was measured with an Orion Model 301 pH meter or a 404-A ionalyzer and a combination pH electrode. The electrophoretic mobility of the colloids was measured with a Zeta-Meter Corp. zeta meter equipped with a Zeiss stereomicroscope and a Plexiglas UVA type II electrophoresis cell.

Reagents. All chemicals used were analytical reagent grade or better. Mineral acids for floc dissolution and pH adjustments were Ultrex or Ultrapure grade. Aqueous solutions of reagents were prepared in water purified in a Corning Nano-pure system. Resistivity of the water used was always greater than 5 MΩ cm. Surfactant solutions were prepared in 50% (v/v) ethanol/water to prevent micelle formation. The concentrations of the surfactants were as follows: laurylammonium chloride (LA), 0.022 M (5 mg/mL); sodium lauryl sulfate (SLS), 0.0017 M (0.5 mg/mL). Freshly prepared solutions of 0.1 M FeCl₃·6H₂O and 0.053 M Fe₂(SO₄)₃·xH₂O were used as a source of adsorbent or coprecipitant for the arsenic in solution.

Commercial atomic absorption spectrophotometry standards of 1000 μg/mL were employed for spiking of brine samples with arsenic and diluted as necessary for use in AAS analyses.

Analytical Procedure. Separated brine samples from the HGP-A well were collected through a heat exchanger coil at the well head into acid-cleaned amber nalgene containers. Flotations were generally carried out within several hours after sample collection in order to avoid complications arising from polymerization of silica with time in the cooled brines. To 100-mL aliquots of brine was added the appropriate amount of ferric salt, the solution was diluted to approximately 180 mL, and the pH was adjusted with NaOH to the desired value. The increase in pH resulted in precipitation of colloidal ferric hydroxide; several minutes after the pH had stabilized, the sample was transferred quantitatively to the flotation cell, and gas flow was initiated at 17 ± 3 mL/min. Three milliliters of the appropriate surfactant solution (laurylammonium chloride or sodium lauryl sulfate) was then injected into the cell, giving an effective surfactant concentration of 2.6 × 10⁻⁵ M SLS or 3.3 × 10⁻⁴ M LA. The foam was allowed to collect at the top of the cell for 3–5 min (sometimes up to 10 min) and then manually removed by means of a Teflon spatula. Several drops of concentrated HCl or HNO₃ were used to remove adhering floc from the spatula, and an additional 2 mL was used to dissolve the foam containing ferric hydroxide enriched with arsenic. The dissolved floc was then transferred to 50-mL volumetric flasks and diluted to the mark with water. Samples were stored in polyethylene bottles for subsequent arsenic analysis. Blank determinations were carried out by using purified water in place of geothermal fluids, and the above procedure was repeated. A minimum of two replicate flotations were performed at various pH values for each set of experimental conditions. Complete sets of flotations as a function of pH were carried out with 1 × 10⁻³ and 2 × 10⁻³ M FeCl₃·6H₂O solution and 0.8 × 10⁻³ and 1.05 × 10⁻³ M Fe₂(SO₄)₃·xH₂O solution to evaluate the effect of increased concentration of precipitating agent and the presence of divalent counterions on the arsenic recovery. Optimization experiments were initially carried out in which the concentration of surfactant was varied at constant pH and iron concentration and also with varying iron concentration at fixed pH and surfactant concentration. ζ potential was determined at selected pH values on the flocs generated from the hydrolysis of ferric chloride and ferric sulfate added to geothermal brines. The electrophoretic mobility of colloidal particles was measured immediately after the pH of the solution had stabilized to the desired value. Reported ζ potentials represent the average for 10 colloid particles tracked at each pH. A potential of 50 or 100 V was applied to the electrodes for the above measurements.

Atomic absorption analysis for arsenic was performed on 250-μL aliquots of the floated sample solutions. In

order to determine the total arsenic present, the samples were oxidized with 5 μL of 0.125 M KMnO_4 prior to addition of NaBH_4 reagent. This preoxidation was necessary because the technique, which results in the production of AsH_3 , is specific for As(V). All analyses were carried out with the method of standard additions to compensate for any matrix effects.

Results and Discussion

Effect of Surfactant Concentration. The effect of surfactant concentration on the ferric hydroxide floc removal was studied over a limited range for SLS and LA. Optimum floc removal was achieved by use of between 3 and 4 mL of either surfactant solution, depending upon the point of zero charge (IEP) of the floc. When smaller volumes of surfactant solution were used, removal of the colloidal ferric hydroxide was incomplete even at low pH values where smaller amounts of hydrolyzed and precipitated Fe^{3+} were present. Large amounts of surfactant effectively recovered all the floc from suspension; however, inordinate quantities of wet foam also were generated. Excessive volumes of foam resulted in a larger carryover of solution into the separated ferric hydroxide floc and sometimes caused overturning of the enriched layer. The use of excessive amounts of surfactant also led to the initial formation of a layer of foam deficient in ferric hydroxide floc followed by a layer containing the collected ferric hydroxide. The last effect, also observed by others, has been attributed to kinetic effects (20). This behavior may also be explained by the formation of hydrophilic micelles from tail to tail bonding of surfactant/floc particles and unbound surfactant locally present in excess, thus rendering them unfloatable. A decrease in the concentration of surfactant available results in the breakup of these micelles and subsequent precipitate flotation of the desired hydrophobic species.

Very low concentrations of surfactant were sometimes ineffective in that a thin and unstable foam layer was generated and readily broke up when disturbed by manual collection procedures. Such a mechanical disturbance of foam layers has been reported to lead to decreased flotation efficiency as a result of floc redistribution into the mother liquor (10, 14, 19). Once redistributed into the underlying solution, the floc did not readily collect at the surface even upon further addition of surfactant.

Effect of Concentration of Precipitating Agent.

The recovery of arsenic from brine fluids was evaluated in solutions containing 1×10^{-3} to 2×10^{-3} M precipitating agent. Complete sets of flotations were carried out with these concentrations of ferric chloride between pH 3.5 and pH 9.0. The experimental data are presented in Figure 2; the lower curve represents the recovery of As(V) whereas the upper curve depicts the removal of both As(III) and As(V). The significance of these two curves will be discussed. At pH 3.5 the efficiency of removal of the arsenic improved significantly as the concentration of added ferric chloride increased. The enhanced recovery in the presence of higher concentrations of ferric ion is a result of the increased extent of iron hydrolysis, which provides a larger surface area available for adsorption of HAsO_4^{2-} , AsO_4^{3-} , and AsO_3^{3-} . No significant improvement in the efficiency of removal was observed when the concentration of ferric chloride was increased above 2×10^{-3} M.

Recovery of Arsenic as a Function of pH with FeCl_3 as Precipitating Agent. In Figure 3 the relative recovery of arsenic is plotted as a function of solution pH. At low pH values the flotations were carried out with SLS as the surfactant because of the positive residual surface charge on the precipitated ferric hydroxide; above pH 6.5 a re-

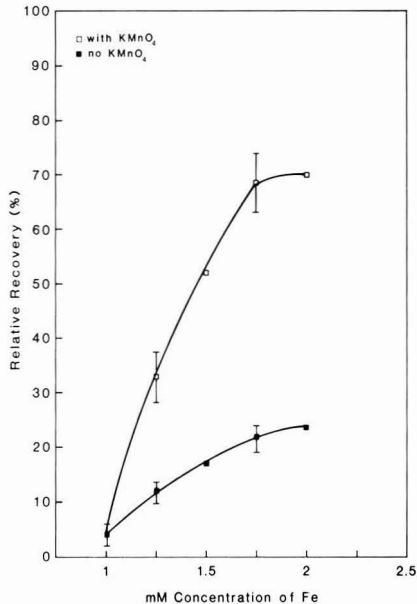


Figure 2. Relative recovery of arsenic as a function of FeCl_3 added. (■) As analysis in the absence of KMnO_4 ; (□) As analysis in the presence of KMnO_4 .

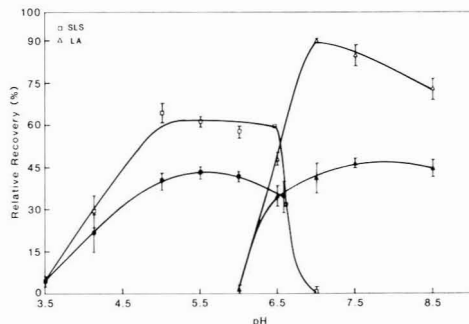


Figure 3. Relative recovery of arsenic as a function of pH in the presence of 10^{-3} M FeCl_3 . (□) SLS; (Δ) LA (open symbols, As analysis in the presence of KMnO_4 ; closed symbols, As analysis in the absence of KMnO_4).

versal in the surface charge characteristics of the floc required the use of LA, a cationic surfactant. Recoveries up to 65% were achieved with SLS, whereas nearly quantitative removal of the arsenic was observed at pH 7.0 (and above) with LA. When the concentration of ferric chloride added prior to pH adjustment and flotation was doubled, the recoveries of arsenic improved significantly. In the arsenic recovery-pH plot of Figure 4, the data show a marked enhancement at low pH because of the increased amount of colloidal ferric hydroxide available to adsorb HAsO_4^{2-} , AsO_4^{3-} , and AsO_3^{3-} . This effect was not as pronounced above the isoelectric point (IEP) and only resulted in a widening of the optimum pH range for flotation.

We believe that the mechanism governing the removal of arsenic from solution at low pH is primarily the electrostatic adsorption of HAsO_4^{2-} , AsO_4^{3-} , and AsO_3^{3-} onto a positively charged surface (ferric hydroxide). This process is termed adsorbing colloid flotation (ACF) (12). Above the IEP there is no strong electrostatic attraction,

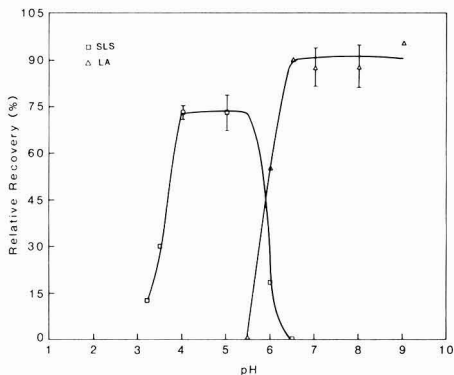


Figure 4. Relative recovery of arsenic as a function of pH in the presence of 2×10^{-3} M FeCl_3 . (□) SLS; (Δ) LA.

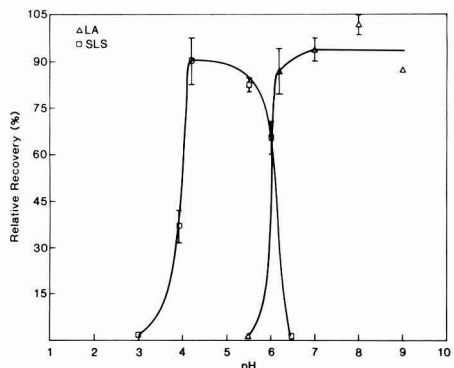


Figure 5. Relative recovery of arsenic as a function of pH in the presence of 8×10^{-4} M $\text{Fe}_2(\text{SO}_4)_3 \cdot x\text{H}_2\text{O}$. (□) SLS; (Δ) LA.

and the controlling mechanism may be that of coprecipitation with the metal hydroxide. Thus, depending on the pH of the brine sample, arsenic is removed either by ACF or precipitate flotation.

Recovery of Arsenic as a Function of pH with $\text{Fe}_2(\text{SO}_4)_3$ as Precipitating Agent. Previous industrial flotation applications and conventional wastewater treatment methods such as clarification by settling have traditionally employed ferric sulfate as a precipitating or coagulating agent (6, 7, 21). Studies to date in our laboratory have primarily concentrated on the use of ferric chloride as a precipitating agent in order to avoid the effects of polyvalent inorganic ions on the surface charge characteristics of ferric hydroxide flocs (9, 10, 19, 22, 23). The high success rate of applications when ferric sulfate was used, however, led us to evaluate this compound as an adsorbing or precipitating agent.

Two complete sets of flotations were carried out between pH 3 and pH 10 with hydrated crystalline ferric sulfate. Because the hydration and composition of the salt were not specified, a solution was prepared and analyzed to determine its iron content. The analysis indicated an iron concentration of 19.7% by weight. Further work was carried out with a solution of 0.053 M $\text{Fe}_2(\text{SO}_4)_3 \cdot x\text{H}_2\text{O}$. Figures 5 and 6 present the flotation recovery of arsenic in the presence of 1.6×10^{-3} and 2.1×10^{-3} M Fe^{3+} , respectively.

A comparison of the recovery curves shows marked similarities in trends to those obtained with ferric chloride used as a source of Fe^{3+} . The increased amount of iron

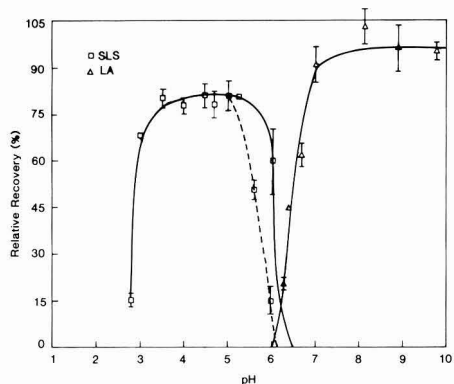


Figure 6. Relative recovery of arsenic as a function of pH in the presence of 1.05×10^{-3} M $\text{Fe}_2(\text{SO}_4)_3$. (□) SLS; (Δ) LA (dashed line represents data obtained 1 day after sample collection).

as depicted by the curve of Figure 6 resulted in a lowering of the minimum pH for effective flotation when SLS was used as the collector. This effect is primarily the result of increased iron hydrolysis in the more concentrated solution. Thus, a widening of the pH range over which flotation can be carried out with SLS was observed in the more concentrated iron solutions. Although recoveries are significantly higher than those obtained with 1×10^{-3} and 2×10^{-3} M FeCl_3 (approximately 85% and 80% recovery vs. approximately 60% and 73% recovery, respectively), the flotation recoveries of arsenic are still not quantitative below the IEP. The incomplete recovery of arsenic in the low pH range may be related to the competition for sites on the positively charged ferric hydroxide floc between the arsenic oxyanions (HAsO_4^{2-} , AsO_4^{3-} , and AsO_3^{3-}) and other anions such as Cl^- , which are present in high concentration (approximately 0.12 M) in the sample solution during flotation.

In order to explain more fully the incomplete removal of arsenic from the brines by ACF below the IEP, let us return to Figure 2. The two curves represent the recovery as determined by arsenic analysis using the method of hydride generation. The lower curve shows the removal of arsenic(V) only because the samples were not preoxidized with KMnO_4 , and the analytical method used is specific for As(V). Analyses of the arsenic oxidation state conducted in freshly collected air-free brines showed that approximately 76% of the arsenic in the brines is present as trivalent arsenic. This value compares well with previous studies conducted on other geothermal fluids (6, 7, 24). In light of the above, a 22% recovery indicates nearly quantitative removal of the As(V) present; the species recovered are believed to be HAsO_4^{2-} or AsO_4^{3-} . The upper curve shows the results of analysis after oxidation of the samples to convert all As(III) present to As(V). The additional recovery is then indicative of arsenic(III) floated from the brines. A simple calculation shows that approximately 61% of the As(III) is then removed by ACF below the IEP. Incomplete removal of As(III) is not unusual, as previous flotation studies have shown that arsenate is preferentially adsorbed over arsenite by ferric hydroxide flocs. Furthermore, at low pH the small acid dissociation constants for H_3AsO_3 favor the undissociated species or H_2AsO_3^- . The presence of these species in significant concentration may contribute to the low recovery of trivalent arsenic with positively charged flocs. Above the IEP the coprecipitation mechanism in effect is not species selective, thus leading to quantitative recovery of

all forms of arsenic (Figure 3). The recoveries are identical above and below the IEP in the absence of KMnO_4 ; i.e., no apparent difference in As(V) removal exists. For the oxidized samples, however, there is a marked improvement indicative of the process described above. The major difference is the initially higher recovery of As(V) , which would indicate that in this case nearly 45% of the total As is present as As(V) . This result is due to oxidation of the samples either prior to flotation (autooxidation after brines are exposed to oxidizing atmospheric conditions) or as a result of the dissolution of the enriched floc with HNO_3 , an oxidizing acid.

The enhanced arsenic removal in the presence of sulfate is probably related to the effect of different anions on the hydrolysis rate of ferric salts (25). Such an enhancement is, however, somewhat unexpected, as polyvalent inorganic ions generally compete more effectively for surface sites than monovalent anions such as Cl^- and NO_3^- (14, 26–28).

A comparison of the recovery of arsenic above the IEP with ferric sulfate used as the precipitating agent with that when ferric chloride was used shows no unexpected trends. Quantitative, or nearly so, removal of arsenic from the geothermal brines is observed above pH 6.5 in all cases. In a manner parallel to the studies that used ferric chloride, the experiments employing higher iron concentration resulted in a wider pH range over which the flotation recovery of arsenic was nearly constant.

In analogy to the previous sets of flotations, it is believed that the arsenic oxyanions are recovered from solution by ACF at low pH. At high pH, where the floc bears a negative surface charge, removal can only be achieved through specific adsorption of the oxyanions or by coprecipitation with ferric hydroxide; the latter is believed to be the more likely mechanism.

ζ Potential of Flocs. The conductivity of the brine samples after precipitation of ferric hydroxide was found to range between 1.3×10^4 and $1.85 \times 10^4 \mu\Omega^{-1} \text{cm}^{-1}$. At both low and high pH values colloid mobility was relatively high and easily timed; consequently, measurements were carried out by using 50-V applied potential to the electrodes. Near the IEP, however, the colloids exhibited very little mobility, and an applied potential of 100 V was often necessary to reliably determine their ζ potential. In several instances the electrophoretic mobility was measured both with 50- and 100-V applied potential. In such cases the reported values represent the average of the two determinations; the relative standard deviation of the average was less than 10%.

The ζ potentials measured for HGP-A brines to which ferric chloride or ferric sulfate was added are presented in Figure 7. These data are compared to the ζ potential of goethite ($\alpha\text{-FeOOH}$) in 0.01 M NaCl solution as determined by Iwasaki and co-workers (28). Although the geothermal fluids are approximately 0.22 M in NaCl, the experimental procedure results in an effective dilution to near 0.12 M. Considering the 10-fold higher ionic strength and the presence of significant quantities of colloidal SiO_2 as well as a variety of other dissolved solids in the geothermal fluids, a remarkable agreement is observed between the ζ potential for goethite and that for the iron floc generated from ferric chloride. The data indicate that the IEP of our system lies between pH 6.3 and pH 6.5 when 10^{-3} M ferric chloride is used as a source of precipitating agent. This range is corroborated by the flotation recovery of arsenic shown in Figure 3 where a crossover in the curves for the two surfactants, SLS and LA, occurs at pH 6.5. The crossover at the IEP compares well with the results of Iwasaki et al., who only evaluated the flotation recovery

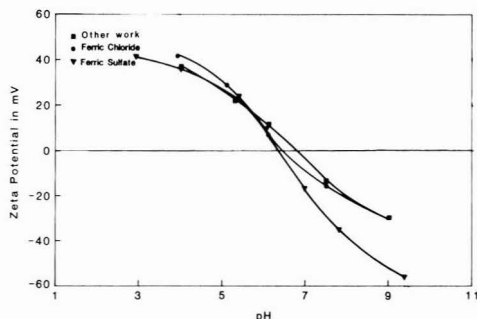


Figure 7. ζ potential of iron(III) flocs as a function of pH. (■) $\alpha\text{-FeOOH}$ in 10^{-2} M NaCl. After Iwasaki et al. (28). (●) FeCl_3 -derived floc in HGP-A brine. (▼) $\text{Fe}_2(\text{SO}_4)_3$ -derived floc in HGP-A brine.

of goethite (28). Although the ζ potentials were not determined for the 2×10^{-3} M FeCl_3 flotations, little change in the charge characteristics was observed other than an apparent shift in the crossover of the recovery curves to near pH 6. The slight shift to lower pH may simply be due to the formation of a $\text{SiO}_2\text{-Fe}(\text{OH})_n^{3-n}$ floc upon aging of the solutions. Although the brines are supersaturated with SiO_2 when cooled to ambient temperature, the kinetics of precipitation of silica are slow below pH 8. Because the experiments using 2×10^{-3} M FeCl_3 were carried out up to a half-day after sample collection, it is possible that a small amount of SiO_2 coprecipitates with the ferric hydroxide floc, thus slightly decreasing its IEP. This type of behavior, a shift in the IEP of flocs, has been shown by Parks to be a function of composition; the shifts typically occur in the direction of the IEP of the contaminant (29). In this case it would lead to a decreased IEP, as the IEP of SiO_2 is between pH 1.8 and pH 3.7 (29, 30). Below pH 6, however, the kinetics of precipitation of silica are much slower, and the effect was not observed. A similar situation was encountered in the flotations using 1.05×10^{-3} M $\text{Fe}_2(\text{SO}_4)_3$ and is shown by the dashed line in Figure 6. In order to test this hypothesis a separate set of experiments was carried out on the brines a day after sample collection. Significant amounts of $\text{SiO}_{2(s)}$ were observed in suspension (pH 7) before the ferric sulfate was added. Flotations using SLS were only effective up to pH 5–5.5, as opposed to pH 5.5–6 when carried out immediately after sample collection. These shifts are interpreted to be an artifact caused by the presence of colloidal silica in the brines.

The third ζ potential curve in Figure 7 is that for ferric hydroxide generated from 2.1×10^{-3} M Fe^{3+} present as $\text{Fe}_2(\text{SO}_4)_3$. Small differences in the ζ potentials are observed below the IEP when compared to the data for flocs generated from 10^{-3} M ferric chloride. A slight decrease in the ζ potential and a shift of the IEP to lower pH are observed in the presence of SO_4^{2-} as can be seen by the crossover in the recovery curves shown in Figure 6. Above the IEP, however, a marked difference exists in the surface charge characteristics of the flocs derived from the hydrolysis of ferric sulfate. Much lower surface potentials are developed; ζ potentials are as much as 20 mV more negative above pH 8. The decrease in surface charge may be due to several possible factors:

- (1) The presence of SO_4^{2-} in solution contributes to lower surface charges because of its adsorption onto the surface of the floc;
- (2) the presence of amorphous SiO_2 physically entrapped in the ferric hydroxide floc forming a mixed precipitate of $\text{SiO}_2\text{-Fe}(\text{OH})_n^{3-n}$;
- (3) the specific adsorption of SO_4^{2-} onto the silica component of the mixed $\text{SiO}_2\text{-Fe}(\text{OH})_n^{3-n}$ floc.

The first phenomenon should affect the surface charge not only above the IEP but also over the entire pH range, because polyvalent anions are preferentially adsorbed onto positively charged flocs and should not result in such a large change in the ζ potential above the IEP. Above the IEP, anions must be held to the surface by specific adsorption because the floc also bears a negative surface charge (14, 27, 28). The coprecipitation of SiO_2 above the IEP is more likely to be the cause of the depressed ζ potentials on these flocs. Indeed, studies in our laboratory have shown that very little precipitation of SiO_2 occurs during the time required for flotation below pH 7 although the solution is highly oversaturated with respect to silica. Above pH 8 significant flocculation of silica occurs, and the flocs generated in the presence of iron contain large amounts of admixed silica. Analysis of the recovered foam fractions after flotation at high pH indicated up to 85% coremoval of silica from the brine. Because the total silica content of the brines is more than 2.5×10^{-2} M (800 mg/L) (or half this value in solution during the flotation), at high pH the recovered flocs are largely composed of SiO_2 . Considering the previously mentioned effect of mixed flocs on IEP as described by Parks (29, 30), it is not surprising that an increased negative surface charge would be observed in the pH range where silica is expected to be a major component of the floc. Contrary to the above argument, though, is the coflotation of SiO_2 observed in the 10^{-3} M FeCl_3 runs.

In this study there does not appear to be any significant depression of the ζ potential above the IEP. An explanation of this discrepancy might be found in the third mechanism proposed above. Analyses of silica scale deposited in the flash tank after steam separation and even at the steam nozzle inlet to the turbine have shown up to 500-fold enrichments in arsenic concentration over the fluid content. Because both the oxyanions of arsenic and silica bear negative charges at the pH values encountered, the enrichment of arsenic is probably through specific adsorption such as that described by Wilson et al. for HAsO_4^{2-} onto ferric and aluminum hydroxides (26). In light of the above and the fact that SO_4^{2-} is equally prone to specific adsorption, one might conclude that SO_4^{2-} is specifically adsorbed onto the silica component of the mixed precipitate and not only onto the ferric hydroxide, thus resulting in a larger depression of the ζ potential above the IEP.

In closing, we add a quote from Park's impressive work on the aqueous surface chemistry of oxides and complex oxide minerals: "The important role of structural charge and the sensitivity of the degree of its compensation of environment force one to conclude that variability of the pzc for minerals and coprecipitated hydroxides will be extreme" (29). We must add that the coflotation of silica observed in our investigations is contrary to the results of Shannon et al., who found that less than 1% of the silica was coflotated in the removal of $\text{Fe}_2(\text{SO}_4)_3$ -derived flocs with Quaternary O (Ciba-Geigy cationic surfactant) using dissolved air flotation (6). This is probably the result of their carrying out flotations at pH 4–4.7 and 85 °C under which conditions the kinetics of polymerization and precipitation of silica are greatly depressed.

Conclusions

A rapid and effective bench scale method for the removal of arsenic species from geothermal brines by adsorptive bubble separations has been described. The use of colloidal ferric hydroxide above the IEP as coprecipitant and laurylammonium chloride as the collector results in nearly quantitative removal of the oxyanions of As(III) and

As(V). The arsenic content of the brines is effectively reduced from 100 ± 10 ng/mL to less than 10 ng/mL, well below the recommended limit for arsenic in drinking waters (50 ng/mL). Separations are carried out in less than 10 min from high ionic strength fluids containing large quantities of dissolved and colloidal silica. Preliminary results indicating a coremoval of silica may prove this technique useful as a treatment method for removal of silica and trace contaminants on a larger continuous flow basis. Surface charge characteristics of the flocs are found to be a function of pH as well as the source of iron used as precipitating agent.

Acknowledgments

I thank Harry Zeitlin and Quintus Fernando for first stimulating my interest in flotation methods. This paper also benefited from discussions with and reviews by Robert L. Grob and Fred T. Mackenzie. We thank M. Tanaka and J. McCullough for various aspects of technical assistance and gratefully acknowledge the Hawaii Electric Light Co., operator of the HGP-A Geothermal Generator Facility, for their cooperation.

Registry No. LA, 929-73-7; SLS, 151-21-3; As, 7440-38-2; ferric hydroxide, 1309-33-7.

Literature Cited

- Thomas, D. M. *Proc. Pac. Geotherm. Conf.* 1982, 273–278.
- Waibel, A. *Trans.—Geotherm. Resour. Counc.* 1983, 7, 205–209.
- Stone, C.; Fan, P. F. *Geology* 1978, 6, 401–404.
- De Carlo, E. H.; Thomas, D. M., University of Hawaii, Honolulu, HI, unpublished work, 1983.
- "International Standards for Drinking Water", 3rd ed.; World Health Organization: Geneva, 1971; pp 1–70.
- Shannon, W. T.; Owers, W. R.; Rothbaum, H. P. *Geothermics* 1982, 11, 43–58.
- Buisson, D. H.; Rothbaum, H. P.; Sharmon, W. T. *Geothermics* 1979, 8, 97–110.
- Lederer, W. H.; Fensterheim, R. J., Eds. "Arsenic: Industrial, Biomedical, Environmental Perspectives"; Van Nostrand: New York, 1983; pp 1–443.
- Chaine, F. E.; Zeitlin, H. *Sep. Sci.* 1974, 9, 1–12.
- De Carlo, E. H.; Zeitlin, H.; Fernando, Q. *Anal. Chem.* 1981, 53, 1104–1107.
- Fuerstenau, M. C., Ed. "Flotation: A. M. Gaudin Memorial Volume I"; American Institute of Mining, Metallurgical, and Petroleum Engineers: New York, 1976; pp 1–621.
- Lemlich, R. "Adsorptive Bubble Separation Techniques"; Academic Press: New York, 1972; pp 1–331.
- Somasundaran, P. *AIChE Symp. Ser.* 1975, 71 (150).
- Wilson, D. J.; Thackston, E. L. Environmental Protection Agency, Cincinnati, OH, 1980, EPA Report 600/2-80-138, pp 1–133.
- Sebba, F. "Ion Flotation"; Elsevier: Amsterdam, 1962; pp 1–154.
- Grieves, R. B. In "Treatise on Analytical Chemistry"; Elving, P. J., Ed.; Wiley: New York, 1982; Part 1, Vol. 5, pp 371–448.
- Hiraide, M.; Mizuike, A. *Rev. Anal. Chem.* 1982, 6, 151–168.
- Clarke, A. N.; Wilson, D. J. "Foam Flotation: Theory and Applications"; Marcel Dekker: New York, 1983; pp 1–418.
- De Carlo, E. H.; Zeitlin, Q.; Fernando, Q. *Anal. Chem.* 1982, 54, 898–902.
- Kawalec-Pietrenko, B.; Selecki, A. *Sep. Sci. Technol.*, in press.
- Sorg, T. J.; Logsdon, G. W. *J.—Am. Water Works Assoc.* 1978, 70, 379–393.
- De Carlo, E. H.; Bleasdel, B.; Zeitlin, H.; Fernando, Q. *Sep. Sci. Technol.* 1982, 17, 1205–1218.
- De Carlo, E. H.; Bleasdel, B.; Zeitlin, H.; Fernando, Q. *Sep. Sci. Technol.* 1983, 18, 1023–1044.
- Creelius, E. A.; Robertson, D. E.; Fruchter, J. S. In "Trace Substances in Environmental Health"; Hemphill, D., Ed.;

University of Missouri Press: Rolla, 1976; Vol. 10.
 (25) Stumm, W.; Morgan, J. J. "Aquatic Chemistry", 2nd ed.; Wiley-Interscience: New York, 1981; pp 1-780.
 (26) Currin, B. L.; Moffat-Kennedy, R.; Clark, A. N.; Wilson, D. J. *Sep. Sci. Technol.* 1979, 14, 669-687.
 (27) Clarke, A. N.; Wilson, D. J.; Clarke, J. H. *Sep. Sci. Technol.* 1978, 13, 573-586.
 (28) Iwasaki, I.; Cooke, S. R. B.; Colombo, A. F. U.S. Bureau of Mines, Avondale, 1960, Report RI 5593.
 (29) Parks, G. A. *Adv. Chem. Ser.* 1967, No. 67, 121-160.

(30) Parks, G. A. *Chem. Rev.* 1965, 65, 177-198.

Received for review September 24, 1984. Accepted December 26, 1984. This research was sponsored in part through a project supported by the Hawaii Natural Energy Institute through Department of Energy Contract DE-FG03-81ER10250M003. The Zeta meter used in these studies was provided by Ed Laus through Solar Energy Research Institute Subcontract XE-09013-01. This is Hawaii Institute of Geophysics Contribution No. 1586.

Using Electrophoresis in Modeling Sulfate, Selenite, and Phosphate Adsorption onto Goethite

Douglas D. Hansmann* and Marc A. Anderson

Water Chemistry Program, University of Wisconsin, Madison, Wisconsin 53706

■ We evaluate methods for determining two quantities generally considered necessary in modeling adsorption. First, the electrical component of net binding constants is determined by electrophoresis in conjunction with pH measurement. Second, three techniques for determining the maximum concentration of available surface sites are compared. We use a Stern model to make out evaluations; however, the results should be applicable to adsorption modeling in general. Electrophoretic mobility data are modeled quite successfully, but the empirically determined maximum surface-site concentration on colloidal goethite (α -FeOOH) varies considerably for sulfate, selenite, and phosphate despite their similar sizes and binding mechanisms. We suggest that aggregation processes, due to both proximity to the isoelectric point of the solid and adsorbate bridging between particles, may have significant effects on surface-site availability.

Introduction

Suspended particles can play a major role in the attenuation and transport of otherwise-dissolved compounds because of combined chemical and electrical interactions resulting in adsorption. The practical value of correlating the extent of adsorption with changes in either particulate or solution character is well recognized and continues to prompt considerable research.

Natural adsorption processes generally occur with a number of distinct adsorbate species and particulate surfaces present. However, current models for predicting the extent of adsorption in relatively simple systems, containing only one or two adsorbates and a single adsorbent, have not always been successful and are often cumbersome in practice. We evaluate some of the methods for determining adsorption model parameters in an attempt to refine our predictive capabilities.

In general, existing models for predicting the extent of adsorption can be divided into two schools of thought. First, there are surface complexation models based on plausible surface reactions between adsorbate molecules and particle-surface sites (1-6). These models have the following form:



where A is a dissolved adsorbate molecule near the particle surface, $\equiv SL$ is a surface site with an attached leaving group, $\equiv SA$ is a surface site with an attached adsorbate molecule, and L is a dissolved leaving-group molecule near the particle surface (in an aqueous solution with only one

adsorbate species A considered, L must be H^+ , OH^- , or a water molecule). Adsorption density is predicted from a simultaneous solution of the equilibrium expression(s) associated with eq 1, an adsorbate mass balance (eq 2), and a surface-site mass balance (eq 3).

$$[A] + N[\equiv SA] = [A]_{total} \quad (2)$$

[A] is the dissolved adsorbate concentration (μM), N is the adsorbent concentration (g/L), $\{\equiv SA\}$ is the adsorbate density on the particle surface ($\mu mol/g$), and $[A]_{total}$ is the total analytical adsorbate concentration (μM).

$$\{\equiv SL\} + \{\equiv SA\} = \{\equiv S\}_{total} \quad (3)$$

$\{\equiv SL\}$ is the density of unfilled adsorbent sites ($\mu mol/g$) and $\{\equiv S\}_{total}$ is the maximum concentration of available adsorption sites ($\mu mol/g$).

Since complexation models are, in theory, based on accurate molecular descriptions of actual reactions, available spectroscopic evidence should confirm surface species predicted by the proposed set of reactions and associated equilibrium constants (K_c). In the case of phosphate adsorption onto goethite (α -FeOOH), infrared spectroscopic studies indicate a binuclear coordination of phosphate ions to two iron atoms on the particle surface (7). However, a complexation model allowing either mononuclear or binuclear coordination among its set of proposed reactions (5) predicts mostly mononuclear species over a wide range of pH and total phosphate concentration. Experimental data are successfully modeled in spite of this discrepancy by using empirically determined equilibrium constants.

Alternatively, there are statistical models where the ratio of adsorbate-occupied to adsorbate-free surface sites is related to the mole fraction of adsorbate remaining in solution (8-13).

$$\{\equiv SA\} / \{\equiv SL\} = K_p X \quad (4)$$

Here, a partition coefficient, K_p , is empirically determined for each type of surface site, and eq 2-4 are solved simultaneously to predict adsorption density. In contrast to the surface complexation approach, this model is not constrained by an a priori knowledge of binding mechanisms or reaction stoichiometry.

Both equilibrium constant (eq 1) and partition coefficient (eq 4) are commonly expressed in terms of the Gibbs free energy:

$$K_{net} = e^{-\Delta G_{net}/(RT)} \quad (5)$$

where ΔG_{net} is the total observed free energy change due to adsorption, RT is the gas law constant times the kelvin

temperature, and K_{net} is the net equilibrium constant or partition coefficient. Since work is involved in bringing charged adsorbate molecules through the electric field produced by a charged particle, the net energy of adsorption is often divided into intrinsic and electrostatic components.

$$\Delta G_{\text{net}} = \Delta G_{\text{intrinsic}} + \Delta G_{\text{electrostatic}} \quad (6)$$

For a given experimental system, both statistical and surface complexation models of adsorption describe the same physicochemical process and should have some features in common. Certainly, both electrostatic energy and concentration of available adsorption sites ($\{=S\}_{\text{total}}$ in eq 3) should be model independent. In the present work, we compare the adsorption of three anions having wide-ranging affinities for colloidal goethite. Quantification of $\Delta G_{\text{electrostatic}}$ and $\{=S\}_{\text{total}}$ is investigated by using classical Stern theory as the framework for a statistical model. In the course of our study we do not mean to suggest that the Stern model is superior to the other available models of adsorption referenced above. However, we feel our results do have implications for adsorption modeling in general.

Theory

The Stern model of adsorption (9) considers both the fraction of surface sites occupied by adsorbate ions and the adsorbate mole fraction in solution. These quantities are related by a Boltzmann distribution based on the difference in energy between dissolved and adsorbed states (14). Mathematically, this model can be expressed by combining eq 3-6 and rearranging:

$$\frac{\{=SA\}}{\{=S\}_{\text{total}} - \{=SA\}} = X e^{-(\Delta G_{\text{intrinsic}} + \Delta G_{\text{electrostatic}})/(RT)} \quad (7)$$

Site Density. An empirical determination of $\{=S\}_{\text{total}}$ can be made by adding a known excess concentration of adsorbate, measuring the remaining dissolved concentration after equilibration with particulate material, and attributing the amount removed to a saturation of available surface sites. This presupposes that there are no competing reactions such as surface precipitation or adsorbate complexation in solution. Our research on goethite indicates that this empirical value is not always consistent with results from alternative methods for site density determination such as the two techniques described below.

(1) Infrared spectroscopic studies suggest that oxyanion surface complexation occurs by displacement of singly coordinated surface hydroxyl groups (15). There is one singly coordinated hydroxyl per unit cell on each of the two predominant goethite crystal faces (16, 17), and unit cell dimensions for each face are well-known (18). Goethite crystal dimensions determined by transmission electron microscopy are used to assign an appropriate fraction of the total N_2 BET surface area attributable to each crystal face, and site density in either moles per mass or moles per surface area can then be calculated.

(2) The second method assumes that an equal number of sites is available for both surface protolysis and oxyanion adsorption (5). Therefore, results from acid-base titration of the surface should simultaneously provide concentration of available oxyanion adsorption sites and the protolyzable site density. However, recent research indicates that cations and anions may bind at different locations (19), so the site density for each type of ion may not be the same.

Electrostatic Energy. Modelers continue to debate how to formulate the electrostatic component of adsorption energy (20). Ion partitioning between particle surfaces and

bulk solution is influenced by charges on both ions and particles, and electrostatic energy can be evaluated by measuring the work required to bring ions from bulk solution to the surface binding plane. Since voltage is defined as work per unit charge, the product of binding-plane potential (ψ_{bp}) relative to bulk solution and the charge (zF) associated with 1 mol of ions yields a measure of electrostatic energy.

$$\Delta G_{\text{electrostatic}} = zF\psi_{\text{bp}} \quad (8)$$

Although there is no method for measuring this binding-plane potential directly, electrophoretic mobility can be used to determine potential at the plane of shear, and this in turn can be related to potential at the binding plane.

Electrophoresis refers to particle movement through a fluid caused by an electromotive force. In addition to this electric field, the particle is affected by Stokes' friction acting in opposition to the field, which is a function of particle size and viscosity of the medium. Calculation of shear-plane, or ζ , potential from electrophoretic mobility was first derived by von Helmholtz (21) and von Smoluchowski (22):

$$\zeta = U\eta/(\epsilon_0\epsilon) = (14.1)U \quad (\text{at } 20^\circ\text{C in water}) \quad (9)$$

where U is electrophoretic mobility [$\mu\text{m}\cdot\text{cm}/(\text{V}\cdot\text{s})$], ϵ_0 is the permittivity of free space ($8.854 \times 10^{-12} \text{ F/m}$), ϵ is the solution dielectric constant, η is viscosity (poise), and ζ is ζ potential (mV). Later work (23, 24) showed that this relationship was valid only for values of $\kappa r > 100$ where r is the particle radius and κ is the reciprocal Debye length. For $\kappa r < 0.1$, this research resulted in a second limiting relationship, the Hückel equation.

$$\zeta = 3U\eta/(2\epsilon_0\epsilon) = (21.2)U \quad (\text{at } 20^\circ\text{C in water}) \quad (10)$$

Between these two limits, additional forces become significant. Just as the particle-surface charge is attracted to one of the poles in the applied direct current field, counterions in the particle atmosphere are repelled by this pole, resulting in the relaxation effect whereby the center of the ionic atmosphere lags behind the particle center itself. Also, ions in the particle atmosphere can experience viscous drag with respect to surrounding solvent molecules. Both effects are accounted for in the theory of Wiersema et al. (25) for spherical particles, and their results have been extended to cylindrical particles by Stigter (26, 27). The relationship between mobility and ζ potential has been experimentally verified by Ottewill and Shaw (28).

Once ζ potential has been determined, the relationship between this quantity and binding-plane potential must be established. The binding plane must be located at or inside the plane of shear, since ions cannot be considered bound to the surface unless they move with the particle. Consequently, $|\psi_{\text{bp}}| \geq |\zeta|$, any difference being due to electrostatic decay across the intervening distance.

If the shear plane is placed at the outer edge of the specifically adsorbed layer (29-31), coincident with the beginning of the diffuse layer (i.e., $\zeta = \psi_{\text{diffuse}}$), we can use a capacitor model of the double layer which assumes a linear potential decay between binding and shear planes. Charge outside the shear plane can be obtained by using Gouy-Chapman theory (31):

$$\sigma_s = -11.74\sqrt{C} \sinh [zF\zeta/(2RT)] \quad (11)$$

σ_s is diffuse layer charge ($\mu\text{C}/\text{cm}^2$), C is total electrolyte concentration in equivalents/liter, and ζ is ζ potential in volts. By use of a value of $20 \mu\text{F}/\text{cm}^2$ for outer-compact-layer capacitance (29, 32), binding plane potential can be calculated.

$$\psi_{bp} = \zeta - \sigma_f/20 \quad (12)$$

This result is used directly in solving eq 8 and is also necessary for ion charge (z) determination in that equation. The average charge on a protolyzable ion in solution is a pH-dependent number and can be calculated by using acid dissociation constants and solution pH. However, pH at the plane of binding is affected by the particle's electric field and, therefore, should be corrected as follows for calculating z (12):

$$\{H^+\}_{bp} = \{H^+\}_{bulk} e^{-F\psi_{bp}/(RT)} \quad (13)$$

where $\{H^+\}_{bp}$ is hydrogen ion activity at the binding plane.

Intrinsic Energy. With the theory developed above, it is now possible to rewrite eq 7 solving for intrinsic free energy of adsorption in terms of measurable quantities.

$$\Delta G_{intrinsic} = -zF(\zeta - \sigma_f/20) - RT \ln \frac{\{SA\}}{(\{S\}_{total} - \{SA\})X} \quad (14)$$

For a given adsorbate-adsorbent pair, this intrinsic energy should be invariant as a function of pH or reactant concentrations. We use this premise to test our ability to determine $\{S\}_{total}$ and ψ_{bp} .

Materials and Methods

All experiments involved batch equilibration of radio-labeled adsorbates with dilute goethite slurries. The phosphate data are from Stanforth (33) in which the equilibration time was 4 h at a goethite concentration of 74 mg/L and 0.002 M ionic strength. Other than these exceptions all experimental conditions were as follows.

Goethite (α -FeOOH) was prepared according to Atkinson et al. (34) by Stanforth (33). Transmission electron microscopy revealed acicular particle monomers, about 35 nm \times 25 nm \times 300 nm in size. Using a 430 \times magnification light-field microscope, aggregates were also seen to be elongated, approximately 0.2 μ m in cross section. The extremes in particle size result in a range of $\kappa\tau$ values from 1.8 to 10 at 10^{-3} M ionic strength. N_2 BET surface area was 33 m²/g, and X-ray diffraction patterns confirmed the absence of noticeable hematite or amorphous Fe(OH)₃ contamination (35).

Preequilibration was accomplished by filling 100-mL polyethylene bottles with a solution containing the adsorbate of interest (ranging between 2×10^{-6} and 2×10^{-5} M) and either HNO₃ or NaOH to achieve the desired pH (generally between 4 and 10). A radioactive label was included (³²P, ⁷⁵Se, or ³⁵S), and the ionic strength was adjusted to 10^{-3} M with NaNO₃. Bottles were kept at 20 °C for 24 h in a New Brunswick shaker, rotating at 160 rpm. Other stock containers and pipets were also filled with preequilibration solutions.

Pretreated bottles were emptied, refilled with fresh solution, and equilibrated for 1 h in the constant-temperature shaker. Next, 0.5 mL of 6.0 g/L stock goethite suspension was added (the final goethite concentration was \sim 30 mg/L), and bottles were immediately returned to the shaker. With these low solids concentrations we were able to achieve high levels of surface coverage with relatively low adsorbate concentrations, thereby minimizing competing reactions such as surface precipitation or solution complexation of the adsorbate. Also, particle collision frequency, and, hence, particle aggregation, was kept to a minimum at these solids concentrations.

After a 24-h equilibration, pH was measured with an Orion 801 pH meter and a Corning combination electrode, and electrophoretic mobility was determined with a PenKem laser zee meter. (The mobility histogram and

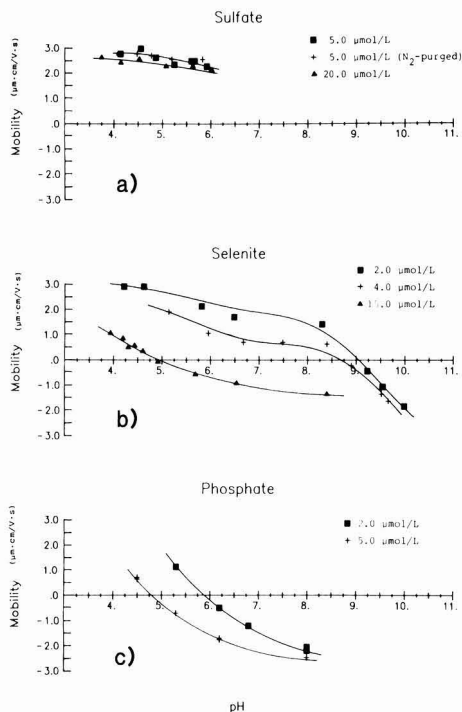


Figure 1. Electrophoretic mobility is a function of both pH and adsorbate concentration for goethite in the presence of sulfate, selenite, and phosphate.

Brownian motion spectra shown in the last two figures were obtained on a PenKem system 3000 electrokinetics analyzer. Here, the goethite was obtained from a second preparation with an N_2 BET surface area of 81 m²/g and monomeric crystals 80 nm in length.) In addition, two aliquots were filtered through a 0.4- μ m Nuclepore filter supported by a polycarbonate apparatus. The first portion was wasted, and the second was used for dissolved adsorbate determination by radioactive counting techniques using a Packard Model 3320 liquid scintillation counter.

Adsorption density was calculated from the difference between initial and dissolved concentrations and normalized with respect to solid mass. Adsorbate pK values were determined by acid-base titration for selenite, since literature values proved unreliable. Under our experimental conditions, $pK_1 = 2.5$ and $pK_2 = 8.45$.

Results and Discussion

The electrophoretic mobility of colloidal goethite in the presence of adsorbed anions is a complicated function of both pH and adsorbate concentration (Figure 1). Given the particle size range and ionic strength of our goethite slurries, and assuming a cylindrical particle shape as a model for our acicular crystals and aggregates, the relationship between shear-plane potential and electrophoretic mobility falls between the two limiting conditions described by eq 9 and 10. By use of data from Stigter (26), Table I lists the appropriate constant to be used in place of "14.1" in eq 9 for a series of mobility ranges. The error terms listed in the table reflect the range in particle size.

By use of eq 8-13 and Table I, the relationship between mobility and $\Delta G_{electrostatic}$ can be established (Figure 2), and it is apparent from Figures 1 and 2 that $\Delta G_{electrostatic}$ has a functional dependence on both pH and total adsorbate

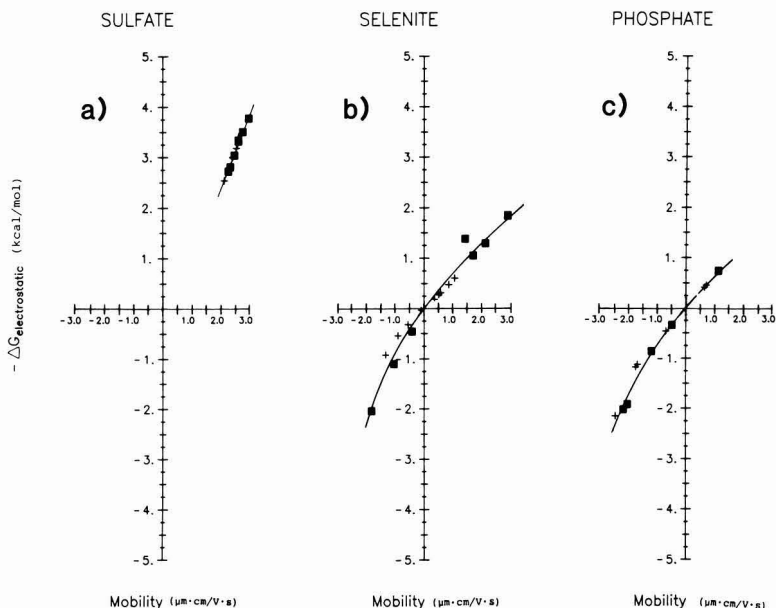


Figure 2. Electrostatic component of the binding energy is related to electrophoretic mobility.

Table I. Constant To Be Used in Place of "14.1" in Equation 9 for a Series of Mobility Ranges^a

U , $\mu\text{m-cm}/(\text{V}\cdot\text{s})$	constant	U , $\mu\text{m-cm}/(\text{V}\cdot\text{s})$	constant
0.0–0.5	18.2 ± 1.9	2.5–3.0	18.9 ± 2.2
0.5–1.0	18.1 ± 1.9	3.0–3.5	19.5 ± 2.1
1.0–1.5	17.9 ± 1.8	3.5–4.0	20.4 ± 2.1
1.5–2.0	18.2 ± 1.9	4.0–4.5	22.3 ± 2.1
2.0–2.5	18.5 ± 2.0	4.5–5.0	24.4 ± 1.8

^aBased on data from Stigter (26) for cylindrical particles.

concentration. For each of the three oxyanions of interest, the net energy of adsorption based on the Stern model (eq 6 and 7) is also a function of pH and adsorbate concentration (Figures 3a–5a). However, when $\Delta G_{\text{electrostatic}}$ is subtracted from these net energy values, the resultant intrinsic energy of adsorption does not show any clear dependence on either variable (Figures 3b–5b). It is apparent that the net energy of adsorption contains a potentially large but relatively constant intrinsic component and a smaller, but highly variable, electrostatic component.

In the above analysis, a value for the maximum concentration of available adsorption sites has been assigned for each anion. For selenite and phosphate, these are empirical values of 80 and 43 $\mu\text{mol/g}$, respectively, based on surface saturation (Figure 6). For sulfate, no surface saturation was observed due to analytical difficulties in obtaining this value. Since $\{=SA\}$ is determined by the difference between $[A]_{\text{total}}$ and $[A]$ in eq 2, the precision of this determination becomes unacceptable as the difference becomes small (e.g., $N\{=SA\} < 0.01[A]_{\text{total}}$) for weakly bound adsorbates such as sulfate.

We describe two alternative indirect methods for site density determination under Theory. By the first technique, using crystal morphology characterization in conjunction with BET surface area measurements, we calculate a maximum site density of 140 $\mu\text{mol/g}$. With the second method $\{=S\}_{\text{total}} = 120 \mu\text{mol/g}$ by using titration results from Sigg and Stumm (5) and adjusting for the differences in BET surface area between their goethite and

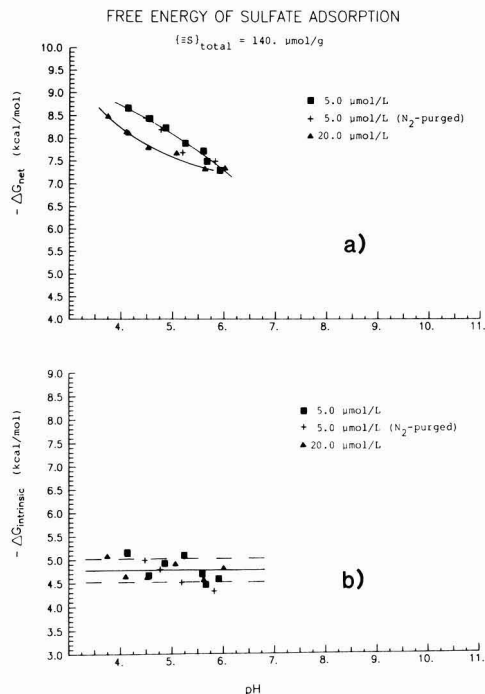


Figure 3. Net energy of sulfate adsorption varies with both pH and total sulfate concentration (a). However, when electrostatic energy is subtracted, the remaining intrinsic component is relatively constant (b). The solid line shows the average value, and the dashed lines depict one standard deviation from the mean.

ours. In both cases we assume binuclear surface coordination exclusively.

In the absence of an empirical value for the maximum site density of sulfate adsorption, we use a theoretical value

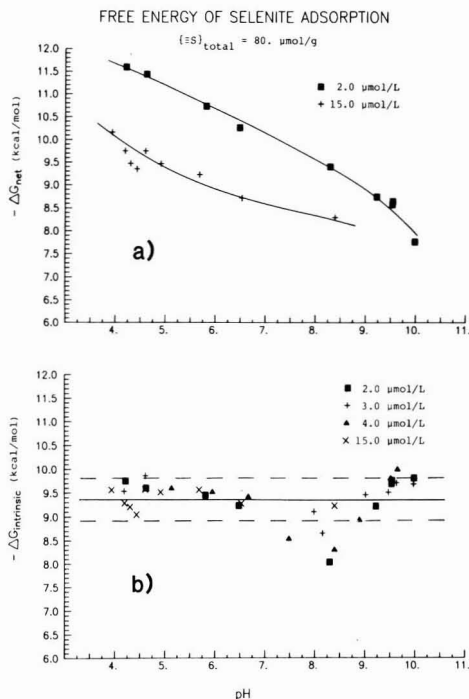


Figure 4. Net energy of selenite adsorption (a) and the intrinsic component (b) are shown as functions of pH and total selenite concentration. Again, the solid line shows the average value, and the dashed line depicts one standard deviation from the mean.

of 140 $\mu\text{mol/g}$ in Figure 3. However, this maximum should apply equally well to all three oxyanions in theory, since their binding mechanisms are thought to be similar and they are all approximately equal in size. We can illustrate the effect of assuming the theoretical $[\text{Se}]_{\text{total}}$ value, as opposed to the empirical values used in Figures 4 and 5, for selenite and phosphate in the following manner.

With the assumption that $\Delta G_{\text{intrinsic}}$ is constant for a given adsorbate-adsorbent pair, eq 6 can be treated as a linear relationship between ΔG_{net} and $\Delta G_{\text{electrostatic}}$ where the slope should be equal to unity and the intercept is $\Delta G_{\text{intrinsic}}$. Figures 7 and 8 show this relationship, comparing the use of empirical vs. theoretical $[\text{Se}]_{\text{total}}$ values for selenite and phosphate, respectively. The dashed lines depict a slope of 1 and an intercept of $-\Delta G_{\text{intrinsic}}$ (determined by averaging the data in Figures 4b and 5b). The ability to fit data with this slope and intercept tests the adherence of the system to a Stern model of adsorption.

In Figure 7 there is little or no qualitative improvement made by choosing either of the two $[\text{Se}]_{\text{total}}$ values for selenite uptake. However, in both cases, noticeably lower $-\Delta G_{\text{net}}$ values are obtained near the isoelectric point (pH_{iep}) where shear-plane potential, and hence $\Delta G_{\text{electrostatic}}$, approach zero. We suggest that particle aggregation reduces the number of sites available for selenite adsorption near the pH_{iep} , and our research is continuing in this area. Clearly, such a decrease in $[\text{Se}]_{\text{total}}$ will increase values for $-\Delta G_{\text{net}}$ (see eq 6 and 7) and, therefore, will increase values near the pH_{iep} in Figure 7.

The empirical $[\text{Se}]_{\text{total}}$ value for phosphate uptake yields a markedly better Stern model fit compared to the theoretical value, as shown in Figure 8. Also, in this system there is no apparent reduction in maximum site density

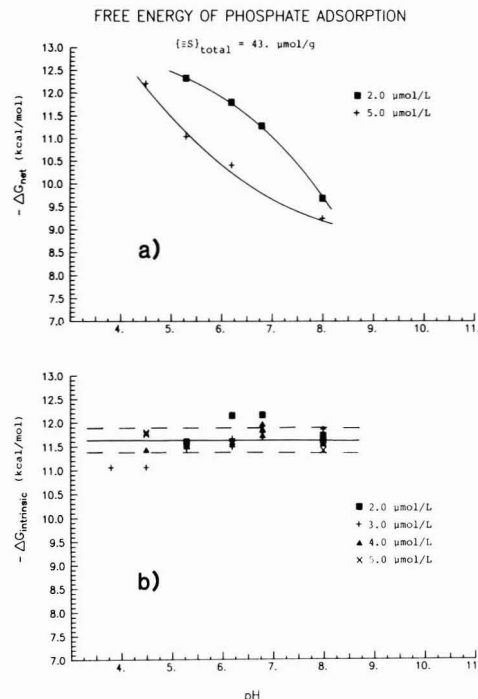


Figure 5. Net energy of phosphate adsorption (a) and the intrinsic component (b) are shown as functions of pH and total phosphate concentration.

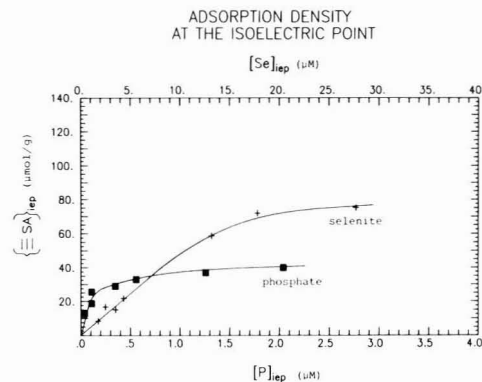


Figure 6. Adsorption density is shown as a function of adsorbate concentration remaining in solution. Each data point is obtained by extrapolation from results obtained on both sides of the isoelectric point (iep), based on electrophoresis measurements.

near the pH_{iep} . Instead, the empirical $[\text{Se}]_{\text{total}}$ value is considerably lower than the theoretical value throughout the range of pH and concentration studied. It has been suggested that phosphate can form bridges between goethite crystals (36), thereby greatly reducing the total number of available sites regardless of proximity to the pH_{iep} .

Our recent research supports this explanation. We have previously shown that particle mobility decreases with phosphate uptake (Figure 1). In addition, the mobility distribution about the mean value narrows considerably with adsorbed phosphate (Figure 9). With a strongly bound ion such as phosphate, a narrow distribution may

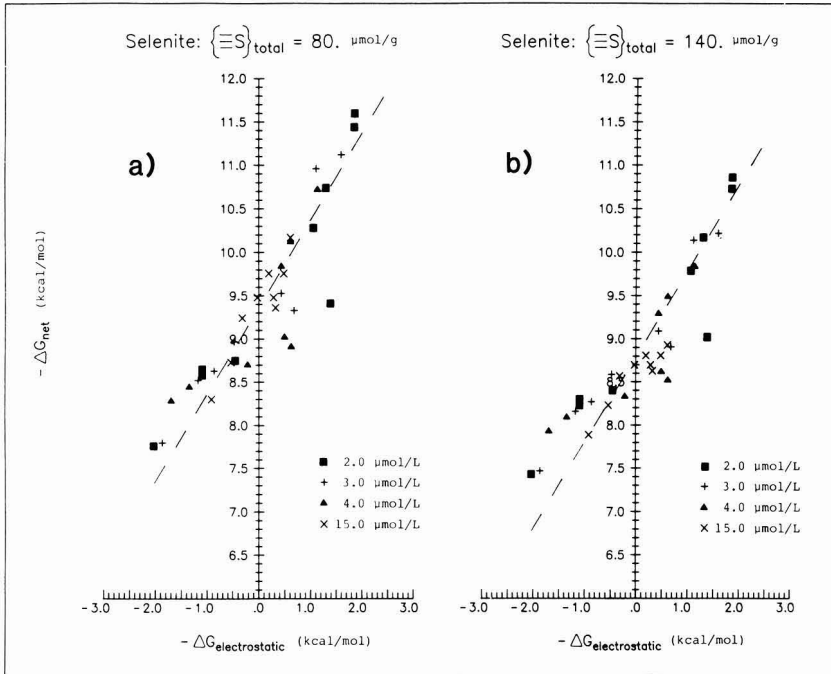


Figure 7. Relationship between net energy of selenite adsorption and its electrostatic component is compared by using both empirical (a) and theoretical (b) values for the maximum concentration of available adsorption sites. The dashed lines depict a slope of 1 and an intercept of $-\Delta G_{intrinsic}$.

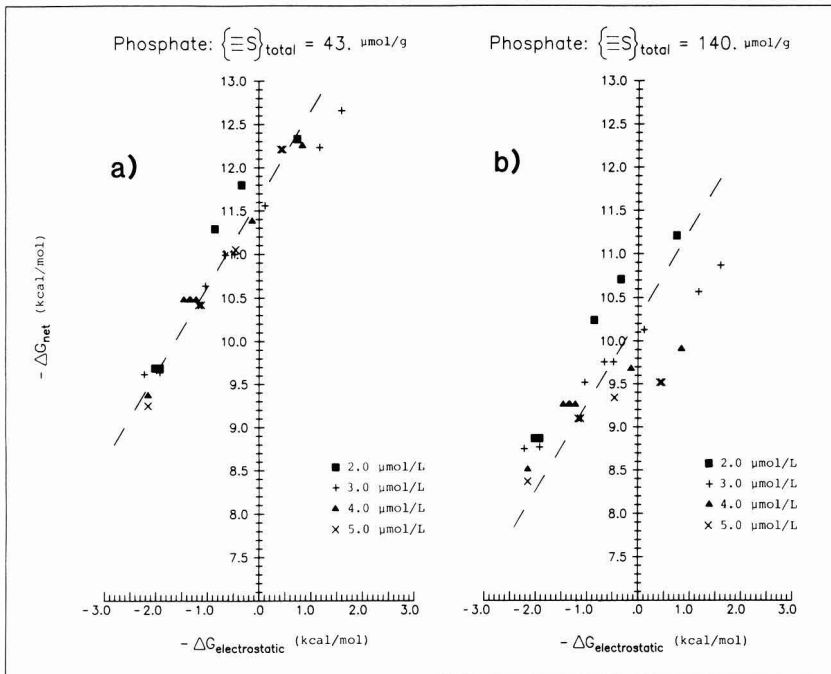


Figure 8. Empirical (a) and theoretical (b) values for the maximum concentration of available phosphate adsorption sites are compared. Again, the dashed lines depict a slope of 1 and an intercept of $-\Delta G_{intrinsic}$.

in part be due to indiscriminant surface coordination at sites that were originally heterodisperse in terms of charge, rendering a more uniform charge distribution (37). How-

ever, an aggregation process, as postulated above, could also narrow the mobility distribution by mitigating the needlelike shape characteristic of monomeric goethite

Mobility Histograms
with and without Adsorbed Phosphate

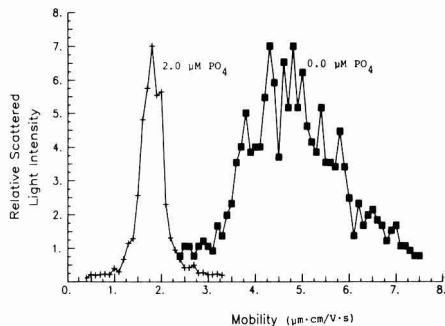


Figure 9. Electrophoretic mobility of goethite shifts from an average of 4.58–1.71 $\mu\text{m-cm}/(\text{V-s})$ with the addition of 2.0 μM phosphate to 30 mg/L goethite at pH 5.71. As described under Materials and Methods, the goethite used here differed from that used for experiments summarized in Figure 1c.

Frequency Spectra
with and without Adsorbed Phosphate

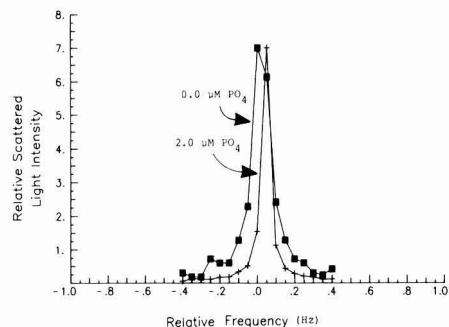


Figure 10. Frequency spectrum based on Brownian movement of the phosphated goethite is considerably narrower than the phosphate-free spectrum. A narrower spectrum indicates that the particle size is larger.

crystals and increasing particle size, thereby limiting the range of Stokes' friction values between various orientations of moving particles during electrophoresis.

Analyzing the Brownian motion of goethite particles lends further support to an increase in particle size in the presence of phosphate. Larger particles exhibit less movement due to molecular collisions, and this is the case for phosphated goethite compared to phosphate-free particles (Figure 10). By use of eq 8–13 and Table I, the electrophoretic mobility of the phosphated goethite described in Figures 9 and 10 corresponds to a value of 1.6 kcal/mol for $-\Delta G_{\text{electrostatic}}$. This value is greater than virtually all of the data presented in Figure 8, indicating that a larger, aggregated particle may characterize phosphated goethite slurries over a wide range of conditions.

Conclusions

Although it would be preferable to predict the maximum concentration of available adsorption sites from some a priori adsorbent characterization, this does not appear to be a feasible approach. Instead, empirical surface saturation results, similar to those presented in Figure 6, appear to be necessary in order to evaluate $(=S)_{\text{total}}$ for each adsorbate species of interest. We feel that aggregation processes are responsible for the discrepancy between

theoretical determinations of the maximum site concentration and empirical results.

Once a realistic value for $(=S)_{\text{total}}$ has been established, it is possible to model data obtained over a wide range of pH and adsorbate concentration with a single value for $\Delta G_{\text{intrinsic}}$ (Figures 3b–5b). This apparently contradicts the opinion that separate intrinsic constants are necessary for each of the several combinations of pH-dependent conjugate acid forms of both the oxyanion and the goethite surface (3, 5, 6).

We have also demonstrated the ability to assign an electrostatic energy value based on an electrophoretic mobility measurement in conjunction with a pH determination (eq 8–13; Figures 3–5). Typically, the determination of electrostatic energy is based on an extensive calibration procedure using potentiometric titrations (5). Although theoretically sound, that approach is cumbersome in practice.

Finally, we note that the relative magnitude of $\Delta G_{\text{intrinsic}}$ influences the effect of electrostatics on anion adsorption. For the weakly bound sulfate ion electrostatic attraction can increase the amount adsorbed; however, the intrinsic energy of sulfate adsorption onto goethite is already too low to allow significant binding, and electrostatic repulsion cannot decrease the amount adsorbed in any meaningful sense. Therefore, sulfate is only bound at low pH values (Figures 1a–3a), and free energy data are difficult to obtain above pH 6 (Figure 3) because $(=SA)$ becomes exceedingly small. Conversely, for the strongly bound phosphate ion, electrostatic repulsion can decrease the amount adsorbed; however, attraction cannot significantly increase coverage because the intrinsic energy is already high enough to cause nearly complete removal from solution. Therefore, phosphate is strongly bound except where pH and/or adsorbate concentration is high (Figures 1c, 2c, and 5a). Selenite has an intermediate value for $\Delta G_{\text{intrinsic}}$ (Figure 4b), and the amount adsorbed is more readily affected by either electrostatic attraction or repulsion as environmental conditions change.

Acknowledgments

We thank R. R. Stanforth and M. I. Tejedor-Tejedor for their technical assistance and are grateful to W. A. Zeltner for valuable discussions and critiques. We thank H. Grogan and J. Schneider for typing this manuscript.

Registry No. Sulfate, 14808-79-8; selenite, 14124-67-5; phosphate, 14265-44-2; goethite, 1310-14-1.

Literature Cited

- (1) Stumm, W.; Hohl, H.; Dalang, F. *Croat. Chem. Acta* 1976, 48, 491–504.
- (2) Davis, J. A.; James, R. O.; Leckie, J. O. *J. Colloid Interface Sci.* 1978, 63, 480–499.
- (3) Davis, J. A.; Leckie, J. O. *J. Colloid Interface Sci.* 1980, 74, 32–43.
- (4) Benjamin, M. M.; Bloom, N. S. In "Adsorption from Aqueous Solution"; Tewari, P. H., Ed.; Plenum Press: New York, 1981; pp 41–60.
- (5) Sigg, L.; Stumm, W. *Colloids Surf.* 1981, 2, 101–107.
- (6) Schindler, P. W. In "Adsorption of Inorganics at Solid-Liquid Interfaces"; Anderson, M. A.; Rubin, A. J., Eds.; Ann Arbor Science: Ann Arbor, MI, 1981; pp 1–49.
- (7) Parfitt, R. L.; Atkinson, R. J.; Smart, R. St. C. *Soil Sci. Soc. Am. Proc.* 1975, 39, 837–841.
- (8) Langmuir, I. *J. Am. Chem. Soc.* 1918, 40, 1361–1413.
- (9) Stern, O. *Z. Electrochem.* 1924, 30, 508–516.
- (10) Hingston, F. J.; Posner, A. M.; Quirk, J. P. *J. Soil Sci.* 1972, 23, 177–192.
- (11) Ryden, J. C.; McLaughlin, J. R.; Syers, J. K. *J. Soil Sci.* 1977, 28, 72–92.

- (12) Anderson, M. A.; Malotky, D. T. *J. Colloid Interface Sci.* **1979**, *72*, 413-427.
- (13) Parfitt, R. L. *Adv. Agron.* **1978**, *30*, 1-50.
- (14) Madrid, L. J. *Soil Sci.* **1980**, *31*, 709-711.
- (15) Parfitt, R. L.; Russell, J. D.; Farmer, V. C. *J. Chem. Soc., Faraday Trans. 1* **1976**, *72*, 1082-1087.
- (16) Rochester, C. H.; Topham, S. A. *J. Chem. Soc., Faraday Trans. 1* **1979**, *75*, 591-602.
- (17) Yates, D. E. Ph.D. Thesis, University of Melbourne, 1975, pp 22-29.
- (18) Bragg, L.; Claringbull, G. F.; Taylor, W. H. "Crystal Structure of Minerals"; Cornell University Press: Ithaca, NY, 1965; p 120.
- (19) Benjamin, M. M. *Environ. Sci. Technol.* **1983**, *17*, 686-692.
- (20) Westall, J.; Hohl, H. *Adv. Colloid Interface Sci.* **1980**, *12*, 265-294.
- (21) von Helmholtz, H. *Ann. Phys. (Leipzig)* **1879**, *7*, 337-343; English Translation: University of Michigan, Ann Arbor, MI, 1951, Engineering Research Bulletin 33.
- (22) von Smoluchowski, M. *Bull. Acad. Sci. Cracovie* **1903**, *1*, 182-190.
- (23) Hückel, E. *Phys. Z.* **1924**, *25*, 204-211.
- (24) Henry, D. C. *Proc. R. Soc. London, Ser. A* **1931**, *133*, 106-112.
- (25) Wiersema, P. H.; Loeb, A. L.; Overbeek, J. Th. G. *J. Colloid Interface Sci.* **1966**, *22*, 78-99.
- (26) Stigter, D. *J. Phys. Chem.* **1978**, *82*, 1417-1423.
- (27) Stigter, D. *J. Phys. Chem.* **1978**, *82*, 1424-1429.
- (28) Ottewill, R. H.; Shaw, J. N. *J. Electroanal. Chem.* **1972**, *37*, 133-142.
- (29) Hunter, R. J. "Zeta Potential in Colloid Science"; Academic Press: New York, 1981; pp 210-216, 296.
- (30) Stigter, D. *Adv. Colloid Interface Sci.* **1982**, *16*, 253-265.
- (31) Lyklema, J. *J. Colloid Interface Sci.* **1977**, *58*, 242-250.
- (32) James, R. O. In "Adsorption of Inorganics at Solid-Liquid Interfaces"; Anderson, M. A.; Rubin, A. J., Eds.; Ann Arbor Science: Ann Arbor, MI, 1981; pp 219-261.
- (33) Stanforth, R. R. Ph.D. Thesis, University of Wisconsin, Madison, WI, 1981.
- (34) Atkinson, R. J.; Posner, A. M.; Quirk, J. P. *J. Inorg. Nucl. Chem.* **1968**, *30*, 2371-2381.
- (35) Tejedor-Tejedor, M. I., University of Wisconsin, Madison, personal communication, 1982.
- (36) Anderson, M. A.; Stanforth, R. R.; Tejedor-Tejedor, M. I. *Environ. Sci. Technol.*, in press.
- (37) Lyklema, J. Agriculture University, Wageningen, The Netherlands, personal communication, 1984.

Received for review July 30, 1984. Accepted January 11, 1985.
This research was funded by a grant from the Department of Energy under Contract DE-AC02-80EV10467.

NOTES

Acidification of Southern Appalachian Lakes

Robert W. Talbot[†] and Alan W. Elzerman*

Department of Environmental Systems Engineering, Clemson University, Clemson, South Carolina 29631

■ Measurements of the dissolved ($<0.4 \mu\text{m}$) major element water chemistry of 10 lakes and reservoirs situated in the southern Appalachian Mountain and Carolina Piedmont regions are used to examine effects of acidic atmospheric deposition inputs on water chemistry. In the mountain region, lakes with low alkalinity and a small watershed/lake area ratio appear to be most susceptible to, and may be undergoing, pH reduction. In the Piedmont region, watershed soils, especially those exposed by man's activities, appear to be effectively neutralizing acid inputs. Weathering of rocks and soils accelerated beyond that expected from carbonic acid alone is probably occurring in the mountain and Piedmont systems. Our analysis suggests that reduction of lake water pH, mobilization of soil chemical constituents, and subsequent changes in the chemical composition of aquatic systems may be a more widespread and potentially serious environmental problem in this area than previous analyses have suggested.

Introduction

Aquatic ecosystems most likely to be adversely affected by inputs of acidic atmospheric deposition are believed to typically have (1) lake waters with low alkalinity, (2) watershed geology dominated by igneous or metamorphic bedrock, and (3) watershed soils characterized as acidic with low buffering capacities. Such conditions are prevalent in the adjacent Appalachian Mountain and Piedmont regions of Southeastern United States. Because the areal bedrock of these regions consists primarily of granites, gneisses, and schists, Galloway and Cowling (1) and Hendrey et al. (2) concluded that the area was generally vulnerable to damage from acid inputs. Norton (3) also evaluated the regions' likelihood to suffering adverse effects from acid inputs but on a more detailed county by county basis using specific geological information. The results of his analysis suggest that the mountain lakes of western North Carolina are located in an area that is particularly vulnerable to damage from acidic atmospheric deposition inputs.

Direct acidic deposition/bedrock interactions in the southern Appalachian Mountain and Piedmont regions may be minimal, however, since the area is highly weathered and bedrock generally lies 5-10 m below the surface. This suggests that at many locations the soils may profoundly influence the interactions of acidic deposition with aquatic and terrestrial ecosystems. Soils in both the mountain and Piedmont regions are characterized as well drained with various sandy clay loams predominating. In addition, the soils are acidic (pH 4.5-5.5), contain little organic matter, are high in K and exchangeable Al, but

contain small amounts of Ca (4). Because the cation-exchange capacities of the soils in these regions are only moderately low (i.e., ~6-15 mequiv/100 g), McFee (5) concluded that the area was only slightly sensitive to adverse effects of acidic deposition inputs. Elzerman and Talbot (6) report, however, that the soils in this area have a small percentage base saturation due to the low Ca and Mg content; yet, acid neutralization in these soils occurs primarily by release of Ca and Mg, suggesting possibly more potential for adverse effects from acid inputs than indicated by total cation-exchange capacities. In summary, the bedrock and soil in the southern Appalachian Mountain and Piedmont regions have little neutralizing capability, and the potential exists for mobilization of chemical constituents from watershed soils to surface waters due to reaction with acidic atmospheric deposition.

Both the mountain and Piedmont regions presently receive acidic rainfall that has a mean volume-weighted H^+ concentration that corresponds to a pH of 4.4 (7). Mean annual precipitation amount averages 132 cm in the Piedmont to 250 cm at the higher mountain elevations and 170 cm at lower mountain elevations (4). Snow usually comprises only a few percent of the total annual precipitation. Precipitation in the mountains may occur continuously for up to 2 weeks or more at a time during any season of the year. The annual precipitation amount in the highest mountain elevations is greater than anywhere else in the United States except for near the Pacific Ocean in the northwest. Consequently, the mountain region is subjected to a potentially large annual atmospheric loading of acidic precipitation as well as possibly long duration wet deposition events.

In this paper we utilize several recently published models (8, 9) to provide an initial qualitative assessment of the effects of acidic atmospheric deposition on the water chemistry of selected aquatic ecosystems situated in the southern Appalachian Mountain and Carolina Piedmont regions. The conceptual model of lake acidification by sulfuric acid inputs recently proposed by Galloway et al. (10) is also used to identify geochemical responses to acidic inputs which may be occurring in this region. Since virtually no reliable or detailed data are available in the open literature describing the water chemistry of lakes in this area, little attention has previously been focused on evaluating the significance of acid inputs to aquatic ecosystems located in this section of Southeastern United States. A recent statistical analysis of stream water chemistry trends at USGS hydrologic bench-mark stations indicated that SO_4^{2-} concentrations have been increasing over the past decade in this region of the United States (11). Because this trend seems to be similar historically to regional atmospheric emission patterns of SO_2 and NO_x , the increased SO_4^{2-} concentrations may be related to inputs of acidic atmospheric deposition, emphasizing the need to

[†]Present Address: Atmospheric Sciences Division, NASA Langley Research Center, Hampton, VA 23665.

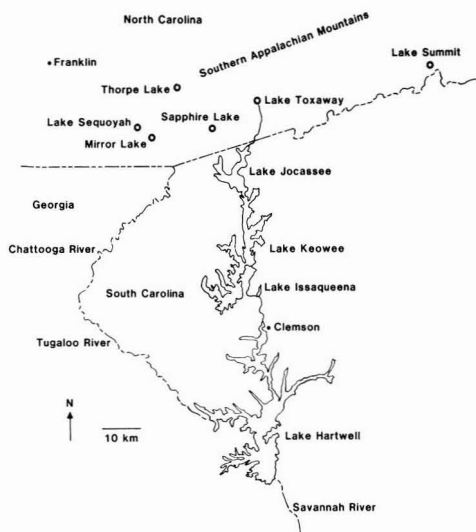


Figure 1. Location of study lakes in the southern Appalachian Mountain and Carolina Piedmont regions.

look at water chemistry changes in the region.

Principal objectives of our study were (1) to obtain a general picture of the current water quality of lakes in this area and generally characterize their water quality in relation to acid inputs, (2) to identify potential problems related to reduction of lake water pH and mobilization of chemical constituents from watershed soils to surface water, and (3) to examine the relationships between acidic deposition inputs and water chemistry responses of various surface waters which are affected by the same regional atmospheric inputs but that are situated in different environmental settings or form a flowing series of interconnected lakes. The latter objective stems from our hypothesis that, when historical data are not available, a comparison of intraregional surface water chemistries can be used to gain insight on net compositional changes induced by acidic deposition inputs.

Sampling and Analysis

After a preliminary survey of 20 lakes, 10 lakes were selected for study (Figure 1) since they provided a wide spectrum of elevations, degrees of development, and watershed/lake area ratios (W/L) and might, therefore, be affected differently by acid inputs. Five of the lakes (Mirror, Sapphire, Sequoyah, Thorpe, and Toxaway) are situated in the southern Appalachian Mountains (NC) at an average elevation of 1012 m. Four of the study lakes (Hartwell, Issaqueena, Jocassee, and Keowee) lie in the Piedmont region of South Carolina and reside at an average elevation of 270 m. Lakes Toxaway, Jocassee, Keowee, and Hartwell are interconnected by rivers and form a chain of lakes extending from the mountain headwater (Toxaway) through Jocassee, then Keowee, and then to the lower Piedmont region (Hartwell). Lake Summit is situated at an intermediate elevation (613 m) in the mountain foothills of southwestern North Carolina.

Surface water samples were collected from each of the study lakes during early May 1982. At the time of sampling, the lake waters were poorly stratified (thermally), and well-mixed conditions existed. Except in the bottom few meters, the lakes exhibited nearly isothermal temperature profiles averaging 18 °C. Since the lake waters

were relatively well mixed, confounding effects of summer stratification on chemical and physical parameters were probably minimal. In addition, effects of biological productivity (e.g., pH and pCO₂) were probably minimal since the samples were collected in the early morning hours (before 10:00 a.m.) on a dark overcast day. Data collected from these lakes on other occasions were similar to the data reported here but were not used in these analyses.

Immediately after collection, approximately 100 mL of lake water was filtered through a 0.4- μ m Nuclepore filter into an acid-cleaned conventional polyethylene (CPE) bottle containing enough HNO₃ (Ultrax) to make the filtrate 0.5% HNO₃. Analyses for Al, Fe, Mn, Ca, Mg, Na, and K were performed on this fraction by using atomic absorption spectrometry. Precision of the cation analyses was estimated to be about $\pm 5\%$. A second water sample was collected (1 L) in a CPE bottle, sealed in a polyethylene bag, and kept on ice in the dark until return to the laboratory. Conductivity, alkalinity, and pH were determined (at 25 °C) on unfiltered subsamples of these samples. Conductivity was determined by using an alternating current conductivity meter. Alkalinity was determined on 100-mL aliquots by titration, using a Metrohm Model 655 Dosimat titrator, to \sim pH 4.5 and then 0.3 pH unit lower in a sealed Teflon apparatus purged with N₂ gas. pH measurements were performed on quiescent solutions by using a Corning combination pH electrode (Model 476223) coupled to an Orion 901 ionalyzer. The technique for pH measurement was essentially that proposed by McQuaker et al. (12) and was designed to minimize the effects of residual streaming and junction potentials on the pH determination. Calibration of the pH-alkalinity system was performed by using pH 4 and 7 certified buffer solutions (± 0.01 pH unit) and carefully prepared low concentration Na₂CO₃ solutions. Analytical precision based on independent analysis of numerous subsamples was estimated to be ± 0.02 units for pH and ± 5 μ equiv/L for alkalinity.

Finally, dissolved Cl⁻, NO₃⁻, and SO₄²⁻ concentrations were measured after filtering approximately 500 mL of lake water through a 0.4- μ m Nuclepore filter. Suspended particulate matter (SPM) concentrations were determined on the basis of the material retained on the filter after drying at room temperature in a desiccator. The technique of Wolfson (13) was used to determine SO₄²⁻ while specific ion electrodes were used for Cl⁻ and NO₃⁻. The precision of anion analyses was estimated to be $\pm 10\%$.

Results and Discussion

Data obtained for the dissolved (<0.4 μ m) major element water chemistry of the study lakes are presented in Table I. For comparison, the mean volume-weighted chemical compositions of rain water for the Piedmont (Clemson, SC and mountain (Franklin, NC) regions have also been included in Table I. Only the H⁺, NO₃⁻, and SO₄²⁻ concentrations were higher in precipitation than in the lake waters. However, lake water concentrations were comparatively low, with the total ionic constituents averaging about 300 μ equiv/L in mountain lakes and 450 μ equiv/L in Piedmont lakes. In addition, alkalinity values were low, ranging from 26 μ equiv/L in Lake Toxaway to 217 μ equiv/L in Lake Issaqueena. The grand average pH of the study lakes was 6.88.

Various chemical acidification models have been proposed to distinguish between acidified and unacidified surface waters. The empirical approach of plotting pH vs. [Ca²⁺] suggested by Henriksen (15) has probably been the most widely used. However, Kramer and Tessier (8) discussed several shortcomings of this method and con-

Table I. Chemical Composition of Areal Rain and Lake Waters in the Southern Appalachian Mountain and Carolina Piedmont Regions

lake	elev, m	SPM, ^a mg/L	cond, μΩ ⁻¹ cm ⁻¹	pH	μM/L										cation/ anion		
					alk ^b	Al	Si	Fe	Mn	Ca	Mg	Na	K	Cl		SO ₄	NO ₃
Toxaway	914	0.90	10	6.71	25.9	0.93	57.0	1.7	0.29	15.0	8.2	28.3	8.7	33.8	15.6	2.4	0.99
Thorpe	1067	1.9	12	6.99	56.6	1.5	78.3	0.34	0.02	20.7	10.3	47.8	11.0	45.1	10.0	3.5	1.0
Sapphire	946	2.3	11	6.61	66.9	2.9	89.0	7.3	0.87	19.7	9.0	47.8	9.0	39.5	14.6	3.9	1.0
Sequoyah	1097	1.3	15	6.78	74.9	2.3	64.1	5.6	0.51	32.4	13.6	69.6	11.5	59.2	19.8	4.5	0.97
Mirror	1037	4.9	16	6.60	77.9	7.3	64.1	12.0	0.98	34.9	14.8	69.6	13.8	81.8	22.9	15.5	1.0
Jocassee	335	2.3	15	7.14	88.7	1.1	117.5	0.15	0.01	25.0	14.0	56.5	13.8	39.5	12.5	3.1	0.97
Keowee	244	2.2	17	7.12	120.1	1.2	121.1	0.20	0.01	32.4	21.0	65.2	18.9	48.0	14.6	4.0	0.97
Hartwell	201	1.3	33	7.13	138.8	1.6	124.6	0.31	0.02	39.9	26.3	104.4	24.6	56.4	25.0	8.1	1.0
Summit	613	1.8	16	7.26	139.0	2.3	121.1	0.75	0.06	42.4	24.7	65.2	14.1	50.8	17.7	5.3	0.97
Issaqueena	300	8.9	37	6.46	216.8	1.0	NA	NA	NA	54.9	41.1	91.3	28.1	67.7	7.4	3.7	1.0
rain ^c																	
Clemson, SC ^d	231		25	4.40 ^e		0.07	0.15	0.03	0.01	3.2	1.6	9.1	0.69	9.3	25.0	17.7	1.1
Franklin, NC	722		24	4.56 ^e		NA ^f	NA	NA	NA	1.7	0.90	10.4	0.56	7.1	17.0	10.2	0.98

^aSPM means suspended particulate matter. ^bExpressed as HCO₃⁻. ^cMean volume-weighted concentrations calculated from ref 7. ^dValues for Al, Si, Fe, and Mn from Talbot (14). ^eCalculated from mean volume-weighted H⁺ concentration. ^fNA means not available.

cluded that a more rigorous approach should be employed, especially when Na, K, and Mg contribute significantly to the total cation concentration. They suggested that pH should be plotted vs. $\sum z_i[M_i]$, where M represents the dissolved Ca, Mg, Na, and K concentrations and z their respective charge. For the lakes investigated in this study, concentrations of K⁺, Mg²⁺, and particularly Na⁺ were significant relative to Ca²⁺ (Table I), suggesting that the Kramer and Tessier (8) approach is relevant for assessing lake acidification effects.

Briefly, Kramer and Tessier (8) recommended that the following equation should be used to define the theoretical line representing carbonic acid weathering (CAW):

$$pH = \log \sum z_i[M_i] - \log *K - \log pCO_2 \quad (1)$$

where z_i and M_i are defined as before. The expression for *K is

$$*K = K_H K_1 = \frac{[HCO_3^-][H^+]}{pCO_2} \quad (2)$$

where K_H is Henry's law constant for CO₂ water-air equilibrium and K₁ is the first dissociation constant for carbonic acid. A fixed pCO₂ value of 10^{-3.52} atm was used in the calculation of the theoretical CAW line depicted in Figure 2.

To correct the measured lake water pH values for variations in pCO₂ and to allow comparison with the theoretical CAW line, a corrected pH value was calculated by using

$$pH_{(corrected)} = pH_{(actual)} - \log pCO_{2(fixed)} + \log pCO_{2(actual)} \quad (3)$$

where values for pCO_{2(actual)} were computed from the measured pH and alkalinity as shown by Kramer and Tessier (8).

To provide a more realistic picture of the cation concentration of the lake waters resulting from weathering processes, the contribution of precipitation-derived Ca, Mg, Na, and K was estimated and subtracted from the measured lake water concentrations. The precipitation component was estimated by using evapotranspiration factors for the mountain (1.6) and Piedmont (2.9) regions calculated from the data reported by Smith and Alexander (11). These calculations indicated that on the average precipitation accounted for approximately 25% (range 13–38%) of the lake water cation concentrations.

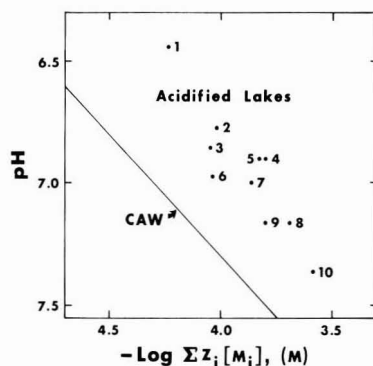
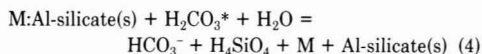


Figure 2. Schematic representation of study lakes relative to the theoretical carbonic acid weathering (CAW) line, where log *K = -7.8 and log pCO₂ = -3.5. Lake identification key: (1) Toxaway, (2) Thorpe, (3) Sapphire, (4) Mirror, (5) Sequoyah, (6) Jocassee, (7) Keowee, (8) Hartwell, (9) Summit, and (10) Issaqueena.

The results of the calculations for the 10 study lakes are depicted in Figure 2. Several important observations can be made from the information provided in Figure 2. First, all of the data points lie in the region above the theoretical CAW line, suggesting that more extensive weathering of watershed soils is apparently occurring than expected from the action of carbonic acid alone. Second, Piedmont lakes have pH values >7.0 while mountain lakes have pH values <7.0. The extreme cases are represented by Lake Toxaway, a mountain headwater lake with the lowest pH, and Lake Issaqueena, a Piedmont lake with the highest pH. These two cases will be examined in greater detail.

Since soils in the study area contain readily exchangeable cations (6, 14), we can write a generalized unbalanced weathering reaction for the incongruent dissolution of silicate minerals as follows:



where M represents various cations such as Ca, Mg, Na, or K. Under natural carbonic acid weathering conditions and ignoring other usually minor constituents, equivalent amounts (mequiv/L) of HCO₃⁻ and cations are produced (16). Thus, a correlation might exist between the W/L ratio and the relative amount of HCO₃⁻ (or cations) in the receiving water.

Table II. Anion and Cation Relationships (Equivalents Based) in Lake Waters^a

lake	W/L ^b	$\Sigma\text{BCs}^c/\text{HCO}_3^-$	$\text{HCO}_3^-/\Sigma\text{anions}$	$\text{SO}_4^{2-}/\text{HCO}_3^-$	$\text{Cl}^-/\text{HCO}_3^-$	$\text{SO}_4^{2-}/\Sigma\text{BCs}$	$\text{Cl}^-/\Sigma\text{BCs}$	$\text{Cl}^-/\text{SO}_4^{2-}$
Toxaway	8	2.2	0.32	1.2	0.86	0.54	0.39	0.72
Thorpe	16	1.7	0.50	0.35	0.60	0.21	0.35	1.7
Sapphire	256	1.3	0.52	0.44	0.42	0.33	0.32	0.96
Sequoyah	61	2.0	0.45	0.53	0.64	0.27	0.32	1.2
Mirror	157	2.0	0.37	0.59	0.90	0.29	0.45	1.5
Jocassee	13	1.0	0.69	0.28	0.14	0.27	0.14	0.50
Keowee	15	1.1	0.61	0.24	0.17	0.22	0.16	0.72
Hartwell	23	1.5	0.69	0.36	0.21	0.24	0.14	0.59
Summit	14	1.1	0.68	0.25	0.17	0.23	0.15	0.67
Issaqueena	84	1.2	0.79	0.07	0.19	0.06	0.16	2.8

^aChloride and base cation concentrations have been corrected for precipitation inputs (see text). ^bW/L means watershed/lake area ratio. ^cBCs mean base cations (Ca + Mg + K + Na).

When values of the ratio $\text{HCO}_3^-/\Sigma\text{anions}$ for the study lakes are compared (Table II), it is apparent that the relative proportion of HCO_3^- in the lake waters is much greater in Piedmont lakes than it is in mountain lakes. In most of the mountain lakes, HCO_3^- was not the most abundant charge balancing anion. The concentrations of SO_4^{2-} and Cl^- in these waters, which are attributed mainly to atmospheric inputs, comprised a significant fraction of the total anionic constituents (Table II). In fact, SO_4^{2-} and Cl^- combined ($\mu\text{equiv/L}$) were 2.5 times greater than HCO_3^- in Lake Toxaway. The opposite was true in Lake Issaqueena where HCO_3^- was the most abundant charge balancing anion.

Obviously, there is not a simple correlation between W/L and the relative proportion of HCO_3^- in the receiving water. More specific information about each lake system is clearly needed. Cultural disturbance of the watershed (e.g., percentage of exposed soil) seems to be a key factor. For example, Lake Issaqueena had a much higher alkalinity than the other Piedmont lakes. The Lake Issaqueena watershed has been subjected to some development, agricultural uses, and controlled forest cutting, potentially exposing large areas of soil. These cultural disturbances of the watershed are undoubtedly facilitated leaching of soil cationic constituents and also contributing alkalinity to the lake waters.

Cronan et al. (17) suggested that, in areas where strong acids from precipitation like H_2SO_4 dominate weathering, the H^+ and SO_4^{2-} provided by atmospheric inputs serve as a major source for cation replacement (H^+) and mobile charge balancing anions (SO_4^{2-}) for subsequent cation transport within watershed soils. This hypothesis lead Burns et al. (9) to suggest that one method of quantifying the importance of strong acid weathering is to compare the sum of base cations (BCs = Ca, Mg, Na, and K) to alkalinity in receiving waters. In this model, the larger the value of the ratio $\Sigma\text{BCs}/\text{HCO}_3^-$, the greater the role strong acids such as H_2SO_4 have in the weathering processes. Values of this ratio for the lakes investigated in this study are shown in Table II. Corrections have been made for the precipitation contribution to the lake water Cl^- and BC concentrations using the appropriate evapotranspiration factors. The largest values of $\Sigma\text{BCs}/\text{HCO}_3^-$ were found in the mountain lakes. Release of cationic constituents to surface waters from strong acid weathering is apparently occurring more extensively in the mountain systems than in the Piedmont systems. This trend is also apparent in Figure 2. The $\Sigma\text{BCs}/\text{HCO}_3^-$ ratio had a value close to unity in most Piedmont lakes, suggesting a lesser effect of strong acid inputs or a difference in neutralizing mechanism compared to the mountain lakes.

Watersheds in the Piedmont, despite being smaller than many mountain systems, are more disturbed by cultural activities than mountain watersheds and thus provide ample interaction with acid precipitation to neutralize excess H^+ inputs. Consequently, leaching of soil constituents may occur, but significant pH reduction in Piedmont lakes is probably unlikely in the near future. This may not be the case, however, for some mountain systems. Of the five mountain lakes investigated, the two lake systems with the smallest W/L ratio (Toxaway and Thorpe) had the lowest pH values. These lake systems are probably the most susceptible to pH reduction since they have little capability for neutralizing excess H^+ inputs. The displacement of Lake Toxaway in Figure 2 from the other mountain lakes indicates that pH reduction and extensive leaching of soil cationic constituents from watershed soils may already be occurring. Lakes Mirror, Sapphire, and Sequoyah have large watersheds and, therefore, may be more resistant to the effects of strong acid inputs than Lakes Toxaway and Thorpe.

Galloway et al. (10) have hypothesized an historical time response of a lake system to acidification effects from atmospheric H_2SO_4 deposition. An important facet of the model is that SO_4^{2-} partially accumulates in watershed soils until saturation is approached. At saturation, SO_4^{2-} enters the lake at a rate equal to the atmospheric input. A concomitant decrease also occurs in the alkalinity concentration (HCO_3^-). As a result of these processes the value of the $\text{SO}_4^{2-}/\text{HCO}_3^-$ ratio in the lake water begins to increase.

The values of the $\text{SO}_4^{2-}/\text{HCO}_3^-$ ratio for our study lakes are presented in Table II. Except in Lakes Toxaway and Issaqueena, the ratio hovers around an average value of 0.40. In Lake Issaqueena, the ratio had a value of 0.07, suggesting that in comparison to the other lakes nearly all the SO_4^{2-} entering the watershed is being retained in the soil. Cultural disturbance of the Lake Issaqueena watershed, directly exposing more soil area, has presumably enhanced SO_4^{2-} retention in this system. In Lake Toxaway the $\text{SO}_4^{2-}/\text{HCO}_3^-$ ratio was 1.2, nearly 20 times its value in Lake Issaqueena. We suspect that the SO_4^{2-} concentration of Lake Toxaway is increasing and the alkalinity decreasing. This interpretation suggests that Lake Toxaway is in stage 3 of the acidification process as described by the Galloway et al. model (10). The other mountain and Piedmont lakes are apparently not as advanced (stage 2) as Lake Toxaway in the acidification process.

During stage 3 of the acidification, the ratio $\text{SO}_4^{2-}/\Sigma\text{BCs}$ should increase in value as the BC concentration decreases (10). The 0.54 value of this ratio in Lake Toxaway is twice the value of the ratio in the other lakes we studied. The low value of the same ratio in Lake Issaqueena (0.06) most

likely reflects effective scavenging of SO_4^{2-} by watershed soils and release of BCs via cation-exchange neutralization reactions.

Another indicator of SO_4^{2-} retention by watershed soils is the relative value of the $\text{Cl}^-/\text{SO}_4^{2-}$ ratio in the lake waters. The ratio had a value greater than 1.0 in most mountain lakes. The lowest value of the ratio in the mountain lake systems was found in Lake Toxaway, where watershed soils are apparently not effectively retaining the atmospheric input of SO_4^{2-} . Of the Piedmont lakes studied, only in Lake Issaqueena was the ratio greater than 1.0. The value of the $\text{Cl}^-/\text{SO}_4^{2-}$ ratio in Lake Issaqueena (2.8) was the largest we observed, and again, it seemingly indicates very efficient SO_4^{2-} retention by watershed soils.

The apparently accelerated weathering of watershed soils in Northeastern United States has resulted in elevated dissolved Al concentrations in receiving waters that may be toxic to fish (18). This same situation may also be developing in some southern Appalachian aquatic systems. Three lakes (Sapphire, Sequoyah, and Summit) had dissolved Al concentrations averaging $70 \mu\text{g/L}$. Lake Mirror had a dissolved Al concentration of $200 \mu\text{g/L}$, essentially the same level found in the Hubbard Brook system located in Northeastern United States (19). Despite the low total organic carbon (TOC) levels present in these lakes (1–3 mg/L), most of the Al (and Fe) may be organically complexed. Filtrates ($0.4 \mu\text{m}$) of Lakes Mirror, Sapphire, and Sequoyah were noticeably colored, suggesting that most of the TOC may have been in dissolved form (DOC). Johnson et al. (19) found a strong correlation between DOC and dissolved Al in Hubbard Brook stream waters, and Pott (20) observed the same relationship in stream waters in the Lake Issaqueena watershed during storm-flow events. As in Northeastern United States, Al is apparently being mobilized in watershed soils of Carolina Piedmont and Mountain systems and released to surface waters. Preliminary leaching studies using soil material collected from the Piedmont and mountain regions and rainwater with a chemical composition typical of areal rainfall indicate that Al, Si, Fe, Ca, Mg, K, Cl, and Pb are readily leachable from these soils by pH 4.4 rainwater (6, 14, 21). Furthermore, investigation of acid precipitation/soil/stream water interactions in the Lake Issaqueena system indicates that stream transport of chemical constituents presumably leached from watershed soils is strongly dependent on rainfall amount, rainwater pH, and local physical features of the watershed (6, 21).

Conclusions

The susceptibility of an aquatic system to detrimental effects from inputs of acidic atmospheric deposition is a complex function of the specific coupling of the chemical and physical (as well as biological) features of the terrestrial-aquatic ecosystems. Detailed analysis of acidic deposition/environment interactions in a suite of carefully selected aquatic systems might reveal generalizations which could be used to address important questions regarding the potential for adverse effects to occur, their extent, and subsequent consequences. In undisturbed watersheds, for example, historical trends in the value of the ratio $\text{HCO}_3^-/\sum \text{anions}$ in surface waters may be useful, with certain caveats, for assessing the relative weathering rates of watershed soils. Lacking the availability of historical data, trends in related or interconnected lakes may present opportunities for acquiring knowledge.

Our analysis of some aquatic systems located in Southeastern United States suggests that some of the lakes in the southern Appalachian Mountain system are probably

highly susceptible to pH reduction. Leaching of chemical constituents from watershed soils and subsequent changes in the chemical composition of surface waters may be widespread and a potentially serious problem in some aquatic systems located in this area of the United States.

Acknowledgments

The help of Janice O'Connor in preparation of the manuscript is gratefully acknowledged.

Registry No. Al, 7429-90-5; Si, 7440-21-3; Fe, 7439-89-6; Mn, 7439-96-5; Ca, 7440-70-2; Mg, 7439-95-4; Na, 7440-23-5; K, 7440-09-7.

Literature Cited

- (1) Galloway, J. N.; Cowling, E. B. *J. Air Pollut. Control Assoc.* 1978, 28, 229-235.
- (2) Hendrey, G. R.; Galloway, J. N.; Norton, S. A.; Schofield, C. L.; Schaffer, P. W.; Burns, D. A. "Geological and Hydrochemical Sensitivity of the Eastern United States to Acid Precipitation". U.S. Environmental Protection Agency, 1980, Report EPA-600/3-80-024.
- (3) Norton, S. A. In "Atmospheric Sulfur Deposition: Environmental Impact and Health Effects"; Shriner, D. S.; Richmond, C. R.; Lindberg, S. E., Eds.; Ann Arbor Science: Ann Arbor, MI, 1980; pp 521-531.
- (4) King, J. M.; Turpin, J. W.; Bacon, D. D. "Soil Survey of Transylvania County, North Carolina"; U.S. Department of Agriculture, Soil Conservation Service and Forest Service: Washington, DC, 1974.
- (5) McFee, W. W. In "Atmospheric Sulfur Deposition: Environmental Impact and Health Effects"; Shriner, D. S.; Richmond, C. R.; Lindberg, S. E., Eds.; Ann Arbor Science: Ann Arbor, MI, 1980; pp 495-505.
- (6) Elzerman, A. W.; Talbot, R. W. "Effects of Acid Deposition (Rain) on a Piedmont Aquatic Ecosystem: Acid Inputs, Neutralization, and pH Changes"; Office of Water Research and Technology, U.S. Department of the Interior, Washington, DC, 1983, SC WRRI Report 108.
- (7) National Atmospheric Deposition Program "Data Report: Precipitation Chemistry"; Natural Resources Ecology Laboratory, Colorado State University: Fort Collins, CO, 1978-1980; Vol. I-III.
- (8) Kramer, J.; Tessier, A. *Environ. Sci. Technol.* 1982, 16, 606A-615A.
- (9) Burns, D. A.; Galloway, J. N.; Hendrey, G. R. *Water Air Soil Pollut.* 1981, 16, 277-285.
- (10) Galloway, J. N.; Norton, S. A.; Church, M. R. *Environ. Sci. Technol.* 1983, 17, 541A-545A.
- (11) Smith, R. A.; Alexander, R. B. "Evidence for Acid-Precipitation-Induced Trends in Stream Chemistry at Hydrologic Bench-Mark Stations". 1983, U.S. Geological Survey Circular 910.
- (12) McQuaker, N. R.; Kluckner, P. D.; Sandberg, D. K. *Environ. Sci. Technol.* 1983, 17, 431-435.
- (13) Wolfson, J. M. *J. Air Pollut. Control Assoc.* 1980, 30, 688-690.
- (14) Talbot, R. W. Department of Environmental Systems Engineering, Clemson University, Clemson, SC, unpublished data, 1983.
- (15) Henriksen, A. *Nature (London)* 1979, 278, 542-545.
- (16) Stumm, W.; Morgan, J. J. "Aquatic Chemistry: An Introduction Emphasizing Chemical Equilibria in Natural Waters", 2nd ed.; Wiley: New York, 1981.
- (17) Cronan, C. S.; Reynolds, R. C., Jr.; Lang, G. E. *Science (Washington, D.C.)* 1978, 200, 309-311.
- (18) Cronan, C. S.; Schofield, C. L. *Science (Washington, D.C.)* 1979, 204, 304-306.
- (19) Johnson, N. M.; Driscoll, C. T.; Eaton, J. S.; Likens, G. E.; McDowell, W. H. *Geochim. Cosmochim. Acta* 1981, 45, 1421-1437.
- (20) Pott, D. B. M.S. Thesis, Clemson University, Clemson, SC, 1982.

(21) Heatley, W. H. Ph.D. Thesis, Clemson University, Clemson, SC, 1982.

Received for review June 20, 1983. Revised manuscript received August 10, 1984. Accepted January 15, 1985. This work was

supported in part by Grant B-151-SC from the U.S. Department of the Interior through the SC Water Resources Research Institute, Clemson University, and Grant ISP-8011451, "Environmental Engineering Chemistry", from the National Science Foundation.

Improved Aqueous Scrubber for Collection of Soluble Atmospheric Trace Gases

Wesley R. Cofer III*

Atmospheric Sciences Division, Langley Research Center, NASA, Hampton, Virginia 23665

Vernon G. Collins

College of William and Mary, Williamsburg, Virginia 23185

Robert W. Talbot

Langley Research Center, NASA-NRC, Hampton, Virginia 23665

■ A new concentration technique for the extraction and enrichment of water-soluble atmospheric trace gases has been developed. The gas scrubbing technique efficiently extracts soluble gases from a large volume flow rate of air sample into a small volume of refluxed trapping solution. The gas scrubber utilizes a small nebulizing nozzle that mixes the incoming air with an aqueous extracting solution to form an air/droplet mist. The mist provides excellent interfacial surface areas for mass transfer. The resulting mist sprays upward through the reaction chamber until it impinges upon a hydrophobic membrane that virtually blocks the passage of droplets but offers little resistance to the existing gas flow. Droplets containing the scrubbed gases coalesce on the membrane and drip back into the reservoir for further refluxing. After a suitable concentration period, the extracting solution containing the analyte can be withdrawn for analysis. The nebulization-reflux concentration technique is more efficient (maximum flow of gas through the minimum volume of extractant) than conventional bubbler/impinger gas extraction techniques and is offered as an alternative method.

Introduction

Gas scrubbing devices (principally bubblers and impingers) have a long history of use for extraction and concentration of atmospheric trace gases (1-4). Many of these techniques are based on the passage of the gas (or gases) of interest through a strongly absorbing liquid in which accumulation of analyte occurs. Typically, chemical analysis is then performed on the collected analyte. Chemical reagents are often incorporated into the liquid medium to facilitate analyte extraction (5-7). Generally this is done to chemically stabilize the analyte in its medium or to increase the extraction efficiency (or capacity), or both. Sometimes an indicating reagent (e.g., color development) is added to the extracting medium (8) to allow direct monitoring of accumulated analyte. Most gas absorption methods (and associated apparatus) possess the virtues of being simple in concept and operation, versatile, and relatively inexpensive to produce and use. Less attractive aspects of these techniques include (a) prolonged periods (minutes to hours) of operation are frequently required before analyte concentrations are sufficient for quantification, (b) the analyses represent integrated values for the sampled period (time-averaged concentrations), and (c) sometimes the accumulated analyte may be significantly altered by uncontrollable and/or unforeseen chemical reactions that occur in the extracting medium (see, e.g.,

ref 9). Nevertheless, gas/liquid absorption techniques remain useful and are commonly applied to atmospheric trace gas analysis.

Many of the currently used analytical procedures employing bubbler/impinger technology for atmospheric trace gas analysis would be significantly improved if shorter sampling periods (more effective concentration) prior to analysis could be realized. In addition, commercial instrumentation for measuring clean air concentrations of certain atmospheric trace gases (e.g., NH_3) are not readily available. To this end, this research was undertaken. Our efforts have focused on the development of an improved gas/liquid scrubbing technique to obtain highly efficient extraction of water-soluble gases from large volume flow rates of air in a minimum of trapping solution.

Scrubber

A schematic representation of the nebulization-reflux concentrator developed during this research is shown in Figure 1. The concentrator is about 20 cm long and weighs about 1 kg. A discussion of the operating principles follows. During sampling, air is drawn through a commercially available (DeVilbiss 40) glass-nebulizing nozzle at about 8 L/min, aspirating solution from the reservoir into the nozzle, where the solution is atomized by impaction into small droplets, forming an air/droplet mist. The solution used for extraction (about 3 mL total) is aspirated from the reservoir at about 2.0 mL/min. The resulting air/droplet mist moves upward through the reaction chamber until it impinges upon a hydrophobic membrane. The hydrophobic membrane was made by shaping a Teflon filter (Zefluor, 2- μm diameter pore size) around a stainless steel screen wire cone used for support. Chemical interaction between the filter and atmospheric trace gases should be minimal (10). Water droplets containing the scrubbed gases collect on the surface of the membrane and coalesce into large droplets, which subsequently roll off the apex of the cone and are redeposited into the reservoir to be recycled. Although the membrane virtually blocks all transport of droplets from the concentrator, it offers little resistance to the existing gas flow.

A principal advantage of the nebulization-reflux concentration technique is the large interfacial surface areas generated in the mist, which promote extremely effective mass transfer between the gas and liquid phases. The apparatus can be partially immersed in an ice-water bath to increase the solubility of most trace gases and, more importantly, to minimize the water loss (as gaseous water)

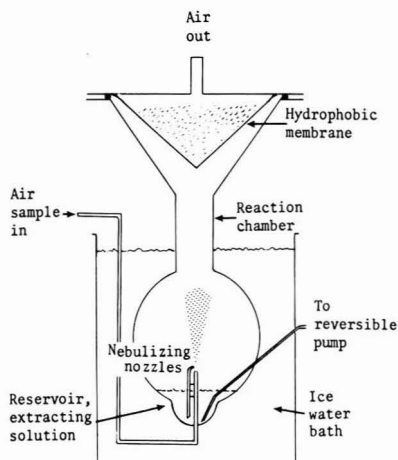


Figure 1. Schematic representation of nebulization-reflux concentrator.

through the hydrophobic membrane during sampling. A reversible peristaltic pumping system is used to add or remove the extracting solution from the reservoir. Filters can be added to the inlet to exclude aerosol particles.

Experimental Section

The extraction efficiency of the nebulization-reflux concentrator was evaluated with trace mixtures of gaseous hydrogen chloride (HCl), ammonia (NH_3), and sulfur dioxide (SO_2). Hydrogen chloride mixtures (in nitrogen) were generated with a commercially available calibration system that utilized the constant diffusion of HCl from a heated (80°C) vial of azeotropic HCl/ H_2O mixture. This system, as it was used, furnished about 175 ppm (volume) (ppmv) of HCl in N_2 at $50\text{ cm}^3/\text{min}$. Ammonia was obtained from a pressurized aluminum cylinder certified by the vendor to contain 92 ± 2 ppmv of NH_3 in N_2 . Sulfur dioxide in nitrogen was supplied from a pressurized aluminum cylinder analyzed at 4.8 ± 0.2 ppmv of SO_2 with a Thermo Electron pulsed fluorescence SO_2 analyzer.

Aqueous extractions of analyte from the trace gas mixtures obtained by using the nebulization-reflux concentrator were compared to their corresponding aqueous extractions made with bubblers. The bubblers were of a design that optimized extraction at high flow rates (11). Chemical analysis of extracted analyte (solvated ions thereof) was performed on an ion chromatograph. For SO_2 evaluations, a 0.1% aqueous hydrogen peroxide (H_2O_2) extracting solution was used. Sulfate analysis was then performed to assess SO_2 capture. Ion chromatographic analysis was performed directly on aliquots withdrawn from the bubblers after runs. Since the potential existed for a small number of concentrated droplets to remain on the membrane and/or walls of the nebulization-reflux concentrator after extractant was removed from the reservoir, a rinse was incorporated into the analysis protocol. About 3 mL of fresh extractant solution was added to the reservoir after each run, refluxed for 2 min with purified nitrogen (or ultrapure air), then removed and added to the original extract before analysis. This was found to effectively scavenge the analyte remaining in the apparatus. After ion chromatographic analysis, calculations were made by relating the measured analyte levels to their original source concentrations. Runs were made at room temperature ($\sim 25^\circ\text{C}$), and all flows were monitored with mass

Table I. Calculated Source Mixing Ratios of NH_3 , HCl, and SO_2 Obtained from Bubbler and Nebulization-Reflex Extractions

gas	no. 1 bubbler, ppmv	no. 2 bubbler, ppmv	scrubber, ppmv
NH_3	92.9 + 2 (12) ^a	3.1 + 0.8 (6)	94.4 + 3 (15)
HCl	165.9 + 8 (10)	not analyzed	172.9 + 10 (15)
SO_2	4.7 + 0.3 (8)	0.2 + 0.1 (4)	4.7 + 0.2 (8)

^a Number of measurements is in parentheses.

flowmeters. Bubbler runs were conducted under optimum conditions for extraction, that is, at trace gas flow rates of $50\text{ cm}^3/\text{min}$ into 25 mL of pH-adjusted extracting solution. Although each trace gas tested was supplied to either bubblers or the nebulization-reflux concentrator at the same rate (based on mass of trace gas per minute), gaseous concentrations were always about 150 times lower for scrubber extractions since it was necessary to incorporate an additional $8\text{ L}/\text{min}$ of prepurified N_2 into the gas stream for effective operation of the scrubber nebulizing nozzles. Resulting scrubber concentrations were 1.1, 0.6, and 0.03 ppmv, respectively, for HCl, NH_3 , and SO_2 .

Results and Discussion

The effectiveness of the hydrophobic membrane in blocking water droplet escape from the concentrator was assessed experimentally. A small buret containing water was plumbed into the nebulization-reflux concentrator in a fashion allowing a small, but steady, feed of water into the reservoir of the apparatus. The concentrator was then immersed in an ice-water bath and operated by using a $8\text{ L}/\text{min}$ flow of cylinder supplied purified dry N_2 . After a few preliminary runs during which settings were established that approximately maintained a constant water level in the reservoir, four runs of about 1 h each were conducted to determine water loss from the concentrator. Water loss for these runs was found to average $0.033 \pm 0.007\text{ mL}/\text{min}$. Calculated water loss, based on assumptions of negligible membrane inhibition for exiting gaseous water molecules and complete water saturation (at 0°C) of the $8\text{ L}/\text{min}$ nitrogen flow, was about $0.038\text{ mL}/\text{min}$. Comparison of the calculated rate of water loss with the experimentally determined measurement suggests that very little droplet water, if any, was lost during operation of the nebulization-reflux concentrator.

The effectiveness of the nebulization-reflux technique for the extraction of highly water-soluble trace gases was evaluated with HCl and NH_3 . Mixtures of HCl in N_2 and of NH_3 in N_2 were first passed through a two-stage fritted bubbler sampling train for quantification. The fritted bubblers were filled with 25 mL of aqueous extracting solution, $1 \times 10^{-5}\text{ M}$ NaOH for HCl extractions, and $4.5 \times 10^{-3}\text{ M}$ HCl for NH_3 extractions. Almost total extraction of gaseous HCl and NH_3 would be expected in these runs. Results from these runs are shown in Table I. It should be noted that the mixing ratios (moles of trace gas per total moles) of HCl and NH_3 determined from these bubbler runs are within 6% of the expected and/or assayed values. Evidence of the efficiency of the single bubbler extractions can be deduced from the low calculated mixing ratios for NH_3 in the gas stream obtained from extractions in a second bubbler in the two-stage train. The average mixing ratios obtained from these bubbler runs were then compared (see Table I) with average mixing ratios obtained from HCl and NH_3 extractions using the nebulization-reflux technique. Again, although these runs were conducted utilizing identical $50\text{ cm}^3/\text{min}$ flows of gaseous HCl

or NH_3 mixture (as with the bubbler extractions), it was necessary to incorporate an additional 8 L/min flow of prepurified dry nitrogen into the gas stream to operate the nebulizing nozzle. Extracting solution for these runs consisted of about 3 mL of either 1×10^{-5} M NaOH for HCl or 4.5×10^{-3} M HCl for NH_3 .

It is apparent from the data displayed in Table I that the mixing ratios determined for HCl and NH_3 from these runs are in excellent agreement with the assayed values and with the bubbler results. Application of Student's *t* distribution to the data sets indicated that bubbler and scrubber results were statistically indistinguishable at the 95% confidence level. This result is even more significant when it is realized that the scrubber results were obtained at about 150 times the flow rate used with the bubbler, into about $1/8$ the volume of extracting solution, and at about $1/150$ of the gas-phase analyte concentration.

A second series of experiments were conducted to evaluate the performance of the nebulization-reflux concentrator in an extraction that involved both an initial gas absorption step and an intentionally induced chemical transformation. In these experiments, runs were conducted in which gaseous SO_2 was either passed (a) through bubblers containing 0.1% H_2O_2 solution at 60 cm^3/min or (b) through the nebulization-reflux concentrator driven with 8 L/min or ultrapure air also using a 0.1% H_2O_2 extracting solution. The H_2O_2 served to convert extracted SO_2 to sulfate. Data obtained during these series of runs appear in Table I. It is immediately clear that the bubbler and scrubber results are in excellent agreement with the cylinder assay and with each other (statistically the same at the 99% confidence level). It is significant to note that the scrubber results were obtained at an effective SO_2 gas-phase concentration of about 30 ppbv.

In previous work Cofer (12) found that it was useful to express the effectiveness of a bubbler extraction process in terms of the ratio of the maximum gas flow rate, V_g (cm^3/min), achievable without resulting loss of captured analyte to the minimum volume of extracting solution V_x (mL). The maximum flow through the minimum volume translates into the most concentrated solution, ultimately facilitating chemical analysis. Though somewhat cursory, this approach allows relative comparisons to be made among extraction techniques and/or apparatus. For single bubbler extractions of HCl and NH_3 , our bubblers were found to perform without significant loss of capturing efficiency for V_g/V_x ratios of about 300. This value is consistent with the flow/volume range suggested by Wartburg et al. (11) for efficient extraction of polar gases with similar apparatus. At higher V_g/V_x (>300), bubbler capturing efficiencies were observed to decline significantly. However, V_g/V_x ratios of about 2700 were routinely used with the nebulization-reflux concentrator without any detectable loss in captured analyte. Several runs were also made at flow rates of 10 L/min ($V_g/V_x = 3300$) with no apparent loss in scrubbing efficiency. The increased efficiency (up to 10-fold) of the nebulization-reflux technique over bubbler/impinger extraction techniques can translate into shorter sampling times and, thus, better temporal resolution for atmospheric trace gas measurements.

Although runs could have been made at flow rates greater than 10 L/min, considerable back-pressure resulted from the nozzle restriction (~ 0.5 atm at 10 L/min). Sampling flows of from 6 to 8 L/min were found most suitable for general scrubbing operations and were, therefore, routinely used in this work.

Several field tests of the nebulization-reflux concentrator were conducted in close proximity to our Langley

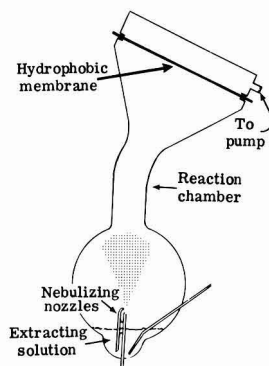


Figure 2. Modified nebulization-reflux concentrator.

Table II. Gaseous Atmospheric Chloride Concentrations Measured during Initial July 1984 Field Sampling Evaluations

date	weather	wind, m/s	time (EDT)	chloride, g/m^3
7-24	hazy	NNE at 0.5	10:00	1.6
7-26	cloudy	N at 0.2	11:00	1.4
7-27	rain	NNE at 0.5	09:30	0.10
7-27	clear	NNE at 1.1	12:00	2.9

laboratory. A metal bellows pump was connected to the system and used to draw ambient air samples at 7 L/min through the scrubber. A $1\text{-}\mu\text{m}$ pore diameter Zefluor Teflon filter was attached to the scrubber inlet to exclude aerosol particles. Air temperatures and relative humidities were highly variable during these initial tests, and significant amounts of condensation were found to accumulate on the back side of the conical membrane (trapped in the cone) at a relative humidity of 90%. To remedy this, the membrane housing was modified and tilted, as shown in Figure 2. As can be readily seen, the new design eliminated the cone and thereby the potential for accumulation of condensate. Initial field tests consisted of 30-min aqueous extractions of ambient HCl. HCl was felt to be a good initial target gas because of its high solubility and the simplicity of its solution chemistry. Although other atmospheric trace gases could release small amounts of soluble chloride in solution, the measurement of solvated chloride should predominately represent an HCl measurement.

Data from these field evaluations of the nebulization-reflux concentrator appear in Table II. A light intermittent rain began on the night of July 26 and continued until morning of July 27, 1984. Scrubber data, other than that presented for the sample acquired between 09:00 and 10:00 eastern daylight time of the morning of July 27, were obtained under nonprecipitating conditions. Gaseous chloride concentrations obtained under dry conditions can be seen to range from about 1.4 to 2.9 $\mu\text{g}/\text{m}^3$. These values lie within the range of gaseous HCl measurements recently reported (0.2–3.0 $\mu\text{g}/\text{m}^3$) for urban areas in Germany by Matusca et al. (13). As would be expected, the HCl measurement made on the morning of July 27 appears to reflect the effect of washout by precipitation. By noon, however, with the emergence of clear skies, gas-phase HCl concentrations dramatically increased.

While the nebulization-reflux technique offers distinct advantages over conventional bubblers with regard to rates of collection and concentration of many soluble atmos-

pheric trace gases, the fundamental limitations for bubbler/impinger application to trace gas measurement apply equally well to our scrubber. For example, complete extraction of gaseous NH_3 occurred in the scrubber only when extracting solution pH was preadjusted to 2.35 or lower. Use of the nebulization-reflux technique, therefore, like any conventional gas/liquid extraction process, requires a thorough understanding of the physical and chemical behavior of the absorbing solution and of the absorbed gases and/or solvated species.

Acknowledgments

We thank Lynn I. Sebacher for her valuable assistance during field testing of the scrubber and Gerald C. Purgold for his help in the fabrication of the scrubber.

Registry No. HCl, 7647-01-0; NH_3 , 7664-41-7; SO_2 , 7446-09-5.

Literature Cited

- (1) Ruch, W. E. "Quantitative Analysis of Gaseous Pollutants"; Ann Arbor-Humphery Science Publishers, Ltd.: Ann Arbor, MI, 1970; pp 209-217.
- (2) Butcher, S. S.; Charlson, R. J. "An Introduction to Air Chemistry"; Academic Press: New York, 1972; pp 44-47.
- (3) Hubert, B. J. "Atmospheric Technology"; National Center for Atmospheric Research: Boulder, CO, 1980; No. 12, pp 30-34.
- (4) Wark, K.; Warner, C. F. "Air Pollution, Its Origin and Control"; Dun-Donnelly Publishers: New York, 1976; pp 245-292.
- (5) West, P. W.; Gaeke, G. C. *Anal. Chem.* **1956**, *28*, 1816-1819.
- (6) Bryers, D. H.; Saltzman B. E. *J. Am. Ind. Hyg. Assoc.* **1958**, *19*, 251-258.
- (7) Fushimi, K.; Miyake, Y. *J. Geophys. Res.* **1980**, *65*, 7533-7536.
- (8) Saltzman, B. E. *Anal. Chem.* **1954**, *26*, 1949-1955.
- (9) Heikes, B. G.; Lazrus, A. L.; Kok, G. L.; Kunen, S. M.; Gandrud, B. W.; Gitlin, S. N.; Sperry, P. D. *J. Geophys. Res.* **1982**, *87*, 3045-3051.
- (10) Apple, B. R.; Tokiwa, Y.; Haik, M.; Kothny, E. L. *Atmos. Environ.* **1984**, *18*, 409-416.
- (11) Wartburg, A. F.; Pate, J. B.; Lodge, J. P., Jr. *Environ. Sci. Technol.* **1969**, *3*, 767-768.
- (12) Cofer, W. R., III 1973, NASA-Langley Research Center Working Paper 1103.
- (13) Matusca, P.; Schwarz, B.; Bachmann, K. *Atmos. Environ.* **1984**, *18*, 1667-1675.

Received for review July 23, 1984. Revised manuscript received November 29, 1984. Accepted January 11, 1985.

Selected Titles

from the Royal Society of Chemistry

Environmental • Health & Safety

Health and Safety in the Chemical Laboratory: Where do we go from here?

Provides an overview of health and safety developments in the chemical laboratory and workplace. Includes Accident and Dangerous Statistics, Morbidity and Mortality Studies, Professional Negligence, Liability and Indemnity, Managing People, Protection of Workers Exposed to Chemicals, and more.

Special Publication No. 51
206 pages. Paper (1984)
\$30.00 (US & Canada only)

Hazards in the Chemical Laboratory, 3rd Edition *L. Bretherick, Ed.*

Vital handbook in all types of laboratory practices. Covers topics such as The Health and Safety at Work etc. Act 1974, Reactive Chemical Hazards, Safety Planning and Management, Fire Protection, Health Care and First Aid, Precautions Against Radiation: Hazardous Chemicals.

Details information on the properties, warning phrases, injunctions, toxic effects, hazardous reactions, first-aid treatments, fire hazards and spillage, disposal procedures for all common laboratory chemicals. Gives short notes on the hazardous properties and reactions of several hundred other less common chemicals.

489 pages. Protective PVC Cover (1981)
\$35.00 (US & Canada only)

Food

Food: The Chemistry of Its Components *T.P. Coultate, Ed.*

Gives a detailed account of the chemistry of the principal substances of food. Discusses both the macro-components, carbohydrates, lipids and proteins, and the micro-components, the colors, flavors, vitamins and preservatives. Shows the relationship between chemical structure of substance and its contribution to the properties and behavior of foodstuffs.

202 pages. Paper (1984)
\$11.00 (US & Canada only)

Recent Advances in the Chemistry of Meat

A.J. Bailey, Ed.

Discusses the problems of the meat industry with reference to the application of chemistry. Reports on The Structure of Muscle and Its Properties of Meat, The

Chemistry of Intramuscular Collagen, The Control of Post-Mortem Metabolism and the Onset of Rigor Mortis, Water-Holding in Meat, The Chemistry of Nitrite in Curing, and more.

Special Publication No. 47
262 pages. Paper (1984)
\$27.00 (US & Canada only)

Analytical

Challenges to Contemporary Dairy Analytical Techniques

Appraises the problems that will be faced by analysts of dairy products in the future and examines the means that are likely to be used to solve them. Looks at quality control, assessment of nutritive content, legal and safety requirements as well as standardized methods of analysis.

Special Publication No. 49
350 pages. Paper (1984)
\$29.00 (US & Canada only)

The Sampling of Bulk Materials *by R. Smith and G.V. James*

Will fill a gap in the literature and stimulate interest in the development of sampling as a field of study. Includes glossary of terms, sampling theories, apparatus for sampling, sampling methods, table of Normal Distribution (single-sided), table for Poisson Distribution, and more.

Analytical Sciences Monograph No. 8
200 pages. Cloth (1981)
\$32.00 (US & Canada only)

Eight Peak Index of Mass Spectra, 3rd Edition

Contains the eight most abundant ions in 66,720 mass spectra covering 52,322 compounds. Indexed by molecular weight, elemental composition, and most abundant ions. Three volumes include molecular weight sub-indexed on formula, molecular weight sub-indexed on fragment ion m/z values, and fragment ion m/z of the two most abundant ions.

3 vols. Cloth (1984)
\$1178.00 (US & Canada only)

Agriculture

The Agrochemicals Handbook

Provides comprehensive data and information on a wide variety of products. Lists trade, chemical, and approved names as well as manufacturers of active components of agricultural products. Covers toxic effects, chemical and physical properties, precautionary measures, and degradation metabolism of active components. Includes herbicides, fungicides, insecticides, nematocides, acaricides, rodenticides, and more. Special feature! Regular updates with announcements and introduction by agrochemical manufacturers of new active ingredients, new pesticidal formulations, and new uses of existing products. (Supplements will be shipped as soon as they are available.)

1,000 pages. Pillar-post binder (1983)
\$248.00 (US & Canada only)
(includes Supplements 1-5)
Replacement Supplements: **\$20.00** each (US & Canada only)

European Directory of Agrochemical Products (EDAP)

Lists over 10,000 agrochemical products manufactured, marketed, and/or used in Western Europe. Details vital information on these products, their active ingredients, and their permitted uses in different countries. Offers three indexes—active ingredients, products, and marketing companies. Does not contain information available in *The Agrochemicals Handbook*.

Four volume flexicover directory includes:

Part I. Fungicides
750 pages (1984)
Part II. Herbicides
1,000 pages (1984)
Part III. Insecticides and Acaricides
1,000 pages (1984)
Part IV. Rodenticides, Nematocides, etc.
450 pages (1984)

Volumes may be purchased individually at **\$114.00** each (US & Canada only)
Special four volume set price: **\$370.00** (US & Canada only)



To charge your books by phone, call TOLL FREE (800) 424-6747 and use your VISA, MasterCard, or American Express.

Order from:

**American Chemical Society
Distribution Office Dept 122
1155 Sixteenth Street, NW
Washington, DC 20036**

Customers outside the U.S. and Canada: please contact *The Royal Society of Chemistry, Distribution Centre, Blackhorse Road, Letchworth, Herts., England* for prices and ordering information.

STANDARD METHODS—16th EDITION

Proven, Time-Tested Methods for the Analysis of Water and Wastewater

The Industry Standard for 80 Years

Originated in 1905 to establish **uniform and efficient methods** for analyzing water, Standard Methods today has earned a reputation as the water and wastewater industries' **most trusted and authoritative source** of water analysis techniques.

Developed and Reviewed by an International Committee of Experts from 16 Different Scientific Disciplines.

The more than **150 analytical methods** described in this valuable reference were developed by specialists from such diverse fields as: organic and analytical chemistry, toxicology, microbiology, civil and sanitary engineering, environmental health, and epidemiology. Its status as an **industry standard** is due in part to the careful review and consensus process by which the 400-member Standard Methods Committee determines the book's contents.

Procedures contained in this 1,340-page laboratory guide are **cited by many state and federal regulatory agencies** for permit compliance purposes as acceptable methods for analyzing the chemical, bacteriological and radiological characteristics of water.

Timely Information of Value to Every Water Quality Analyst

Published in February of this year, the 16th Edition continues the tradition of providing practical information in a **well-organized, easy-to-read** format that permits quick referencing of methods, tables, and bibliographies.

The text's general introduction addresses topics of importance to all water quality laboratory professionals and includes discussions on:

- Current laboratory safety and quality assurance practices

- Proper collection and preservation of samples
- Precision, accuracy and correctness of analyses

Subsequent sections on specific chemical analytic techniques describe the chemical reactions taking place during analysis and alert analysts to potential interferences.

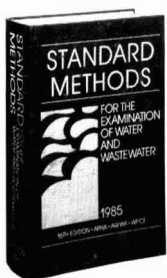
The Most Comprehensive, Up-To-Date Source for Instrumental and Non-Instrumental Methods

More than 50 percent of this industry classic has been **revised, updated or rewritten** to reflect new developments in water analysis techniques over the past 5 years. Classical wet chemical methods (e.g. colorimetric method) are still included but new emphasis is given to **contemporary instrumental techniques**.

Changes in the **16th Edition** of importance to chemists include:

- METALS**
 - A new general discussion of emission spectroscopy using an inductively coupled plasma source.
- INORGANICS**
 - Addition of a new instrumental method using an ion chromatograph for measuring most anions.
 - A change of indicators used for acidity and alkalinity
- ORGANICS**
 - A new method for total organic halide (TOX)
 - Instrumental identification of taste and odor-producing compounds using closed-loop stripping and GC/MS.

Whether you're involved in permit compliance, water supply or wastewater monitoring, Standard Methods is your key to confidence in acquiring quality test results.



Standard Methods is published jointly by three leading scientific organizations: American Public Health Association, American Water Works Association, and the Water Pollution Control Federation.

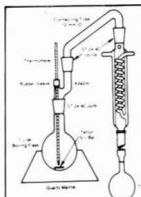


Figure 4131. Direct distillation apparatus for fluoride.

Helpful tables, illustrations and bibliographic references are included throughout this comprehensive text.

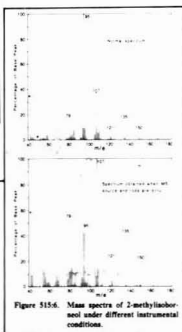


Figure 3156. Mass spectra of 2-methylfluorobenzene under different instrumental conditions.

Normality of NaOH Solution	Required Weight of NaOH to Prepare 1,000 mL of Solution #	Required Volume of 15% NaOH to Prepare 1,000 mL of Solution #
6	240	400
1	40	67
0.1	4	6.7

Make sure there's a copy in your water quality lab!

ORDER FORM

Mail order form to:
Computer Services Department
American Water Works Association
 6666 West Quincy Avenue, Denver, CO 80235

YES! Send me the new 16th edition of Standard Methods.

Send me _____ copies of **Standard Methods for the Examination of Water and Wastewater—16th Edition** (Members \$72.00; nonmembers, \$90.00; 10035LC)

Payment enclosed. (Make check payable to AWWA in U.S. or Canadian funds. If Canadian funds, add 15% to total. If this order is to be shipped outside of North America, please add 40% to above prices.)

Personal check Company check _____ Check no.
 Visa Mastercard American Express

_____ Exp. date
 _____ Card no.

Bill me (AWWA members only).

PLEASE PRINT

NAME _____

ORGANIZATION _____

ADDRESS _____

CITY _____ STATE _____ ZIP _____

PROVINCE _____

PHONE _____ MEMBER NO. _____

